UNIVERSITÀ
DEGLI STUDI
FIRENZE

DOTTORATO DI RICERCA IN
AREA DEL FARMACO E TRATTAMENTI INNOVATIVI

CURRICULUM: SCIENZE FARMACEUTICHE

CICLO XXXI

COORDINATORE Prof. Teodori Elisabetta

Design and synthesis of new adenosine receptor antagonists as neuroprotective agents

Settore Scientifico Disciplinare CHIM/08

Dottorando
Dott. Falsini Matteo

Tutore Scientifico
Prof.ssa Colotta Vittoria

Tutore Teorico
Dott.ssa Varano Flavia

Coordinatore
Prof.ssa Teodori Elisabetta

Anni 2015/2018

TABLE OF CONTENTS

1. INTRODUCTION

1.1. Neurodegenerative disorders

Neurodegenerative disorders affect over 30 million of individuals in the world leading them to disability and death. They are characterized by important pathological changes in specific areas of the central nervous system (CNS) and degeneration of distinct neuron subsets. Despite the different symptomatology and neuronal vulnerability, the pathological processes seem to be similar, suggesting common neurodegenerative mechanisms. Neurodegenerative disorders include common diseases, such as the well-known Parkinson's disease (PD), Alzheimer's disease (AD), but also uncommon conditions, such as Huntington's disease (HD)[1].

Some diseases, such as AD, are characterized by cognitive decline, while others, such as PD, are mainly characterized by motor impairments. HD shows simultaneously motor, psychiatric, and cognitive symptoms as predominant features early on.

- **Alzheimer's disease (AD)**

Alzheimer's disease is the most common neurodegenerative disorder and it is characterized by memory decline. In the early stage, patients present episodic memory dysfunctions, with more recent events being more difficult to remember while more distant memories are generally preserved. Patients also have early impairment in semantic memory regarding the knowledge of facts about the world while procedural memory is not affected. Other cognitive disfunctions of AD include language, visuospatial function, and executive function[1]. AD patients also present language difficulties that manifest early in the disease as reduced verbal fluency and naming. Patients often have neuropsychiatric disturbances, including depression, delusions, hallucinations, behavioral disturbances, such as agitation, and personality changes.

- **Parkinson's disease (PD)**

PD has been defined as a motor disorder. The motor symptoms include resting tremor, bradykinesia, rigidity, and gait imbalance. However, also nonmotor features have been observed such as cognitive impairment, psychiatric symptoms, autonomic dysfunction, and sleep disturbances[1]. Autonomic dysfunction includes constipation, gastrointestinal

motility issues, urinary symptoms, orthostatic hypotension. Common psychiatric features include depression and anxiety. In later stage of the pathology patients develop cognitive decline and in some cases dementia. Differently from AD, memory decline is rare while cognitive impairments such as deficits in attention, hallucinations, or psychosis often occur in PD. Sleep disturbances include sleep apnea, daytime sleepiness, and rapid eye movement sleep behavior disorder (RBD).

- **Huntington's disease (HD)**

This disorder is characterized psychiatric illness, cognitive impairment, and motor dysfunction. When HD manifests during adulthood, patients can show simultaneously either motor symptoms or behavioral symptoms. Psychiatric symptoms include depression, anxiety, and less likely mania and psychosis. Suicide is also a very common event in patients with HD. Patients may also be aggressive toward others. Cognitive impairments are also not rare with decline in attention, motivation, problem solving, and executive function. The motor dysfunction is typically marked by choreiform movements, which are excessive, together with involuntary movement. Differently from AD and PD, HD occurs during childhood and the clinical manifestations are quite different and include akinesia, rigidity along with cerebellar ataxia and seizures.

Mechanisms implicated in neurodegeneration

Despite causes of each neurodegenerative disorder are different, some mechanisms involved in neurodegeneration seem to be similar. In fact, the mechanisms leading to neurodegeneration and cell death include:

- Mitochondrial Dysfunction.
- Oxidative Stress.
- Excitotoxicity.
- Protein Aggregation.
- Prion-Like Spread.
- Neuroinflammation.

Among these mechanisms, no one appears to be the main cause of neurodegeneration, and these pathogenic mechanisms act synergistically through complex interactions to promote neurodegeneration.

Current treatment options

At present, the therapeutic treatments available to patients with neurodegenerative disorders are few and those that are available address only symptoms and not affecting the mechanisms underlying the disease. Despite these therapies can make a big difference in the quality of life of patients, it is urgent to develop effective and safe therapies able to stop or slow the progression of diseases. To achieve this we need a better understanding of the mechanisms and causes regulating the neurodegeneration that could provide new promising targets for drug the discovery programs[1].

1.2 Adenosine in brain disorders

In central nervous system (CNS), adenosine plays the double role of neuro- and homeostatic modulator. The neuromodulatory effect results from a balanced activation of inhibitory A_1 receptors and facilitatory A_{2A} receptors, mostly controlling excitatory glutamatergic synapses[2]. A_1 adenosine receptor (AR) induces a tonic brake on excitatory transmission, whereas the A_{2A}AR is involved in promoting synaptic plasticity phenomena. The neuromodulatory role of adenosine is very similar to the role of adenosine in the control of brain disorders; in fact, A_1ARs mostly act as a hurdle that needs to be overcame to begin neurodegeneration and, accordingly, A_1AR only effectively control neurodegeneration if activated in the temporal vicinity of brain insults; in contrast, the blockade of A_{2A}AR leads to beneficial effects in different neurodegenerative conditions such as ischemia, epilepsy, Parkinson's or Alzheimer's disease and also seem to afford benefits in some psychiatric conditions[2]. Despite this qualitative agreement between neuromodulation and neuroprotection by A_1AR and A_{2A}AR, it is still not clear if the role of A_1AR and A_{2A}AR in the control of neuroprotection is mostly due to the control of glutamatergic transmission, or if it is instead due to the different homeostatic roles of these receptors related with the control of metabolism, of neuron–glia communication, of neuroinflammation, of neurogenesis or of the control of action of growth factors.

Althoughthis current mechanistic uncertainty, it seems evident that targeting the A_1 and A_{2A}ARs might constitute a novel strategy to control the progression of different neurological and psychiatric disorders. Based on these premises, I focused my PhD research activity on the identification of new compounds designed as antagonists of the human (h) A_{2A}AR or of both hA_1 and hA_{2A}ARs.

1.3 Adenosine

Adenosine is an endogenous purine nucleoside that plays an important role in the human body. Its existence was demonstrated for the first time in 1927 when a adenine compound able to slow the heart rhythm and rate was discovered in extracts from cardiac tissues[3]. Since then, adenosine physiopathological roles have been investigated in various disciplines (biology, physiology, medicine,) thus generating a new field of research. Fifty years later, this findings led to the introduction of adenosine in the diagnosis and treatment of supraventricular tachycardia[4,5]. At present, adenosine is known to be an ubiquitous endogenous molecule involved in several biological functions, both physiological and pathological[6,7]. These include cardiac rhythm and circulation[8,9] lipolysis[10] , renal blood flow[11,12], immune function[13] , sleep regulation[14,15] and angiogenesis[16] , as well as inflammatory diseases[17,18], ischaemia–reperfusion[19] and neurodegenerative disorders[20].

1.3.1 Origin and metabolism of adenosine

In physiological conditions, extracellular adenosine levels are between 20 and 300 nM, rising to a low micromolar values in particular situations (physical exercise or low atmospheric oxygen levels) and high micromolar levels (30 µM) in pathological conditions. The concentration of adenosine in the extracellular compartment is the consequence of biological processes such as extracellular adenosine production, adenosine transport, adenosine formation from intracellular pathways or adenosine breakdown to inosine or AMP (Figure 1). Extracellular adenosine derives from two sources. First, it may be derived from the external transport of intracellularly generated adenosine otherwise may also be formed as a consequence of extracellular hydrolysis of adenine nucleotides. In many

instances, extracellular adenosine arises from the degradation of extracellular nucleotides ATP and ADP.

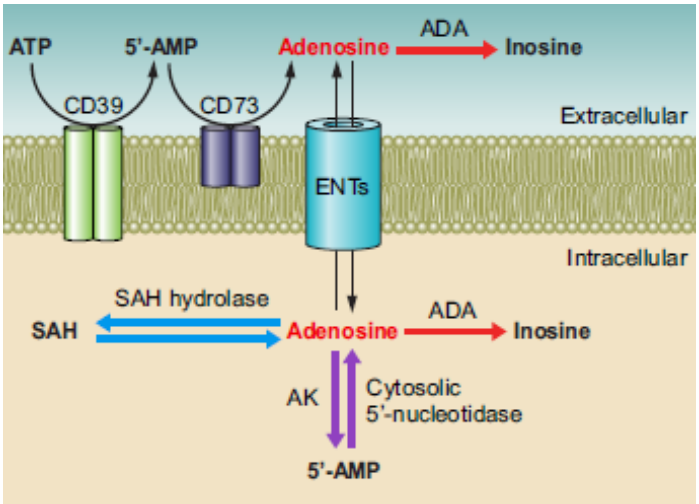

Figure 1. Adenosine metabolism and transport in the extra-intracellular milieu.[21]

In particular, adenosine originates from ATP through a two-step enzymatic reaction in which ATP or ADP are turned into AMP by ectonucleoside triphosphate diphosphohydrolase 1 (ENTPD1; also known as CD39) and followed by AMP hydrolysis to adenosine by ecto-5'-nucleotidase (NT5E; also known as CD73). ATP can be released from different cell types by various mechanisms including the releasing from storage vesicles together with other hormones but it can be also released via a 'kiss and run' mechanism[22] (a type of synaptic vesicle release where the vesicle opens and closes transiently) or from the lysosome by exocytosis[23]. The ATP is also released by mechanisms including uncontrolled leakage from necrotic cells[9] or from cells undergoing other forms of cell death[24,25] as well as release from inflammatory cells or vascular endothelia through connexin hemichannels and channels such as P2X purinergic receptor 7[26-28]. In physiological conditions, adenosine is mainly originated intracellularly, from hydrolysis of AMP and *S*-adenosylhomocysteine (SAH) through the endo-5-nucleotidase, and SAH hydrolase, respectively[29]. Also the extracellular adenosine, once generated, is captured at the intracellular level trough the SLC28 family of cation-linked concentrative nucleoside transporters (CNTs) and the SLC29 family of energy-independent, equilibrative nucleoside transporters (ENTs), which regulate the free passage of adenosine across the cell

membrane. The adenosine passage across the membrane is regulated by a concentration-dependent mechanism which suggests how the uptake or release from cells is determined by the adenosine gradient. The role of ENTs in this transfer is more important than that of CNTs, indeed, the four isoforms of ENT (1–4) allows the passage into or out of cell membranes on the basis of adenosine concentrations, while the three isoforms of CNT (1–3) facilitate adenosine influx against a concentration gradient, using the sodium ion gradient as a source of energy. Normally the adenosine flux is from the extracellular to intracellular compartment, while during hypoxia, it is reversed. After intracellular uptake, adenosine is rapidly metabolized to inosine by adenosine deaminase (ADA) or phosphorylated to AMP through adenosine kinase (AK). The Michaelis constant (K_m) values for these enzymes are 2 µM (AK) and 17–45 µM (ADA) respectively thus suggesting that AK is the principal means of adenosine clearance in physiological conditions, while deamination occurs preferentially in case of pathological processes featuring higher adenosine levels. In such situations, deamination through ecto-ADA or influx through ENTs may occur to reduce the extracellular adenosine concentration[30-32].

1.3.2 Adenosine receptors (ARs)

Adenosine mediates its effects through specific interactions with G protein-coupled receptors (GPCRs) divided into four subtypes termed A_1, A_{2A}, A_{2B}, and A_3 (ARs, Figure 2).

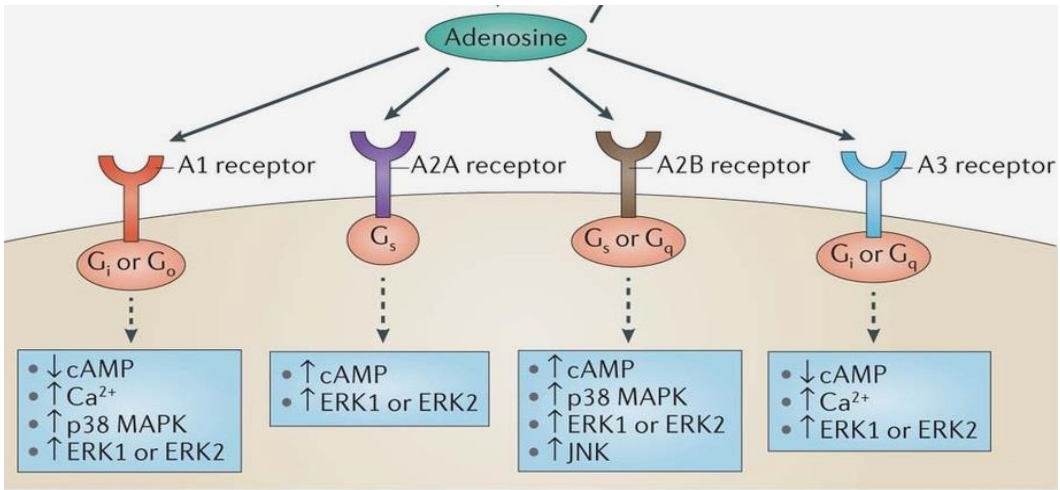

Figure 2. Adenosine receptors (ARs) and their corresponding intracellular signal pathways.[33]

ARs are widely expressed in the human body, and are present in the nervous, cardiovascular, respiratory, gastrointestinal, urogenital, and immune systems as well as in bone, joints, eyes, and skin[34]—a pattern of distribution that explains the role of adenosine in the control of a broad spectrum of physiological and pathophysiological conditions.

Each AR is characterized by specific cell and tissue distribution (Figure 3), secondary signaling transductors (Table 1), and physiological effects.

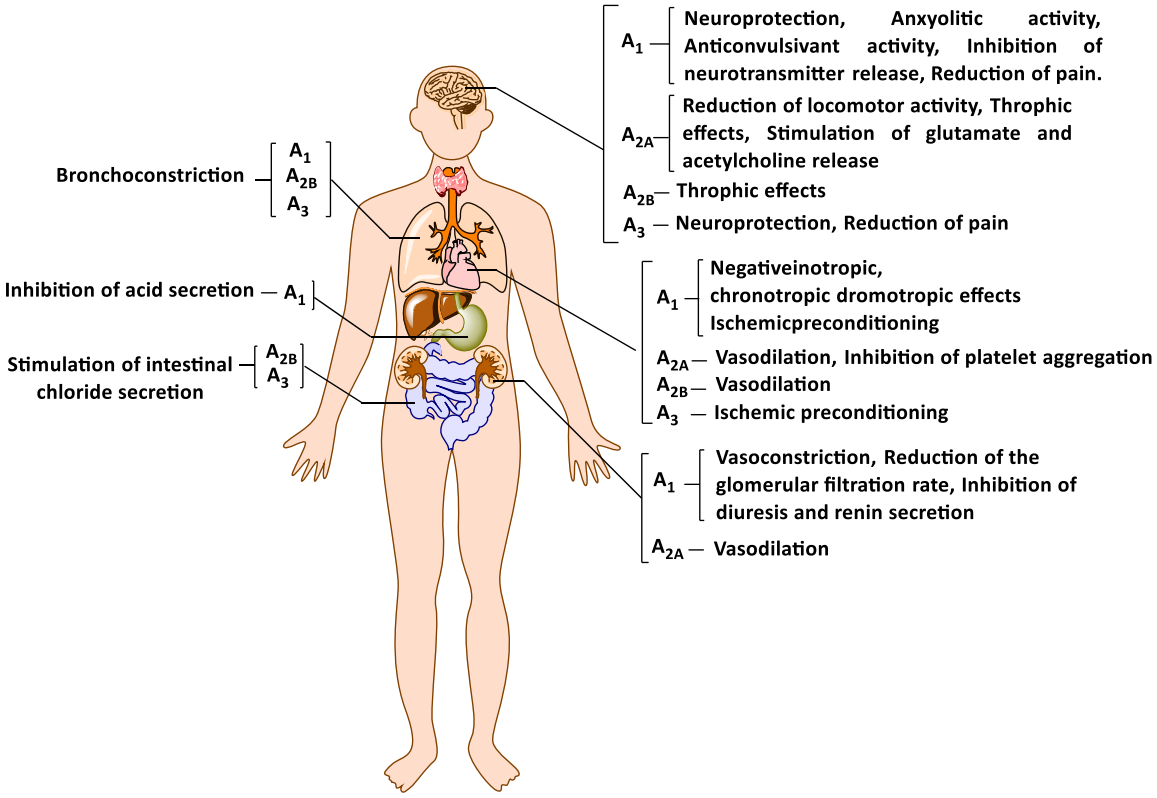

Figure 3. ARs anatomical distribution and corresponding physiological effects.

In particular, A_1AR and A_3AR signals are mediated through G_i and G_o which are able to reduce adenylyl cyclase (AC) activity and cAMP levels, while A_{2A}ARs and A_{2B}ARs are coupled to G_s proteins, through which they stimulate AC and increase cAMP levels, thus leading to the activation of a plethora of effectors, depending on the signaling triggered by cAMP in specific cells[35] (Table 1).

Table 1. Classification and mechanism of action of adenosine receptors				
Name	**A_1**	**A_{2A}**	**A_{2B}**	**A_3**
G protein coupling effector system	**$G_{i/0}$**	**G_s**	**$G_{s/q11}$**	**$G_{s/q11}$**
	Adenylyl cyclase ↓	**Adenylyl Cyclase ↑**	**Adenylyl cyclase ↑**	**Adenylyl cyclase ↓**
	Phospholipase C ↑	**MAP kinase ↑**	**Phospholipase C ↑**	**Phospholipase C ↑**
	K^+/Ca^+ ↑		**MAP kinase ↑**	**PI 3-Kinase ↑**
	PI 3-Kinase ↑			**MAP kinase ↑**
	MAP kinase ↑			
Adenosine affinity	**1-10 nM**	**0.1-1 µM**	**>10 µM**	**100 nM**

1.3.3 Adenosine receptor molecular structures

All four ARs have been well identified, cloned and pharmacologically studied, and present a common structure consisting in a core domain which crosses the plasma membrane seven times, in which each helix is 20–27 amino acids long and linked by three intracellular and three extracellular loops[36]. The extracellular amino-terminal contains one or more glycosylation sites, while the intracellular carboxylic-terminus provides sites for phosphorylation and palmitoylation thus regulating desensitization and internalization processes. The AR subtypes present different numbers of amino acids. For instance, a longer COOH terminus, with 122 amino acids, is found on A_{2A}AR, whereas A_1AR, A_{2B}AR, and A_3AR bear COOH-terminal tails consisting of ~30–40 amino acids[35]. The sequence identity between the hA_1 and hA_3 ARs is 49%, and the hA_{2A} and hA_{2B} ARs are 59% Some of these charateristic conserved residues are involved in specific functions. In particular, there are two peculiar His residues in TMs 6 and 7 of hA_1, hA_{2A}, and hA_{2B} ARs while in the hA_3 AR, one of this His residue is lacking but another His residue can be found in TM3. All this His residues have been indicated by mutagenesis studies to be important in recognition and/or activation of the receptor[35,37]. In the beginning, adenosine receptors were divided in subtypes A_1 and A_2 following their ability to increase or decrease the activity of adenylate cyclase (AC), respectively[38,39]. Then, A_2 receptors were further classified, by Daly and collaborators[40], on the basis on their affinity for the endogenous ligand adenosine, indeed, A_{2A} affinity (0.1-1 µM) is higher than and A_{2B} one (>10 µM). A_3

AR was identified fort the first time in 1991 through a polymerase chain reaction (PCR) performed on rat cDNA encoding a GPCR that showed high affinity (58%) with A_1 and A_{2A} AR[41]. This "new" receptor revealed an unconventional low homology between its homologous in other species (e.g. 72% versus rat A_3 AR) considering the other ARs (85-95 % of homology versus rat). Moreover, the presence of several GPCRs (including ARs) in homomer, oligomer or heteromer forms has been observed[42-47]. GPCR heteromers are considered to be new signaling entities characterized by different functional properties when compared with homomers. In this field, the adenosine A_1AR-A_{2A}AR unit represents the first reliable structure of a macromolecular complex, including two different receptors but also two different G proteins coupled to them[42,45]. Indeed A_1AR is coupled to G_i and A_{2A}AR to G_s, thus making this heteromer able to activate opposite signals affecting the cAMP-dependent intracellular pathway. In particular, this entity plays the role of sensor a cell surface of adenosine concentration, able to discriminate between low and high levels of nucleoside[45]. In the case of low adenosine levels, it binds preferentially the A_1AR protomer of the heteromer and activates $G_{i/o}$ protein, thus inhibiting adenylate cyclase (AC), protein kinase A (PKA), and GABA uptake. Instead, when adenosine levels are higher, its binding is favored to A_{2A}R component of the complex, which reduces A_1AR activation and, through G_s protein, associates with the AC/cAMP/PKA cascade, resulting in the increase of GABA uptake[48]. Interestingly, the heteromerization phenomenon appears as a general mechanism affecting also A_3ARs, forming homodimers and A_1AR-A_3AR heterodimers[49,50]. This opens up new perspectives in the drug development[44], in particular, A_{2A}AR-D_2 dopamine receptor heterodimers have been detected in the striatum and may be a viable therapeutic target in PD[51-53].

1.3.4 A_1 adenosine receptor

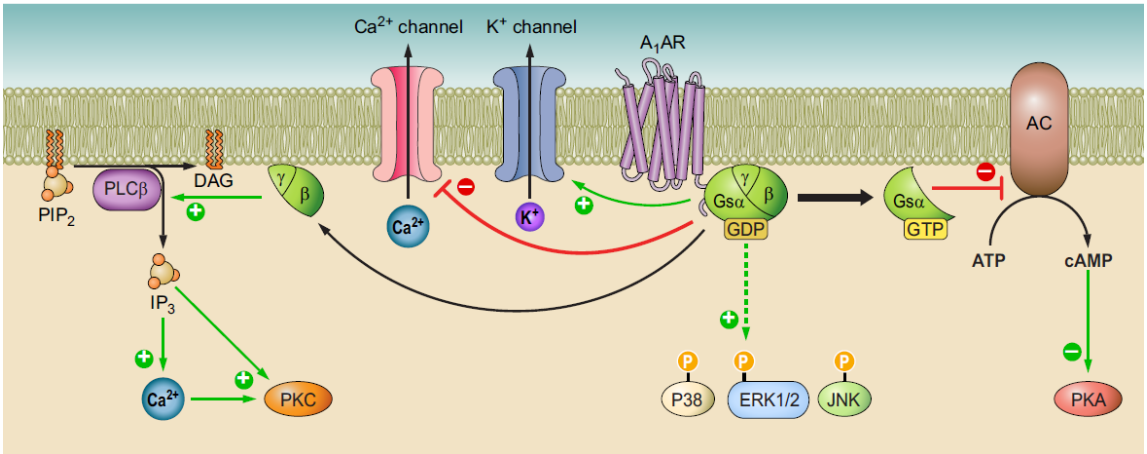

Figure 4. Overview of A_1AR intracellular signaling pathways. A_1AR stimulation decreases adenylate cyclase (AC) activity and cAMP production, thus inhibiting protein kinase A (PKA), while activated phospholipase C (PLC)-β and Ca^{2+}. K^+ and Ca^{2+} channels are opened and closed, respectively, by A_1AR enrollement. Mitogen activated protein kinases p38, ERK1/2, and JNK1/2 phosphorylation are induced by A_1AR activation.[21]

The A_1AR is expressed in the central nervous system (CNS) especially in the brain cortex, cerebellum, hippocampus, autonomic nerve terminals, spinal cord, and glial cells[29]. This broad distribution reflects the wide range of physiological functions regulated by A_1AR in the brain incuding neurotransmitter release, dampening of neuronal excitability, control of sleep/wakefulness, pain reduction, as well as sedative, anticonvulsant, anxiolytic, and locomotor depressant effects[54-56]. This subtype is also present at high levels in peripheral organs such as the heart, kidney, adipose tissue, and pancreas, where it induces negative chronotropic, inotropic, and dromotropic effects, reduces renal blood flow and renin release, and inhibits lipolysis and insulin secretion, respectively[57-63]. It is also located on airway epithelial and smooth muscle cells, where it stimulates a bronchoconstrictory response, and in several immune cells such as neutrophils, eosinophils, macrophages, and monocytes in which it modulates essentially proinflammatory effects[64-66]. A_1AR also stimulates phospholipase C (PLC)-β activation, thereby increasing inositol 1,4,5-trisphosphate (IP3) and intracellular Ca^{2+} levels, which induces calcium-dependent protein kinases (PKC) and/or other calcium-binding proteins. At the neuronal and myocardial level, A_1AR stimulates potassium (K) pertussis toxin-sensitive and K-ATP channels, while reducing Q-, P-, and N-type Ca^{2+} channels. Furthermore, involvement of A_1AR in the intracellular phosphorylative cascade of the mitogen-activated protein kinase

(MAPK) family—including extracellular signal-regulated kinase (ERK), p38, and Jun NH_2-terminal kinase (JNK)— has been reported[67,68](Figure 4).

1.3.4.1 A_1AR in neurological diseases

The A_1AR subtype is widely and homogeneously expressed in the CNS, mainly in excitatory synapses, and plays an important role in regulating the physiological synaptic transmission. In detail, A_1AR stimulation inhibits the excitatory transmission through the inhibition of N-type calcium-channel and neuronal hyperpolarization by regulation of potassium current[69,70]. This leads to a reduction in glutamate release and inhibition of NMDA effects, which maintains an A_1ARs-dependent inhibitory tonus in the brain[71-73], an effect that is beneficial in several central disfunctions such as epilepsy, pain, and cerebral ischemia[74].

- **A_1AR in epilepsy, pain and cerebral ischemia**

During investigations, adenosine proved to be an endogenous anticonvulsant molecule, able to reduce the frequency of action potentials induced by electrical stimulation through involvement of overexpressed A_1ARs[75]. Several studies have reported protection against seizures resulting from an increase in adenosine levels produced by a ketogenic diet, which apparently inhibits adenosine kinase[76] (ADK). It seems that this effect may also be related to adenosine interfering with the *S*-adenosyl methionine (SAM)-induced DNA methylation pathway— involved in epileptogenesis—as a result of ADK reduction, adenosine increase, SAH accumulation, and SAM inhibition[77]. These data constitute the rationale supporting ADK inhibitors as therapeutic agents. However, despite these may increase adenosine and reverse such epigenetic changes, their toxic side effects have not yet been overcome[78]. As an alternative, adenosine-based treatments have been proposed. For example, adenosine administration might be useful as a preventative treatment or following surgical resection of an epileptogenic focus[79].

The neuroprotective properties of A_1ARs have been investigated in several models of inflammation and neuropathic pain, in which A_1AR agonists showed antinociceptive and/or antihyperalgesic properties. A_1AR activation reduces pain by acting on spinal, supraspinal, and peripheral neurons as well as in glial cells. The molecular mechanisms involved in pain mitigation include the classical signal pathways described for A_1AR-AC

and PKA reduction; PLC induction; Ca^{2+} and K^{+} channel regulation; and ERK, CREB, calmodulin kinase (CaMKIIα) inhibition, as well as reduction of excitatory amino acid release[55]. In addition, the pathway involving the nitric oxide/cGMP/protein kinase G/KATP channel emerged as a molecular effector in the A_1AR-mediated pain suppression through induction of nociceptive neuron hyperpolarization and inhibition of microglia hyperactivation[80]. However, since the systemic administration of A_1AR agonists may lead to central and cardiovascular side effects, several candidates have failed in clinical trials. In this sense, partial agonists or allosteric modulators could represent a solution to this problem. Furthermore, the A_1AR's inhibitory effect on the glutamate release appears to be fundamental in the prevention/protection against ischemic damage. However, A_1AR only seems to be effective in the early hours after damage while the chronic stimulation is responsible for the opposite effects. Indeed, a role for A_1AR has been retrieved during preconditioning—a state of tissue protection by exposure to sublethal insults— probably occurring through modulation of NMDA preconditioning- mediated increase of glutamate uptake[81].

- **A_1AR in Alzheimer's disease**

A_1 receptors reduces the synaptic transmission and release of various neurotransmitters[82]. In the hippopcampus, adenosine inhibits the release of acetylcholine and the excitatory amino acid glutamate[82-84]. This latter and its receptors have been recognized to play a central role in the pathogenesis of AD and the dysfunction of this excitatory amino acid system may be responsible for some of the AD clinical manifestations[85,86]. Alexandre de Mendoca first described that endogenous adenosine, through A_1 receptor activation, modulates long-term synaptic plasticity phenomena, such as long-term potentiation[87] (LTP), and then showed that tonic activation of A_1 receptors decreases[88] LTP. In accordance with the notion that synaptic plasticity is the basis for learning and memory in different brain areas[89], adenosine correspondingly modulates rodent performances in various learning and memory paradigms[90]. Administration of adenosine receptor agonists (mainly A_1) disrupts learning and memory in rodents[91,92] while the nonselective adenosine receptor blockade by caffeine/theophylline or selective blockade of A_1 and A_{2A} receptors improve the performances of rodent different behavioral tasks[92,93]. A_1 receptors are highly expressed in the CA1 region of

hippocampus[94] in a normal healthy brain. A change in the pattern of A_1 receptor expression has been found in AD patients when compared with age-matched control brains[95]. Most of the studies regarding the AD models for adenosine receptors were performed in hippocampus and striatum and showed reduced levels of A_1 receptors in these areas[96]. In AD patients, a reduced density of A_1 receptors, along with reduced binding sites for adenosine agonists and antagonists, has been found in the molecular layer of the dentate gyrus. In addition, altered binding of adenosine agonists and antagonists to A_1 receptors in CA1 and CA3 regions of hippocampus has been observed[97]. Kalaria and colleagues have demonstrated that A_1 receptors are significantly reduced by 40-60% in AD after assessing the hippocampal samples collected from postmortem AD subjects as well as they observed an highest reduction of A_1 receptors in the molecular layer of the dentate gyrus including perforant pathways[98], which is the principal source of cortical input to the hippocampal formation[99]. On the contrary, Albasanz and co-workers highlighted that an upregulation of both the A_1 and A_{2A} receptors take place in frontal cortex both in early and advanced stages of AD[100], associated with sensitization of the corresponding transduction pathways. In agreement with theses results, a study carried-out in a transgenic mouse model (APP Swedish mutation) also found the higher levels of cortical A_1 and hippocampal A_{2A} receptors as compared with the non-transgenic mouse[101]. On the other hand, it is not clear if A_1 receptors influence the processes involved in the formation of abnormal APP and hyperphosphorylated tau proteins in AD patients. However, the role of A_1 receptors in APP processing, tau phosphorylation and cellular signaling has been investigated in a model of human neural cells (neuroblastoma SH-SY5Y cells) that naturally express A_1 receptors[95]. This study shows that activation of A_1 receptors led to the production of soluble APP, mediate tau phosphorylation and its translocation towards the cytoskeleton of neuroblastoma cells. A marked increase in A_1 receptor immunoreactivity was also observed in degenerating neurons with neurofibrillary tangles and in dystrophic neurites of Aβ plaques in the hippocampus and frontal cortex of AD. The positive involvement of A_1 receptors in in vitro APP processing, tau phosphorylation and the presence of A_1 receptors in the neurodegenerative structures of AD suggest that A_1 receptors may play a role in the pathogenesis of AD.

- **A_1AR in Parkinson's disease**

Regarding the involvement of A_1 adenosine receptor in Parkinson's diesease, quantitative autoradiographic studies in rodent, postmortem human brain samples[102], as well as [11C-MPDX] PET imaging in human subjects[103] highlighted that adenosine A_1 receptors are highly expressed in neocortex, hippocampus, and striatum. Based on anatomical and in vivo microdialysis studies, A_1ARs seem to be localized presynaptically of dopamine (DA) axon terminals where they reduce the DA release[104]. Futheremore it was been observed that A_1ARs blockade improves DA release in the striatum and similarly to the A_{2A} receptors, potentiate DA-mediated responses. Furthermore, the A_1 receptor is also concentrated in neocortical and limbic brain areas that are important for cognitive function and have been implicated in antidepressant action. Inhibition of A_1 receptors enhances neurotransmitter release in the hippocampus[105] and is effective in improving performance in animal models of learning and memory[106]. ASP-5854 is a dual A_{2A}/A_1 antagonist able to bind the A_{2A} and A_1 ARs with affinity values of 1.8 and 9.0 nM, respectively[107]. ASP-5854 turned out to be effective in a number of animal models of PD[108,109], and it has shown beneficial effects in two models of cognition, the scopolamine-induced memory deficits in the mouse Y-maze and the rat passive avoidance test[110]. On the contrary, the highly selective A_{2A} antagonist KW-6002 showed minimal or no effect in the same models thus indicating that the A_1 component could provide added benefit to PD patients. These data suggest that a dual A_{2A}/A_1 adenosine receptor antagonist may offer a unique and exciting approach to treating both the motor and the nonmotor disturbances of PD.

A_1 receptors play an active role in protecting astrocytes from damage and cell death[111-113] through the activation of PI3K and ERK 1/2 phosphorylation. A_1ARs on microglial cells have been demonstrated to reduce excessive activation of microglial cells following immune activation[114]. Activation of these receptors may secondarily affect oligodendroglial cells[114] and also astrocyte proliferation[115], which emphasizes the possibility of an extended glial network of signaling. A_1 receptors on neurons (especially at nerve terminals) are involved in mediating the dampening effect on neuronal activity mediated by adenosine generated from ATP released from astrocytes[116,117].

1.3.5 A_{2A} adenosine receptor

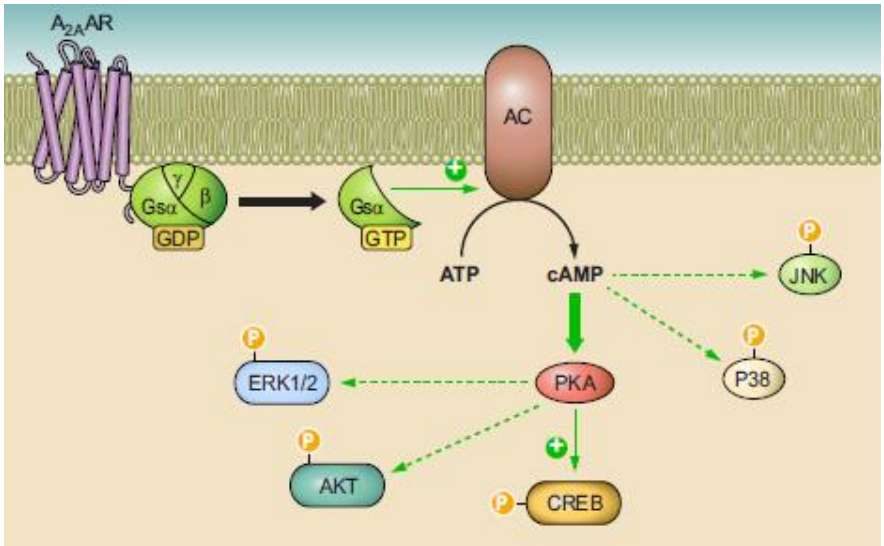

Figure 5. Overview of $A_{2A}AR$ intracellular signaling pathways. $A_{2A}AR$ stimulation increases adenylate cyclase (AC) activity, cAMP production, protein kinase A (PKA), and cAMP-responsive element-binding protein (CREB) phosphorylation. AKT and mitogen- activated protein kinases p38, ERK1/ 2 and JNK1/2 are activated following by $A_{2A}AR$ recruitment.[21]

The $A_{2A}AR$ subtype is localized both in the CNS and peripherally showing the greatest expression is in the striatum, olfactory tubercle and the immune system, while lower levels were observed in the cortex, hippocampus, heart, lung, and blood vessels. Furtheremore, $A_{2A}AR$ is expressed on both pre and postsynaptic neurons and in glial cells, astrocytes, microglia and oligodendrocytes, where it regulates several functions related to excitotoxicity, spanning neuronal glutamate release, glial reactivity, blood-brain barrier (BBB) permeability, and peripheral immune cell migration. The $A_{2A}AR$ subtype is also expressed in the immune system, in leukocytes, platelets, and the vasculature, where it mediates anti-inflammatory, antiaggregatory, and vasodilatory effects, respectively[118].

In the brain, $A_{2A}ARs$ modulate the activation of a particular neuron-specific type of G_s protein, known as G_{olf}, which is also linked to AC[119]. cAMP-dependent PKA is the most common effector raised by $A_{2A}AR$ activation; this phosphorylates and activates numerous proteins, including receptors, phosphodiesterases, cAMP-responsive element binding protein (CREB), and dopamine- and cAMP-regulated phosphoprotein (DARPP-32)[120]. Moreover, according to several literature reports on different cellular models, the $A_{2A}AR$ appears to be involved in the modulation of MAPK signaling[121,122] (Figure 5). $A_{2A}AR$ may also interact with different accessory proteins, D_2-dopamine receptors, α-actinin, ADP-

ribosylation factor nucleotide site opener (ARNO), ubiquitin-specific protease (USP4), and translin associated protein X (TRAX) through the COOH terminus, which would explain the contrasting results found in terms of A_{2A}AR-mediated effects[121].

1.3.5.1 A_{2A}AR in neurological diseases

- **A_{2A}AR in Parkinson's disease**

A_{2A}Rs are highly expressed in the basal ganglia and depend on G_s and other interacting proteins for correct transduction of their signals[123]. The striatum is the anatomical region in mammals that most strongly expresses A_{2A}Rs, which have been established to play an important role in the regulation of dopaminergic transmission in the basal ganglia[124]. A_{2A}AR are co-localized postsynaptically with D_2Rs in GABAergic striatopallidal enkephalinergic MSNs. Stimulation of the A_{2A}AR at this level counteracts the inhibitory modulation of NMDA receptor activity mediated by D_2Rs, which includes regulating Ca^{2+} influx, transition to the firing "up" state and modulation of neuronal firing in the "up" state[125,126] . This interaction is the main cause of most of the locomotor inhibition and activation induced by A_{2A}R agonists and antagonists, respectively[127]. Adenosine A_{2A}AR-mediated activity is usually antagonistic to that mediated by D_2R in MSNs and functional antagonism between A_{2A} and D_2 receptors was recently reported in striatal cholinergic interneurons[128]. Overall, adenosine-dopamine antagonism underlies the potential therapeutic benefits of A_{2A}R-selective antagonists in PD. Related to this, blockade of A_{2A} receptors showed beneficial effects in preclinical animal models of PD, showing potentiation of dopamine induced responses in dopamine 6-OHDA-treated[129,130] animals and significant relief of parkinsonian symptoms in MPTP-treated[131,132] nonhuman primates[133-135]. A_{2A} antagonists facilitate dopamine receptor signaling thus normalizing motor function in animal models of dopamine dysregulation. Despite most of adenosine A_{2A} receptors are located in the basal ganglia, some have been also found in other areas of the CNS such as the nucleus accumbens and olfactory tubercle. This suggests that adenosine A_{2A} receptors might be actively involved in the neuropsychiatric nonmotor symptoms occurring in PD including anxiety, depression, and cognitive impairment. Only little investigation was carried out about of this possibility until recently but an association with A_{2A} receptors had been demonstrated using A_{2A} receptor knock-out mice and

pharmacological manipulation of A_{2A} receptor function[136,137]. This is potentially important since the PD non-motor impairments, such as anxiety and depression, are not well controlled by classical antidepressant and anxiolytic drugs and changes in cognition only show a small improvement in response to cholinesterase inhibitors which can, in some cases, worsen motor features. Another issue to be investigated is the potential ability of A_{2A} receptor antagonists to modify and slow the disease progression. At this regard, several epidemiological studies revealed that caffeine intake is related to a decrease risk of developing PD[138]. Among its many actions, caffeine also acts as an adenosine A_{2A} receptor antagonist and this led to investigation of the potential of A_{2A} receptor manipulation as a means of controlling disease progression in PD.

- **A_{2A}AR in Alzheimer's disease**

Limited data are available about the role of A_{2A} in AD. An increased expression of A_{2A} receptors in microglial cells in the hippocampus and cerebral cortex of AD patients has been found[95]. Modulation of A_{2A} receptors could have neuroprotective effects in AD since they might interfere the pathogenesis of AD increasing the resistance of neuronal cells to insults. The main hypothesis underlyng the progressive neurodegeneration in AD is the neurotoxicity caused by Aβ[139] and current evidence favors the idea that soluble Aβ plays the pivotal role in the pathogenesis of AD. Primary cultures of cerebellar granule cells with Aβ25-35 in the presence of adenosine receptor blockers revealed that the blockade of A_{2A} receptors almost completely prevented Aβ-induced neurotoxicity[140]. So it appears that the presence of A_{2A} receptor is essential for Aβ toxicity and inhibition of this receptor might counteract the Aβ induced neurotoxicity in AD. Nevertheless, the neuroprotective mechanism of A_{2A} receptor antagonists against Aβ induced neurotoxicity is not well known. A possible explanation might be the A_{2A}AR ability to modulate neuro-inflammation by its anti-inflammatory properties[141]. Symptomatic relief from cognitive impairments in AD patients might be achieved by modulating A_{2A} receptors, in fact, these receptors are able to positively modulate the neurophysiological mechanisms of learning and memory[142,143]. Furtheremore, severeal studies highlighted the efficacy of caffeine or selective A_{2A} receptor antagonists in preventig delayed memory deficits induced by intracerebroventricular Aβ[144]. This result indicates that caffeine affords its beneficial effects through A_{2A} receptors, which were found to be overexpressed in cortical regions

both in animal models[101] as well as in cortical tissues of AD patients[95, 100]. The data collected from a recent report showed a reduction in memory loss induced by Aβ after the pharmacological blockade or genetic inactivation of A_{2A} receptors[142]. Moreover, in A_{2A} receptor knockout mice, administration of Aβ did not cause learning deficits or synaptotoxicity[145], thus proving the important role of A_{2A} receptors in cognitive function. The beneficial effects usually exerted by A_{2A} receptor antagonists have also been found in different behavioral studies in vivo.

- **A_{2A}AR in Huntington's disease**

Several studies support the hypothesis[146] that cortico-striatal glutamatergic deregulation should be involved in pathogenesis of HD. Indeed, mutated huntingtin induces glutamatergic dysfunctions such as the increased glutamate release and decreased astrocytic glutamate clearance[147,148], as well as an overexpression and activation of NMDA receptors[149] which are able to induce changes in NMDA receptor subunits[150-152]. A_{2A}AR is mainly located postsynaptically in medium spiny neurons (MSNs)[153] but it can also be found presynaptically on the cortico-striatal glutamatergic afferents[154], where it modulate glutamate release[155,156]. Besides neurons, A_{2A}R is also present in non-neuronal cells, such as endothelial and glial cells which allow a control of vasodilation and glial responses to injury and inflammation[157-159]. Several lines of evidence point towards a pathophysiologic role for adenosine A_{2A}R in HD, since changes in A_{2A}R gene expression, density and signaling, as well as early vulnerability of MSNs selectively expressing A_{2A}R, has been observed[160-163]. Moreover, recent evidence indicates that a polymorphism of the A_{2A}R gene (ADORA2A) can influence the age of onset of HD patients[164]. As reported above, continued exposure to glutamate and persistent opening of NMDA channels, make MSNs vulnerable to excitotoxic damage, in particular those expressing A_{2A}R, which receive more glutamatergic inputs from the cortex[165], further supporting a role for A_{2A}R in HD physiopathology[165]. Neuroprotective effects attributed to A_{2A}R antagonists correlate well with their ability to decrease glutamate levels by preventing[166-169] or decreasing its release and enhancing its uptake by glial cells[170-173]. A_{2A}R in glutamatergic synapses is also able to control the activation/expression of NMDA receptors[174,175], their subunit composition[176] and plastic changes in cortical glutamatergic inputs. Whereas the presynaptic role of A_{2A}R antagonists is increasingly accepted as neuroprotective, an effect mainly attributed to the modulation of

glutamatergic transmission, the postsynaptic and extra-synaptic effects of $A_{2A}R$ blockade have been speculative and most studies favor $A_{2A}R$ agonists, rather than antagonists as protective agents in the particular case of the degeneration of MSNs. These were attributed to the ability of $A_{2A}R$ antagonists to potentiate NMDA-mediated toxicity and to the ability of agonists to reduce NMDA currents in striatal MSNs[168,169,174,177,178]. Finally, $A_{2A}R$ blockade is generally accepted as a protective strategy in the control of neuroinflammation in several degenerative conditions, including HD. However, despite the established pathophysiologic role of $A_{2A}R$ in HD,further investigations areneeded to understandjjj if it is the activation or the blockade of $A_{2A}R$ that can bring about clinical benefits. The complexity of functions operated by $A_{2A}R$ in specific cellular and regional locations specifically in the striatum may suggest that neither stimulation nor blockade are beneficial or that both can be advantageous, depending on the time-frame of the disease taken into account. Thus, HD is a special case of a brain disorder where both $A_{2A}R$ agonists and antagonists have been shown to provide protection in animal models of HD.

- **A_{2A}AR in cerebral ischemia**

The role of $A_{2A}R$ in ischemic brain damage was described in parallel by the group of John Phillis and that of Ennio Ongini at Schering-Plough; they first observed that the blockade of $A_{2A}R$ afforded protection against ischemic brain damage[179-182]. This effect was then confirmed in experiments carried out by Jiang-Fan Chen, showing that the genetic elimination of $A_{2A}R$ was effective in protecting from the ischemic brain damage[183]. Subsequent investigations in different brain preparations also confirmed that the pharmacological or genetic blockade of the $A_{2A}R$ consistently decreased the infarted area and/ or the outcome (neurological score) upon ischemic insults[184-186]. Although the collected data are consistent in indicating the important role for $A_{2A}R$ in counteracting ischemia-induced brain damage, there are still open questions before to consider this receptor as a concrete therapeutic target. In fact, is not yet known the exact time window in which the A_{2A} AR manipulation might be beneficial and if its blockade might only be considered as a prophylactic strategy or if it might also have therapeutic utilities[187]. Also the comprehension of the mechanisms underlying the $A_{2A}R$ ability to control ischemic neuronal damage should be tackled to ensure a sustained translational rationale. In fact, several evidences in animal models have suggested the possible involvement of

mechanisms, either controlling glutamate release[188,189], central inflammatory processes and glial reactivity[190-192] or the permeability of the blood-brain barrier[193,194] and infiltration of peripheral myeloid cells[195]. Recent studies highlighted also that caffeine improves both the stroke recovery[196] and post-traumatic injury[197] thus suggesting to further investigate the potential therapeutic effects of $A_{2A}R$ antagonists in the regulation of the post ischemic recovery of brain function.

- **$A_{2A}AR$ in cerebral glial cells**

Many functional measurements (such as cAMP levels and cytokine release) in association with pharmacological tools have clearly shown the presence and function of $A_{2A}Rs$ in glial cells. Expression of this receptor in glial elements both the striatum and the solitary tract has been also confirmed by electron microscopic studies[198]. Under physiological conditions, the A_{2A} AR expression in microglia and astrocyte is usually low and frequently below the detection limit of histological methods (i.e., immunohistochemistry, autoradiography, or in situ hybridization)[116,199,200]. On the contrary, $A_{2A}Rs$ in glial cells is overexpressed following the brain insults as clearly shown by double immunohistochemistry analysis, in which, A_{2A} AR expression is increased in microglial cells and astrocytes of mouse substantia nigra at 24 h after 1-methyl-4-phenyl-1,2,3,6-tetrahydropyridine (MPTP) intoxication. The induction of glial $A_{2A}Rs$ by brain insults and inflammatory signals, couple with local increase in adenosine and proinflammatory cytokine levels (such as IL-1b, which further induces $A_{2A}R$ expression) and take part to an important feed-forward mechanism to locally control neuroinflammatory responses in the brain. Moreover, A_{2A} AR in glial cells might be involved in complex actions regulating neuronal cell death (both, potentially deleterious as well as neuroprotective) and possibly other functions such as modulation of synaptic transmission. In astrocytes, $A_{2A}AR$ stimulation by extracellular adenosine increases astrocyte proliferation and activation[201,202], inhibits the expression of iNOS and the production of NO[203], as well regulates glutamate efflux by astrocytes [170]. Regarding the microglial cells, activation of $A_{2A}ARs$ has mixed effects on their proliferation, but clearly shows facilitating effects on the release of cytokines, including upregulation of cyclooxygenase 2 and release of prostaglandin E2 (PGE2)[204]. The $A_{2A}R$ stimulation at this level was also observed to be

effective in increasing the nitric oxide synthase (NOS) activity and NO release[205] as well as the nerve growth factor expression[206].

1.3.5.2 A_{2A}AR in cardiovascular disorders

A_{2A}ARs are largely involved in coronary vascular control due to their expression in the smooth muscle and endothelium, where they induce vasodilation. The A_{2A}AR-mediated coronary response seems to involve PKA activation, and some studies have indicated the participation of p38 MAPK and IP3 signaling[207,208]. It has also been reported that adenosine induces the generation of large amounts of nitric oxide, a well-known vasodilator, through A_{2A}AR-mediated activation of endothelial nitric oxide synthase[209]. The cardioprotective actions of A_{2A}ARs are also related to their potent anti-inflammatory effects, and it has been proposed that A_{2A}AR stimulation results in cardioprotection by reducing neutrophil accumulation[210]. Furtheremore, A_{2A}AR overexpression has been associated with spontaneous calcium release from the sarcoplasmic reticulum in atrial fibrillation patients, and blocking A_{2A}ARs results incalcium inhibition[211]. Moreover, stimulation of A_{2A}ARs in human atrial myocytes can induce beat-to-beat irregularities in the calcium transient, thus suggests a novel role for A_{2A}AR antagonists in atrial fibrillation: maintaining uniform beat-to-beat responses at higher beating frequencies[212].

1.3.5.3 A_{2A}AR in Inflammation

A_{2A} receptor is coupled to a G_s protein and its stimulation leads to increased intracellular cAMP levels[213], which is a key regulator of immune and inflammatory responses. cAMP exerts its functions mainly through the protein kinase cAMP-dependent (PKA) that activates the nuclear substrate cAMP responsive element-binding protein (CREB) by phosphorylation at the level of Ser-133[214]. This latter binds to the nuclear co-factor CBP and to p300, and the complex in turn modulates the expression of many genes by binding to cAMP responsive elements in their promoter regions[214]. Importantly, CREB can indirectly regulate the transcription of many inflammatory genes competing with nuclear factor-κB (NF-κB)/p65 for CBP[215]. The latter is probably one of the major mechanisms by which A_{2A}R stimulation inhibits the transcriptional activity of NF-κB in a PKA/CREB-dependent manner, subsequently suppressing the expression of pro-inflammatory cytokines, such as tumour necrosis factor (TNF-α). cAMP can also activate other

substrates such as EPAC 1 (exchange protein directly activated by cAMP), altering proinflammatory genes expression[216]. Related to this, Sands and collaborators demonstrated that following $A_{2A}R$ stimulation, the accumulation of cAMP and the activation of EPAC1 in vascular endothelial cells might inhibit proinflammatory cytokines-induced Janus kinases (JAKs) and signal transducer and activator of transcription (STAT) pathways, effect related to the suppressor of cytokine signaling-3 (SOCS-3)[217,218]. Furtheremore, expression of $A_{2A}R$ was increased by lipopolysaccharide (LPS) or by inflammatory cytokines such as TNF-α and IL-1β because of the presence of putative NF-κB consensus sites in its promoter region[219-222]. Hence, during inflammatory conditions the overexpression of $A_{2A}R$ by inflammatory cytokines could imply an endogenous protective mechanism avoiding devastating effects. $A_{2A}R$ essentially suppress inflammatory and immune responses by reducing production of many pro-inflammatory cytokines from different cell types. One of the first pieces of evidence on this matter was shown by Sullivan et al who highlighted that CGS21680 inhibits TNF-α production from monocytes and macrophages in response to microbial products, such as endotoxin[223].At this regard, CGS21680-mediated effects on accumulation of pro-inflammatory cytokines, such as TNF-α and IL-12, in macrophages activated via Toll-like receptor (TLR) agonists or by cytokines, is related to cAMP-mediated inhibition of NF-κB, via inhibition of IκB phosphorylation[224]. CGS21680 have been also observed to be capable in stimulating cycloxygenase-2 expression in neutrophils thus increasing the capacity of these cells to produce prostanglandins E2, that have potent anti-inflammatory activities on leukocytes and other inflammatory cells[225-228]. Interestingly, in human neutrophils stimulated with known inflammatory agents, it has been recently demonstrated that CGS21680 and other c-AMP-elevating compounds could regulate the expression profile of many genes, encoding transcription factors, enzymes and regulatory proteins, as well as cytokines and chemokines involved in molecular signaling pathways associated with the resolution of inflammation[229].

1.3.6 A_{2B} adenosine receptor

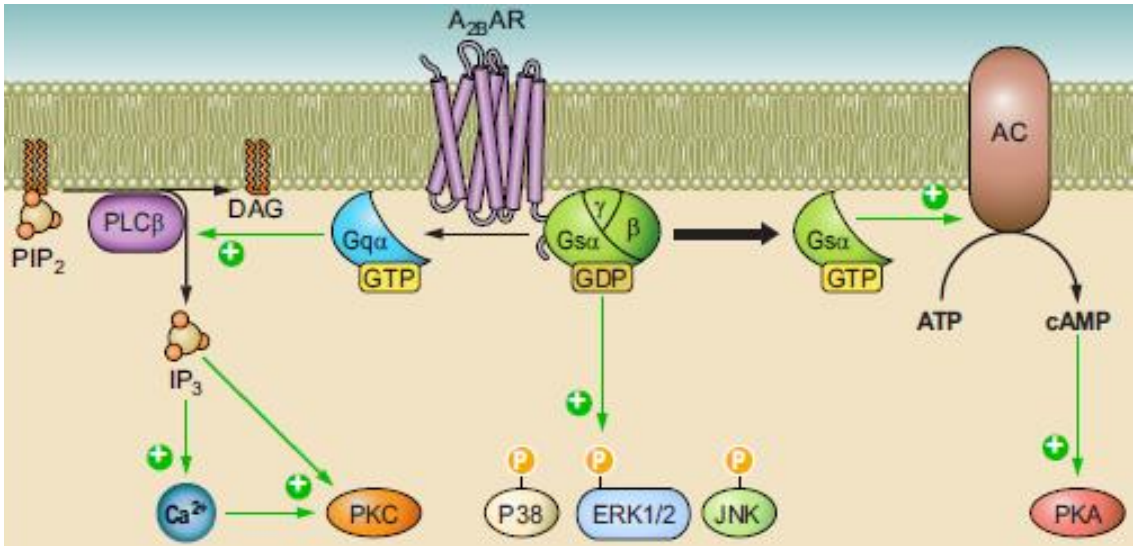

Figure 6. Overview of $A_{2B}AR$ intracellular signaling pathways. $A_{2B}AR$ stimulation increases adenylate cyclase (AC) activity, cAMP production, and protein kinase A (PKA) phosphorylation. $A_{2B}AR$ enrollement activates phospholipase C (PLC)-β and increases Ca^{2+}. Mitogen-activated protein kinases p38, ERK1/2, and JNK1/2 phosphorylation are induced by $A_{2B}AR$ activation[21].

The $A_{2B}AR$ is highly expressed essentially in peripheral organs including bowel, bladder, lung, vas deferens, and different cell types such as fibroblasts, smooth muscle, endothelial, immune, alveolar epithelial, cells, and platelets. In the CNS are found in astrocytes, neurons, and microglia[230-232]. Its expression is upregulated in different injurious conditions such as hypoxia, inflammation, and cell stress. $A_{2B}AR$ signaling pathways involve AC activation through G_s proteins, leading to PKA phosphorylation and enrollment of different cAMP-dependent effectors like exchange proteins, which are directly activated by cAMP (Epac). Moreover, $A_{2B}ARs$ can stimulate PLC through the G_q protein, resulting in Ca^{2+} mobilization, and can regulate ion channels through their βγ subunits (Figure 6). This subtype acts as stimulator of MAPK activation in several cell models in both central and peripheral systems[233]. In addition, $A_{2B}ARs$ have multiple binding partners that modulate $A_{2B}AR$ responses and functions; these include netrin-1, E3KARPP-EZRIN-PKA, SNARE, NF-κB1/ P105, and α-actinin-1. Netrin-1, the neuronal guidance molecule, induced during hypoxia, reduces inflammation by activating $A_{2B}AR$, which inhibit neutrophils migration[234]. Interestingly, binding of $A_{2B}AR$ to P105 inhibits NF-κB activity, thereby explaining its anti-inflammatory effects[235]. Furthermore, α-actinin- 1

might favor A_{2A}AR and A_{2B}AR dimerization, thus inducing A_{2B}AR expression on the cell surface[236].

1.3.6.1 A_{2B}AR in neurological diseases

A_{2B}ARs are located in the CNS and spinal cord in low concentrations, while higher levels have been observed in astrocytes, in which A_{2B}AR expression is upregulated following lipopolysaccharide (LPS) and hypoxic stimulation[237]. It has been reported that A_{2B}AR blockade in the brain inhibits the inflammatory cascade and neuronal injury following global cerebral ischemia by interfering with the p38 pathway[238]. Whatever the case, A_{2B}ARs may have a potential indirect role in hypoxia/ ischemia as a consequence of angiogenesis resulting from increased endothelial cell functions [239]. Recently, it has been shown in two different chronic pain models that A_{2B}ARs on myeloid cells contribute to pain perception by stimulating IL-6 receptor signaling and promoting immune-neuronal interactions[240]. Even more recently, secretion of IL-6 and a consequent increase in cell proliferation mediated by A_{2B}ARs and a pathway involving p38 has been observed in microglial cells, suggesting that this subtype may have a proinflammatory role[241]. However, an anti-inflammatory effect, linked to IL-10 production and TNF-α inhibition, has also been observed following the A_{2B}AR activation[242,243].

1.3.7 A_3 adenosine receptor

The A_3AR subtype expression has been found in a variety of primary cells, tissues, and cell lines. Low levels have been reported in the brain, where it is located in the thalamus, hypothalamus, hippocampus, cortex, and retinal ganglion cells, as well as at motor nerve terminals and the pial and intercerebral arteries. A_3ARs are also expressed in microglia and astrocytes, and the inhibition of a neuroinflammatory response in these cells has been associated with their induction of an analgesic effect[244]. Despite A_3AR is also known to exert cardioprotective effects, and to be greatly expressed in the coronary and carotid artery, its precise location in the heart has not yet been reported. At the peripheral level, however, A_3AR has been found in enteric neurons, as well as epithelial cells, colonic mucosa, lung parenchyma, and bronchi. Moreover, A_3AR is widely expressed in inflammatory cells like mast cells, eosinophils, neutrophils, monocytes, macrophages, foam cells, dendritic cells, lymphocytes, bone marrow cells, lymph nodes, chondrocytes,

and osteoblasts, where it regulates anti-inflammatory effects[74]. Interestingly, A_3AR is overexpressed in several cancer cells and tissues and is therefore likely to have an important antitumoral role[245].

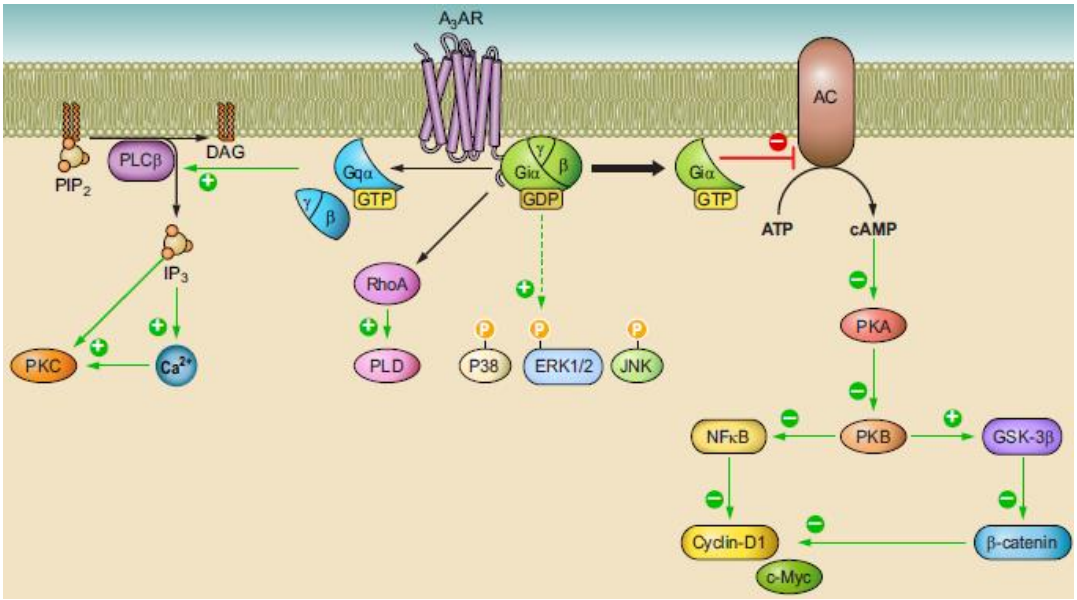

Figure 7. Overview of A_3AR intracellular signaling pathways. A_3AR stimulation triggers decrease of adenylate cyclase (AC) activity and cAMP production, activation of glycogen synthase kinase-3β (GSK-3β), and consequent decrease of β-catenin, cyclin D1, and c-Myc. Increase induced by A_3AR activation of phospholipase C (PLC)-β and Ca^{2+}, as well as of RhoA and phospholipase D (PLD) is shown. Mitogen-activated protein kinases p38, ERK1/2, and JNK1/2 phosphorylation are induced by A_3AR activation[21].

$A_{3A}Rs$ activates a variety of intracellular signaling by preferentially coupling to G_i proteins, by which they inhibit AC, and, a high concentrations of $A_{3A}R$ agonists, to G_q proteins or $G_{\beta\gamma}$ subunits, thereby inducing an increase in both PLC and calcium (Figure 7). A reduction in cAMP results in PKA inhibition, which leads to an increase in glycogen synthase kinase-3β (GSK-3β); downregulation of beta-catenin, cyclin D1, and c-Myc; and reduction of nuclear factor (NF)-κB DNA-binding ability[246]. A different pathway from GPCR signaling—involving monomeric G protein RhoA and phospholipase D—is important for A_3AR-mediated neuro- and cardioprotection. A_3ARs are also known to regulate MAPK, PI3K/Akt, and NF-κB signaling pathways, by which they exert anti-inflammatory effects. Stimulation or inhibition of HIF-1 has been also proved to have protumoral and neuromodulatory effects in cancer cells and astrocytes, respectively[245].

1.3.7.1 A_3AR in neurological diseases

Despite the A_3ARs expression in the brain is not abundant as in the periphery, these receptors are influential in some neuronal diseases. In cerebral ischemia, A_3ARs play an initial protective role in synergy with A_1ARs by inhibiting excitatory synaptic transmission. However, longer activation raises excitotoxicity and the risk of damage through the activation of PKC and consequent calcium increase. This suggests that the protective or deleterious role of A_3ARs depends on the severity and duration of the ischemic episode[247]. In addition, plastic changes in A_3ARs may occur following prolonged stimulation by both agonists and antagonists before and after ischemia/ hypoxia with similar results[248]. Specifically, A_3ARs affect glial functions by regulating cell migration and TNF-α production in microglial cells[249-251]. In astrocytes, it has been demonstrated that A_3 ARs decrease HIF-1 expression in both normoxic and hypoxic conditions thus inhibiting proinflammatory genes including those for inducible nitric oxide synthse and A_{2B}AR and suggesting an anti-inflammatory role of this AR subtype in the CNS[237]. A_3ARs involvement in pain conditions has also been investigated even if with mixed results. Despite some studies, performed with nonselective ligands as well as KO mice, have attributed them a pronociceptive function, several other studies have suggested A_3ARs as an antinociceptive drug target[252-254] . In fact, A_3ARs agonists show beneficial effects in neuropathic pain models by inhibiting the mechano-allodynia onset after chronic constriction injury and by increasing the potency of classical analgesic drugs such as morphine and gabapentin[255,256]. Interestingly, the antinociceptive activity of these agents has been demonstrated in neuropathic pain induced by chemotherapy in animal models of bone metastasis associated with breast cancer[54,244,257,258].

1.4. Adenosine receptors oligomerization

For long time, adenosine receptors have been thought to exclusively exist in a monomeric state. Monomeric receptors are sufficient to induce signaling[260-263]. At least some studies suggest signaling via dimers occurs only at higher receptor densities[263]. However, several studies highlighted that adenosine receptors can form dimeric, multimeric or oligomeric structures. Through self-association, homo-oligomers ("homomers") can be formed. Hetero-oligomerization leading to "heteromers" may be the consequence of the

association between adenosine receptors and preferred partners, preferably other GPCRs, including other adenosine receptor subtypes. This event has been observed through several experimental techniques, mostly in artificial cell lines. The use of overexpressed recombinant receptors may result in the creation of many more oligomers than naturally exist. Furthermore, GPCRs contain hydrophobic regions that can oligomerize, even after solubilization in SDS. Hence, receptor dimerization or oligomerization may occur after solubilization in detergent without being representative of receptor structure and organization in the membrane.

1.4.1 Adenosine homomers

Despite four homomeric pairs might be possible for adenosine receptors (A_1-A_1, A_{2A}-A_{2A}, A_{2B}-A_{2B}, and A_3- A_3) only experimental reports for the occurrence of A_1-A_1 and A_{2A}-A_{2A} homomers have been published.

- ***A_1-A_1***

The existence of A_1 receptor homomers were observed for the first time in 1995 by Ciruela [263] and then by Yoshioka[264] in 2002 by using (different) antibodies against the wild-type adenosine A_1 receptor and observing after the immunoprecipitation experiments, analyzed with Western blotting, the presence of higher order bands in some instances (e.g., in HEK_{293} cells expressing the human adenosine A_1 receptor, but also in brain tissues). In another study, A_1-A_1 homomers, predominantly located at the cell surface, has been identified with BiFC (Bimolecular Fluorescence Complementation) techniques in CHO cells expressing yellow fluorescent protein (YFP)-tagged receptors[265].

- ***A_{2A}-A_{2A}***

The first experimental evidence of the A_{2A}-A_{2A} homodimer existence was reported in 2004 by Canals and coworkers. The authors used both FRET (Fluorescence Resonance Energy Transfer) and BRET (Bioluminescence Resonance Energy Transfer) techniques as well as immunoblotting to show that in transfected HEK_{293} cells, overexpressed recombinant adenosine A_{2A} receptors exist as both homodimers and monomers. A_{2A} receptor homodimerization was also demonstrated by Vidi (2008) with BiFC techniques [266], who also used a combination of FRET and BiFC techniques to demonstrate that recombinant adenosine A_{2A} receptors exist as higher order oligomers, consisting of at least three

monomers, at the plasma membrane of differentiated neuronal cells[267]. In another study, recombinant A_{2A}-A_{2A} homodimers, mainly located intracellularly, were identified with BiFC techniques in CHO cells expressing YFP-tagged receptors[265].

1.4.2 Adenosine heteromers

Available evidence points to the interaction of both adenosine A_1 and A_{2A} receptors with other GPCRs, no direct data have been reported for adenosine A_{2B} and A_3 subtypes.

- **A_1-A_{2A}**

Ciruela and coworkers[155] in 2006 investigated the heteromerization of adenosine A_1 and A_{2A} receptors. The two receptors are colocalized in striatal glutamatergic terminals, both pre- and postsynaptically. This was demonstrated in immunogold blotting and, after detergent solubilization, coimmunoprecipitation experiments. In HEK293 cells transfected with suitably tagged adenosine A_1 as well as A_{2A} receptors, evidence in BRET and TR- FRET experiments was found for a direct interaction between the two recombinant receptors. The major receptor-receptor interaction found appears to be an A_{2A}R agonist produced reduction of A_1R affinity. Therefore, at high concentrations of adenosine, which can activate A_{2A}Rs, an increase of glutamate release is found. In astrocytes a similar mechanism maybe found involving A_1R-A_{2A}R heteromers which via $G_i/_o$ and G_s proteins modulate GABA transport[268,269].

- **D_2-A_{2A}**

The heteromeric couple of adenosine A_{2A} and dopamine D_2 receptor is probably the deeply studied combination. Hillion and coworkers performed double immunofluorescence experiments with confocal laser microscopy showing substantial colocalization of recombinant adenosine A_{2A} and dopamine D_2 receptors in cell membranes of SH-SY5Y human neuroblastoma cells stably transfected with human D_2 receptor as well as in cultured striatal cells (2002)[270]. Heteromerization between the two detergent-solubilized receptors was demonstrated in coimmunoprecipitation experiments, for which membrane preparations were used from D_2 receptor-transfected SH-SY5Y cells and from mouse fibroblast Ltk– cells stably transfected with the long form of the human D_2 receptor. In the latter case, the A_{2A} receptor (doubletagged with hemagglutinin) was transiently cotransfected. Similar studies were done by Kamiya et al.

(2003) in HEK293 cells[271]. Resonance energy transfer techniques (BRET and FRET) with suitably tagged receptors were used to demonstrate the same heteromerization in intact HEK293 cells[271,272]. Heteromerization seemed to be constitutive and not ligand-induced, and involved the long C-terminal tail of the adenosine A_{2A} receptor[273] , in contrast to A_{2A} receptor homomerization. Related to PD, a large wide of evidence clearly showed the important role of the A_{2A}-D_2 heteroreceptor complex in modulation of motor activity. In fact, due the allosteric receptor-receptor interactions in this complex, adenosine reduces the affinity of agonists for the D_2 receptor thus behaving as negative modulator of D_2 receptor-mediated neurotransmission[52,230,274]. In this scenario, A_{2A} AR antagonists have demonstrated therapeutic value in the treatment of PD because they potentiate dopamine D_2 receptor-mediated neurotransmission.

1.5 Adenosine receptors ligands

Several chemical methods have been applied to obtain selective agonists and antagonists for all four AR subtypes (A_1, A_{2A}, A_{2B}, and A_3). Availability of selective compounds has facilitated research on therapeutic applications of modulating ARs and in some cases has provided clinical candidates. The Prodrug approach have been also applied to improve the bioavailability of some compounds and minimize side-effects. The A_{2A} agonist regadenoson (Lexiscan®), a diagnostic drug for myocardial perfusion imaging, was the first selective AR agonist to be approved. Other selective ligands (agonists and antagonists) are or were undergoing clinical trials for a broad range of therapeutic applications, including capadenoson and tecadenoson (A_1 agonists) for atrial fibrillation, or paroxysmal supraventricular tachycardia, respectively, apadenoson and binodenoson (A_{2A} agonists) for myocardial perfusion imaging, preladenant and tozadenant (A_{2A} antagonists) for the treatment of Parkinson's disease, and CF101 and CF102 (A_3 agonists) for inflammatory diseases and cancer, respectively.

1.5.1 Adenosine receptor agonists

The structure–activity relationship (SAR) of adenosine analogues as AR agonists has been deeply investigated and almost all are purine nucleoside derivatives, either adenosine or xanthosine. One exception to this role is represented by the class of 2-aminopyridine-3,5-

dicarbonitrile derivatives that act as agonists at ARs with different degrees of subtype selectivity[275-277].

- **A_1AR selective agonists**

In general, substitution of adenosine at the N^6 -position with a wide range of alkyl, cycloalkyl, and arylalkyl groups henances selectivity for the A_1AR. In addition, any modification at the N^6-position prevents the action of adenosine deaminase, which rapidly degrades adenosine itself, in vivo. N^6-Cycloalkyl substitution has been the most successful and general means of achieving selectivity for the A_1AR. N^6-Cyclopentyladenosine (CPA) and its 2-chloro analogue (CCPA) are the most potent and selective A_1AR agonists in wide use as pharmacological agents. The bicyclic analogue S-ENBA shows subnanomolar affinity at the A_1AR with lower residual affinity than CPA or CCPA for other AR subtypes[278]. Bayer Co. (Germany) discovered 2-amino-3,5-dicyanopyridine derivatives, e.g. capadenoson, as non-nucleoside-derived adenosine receptor agonists[275,279] (Figure 8). Several A_1-selective adenosine derivatives, including, selodenoson, capadenoson, NNC-21-0136 and others have been clinically investigated for various indications (Figure 8).

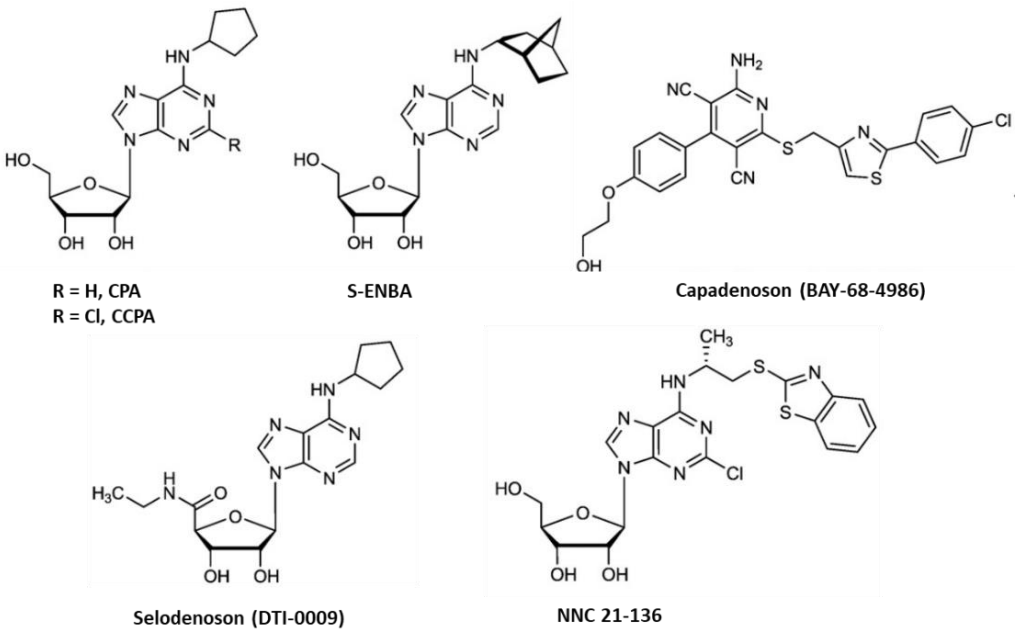

Figure 8. A_1 AR agonists.[280]

Diagnostic and therapeutic uses

A_1-selective (partial) agonists have been clinically investigated for therapeutic application in paroxysmal supraventricular tachycardia, atrial fibrillation, angina pectoris or neuropathic pain. In this sense, partial agonists are preferred to avoid receptor desensitization and to possibly achieve a certain tissue selectivity of the effects. A_1AR agonists have antiischemic effects in the heart and brain. Recently, A_1AR activation was shown to mediate neuroprotective effects through microglial cells[281]. Various A_1AR agonists have been shown to be neuroprotective in ischemic and seizure models. However, the peripheral side effects of A_1AR agonists could be severe. The A_1AR agonist NNC-21-0136 was previously in clinical development for the treatment of stroke and other neurodegenerative conditions[282]. A_1AR agonists are of interest for applications in treating cardiac arrhythmias, and recently was suggested that a partial agonist of this subtype would have advantages over a full agonist for this use[283]. The A_1AR-selective agonist selodenoson (Figure 8) has been in clinic trials for treatment of acute and chronic control of tachycardia and topical treatment of diabetic foot ulcers (Aderis Pharmaceuticals). It was formulated for intravenous administration to control heart rate during acute attacks and for oral administration in the chronic management of atrial fibrillation. The non-nucleoside AR agonist BAY 68-4986 (capadenoson) is under investigation for atrial fibrillation and for the treatment of angina.

- **A_{2A}AR selective agonists**

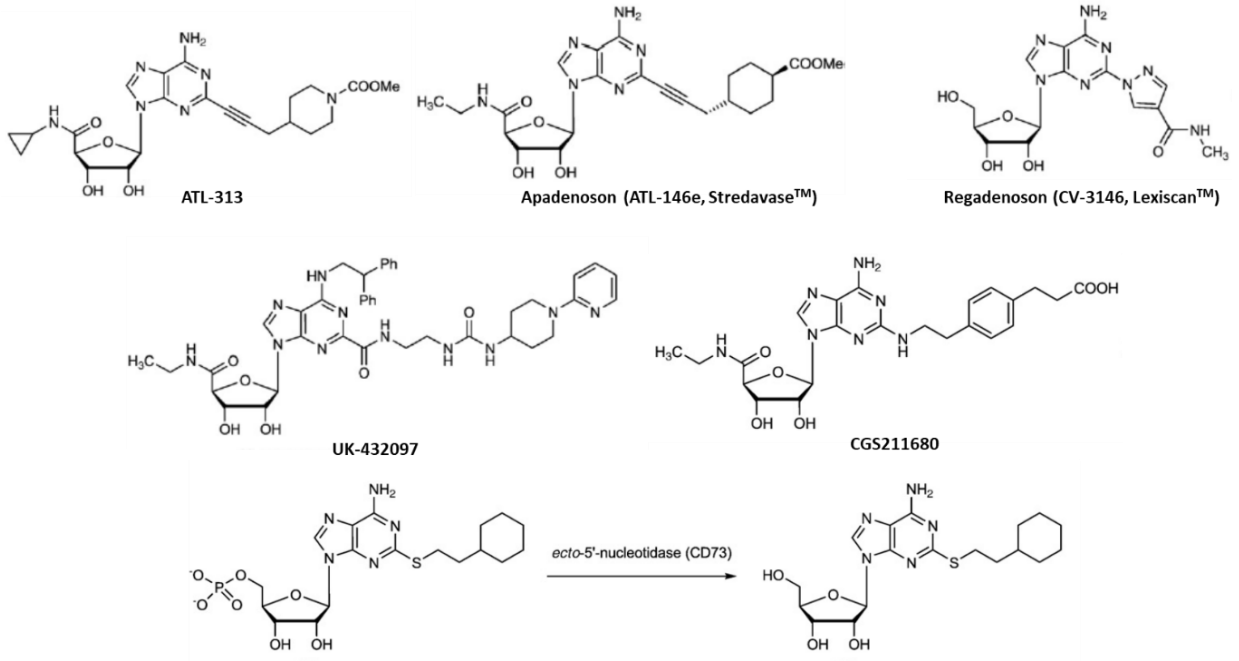

Figure 9. A_{2A} AR agonists[280].

Regarding the SARs for the A_{2A}AR agonists, introduction of (thio)ethers, secondary amines, and alkynes groups at the 2-position of adenosine enhanced A_{2A}AR selectivity in many synthetic analogues. The presence of a 5'-N-alkyluronamide modification, as found in the potent nonselective agonist NECA (5'-N-ethyluronamide), tends to maintain or enhance the selectivity for the A_{2A}AR. Also, the 2-(2-phenylethyl)amino modification of adenosine was particularly advantageous in increasing the affinity at the A_{2A}AR and is present in an extended chain in CGS21680 . In some cases also substitutions at the N^6 -position have been observed to increase the affinity at the A_{2A}AR. An example of this is the class of N^6 -(2,2-diphenylethyl)adenosine analogues, such as UK-432097. Regadenoson (Lexiscan™)[284] has been introduced as a diagnostic for stress testing due to its vasodilatatory effects, and apadenoson was developed for the same application. Several A_{2A}-selective agonists including UK-432097, sonedenoson, and binodenoson have been clinically evaluated. Unfortunately, their potent hypotensive effects following the systemic administration was the main problem associated to the application of A_{2A} agonists as anti-inflammatory agents. Recently, efforts have been undertaken to obtain A_{2A} agonists which show site-specific action. A_{2A} agonists, such as UK-432097 have been

developed for the treatment of bronchial inflammation (constructive pulmonary disease, COPD) by inhalation with limited systemic exposure[285]. As an alternative, 5'-phosphate prodrugs (Figure 9) of A_{2A} agonists have been prepared to obtain a selective cleveage and release of the A_{2A} agonist at inflammation site where ecto-5'-nucleotidase (CD73) is highly expressed[286].

Diagnostic and therapeutic uses

The 2-substituted A_{2A}AR agonist apadenoson and other analogues (binodenoson and sonedenoson, were investigated as cardiovascular clinical candidates[287-289]. Some agonists are of interest for use as vasodilatory agents in cardiac imaging (like adenosine itself, marketed as Adenoscan®) and in suppressing inflammation[290]. Regadenoson (Lexiscan®) is already approved for diagnostic imaging[291]. Two selective A_{2A} agonists developed by Adenosine Therapeutics (now Clinical Data) were selected for clinical trials as therapeutic agents for acute inflammatory conditions (ATL-1222, structure not disclosed) and ophthalmic disease (ATL-313).

1.5.2 Adenosine receptor antagonists

The prototypical AR antagonists were alkylxanthine derivatives such as the natural products caffeine and theophylline that behave as weak and nonselective AR antagonists. The structure–activity relationship (SAR) of xanthine derivatives as AR antagonists has been exhaustively investigated. The effects on the receptor subtype selectivity of substitution at the 1-, 3-, 7-, and 8-positions have been explored in detail[292]. However, several new highly selective AR antagonists are chemically diverse than the xanthines and contain non purine heterocyclic scaffolds (Figure 10-11).

- **A_1AR selective antagonists.**

Introduction of aryl or cycloalkyl groups at the 8-position of the xanthine core structure led to high affinity and selectivity for the A_1AR. For example, the 8-cyclopentyl derivative DPCPX (CPX) (Figure 10) is highly selective and showed nanomolar affinity at the rat A_1AR and is still selective, to a lesser degree, at the human A_1AR. A bicycloalkyl group is present in the 8-(3-noradamantyl) group of rolofylline[293] (KW-3902, NAX). Another 8-bicycloalkyl

xanthine analogue naxifylline (BG9719, Figure 10) was even more selective for the A_1AR, with a K_i ratio human A_{2A} /A_1 of 2400 compared with a ratio of 150 for rolofylline

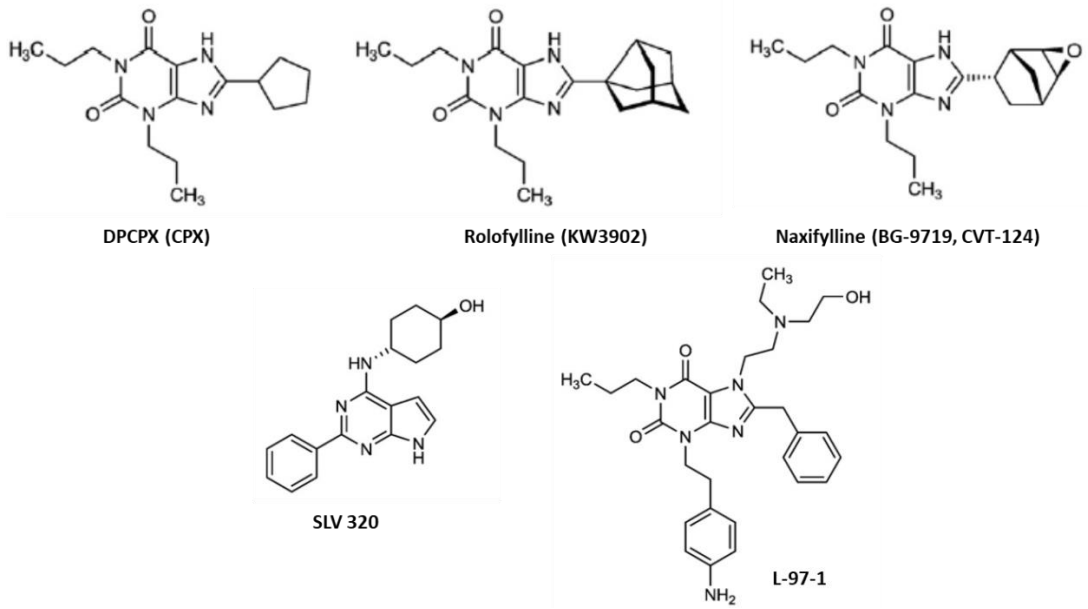

Figure 10. A_1 AR antagonists[280].

Diagnostic and therapeutic uses

Various A_1AR antagonists, xanthines and non-xanthines, have been or are currently being explored for clinical applications[294] for heart failure, and for improving renal function and treatment of acute renal failure. The 8-cyclopentyl derivative DPCPX has been in clinical trials for cystic fibrosis through a non-AR related mechanism[295] . The highly selective A_1AR antagonist L-97-1 (Endacea Inc.) is relatively well water-soluble and in late preclinical development for the treatment of asthma and sepsis[296] . Disappointedly the low water-solubility and low bioavailability of DPCPX, rolofylline, naxifylline and others has always been a problem in the development of A_1AR antagonists[297,298]; thus, A_1AR antagonists such as toponafylline and L-97-1 endowed with good water solubility are better clinical candidates. Some nonxanthine A_1AR antagonists including SLV 320[299] (Solvay Pharmaceuticals) have also been shown to have high receptor subtype selectivity. SLV 320 has been selected for clinical trials as an intravenous treatment for acute decompensated heart failure with renal impairment.

- **A_{2A}AR selective antagonists**

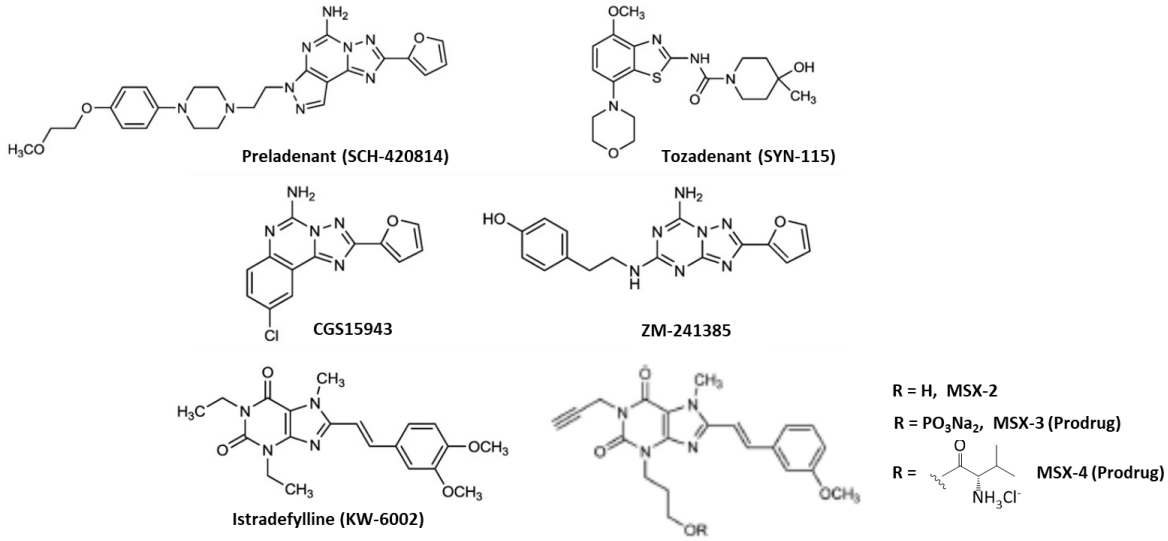

Figure 11. A_{2A} AR antagonists[280].

Recent discoveries led to the identification of new A_{2A} antagonists[300-302]. Modification of xanthines at the 8-position with alkenes (notably styryl groups) henanced the selectivity for the A_{2A}AR. The 8-styrylxanthine istradefylline was among the first A_{2A}AR antagonists reported (Figure 11). The phosphate prodrug MSX-3 and the L-valine ester prodrug MSX-4 have been synthesized to improve the water-solubility of the potent and selective A_{2A} antagonist MSX-2[303,304]. Both are now broadly used as pharmacological tools in particular for in vivo studies[305,306]. Replacement of the xanthine core with various heterocyclic ring systems has led to exceptionally high affinity and selectivity at the A_{2A}AR. The triazolotriazine ZM241385, the triazolopyrimidine vipadenant and the pyrazolotriazolopyrimidine SCH442416 (structure not reported) are examples of highly potent A_{2A}AR antagonists of later generation. ZM241385, in both tritiated and iodinated form, has been employed as a radioligand at the A_{2A}AR. SCH442416 related compounds include preladenant (SCH 420814). The latter proved to be effective in phase II clinical trials for the treatment of Parkinson's disease but it was discontinuetd in may 2013 since it showed scarse efficacy than the Placebo in phase III clinical trials. Novel A_{2A} antagonists, such as the benzothiazole derivative tozadenant (Figure 11) that are structurally neither related to xanthines nor to adenine have been identified by highthroughput screening.

Diagnostic and therapeutic uses

The well-known regulation of motor control mediated by A_{2A}Rs under conditions of dopamine depletion is solid enough to merit the clinical trials currently underway, which aim to demonstrate the therapeutic efficacy of A_{2A}R antagonists in PD. Thus far, several A_{2A}AR antagonists have been developed and brought to the clinical arena. Istradefylline is the only drug that has been approved, but only in Japan, in combination with levodopa (L-DOPA), and is currently awaiting global approval following new clinical trials performed by Kyowa Hakko Kirin. Indeed, the American Food and Drug Administration (FDA) has thus far not approved this drug, due to its lack of efficacy with respect to L-DOPA. Similarly, another A_{2A}AR antagonist, Preladenant, did not significantly decrease off-time in comparison with a placebo. Tozadenant appears more promising, and following positive results from phase IIb trials, a phase III clinical study has begun for this A_{2A}R antagonist[308]. Furthermore, a functional link between A_{2A}AR and α-synuclein (α-Syn) has recently been reported, which may open new avenues. Indeed, A_{2A}AR knockout (KO) mice prevented α-Syn-induced toxicity[309], and α-Syn aggregation and associated toxicity were reduced by A_{2A}AR blockade, suggesting a strong relationship between these two proteins, which are both harmful in PD[310]. More extensively, the involvement of aberrant A_{2A}AR signaling has been found in the pathogenesis of synucleinopathy, as its genetic deletion reduces hippocampal pathological α-Syn aggregation[311].

1.6 Oxidative Stress and Neurodegenerative Disorders

As widely known, oxygen plays a central role for the survival and normal functions of most eukaryotic organisms. Along the respiratory chain, oxygen is partially converted, at low ratio, into superoxide, a basic free radical that can generates other reactive oxygen species (ROS). Cell metabolism could generate other free radicals from nitrogen, classified into the family of reactive nitrogen species (RNS). ROS and RNS at physiological concentrations have recently been proved to regulate several normal functions, such as regulation of signal transduction, induction of mitogenic response, and involvement in defense against infectious agents, *etc.*[312]

ROS levels are under the control of antioxidant systems which are responsible for keeping their level constant in living organisms. These antioxidant systems are both enzymatic and

non-enzymatic. Breaking the balance by over production of ROS and/or reduction of antioxidants can be deleterious, and is termed oxidative stress. Under these conditions, excessive free radicals could freely pass through the plasma membrane, damaging the cell membrane via lipid peroxidation, modifying signal and structural proteins to lead to misfolding and aggregation, and oxidizing RNA/DNA to interrupt transcription thus resulting in gene mutation.

1.6.1 Reactive oxygen species (ROS)

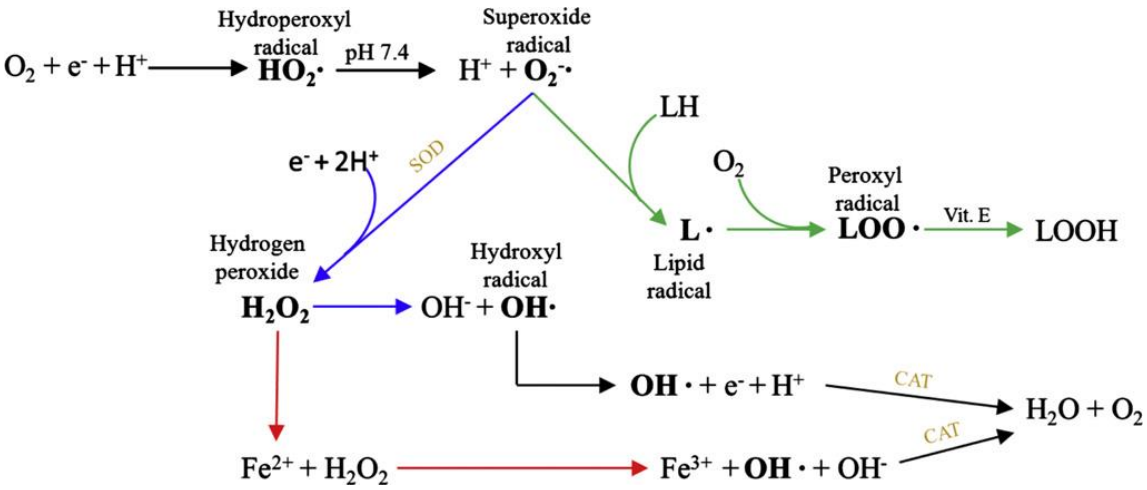

Figure 12. Overview of the reactions leading to the formation of ROS. Green arrows represent lipid peroxidation. Blue arrows represent the Haber–Weiss reactions and the red arrows represent the Fenton reactions. The bold letters represent radicals or molecules with the same behavior (H_2O_2). SOD refers to the enzyme superoxide dismutase and CAT refers to the enzyme catalase.[313]

ROS principal production sites include mitochondria, endoplasmic reticulum (ER), plasma membrane and cytoplasm. During the aerobic metabolism, the 1–2% of electrons leak from the electron transport chain and form $O_2^{\bullet-}$ by cycling the ubiquinol in the inner mitochondrial membrane. In this sense, the NADH-ubiquinone oxidoreductase (Complex I) and ubiquinol-cytochrome c oxidoreductase (Complex III) are the two enzymatic sources for $O_2^{\bullet-}$ production[314]. $O_2^{\bullet-}$ is also produced by cytochrome P450-dependent oxygenases in the ER of the liver, lung and small intestine[315,316] as well as by NADPH oxidase (Nox) of phagocytes cell membrane[317,318]. Xanthine oxidase (XO), instead, provides for the $O_2^{\bullet-}$ and H_2O_2 in the cytosol[319]. In addition, $O_2^{\bullet-}$ is generated non-enzymatically by transferring a single electron to oxygen by reduced coenzymes, prosthetic groups (e.g., flavins or iron sulfur clusters) or previously reduced xenobiotics[314].

$O_2^{\bullet-}$ is the precursor of most ROS and a mediator in oxidative chain reactions. It is spontaneously converted or catalyzed by superoxide dismutases (SOD) into H_2O_2, which is then partially reduced to $^{\bullet}OH$ in the presence of Fe^{2+} by the Fenton reaction[320]. $NO^{\bullet}$, istead, is enzymatically synthesized from L-arginine by the family of nitric oxide synthases (NOS), including neuronal NOS (nNOS), endothelial NOS (eNOS) and inducible NOS (iNOS), which are all located in the cytosol. On the contrary, mitochondrial NOS (mtNOS) and α-isoform ofnNOS, are localized in the mitochondria where NO and $O_2^{\bullet-}$ lead to the formation of $ONOO^-.NO^-$ as the result of NO reaction with Heme-Fe^{2+} while a NO^+ originates from a reaction of NO with Heme-Fe^{3+}, [321,322].

1.6.2 Antioxidant systems

ROS over-accumulation is counteracted in the body thanks to enzymatic and non-enzymatic systems. Enzymatic antioxidants are divided into primary and secondary enzymatic defences. Regarding the primary defence, it consists of three important enzymes:

- Superoxide dismutase (SOD)
- Glutathione peroxidase (GPx)
- Thioredoxin reductase (TR)
- Catalase (CAT) [10]

SOD converts $O_2^{\bullet-}$ to O_2 and H_2O_2 which is destroyed by GPx to form H_2O in the presence of the tripeptide glutathione (GSH). Thioredoxin reductase (TR) is also essential for keeping low levels of H_2O_2 by converting it into H_2O and O_2 as well[323,324]. CAT, another enzyme that converts H_2O_2 to H_2O and O_2, is present in the cells. Despite their high efficiency, the enzymatic antioxidant systems does not suffice thus forcing the human body to use non enzymatic resources able to maintain free radical at low levels. These include, ascorbic acid (vitamin C), α-tocopherol (vitamin E), glutathione (GSH) and flavonoids[325]. Ascorbic acid is effective in scavenging the superoxide radical anion, hydrogen peroxide, hydroxyl radical, singlet oxygen and reactive nitrogen oxide[326], while Vitamin E stops the lipid peroxidation by donating its phenolic hydrogen to the peroxyl radicals forming tocopheroxyl radicals that are unreactive and unable to continue the oxidative chain reaction. Vitamin E is the principal lipid-soluble antioxidant found in plasma, red cells and tissues, allowing it to protect the integrity of lipid structures, mainly membranes[327]. These two vitamins also

display a synergistic behavior with the regeneration of vitamin E through vitamin C from the tocopheroxyl radical to an intermediate form, therefore reinstating its antioxidant potential[328]. Glutathione (GSH) is an endogenous tripeptide, which is the most abundant thiol in most tissues. It plays a crucial role in the cellular protection against oxidative stress (Figure 13) being active at various different levels. In particular, it acts as a direct free radical scavenger by hydrogen atom donation, and the resulting much less reactive radicals decay bimolecularly or through an oxygen-dependent mechanism forming in both cases the GSH disulphide[329] (GSSG). Moreover, GSSG can quench radicals through electron donation by short living disulphide radical anions[330]. GSH also acts as as a hydrogen donor for several other endogenous antioxidants such as ascorbate, which in turr regenerates α -TOC[331]. In this way, GSH can potentiate the protective efficacy of a wide range of endogenous mechanisms that are active against different reactive intermediates. Flavonoids constitute the most important single group of polyphenols, acting as antioxidants by terminating free radical chain reactions. Flavonoids stop the oxidation of lipids and other molecules by the rapid donation of hydrogen atoms to radicals, becoming the phenoxy radical intermediates by themselves. However, these intermediates are relatively stable, and thus do not initiate further radical reaction. Other non-enzymatic antioxidants in the body, such as selenium, carotenoids, lipoic acid, coenzyme Q and melatonin were also recognized as nicely reported in recent reviews [325, 332].

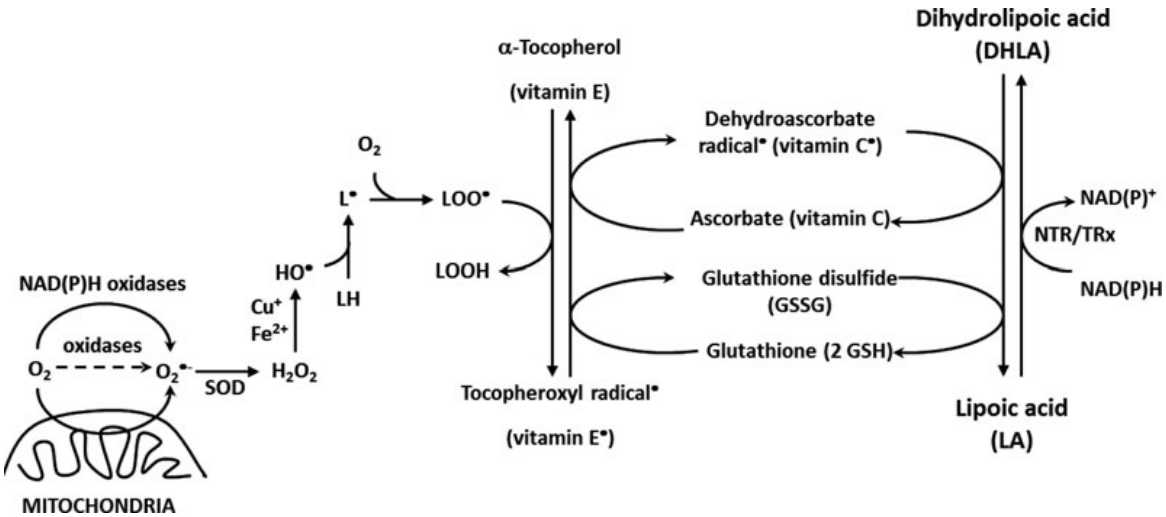

Figure 13. The pathways of the antioxidants: glutathione (GSH), Lipoic acid (LA), and dihydrolipoic acid (DHLA). LA and DHLA increase the efficiency of the vitamin C cycle and activate the vitamin E cycle. [333]

1.6.3 Other antioxidants

- **Lipoic acid**

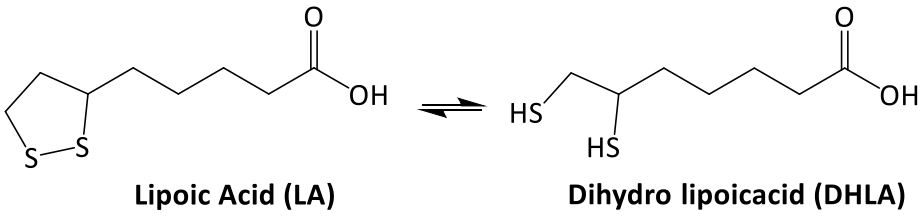

Figure 14. Chemical structure of Lipoic acid (LA) and dihydrolipoc acid (DHLA).

Lipoic acid (LA, Figure 14) is an endogen organosulfur compound that plays an essential role in the metabolism as a cofactor for several mitochondrial enzymes[334,335]. It can be synthesized by a enzymatic reaction from octanoic acid or ingested with food[336,337].LA is better known than its reduce form, dihydrolipoic acid (DHLA) and both forms have been demostrated to exert antioxidant properties[338-341]. The chemical reactivity of LA is mainly conferred by its dithiolane ring. The oxidized (LA) and reduced (DHLA) forms create a potent redox couple, in fact, it has been reported that LA/DHLA has a redox potential of −320 mV while the redox potential of GSH/oxidized glutathione is −240 mV. This difference suggests that DHLA is more effective in protecting from oxidative damage than GSH. The LA/DHLA couple has been called "universal antioxidant" since it is able to regenerate several antioxidants[333]. Furtheremore, differently from ascorbic acid DHLA is not destroyed while quenching free radicals and can be recycled from LA. Several studies higlighted that LA and DHLA are able to inactivate hydroxyl radicals, hypochlorous acid, and singlet oxygen[339]. Recently, LA and DHLA were also shown to react with peroxynitrite ($ONOO^-$), a highly reactive oxidant species resulting from the rapid reaction of nitric oxide ($^{\bullet}NO$) with superoxide anion ($O_2^{\bullet-}$), which is thought to be the main mediator of all the nitric oxide cytotoxic effects. However, Trujillo and Radi showed that the direct reaction between the LA/DHLA couple with peroxynitrite was not fast enough to be effective under in vivo conditions[342]. In addition to its ability to directly quench ROS in biological systems, LA also exerts antioxidant effects by acting on transition metal chelation. In fact, LA is a potent chelator of divalent metal ions in vitro, and forms stable complexes with Mn^{2+}, Cu^{2+}, Fe^{2+}, and Zn^{2+}. It has been demonstrated that LA had a profound dose-dependent

inhibitory effect upon Cu^{2+} -catalyzed ascorbic acid oxidation[343]. LA also inhibited Cu^{2+} catalyzed liposomal peroxidation. Futhermore, have been also reported the protective effect of R- LA on cortical iron content in aged rats with lowering age-related oxidative stress[344]. DHLA-mediated chelation of iron and copper in the brain showed also a positive effect in the pathobiology of Alzheimer's disease by lowering free radical damage[345]. Lipoic acid (LA), is used in combination with epalrestat in the treatment of diabetic peripheral neuropathy (DPN) Experimental evidences higlighted that LA enhances nerve blood flow, reduces oxidative stress, and improves distal nerve conduction[346]. A study revelead that intravenous (IV) administrations of LA (600 mg IV/day) ameliorated the symptoms of neuropathy after 3 weeks[347], with i.v. therapy being more effective than oral treatment[348] (SMD =−2.8 vs SMD =−1.8).Epalrestat is an aldose reductase inhibitor that relieves oxidative stress and suppresses the polyol pathway, which delays the progression of DPN and effectively and safely improves both diabetic neuropathy symptoms and the motor nerve conduction velocity[349-351]. Accumulating evidence has shown that LA combined with epalrestat may be a viable alternative for patients with DPN due to its marked beneficial effect on clinical symptoms and nerve conduction velocity[352].

1.6.4 Oxidative stress

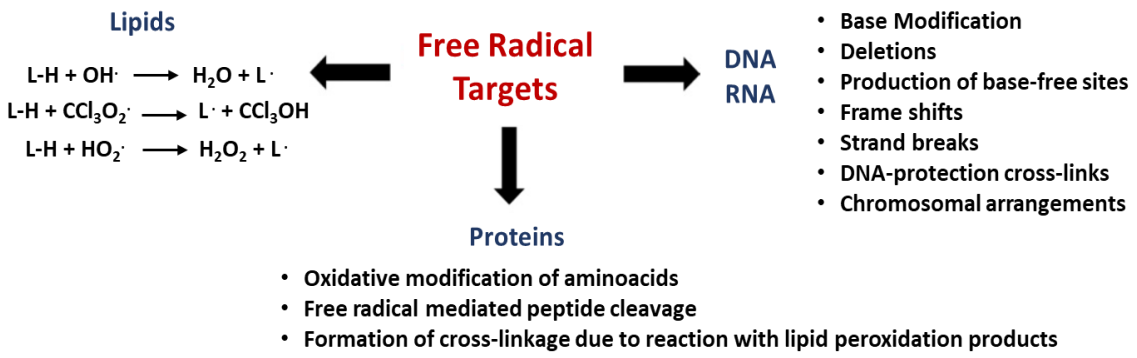

Figure 15. Targets of free radicals[313].

The equilibrium between production and neutralization of ROS is very delicate, and in the case this balance tends to a ROS overproduction, the cells start to suffer the consequences of oxidative stress[353]. Under normal conditions ROS mediate and regulate physiological functions of the body while in case of an over-accumulation they lead to severe deleterious effects for cells, tissues and organs. Oxidative stress and ROS accumulation are the result of several conditions including injury, inflammation, aging or chronic

diseases. Alternatively, their overproduction might originate from a diminished ability in the elimination of ROS. These compounds pass freely through cell and nucleus membranes, causing the oxidation of biomacromolecules such as lipids, proteins and nucleic acids (DNA and RNA) (Figure 15). The ROS-induced lipid peroxidation leads to membrane leakage[354], while oxidation of amino acids (especially cysteine residues) results in the formation of protein-protein cross-links with dysfunction of these proteins. DNA peroxidation induced by ROS interrupts gene transcription and causes gene mutations, microsatellite instability, and effects on transcription binding factor[355]. RNA is even more vulnerable to oxidative stress than DNA due to its generally single-stranded state and accessibility to the oxidant-producing mitochondria. As a consequence of these processes, high levels of ROS cause damage to various cellular components and ultimately result in cell death. ROS overproduction results in a number of chronic diseases typified by neurodegenerative diseases and also mediate therapeutic side effects, such as chemotherapy-induced neuropaty.

1.6.5 Oxidative stress and neurodegeneration

A common feature in neurodegenerative disorders is the presence of specific protein(s) including Tau and beta-amyloid (Aβ) for Alzheimer's disease (AD), alpha-synuclein (αSyn) for Parkinson's disease, mutant huntingtin protein (mHtt) for Huntington's disease, and TAR DNA binding protein (TDP-43) for Amyotrophic lateral sclerosis. ROS mediate neurotoxicity in each of these diseases through the oxidative modifications of the hallmark protein. It is well known that AD is characterized by the presence of intracellular neurofibrillary tangles (NFT) and extracellular Aβ deposits. NFT mainly consist in bundles of paired helical filaments (PHF), whose major component being the microtubule-associated protein Tau. At this regard, hyperphosphorylation appears to be the critical event in leading the Tau protein to an abnormal aggregation and alterated function and in which ROS seem to be actively involved. In AD, ROS can also activate the c-Jun *N*-terminal kinases (JNK), p38 and deactivate protein phosphatase 2A (PP2A). JNK and p38 promote the expression of Tau, and stimulate AβPP cleaving enzyme 1 (BACE1), causing Aβ1-42 accumulation which leads to activation of NADPH oxidase (Nox) and producion of additional $O_2^{\bullet-}$, and results in Ca^{2+} influx to elicit excitatory neurotoxicity. Once phosphorylated, Tau and other cytoskeletal proteins are subject of modification by

carbonyl products of oxidative stress[356,357] and consequent aggregation into fibrils[356]. Furtheremore, Aβ presence in senile plaques is considered to have a causal role in AD and related to this H_2O_2 at 100–250 μM results in increased levels of intracellular Aβ in human neuroblastoma SH-SY5Y cells[358]. Oxidative stress have been also demonstrated to induce accumulation of potentially neurotoxic Aβ peptide by inducing the amyloidogenic process of AβPP and increasing the activity of β-secretase[359,360]. Cerebral amyloid angiopathy is associated with most cases of AD and characterized by Aβ deposits in brain vessels[361]. Oxidative stress is found triggering the amyloidogenic pathway in human vascular smooth muscle cells by up-regulation of AβPP cleaving enzyme 1 (BACE1) expression and secretion of Aβ1–40 and Aβ1–42 with mediation of c-Jun *N*-terminal Kinase and p38 MAPK[362]. Oxidative stress plays also a central role in the protein aggregation mechanism in PD. Post translational modifications of the αSyn induced by oxidative stress, including those by 4-hydroxy-2-nonenal (HNE-αSyn), nitration (n-αSyn), and oxidation (o-αSyn), have been observed in αSyn oligomerization. Especially the HNE-αSyn and n-αSyn tend to be more inclined in forming oligomers than the unmodified one. The cellular toxicity of HNE-αSyn is significantly higher than other postranslationally modified species[363]. Related to HD, the mHtt aggregation is actively involved in the pathogenesis of the disease. The mHtt can aggregate at distinctive conformations that have different neurotoxicity, and different conformations of mHtt exist in different brain regions in HD mice[364]. Oxidative modification of the aggregated mHtt facilitates an increase in the size of aggregates and changes the conformation of aggregated mHtt[365]. Furtheremore, oxidative stimulations have been found to enhance the polyglutamine-expanded truncated *N*-terminal Huntingtin aggregation and mHtt-induced cell death[366].

1.6.6 Oxidative stress and neuropatic pain

Neuropathic pain (NP) is a common and unique type of chronic pain. In developed countries, about the 3% of the population suffer from NP. It manifests as spontaneous burning, shooting pain, hyperalgesia and in most patients is usually chronic. This condition is the result of several factors with impairment in nerve function. The pathophysiology is relatively complex and involves both central and peripheral mechanisms with alteration in the ion channel expression, neurotransmitter release, and pain pathways are involved in the pathophysiology of pain[367]. Although infomations on molecular basis of the

neuropathy are insufficient, it has been reported that oxidative stress might contribute to the pathophysiology of NP[368]. In fact, in chronic constriction injury (CCI) model of rat neuropathic pain, heat hyperalgesia was reduced by systemically injections of antioxidants[369,370]. Another study, in spinal nerve ligation (SNL) model of neuropathic pain, showed that systemic administration of ROS scavenger phenyl-N-tert-butylnitrone (PBN) relieved mechanical allodynia[371]. Furthermore, increased levels of the antioxidant enzyme SOD together with a reduction in the concentration of the ROS-scavenger glutathione have also been observed in the CCI model of rat neuropathic pain[372]. In addition to this, beneficial effects in reliefing the hyperalgesia in CCI-induced neuropathic rats was demonstrated after the intraperitoneal administration of the antioxidant N-acetyl-cysteine[372].

Neuropathy is a commonly found condition with the oxaliplatin anticancer treatment. In fact, patiens treated with oxaliplatin tend to develop a neuropathic syndrome with paresthesia, dysesthesia, and pain adversely affecting the quality of the daily life until suspension of the therapy[373]. At this regard, in a rat model of painful oxaliplatin-induced neuropathy an important component of oxidative stress have been observed[374]. Furtheremore, high levels levels of carbonylated protein and thiobarbituric acid reactive substances in the plasma of oxaliplatin-treated rats are index of the resultant protein oxidation and lipoperoxidation, respectively. The same pattern of oxidation was revealed also in the sciatic nerve, and in the spinal cord where the damage reached the DNA level[374]. Treatment with the antioxidant derivatives silibinin and α-tocopherol (100 $mgkg^{-1}$ per os) proved to be effective in preventing oxidative damage and reducing oxaliplatin-dependent pain induced by mechanical and thermal stimuli. These compounds have been also demostrated to improve motor coordination and reverse about 50% of the oxaliplatin-induced behavioral alterations[374]

2. AIM OF THE WORK

Adenosine elicits its physiological effects interacting with four receptor subtypes, whose activation mediate many physiophatological functions. Among adenosine receptors, the A_{2A} subtype have attracted much interest as druggable target for therapeutic intervention in neurodegenerative diseases[95,101,124,163]. The A_{2A}AR is widely expressed in the CNS and is involved in the control of motor activity, learning, memory[90, 375-377] and in excitotoxicity[176,378]. Blockade of A_{2A}ARs may be useful in brain disorders such as Parkinson's disease (PD)[53,379], cerebral ischemia[232,380,381], Huntington's disease[176,378](HD), or Alzheimer's disease[382,383] (AD) and also affords benefits in some psychiatric disorders[142]. Thus, identification of new A_{2A} AR antagonists remains an attractive goal in drug discovery. Also the A_{2A}/A_1 AR dual targeted antagonism have emerged as promising therapeutic approach for the treatment of PD[107,109,384]. A_1 ARs are presinaptically expressed on striatal dopaminergic neurons where they inhibit dopamine release[385,386]. Hence, A_1/A_{2A} AR antagonists would both facilitate dopamine release (A_1) and potentiate the post-synaptic response to dopamine (A_{2A}). A_1 AR are also located in the hippocampus, neocortex and limbic system which are brain areas implicated in the control of cognitive and emotive functions[6]. Thus, A_1 AR antagonists could ameliorate cognitive impairments associated to PD since they improve performance in animal model of learning and memory[109,384].

The research group I joined has been interested for years in the design, synthesis and pharmacological evaluation of heterocycle derivatives as adenosine receptor antagonists. In searching for a new byciclic chemotype to obtain selective hA_{2A} AR antagonists, a molecular simplification approach was applied to the 1,2,4-triazolo[4,3-*a*]quinoxaline-1-one scaffold (Figure 16), successfully employed in the past to synthesize potent and selective antagonists of A_1, A_{2A} and A_3 ARs[387-391]. Thus, the 8-amino-1,2,4-triazolo[4,3-*a*]-pyrazine-3-ones series was designed, also considering that its synthetic accessibility would have permitted to functionalize the 6 position with different moieties (methyl, aryl, arylalkyl, heteroaryl) and the 2 position with suitable aryl and benzyl groups.

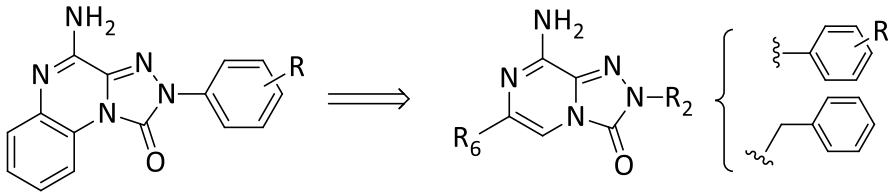

1,2,4-triazolo[4,3-*a*]quinoxalin-1-ones TQX series **1,2,4-triazolo[4,3-*a*]pirazin-3-ones**

1-86 { R = H, OCH_3, OH, NO_2, NH_2 ; R_6 = CH_3, Arylalkyl, Aryl, Heteroaryl }

Figure 16. Molecular simplification of 1,2,4-triazolo[4,3-*a*]quinoxaline-1-one scaffold to obtain the new 8-amino-1,2,4-triazolo[4,3-*a*]-pyrazin-3-ones series.

Hence, this PhD thesis focused on the identification of new compounds designed to target the $hA_{2A}AR$, or both the hA_1 and hA_{2A} ARs, and based on the 8-amino-1,2,4-triazolo[4,3-*a*]pyrazin-3-one scaffold (Figure 16).

2.1 Preliminary structure-affinity relationship investigations: synthesis of 8-amino-2-aryl-1,2,4-triazolo[4,3-*a*]pyrazin-3-ones 1-10

The first aim of the work was the synthesis of compounds **1-10** (Figure 17) to carry out a preliminar SAR study. Hence, a methyl and the bulkier and more lipophilic phenyl moiety were appended at the 6-position (R_6), while different small subtituents (R), endowed with different electronic and lipophilic properties, were placed on the 2-phenyl ring. The R groups were also selected as suggested by the affinity data of the TQX series[387]. Anticipating the obtained binding activities, it was observed that the phenyl was better than the methyl group for the 6-position, while the unsubstituted phenyl ring at position 2 emerged as the best group for obtaining an efficient hA_{2A} receptor interaction.

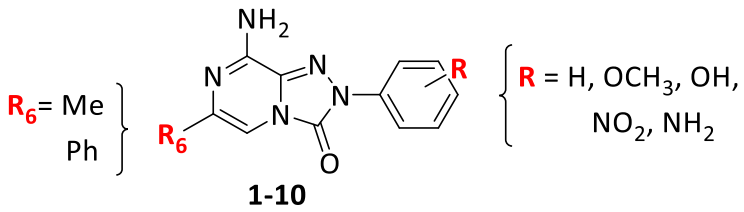

Figure 17. Modifications performed on the 2-phenyl and at the 6-position of the 8-amino-1,2,4-triazolo[4,3-*a*]-pyrazin-3-one scaffold.

The 2,6-diphenyl substituted compound **2** was the most notable within the first set of synthesized compounds, possessing nanomolar for hA_1, hA_{2A} and hA_3 ARs (K_i = 10-13 nM).

Based on these premises, in the subsequent derivatives, the 2-phenyl was maintained unmodified while structural changes were made at the 6-phenyl level.

2.2 Structural modifications on the 6-phenyl ring: synthesis of 8-amino-6-aryl-2-phenyl-1,2,4-triazolo[4,3-*a*]pyrazin-3-ones 11-39

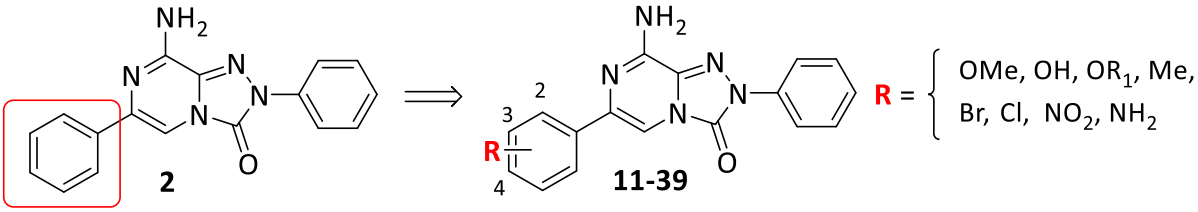

Figure 18. Modifications on the 6-phenyl ring of the 8-amino-2-phenyl -1,2,4-triazolo[4,3-*a*]-pyrazin-3-one scaffold.

The subsequent modifications were carried out on the 6 phenyl ring of derivative **2**, where substituents with different lipophilicity, electronic and steric properties (OR_1, NO_2, NH_2, Br, Cl, Me) were introduced at 2, 3 and 4 positions (Figure 18). In particular, several alkoxy moieties, containing either linear, unsaturated, branched or cyclic alkyl and benzyl chains (compounds **18**-**28**) were investigated at position 3 and 4. Introduction of hindering moieties was performed taking into account the SARs of different series of hA_{2A} AR antagonists with similar size and shape, indicating that the presence of bulky substituents at suitable positions was often profitable for an effective and selective recognition of the hA_{2A} AR[380].

2.3 Structural modifications to improve drug-like properties: synthesis of 8-amino-1,2,4-triazolo[4,3-*a*]pyrazin-3-ones 40-61 and 62-68

To expand SAR studies and especially to ameliorate the drug-like properties of these AR antagonists, a third set of compounds was designed and synthesized by derivatization of the $-NH_2$ and -OH functions of the previously obtained derivatives **16**, **37**-**39**.

First, hydrophilic substituents were used to decorate some triazolopyrazines (**40**-**51**, Figure 19). In particular, substituted piperazine rings were introduced at the ortho, meta and para position of the 6-phenyl ring (compounds **40**-**45**). Furthermore, substituted piperidine, pyrrolidine and morpholine moieties were appended at the para position of the 6-phenyl ring by using different length linkers (derivatives **52**-**61,** Figure 19) endowed

with diverse flexibility. These basic moieties were selected since they are a common feature of known potent and selective hA_{2A} AR antagonists[380] and are known to improve the drug-like properties of the compounds.

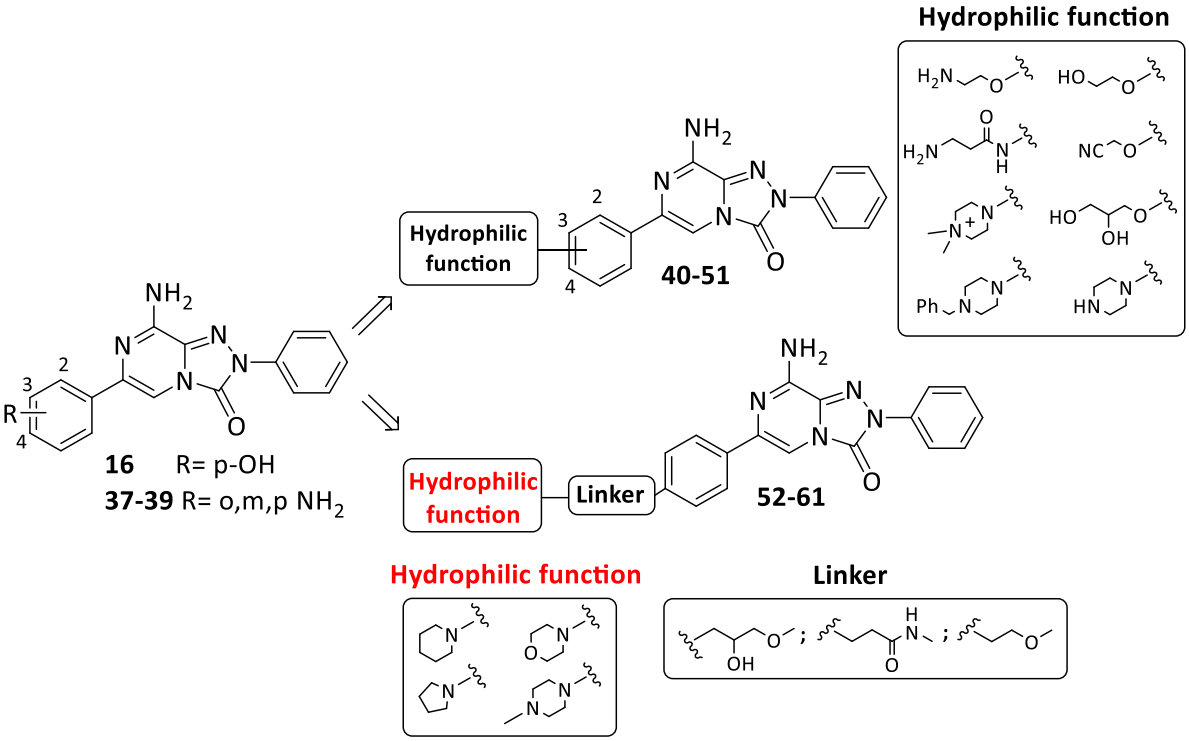

Figure 19. Introduction of hydrophilic and/or basic moieties at the 6-phenyl level to improve drug-like properties.

Next, the 6-phenyl ring of compound **2** was replaced with heteroaryl groups (2-furyl, 2-(5-methylfuryl), 2-thienyl and 2-pyridyl) which were thought to enhance compound solubility (compounds **62-65,** Figure 20). Derivatives **66-68** (Figure 20) featuring a benzyl chain at position 2, combined with a phenyl, a 2-furyl and a 2-(5-methylfuryl) at position 6, were synthesized because the benzyl pendant, being more flexible than the 2-phenyl moiety, was thought to improve the solubility of the compounds. Combination of a benzyl with a 2-furyl substituent was also suggested by the binding results previously obtained in our pyrazolopyrimidine series[392] in which this type of decoration shifted affinity toward the hA_{2A} AR.

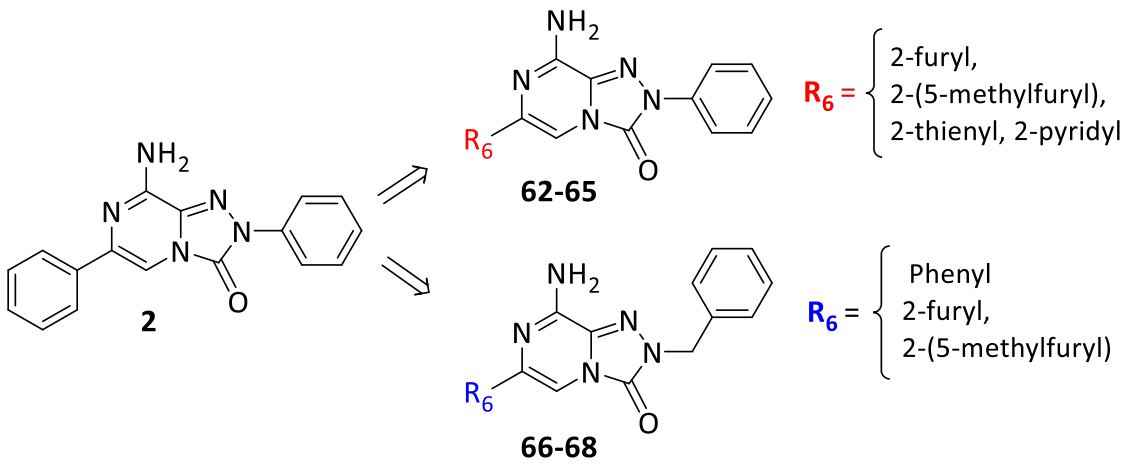

Figure 20. Introduction of heterocyclic moieties at the 6-position and of a benzyl pendant at position -2 of the 8-amino-1,2,4-triazolo[4,3-*a*]-pyrazin-3-one scaffold (compounds **62**-**68**)

2.4 Design of dual hA_{2A} AR antagonists-antioxidants: synthesis of 8-amino-6-aryl-2-phenyl-1,2,4-triazolo[4,3-*a*]pyrazin-3-ones 74-86.

Finally, a set of triazolopyrazines bearing a potential antioxidant function (compounds **74-86**) were designed because we envisaged as an attractive aim to combine in the same molecule the ability of blocking the hA_{2A} AR and that of counteracting oxidative stress and ROS formation, the latter processes being among the main causes of cellular and neuronal degeneration. The oxidative stress state is a condition in which antioxidant defenses are overwhelmed and not able to protect cells from oxidative damage. With this in mind, substituted phenolic residues were placed at the 6-position of the bicyclic scaffold (compounds **74**-**78,** Figure 21).

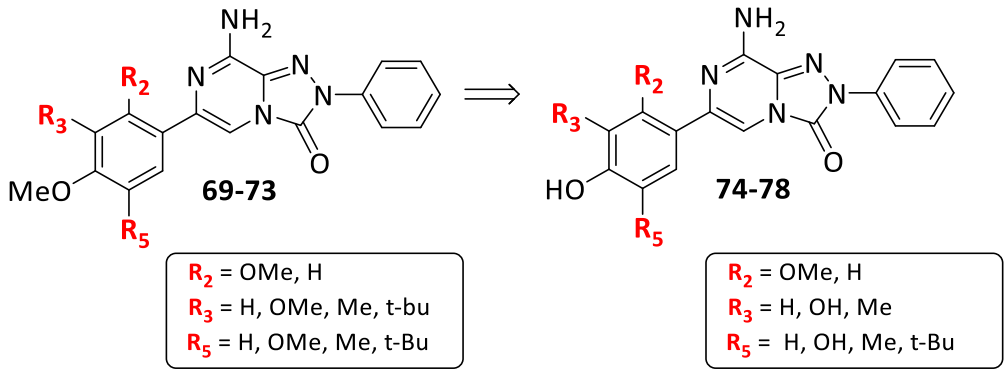

Figure 21. Newly synthesized 8-amino-2-phenyl-1,2,4-triazolo[4,3-*a*]-pyrazin-3-ones featuring substituted phenol moieties at the 6-position

The choice of these 6-substituents ensued from the evidence that substituted phenolic compounds, together with polyphenolic rings, are a common feature of both natural and synthetic antioxidant compounds. At this regard, the phenolic endogenous antioxidant α-tocopherol (Vitamin E), as well as natural phenolic acids such as hydroxycinnamic and hydroxybenzoic acids, deserve to be mentioned. These latter exert antioxidant activity as chelators and free radical scavengers with special impact over hydroxyl and peroxyl radicals, superoxide anions and peroxynitrites[393,394]. As synthetic antioxidant compounds, butylhydroxytoluene (BHT), butylhydroxyanisole (BHA) and tert-butylhydroquinone (TBHQ) can be mentioned. With regard to BHT, it is a well known antioxidant used for several products including food, pharmaceuticals *etc*[395]. Moreover, several studies indicated that compounds containing di-tert-butylphenol groups exert several biological functions including antioxidant, anti-inflammatory, anticancer activities[396-399].

Other groups, thought to exert antioxidant properties, were selected and appended, directly or through spacers, to the para-OH and para-NH_2 function of derivatives **16** and **39**, respectively, to provide compounds **79-86** (Figure 22).

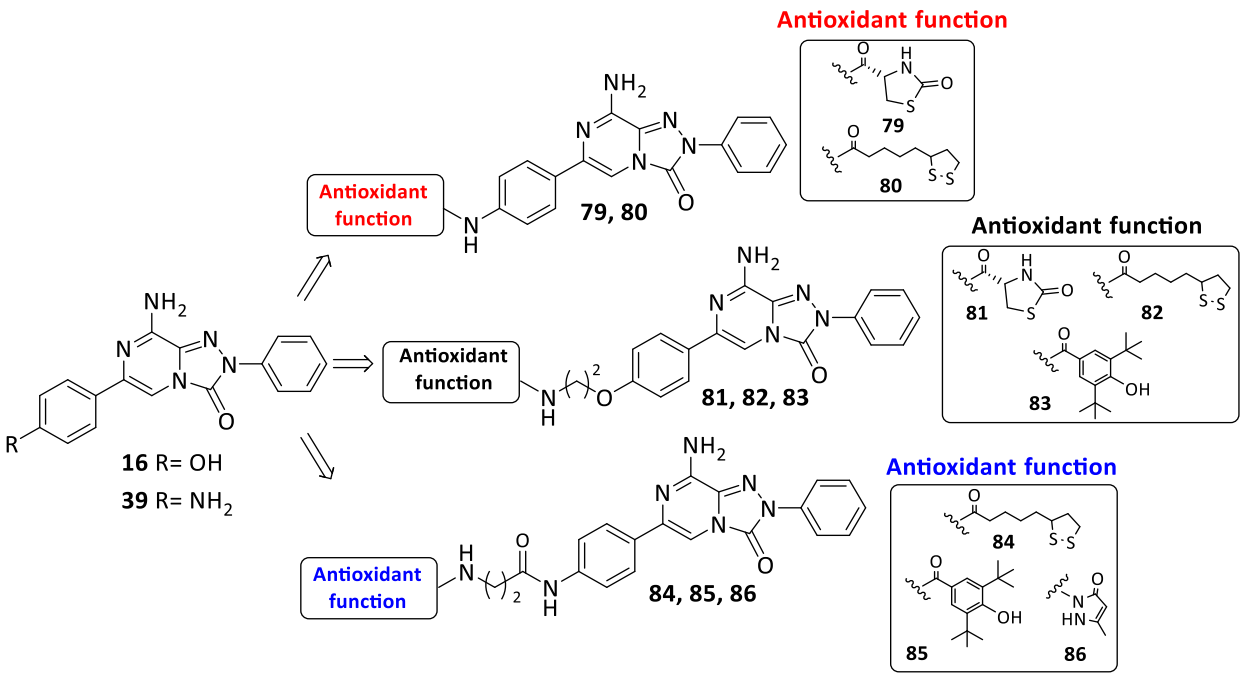

Figure 22. Introduction of potential antioxidant moieties at 6-phenyl level of the 8-amino-2-phenyl -1,2,4-triazolo[4,3-*a*]-pyrazin-3-one scaffold.

The antioxidant lipoic acid (LA) residue (compounds **80**, **82**, **84**) was selected since LA turned out to be effective in scavenging free radicals in polar media by a one-electron transfer mechanism[333] and also exerts antioxidant effects by acting on transition metal

chelation[333]. There are also evidences, from both in vitro and physiological studies, that LA increases or maintains cellular GSH levels by acting as a transcriptional inducer of genes governing GSH synthesis[400] (see "Introduction").

The (S)-2-oxothiazolidine-4-carboxylic acid residue (OTC, derivative **79, 81**), together with the 3,5-di-tert-butyl-4-hydroxybenzoic acid (compounds **83**, **85**) and the 5-methyl-1,2-dihydro-3H-pyrazol-3-one (compound **86**) moiety, were also chosen for the ibridization approach. OTC is a prodrug of cysteine which acts as antioxidant since it is able to inactivate the hydroxyl radicals[401] or maintain free sulfhydryl groups[402]. Introduction of the 3,5-di-tert-butyl-4-hydroxybenzoic acid residue was undertaken due to its structural similarity to the butylhydroxytoluene (BHT, see above) which is able to break radical chain reactions through atom transfer[403]. Instead, the 5-methyl-1,2-dihydro-3H-pyrazol-3-one ring was selected since it plays a key role in the antioxidant mechanism of edaravone, an approved drug for brain ischemia[404] which turned out to to be effective also in counteracting the myocardial ischemic insult[405]. Edaravone can exist in three tautomeric forms **A**, **B**, **C**[406-408] (Figure 23) and it is currently accepted that the anionic form is very effective in scavenging free radicals in polar media by a one-electron transfer mechanism[409] (Figure 23, pathway A).

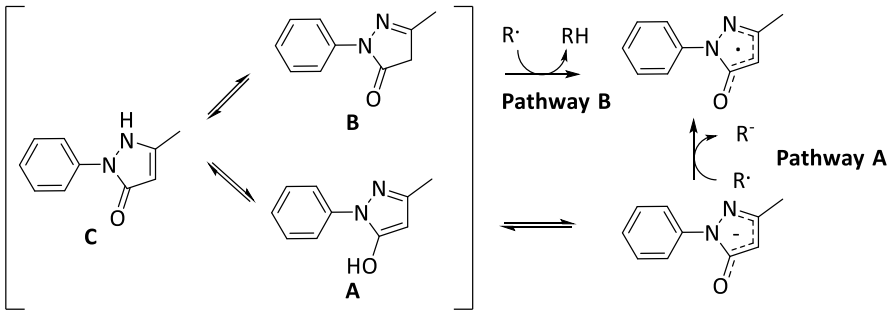

Figure 23. Edaravone antioxidant mechanism of action.

All the synthesized 8-amino-1,2,4-triazolo[4,3-*a*]pyrazin-3-ones **1-86** were investigated for their affinity and selectivity at hARs. Based on the binding data, some of the compounds endowed with the highest affinities at the hA_1 and hA_{2A} subtypes (**13**, **31**, **32**, **68, 47**, **78**, **82**, **84** and **85**) were selected to determine their antagonistic properties by evaluating their effect on cAMP production in CHO cells, stably expressing the hA_1 and

hA_{2A} ARs. The same derivatives were further pharmacologically profiled to evaluate their potential protective effects in vitro models of neuroprotection.

3. CHEMISTRY

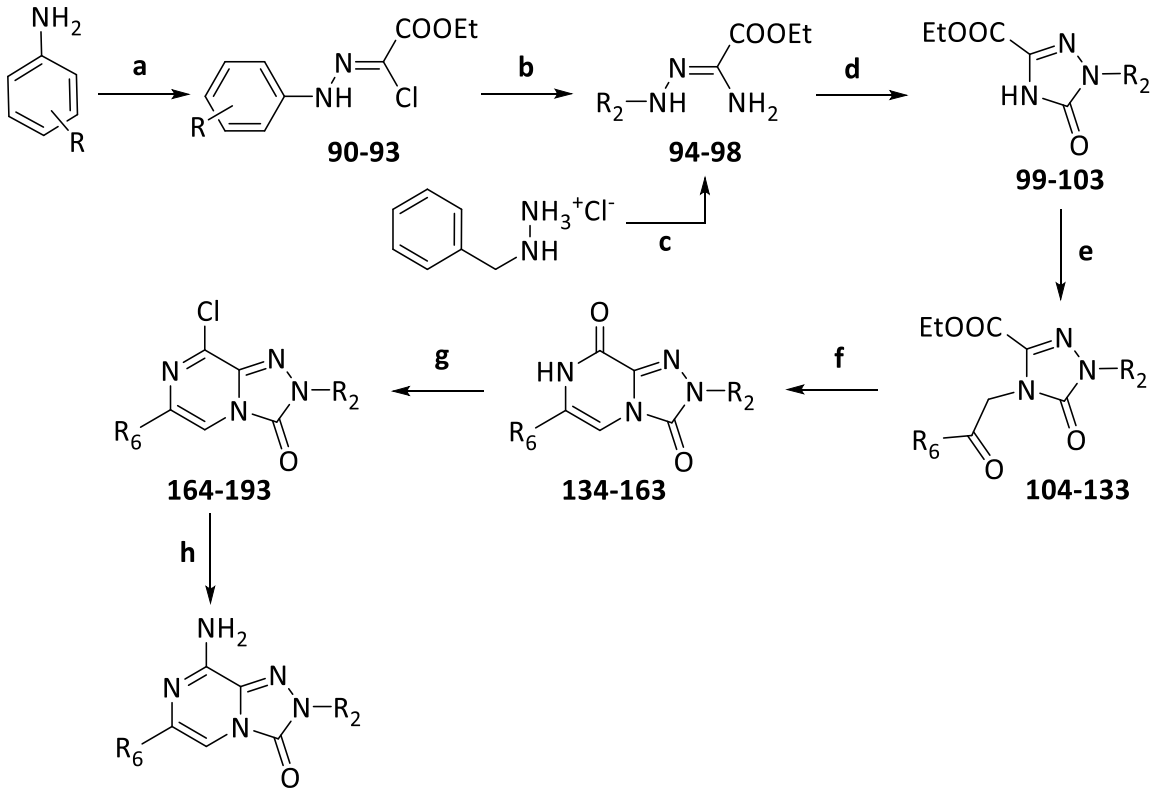

1-6, 11-13, 17, 29-36, 62-73

Scheme 1. **a**) $NaNO_2$, 2-Chloroacetoacetate, NaOAc, MeOH 0-5 °C; **b**) 33% aqueous NH_3, 1,4-dioxane, r.t.; **c**) absolute EtOH, Ethyl 2-amino-2-thioxoacetate K_2CO_3, r.t.; **d**) for **99-102**, Triphosgene, anhydrous THF, r.t.;[410] for **103**, Carbonyldiimidazole, dichloromethane, r.t.; **e**) R_6-$COCH_2Br$, K_2CO_3, DMF/acetonitrile, r.t.; **f**) NH_4OAc, mw or conventional heating 130-190 °C sealed tube; **g**) $POCl_3$, mw or conventional heating, 140-180 °C; **h**) NH_3, absolute EtOH, 130 °C. For R_2 and R_6 see Table 2.

The new 8-amino-1,2,4-triazolopyrazin-3-one derivatives **1-6, 11-13, 17, 29-36, 62-73** were prepared as depicted in Schemes 1. The starting ethyl 2-arylhydrazono-2-chloroacetates **90-93**[393,411,412] were prepared by reacting the suitable aryldiazonium chloride with ethyl 2-chloroacetoacetate, in the presence of sodium acetate in MeOH. Compounds **94-97**[413,414] were prepared by reacting the ethyl 2-arylhydrazono-2-chloroacetates **90-93** with 33 % aqueous ammonia solution in 1,4-dioxane at room temperature, while ethyl 2-amino-2-(2-benzyl-hydrazono)acetate **98** was obtained by reacting benzylhydrazine dihydrochloride with ethyl 2-amino-2-thioxoacetate in absolute ethanol and in the presence of potassium bicarbonate. Treatment of derivatives **94-97** with triphosgene yielded the ethyl 1-phenyl-5-oxo-1H-1,2,4-triazole-3-carboxylates **99-102**[410,415]**.** The 1-benzyl-substituted derivative **103,** instead, was obtained by reacting

ethyl 2-amino-2-(2-benzyl-hydrazono)acetate **98** with carbonyldiimidazole in methylene chloride at room temperature[416]. N^4-alkylation of **99-103** with commercial or properly synthesized α-aloketones in DMF/CH_3CN, in the presence of potassium carbonate, afforded the ethyl 1-aryl-5-oxo-1,2,4-triazole-3-carboxylates **104-133** whose cyclization with ammonium acetate, performed by conventional heating or under microwave irradiation, gave the 1,2,4-triazolo[4,3-a]pyrazine-3,8-dione derivatives **134-163**. The latter were chlorinated with phosphorus oxychloride, under microwave irradiation, to obtain the related 8-chloro derivatives **164-193** which were allowed to react with a saturated solution of ammonia, in absolute ethanol, to afford the desired 8-amino-1,2,4-triazolo[4,3-a]pyrazine-3-one derivatives **1-6, 11-13, 17, 29-36, 62-73**.

Table 2.	R_6	R_2		R_6	R_2
104, 134, 164, 1	Me	Ph	**119, 149, 179, 34**	C_6H_4-2-NO_2	Ph
105, 135, 165, 2	Ph	Ph	**120, 150 ,180, 35**	C_6H_4-3-NO_2	Ph
106, 136, 166, 3	Me	C_6H_4-4-OMe	**121, 151, 181, 36**	C_6H_4-4-NO_2	Ph
107, 137, 167, 4	Ph	C_6H_4-4-OMe	**122, 152, 182, 62**	2-furan	Ph
108, 138, 168, 5	Ph	C_6H_4-4-NO_2	**123, 153, 183, 63**	2-(5-methylfuryl)	Ph
109, 139, 169, 6	Ph	C_6H_4-2-OMe	**124, 154, 184, 64**	2-thienyl	Ph
110, 140, 170, 11	C_6H_4-2-OMe	Ph	**125, 155, 185, 65**	2-pyridyl	Ph
111, 141, 171, 12	C_6H_4-3-OMe	Ph	**126, 156, 186, 66**	Ph	CH_2Ph
112, 142, 172, 13	C_6H_4-4-OMe	Ph	**127, 157, 187, 67**	2-furan	CH_2Ph
113, 143, 173, 17	C_6H_4-4-Me	Ph	**128, 158, 188, 68**	2-(5-methylfuryl)	CH_2Ph
114, 144, 174, 29	C_6H_4-3,4-OCH_2O	Ph	**129, 159, 189, 69**	C_6H_4-2,4-diOCH_3	Ph
115, 145, 175, 30	C_6H_4-3-Br	Ph	**130, 160, 190, 70**	C_6H_4-3,4-diOCH_3	Ph
116, 146, 176, 31	C_6H_4-4-Br	Ph	**131, 161, 191, 71**	C_6H_4-3,4-triOCH_3	Ph
117, 147, 177, 32	C_6H_4-3-Cl	Ph	**132, 162, 192, 72**	C_6H_4-4-OCH_3-3,5-diCH_3	Ph
118, 148, 178, 33	C_6H_4-4-Cl	Ph	**133, 163, 193, 73**	C_6H_4-4-OCH_3-3,5-di-t-but	Ph

Demethylation of the (methoxyphenyl) derivatives **3, 4, 6, 11-13** with 1M solution of BBr_3 in methylene chloride gave the corresponding (hydroxyphenyl)-substituted compounds **7-9, 14-16** (Scheme 2).

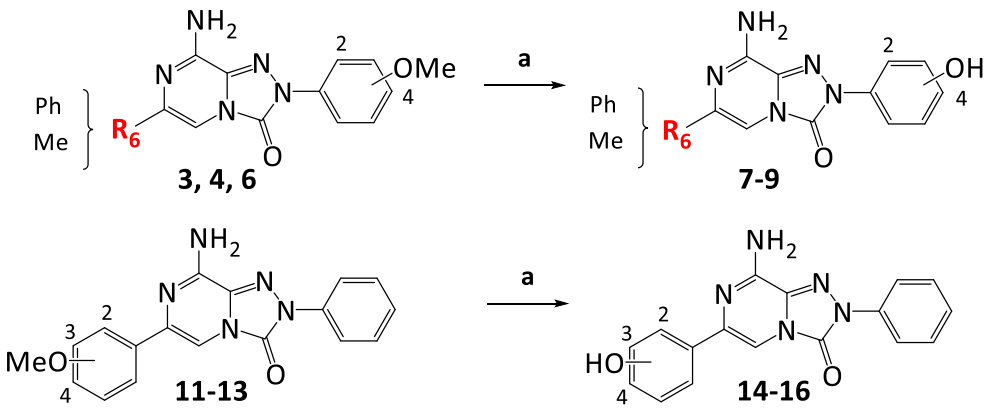

Scheme 2. **a)** BBr_3 1M in dichloromethane, anhydrous dichloromethane, 0 °C, r.t.

Finally, the (nitrophenyl) derivatives **5, 34-36** were reduced (H_2, Pd/C) in a Parr apparatus to yield the corresponding (aminophenyl) derivatives **10, 37-39** (Scheme 3).

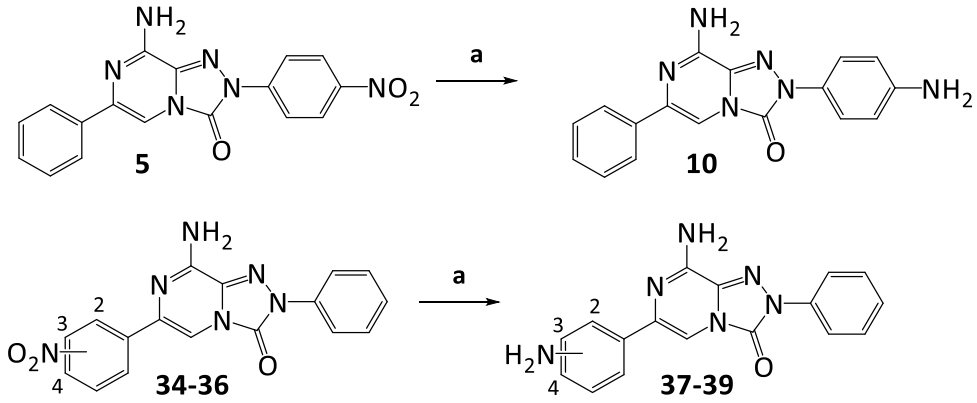

Scheme 3. a) H_2, Pd/C, DMF, Parr apparatus, 40 psi, r.t.

The 6-(alkoxyphenyl) compounds **18**–**28** (Table 3) were synthesized as outlined in Scheme 4, i.e. by alkylation of the 6-(hydroxyphenyl) derivatives **15** or **16** with the suitable alkyl bromides in refluxing 2-butanone and in the presence of potassium carbonate.

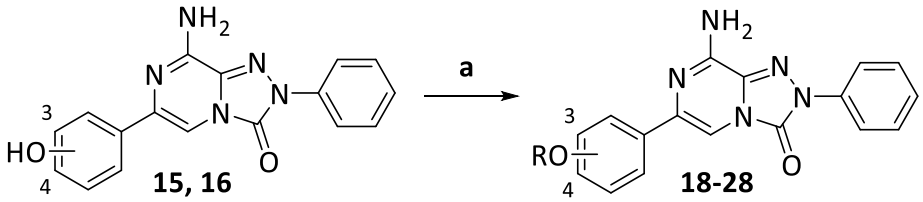

Scheme 4. a) Alkyl bromide, K_2CO_3, 2-Butanone, reflux.

Table 3.

	R		R
18	3-O-propargyl	**24**	4-O-iC_3H_7
19	4-O-propargyl	**25**	4-OCH_2-iC_3H_7
20	3-OCH_2Ph	**26**	4-$OCH_2cC_3H_5$
21	4-OCH_2Ph	**27**	4-$OCH_2cC_4H_7$
22	4-OC_2H_5	**28**	4-OCH_2-$CH=CH_2$
23	4-O-nC_3H_7		

It has to be pointed out that the 6-aminophenyl substituted compounds **37-39** and the 6-(4-hydroxyphenyl) derivative **16** were employed as key intermediates for the synthesis of the new sets of compounds **40-61** and **79-86**.

The 2-phenyl-triazolopyrazines **40-61,** bearing, on the 6-phenyl ring, substituents which were thought to enhance water solubility and drug-like properties, were synthesized as depicted in Scheme 5-9. Compounds **40-42**, featuring a piperazine residue at the three positions of 6-phenyl moiety, were achieved as described in Scheme 5. The piperazine ring was constructed by alkylation of the aromatic amino group of derivatives **37-39** with bis(2-chloroethyl)amine in sulfolane at 150 °C. Reaction of the 6-(3-piperazin-1-yl)-substituted compound **41** with methyl iodide gave rise to the N,N-dimethylpiperazinium salt **43** while allowing to react compounds **41** and **42** with benzyl bromide, the respective N-benzylpiperazin-1-yl-derivatives **44** and **45** were obtained.

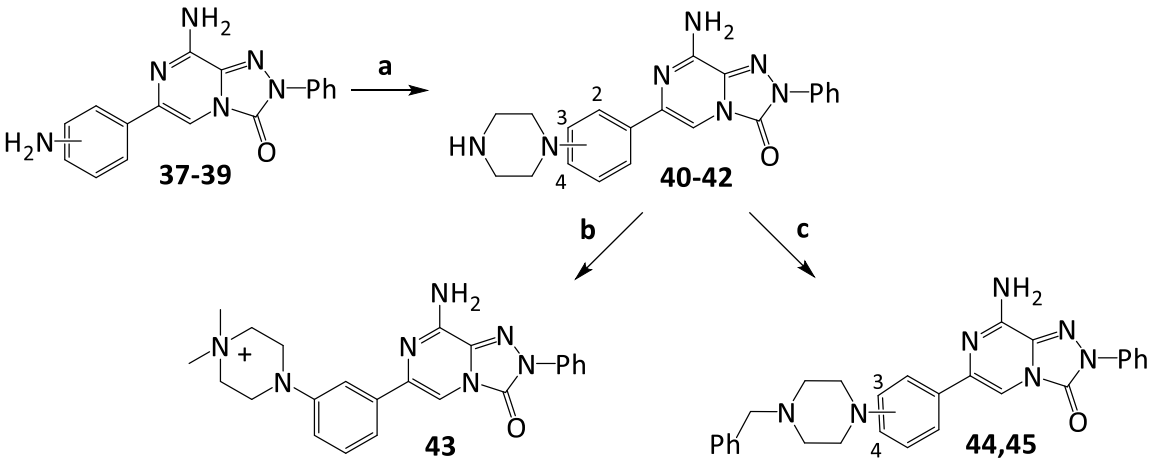

Scheme 5. a) Bis(2-chloroethyl)amine hydrochloride, sulfolane, 150 °C; **b)** From **41,** CH_3I, anhydrous DMF, r.t.; **c)** From **41** and **42,** Benzyl bromide, Et_3N, anhydrous 1,4-dioxane, reflux.

Derivatives **46-50,** featuring small hydrophilic chains on the *para* position of the 6-phenyl ring, were synthesized as outlined in Scheme 6. Reaction of the 6-(4-hydroxyphenyl)-

derivative **16** with suitable alkyl halides and in presence potassium carbonate in anhydrous acetone, afforded the desired 6-(4-O-alkylated) compounds **46** and **47**. Reduction of the nitrile **47** with lithium aluminium hydride in anhydrous THF at room temperature gave the corresponding 6-(4-(2-aminoethoxy)phenyl compound **48**. Compounds **49** and **50** were achieved by reacting the 6-(4-hydroxyphenyl) intermediate **16** with ethylene carbonate, in presence of potassium carbonate and in anhydrous DMF at 110 °C, (compound **49**) or with 3-chloropropane-1,2-diol in anhydrous acetonitrile at room temperature (compound **50**).

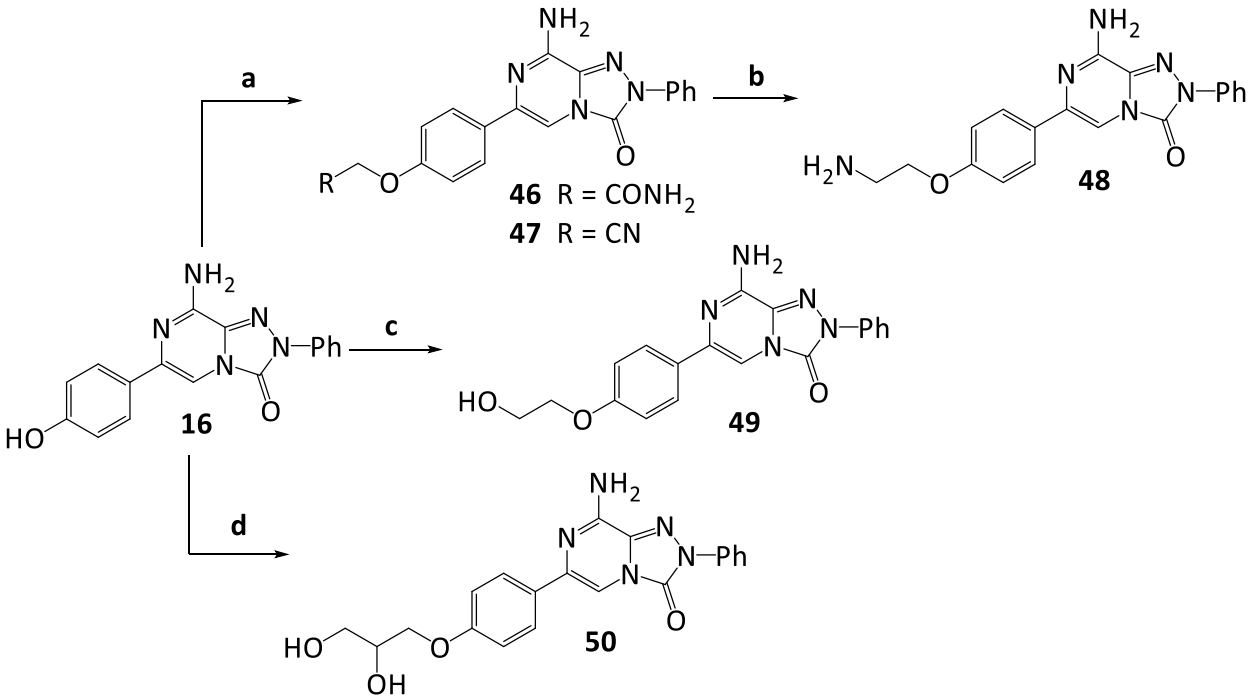

Scheme 6. a) Chloroacetamide (for compd. **46**) or Chloroacetonitrile (for compd. **47**), K_2CO_3, anhydrous acetone, r.t.; **b)** from **47,** $LiAlH_4$, anhydrous THF, 0 °C; **c)** Ethylene carbonate, K_2CO_3, anhydrous DMF, 110 °C; **d)** 3-Chloropropane-1,2-diol, K_2CO_3, anhydrous Acetonitrile, r.t.

Other basic hydrophilic functions were appended, by suitable spacers on the *para*-position of the 6-phenyl ring (Schemes 7, 8 and 9). Reaction of the 6-(4-aminophenyl)-derivative **39** with 3-chloropropionic acid in presence of EDCI hydrochloride, DIPEA in anhydrous DMF, gave the N-(4-(8-amino-3-oxo-2-phenyl-2,3-dihydro-[1,2,4]triazolo[4,3-a]pyrazin-6-yl)phenyl)acrylamide **194** which was treated with a saturated ammonia solution at 130 °C in absolute ethanol to afford 3-amino-N-(4-(8-amino-3-oxo-2-phenyl-2,3-dihydro-[1,2,4]triazolo[4,3-a]pyrazin-6 yl)phenyl)propanamide **51**. Instead, the 8-amino-1,2,4-triazolopyrazin-3-one derivatives

52-55, bearing in the side chain cyclic amines, were achieved by refluxing the intermediate **194** with the suitable amine in anhydrous THF (Scheme 7).

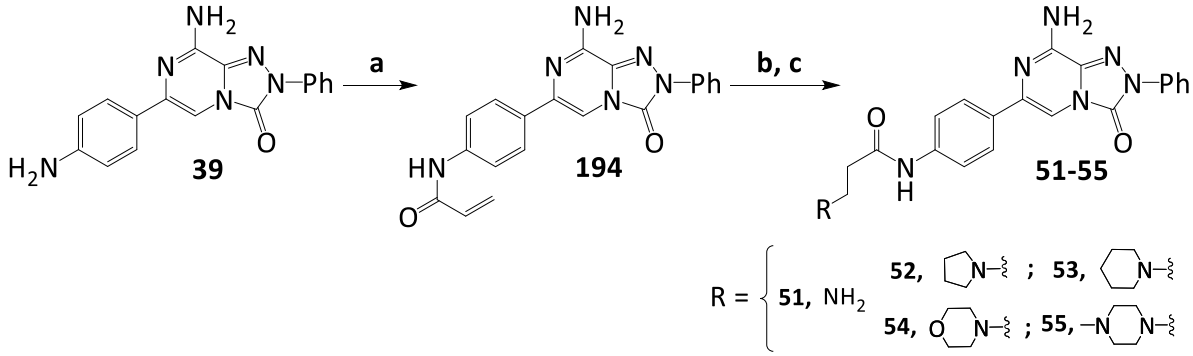

Scheme 7. a) 3-Chloropropionic acid, EDCI.HCl, DIPEA, anhydrous DMF, r.t.; **b)** NH_3, absolute EtOH, 130 °C; **c)** Cyclic amine, anhydrous THF, reflux.

Reaction of the 6-(4-(2-hydroxyethoxy)phenyl) derivative **49** with thionyl chloride in anhydrous toluene, and in presence of pyridine, afforded the 6-(4-(2-chloroethoxy)phenyl) derivative **195** which was reacted with suitable cyclic amines in presence of potassium carbonate, and catalytic amount of potassium iodide, in anhydrous DMF at 110 °C, to yield the desired final compounds **56-59** (Scheme 8).

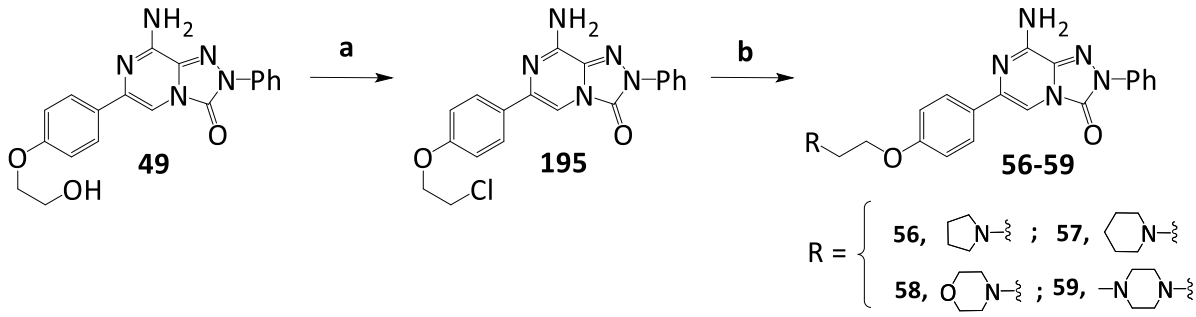

Scheme 8. a) $SOCl_2$, pyridine, anhydrous toluene, reflux; **b)** Cyclic amines, K_2CO_3, KI, anhydrous DMF, 110 °C.

Treatment of the 6-(4-hydroxyphenyl)-derivative **16** with epichlorohydrin, potassium carbonate in anhydrous acetonitrile at 85 °C, afforded the 6-(oxiran-2-ylmethoxy)phenyl substituted derivative **196** which was reacted with piperidine or morpholine, in boiling ethanol and in presence of potassium carbonate, to yield the desired triazolopyrazines **60-61** (Scheme 9).

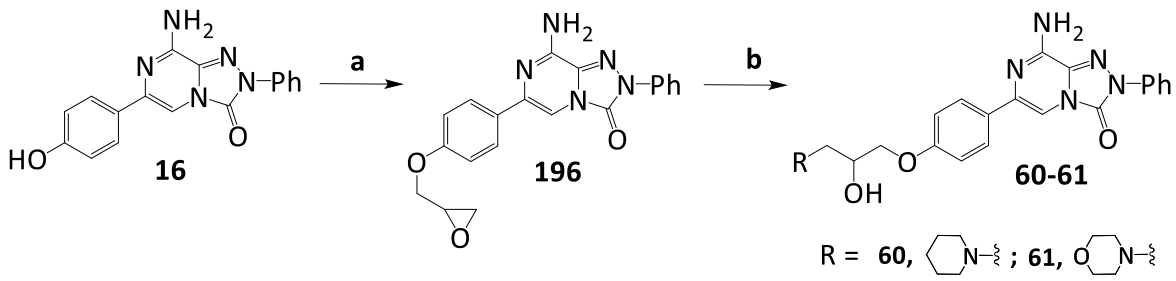

Scheme 9. a) Epichlorohydrin**,** K_2CO_3, anhydrous acetonitrile, reflux; **b)** Cyclic amines, K_2CO_3, absolute EtOH, reflux.

Finally, a set of 8-amino-1,2,4-triazolopyrazin-3-one derivatives **74-86,** containing moieties which were thought to confer antioxidant properties were synthesized (Scheme 10-14)**.** Compounds **74-77**, bearing substituted phenolic rings at position 6, were obtained by reacting the corresponding methoxy derivatives **69-72** with BBr_3 1M dichloromethane solution in anhydrous methylene chloride at room temperature. This conditions did not work to demethylate the 3,5-di-tert-butyl-4-methoxyphenyl-derivative **73,** due to the steric hindrance of the two tert-butyl groups. More drastic conditions, i.e. 48% aqueous HBr in boiling acetic acid, permitted demethylation of **73**, but also caused elimination of one tert-butyl group, thus affording the 3-(tert-butyl)-4-hydroxyphenyl derivative **78** (Scheme 10).

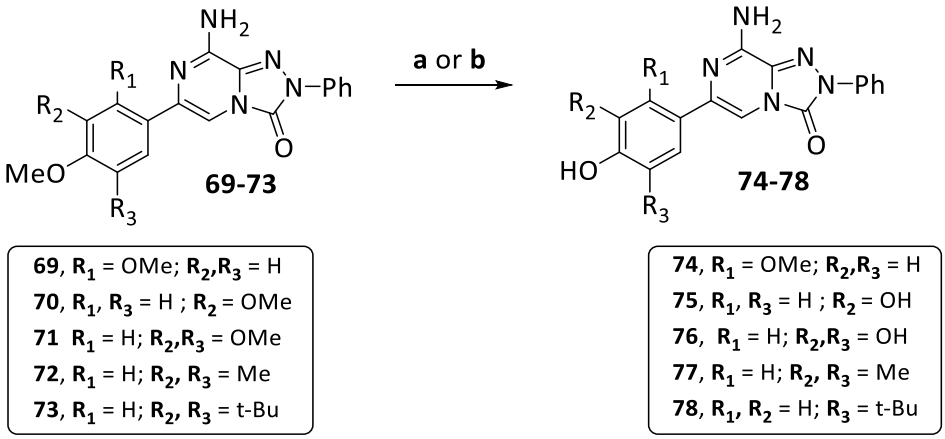

Scheme 10. a) from **69-72**, BBr_3 1M in dichloromethane, anhydrous dichloromethane, r.t.; **b)** from **73**, 48% HBr, acetic acid, reflux.

The set of 8-amino-1,2,4-triazolopyrazin-3-one derivatives **79-86**, featuring different possible antioxidant groups on 6-phenyl ring, were synthesized as depicted in Schemes 11-14. Compounds **79**, **80** were prepared as shown in Scheme 11, i.e. starting from the 6-

(4-aminophenyl)-derivative **39** which was reacted at room temperature with (S)-2-oxothiazolidine-4-carboxylic acid (compound **79**) or racemic lipoic acid (compound **80**) and EDCI hydrochloride, 1-hydroxybenzotriazole hydrate, DIPEA, in anhydrous DMF.

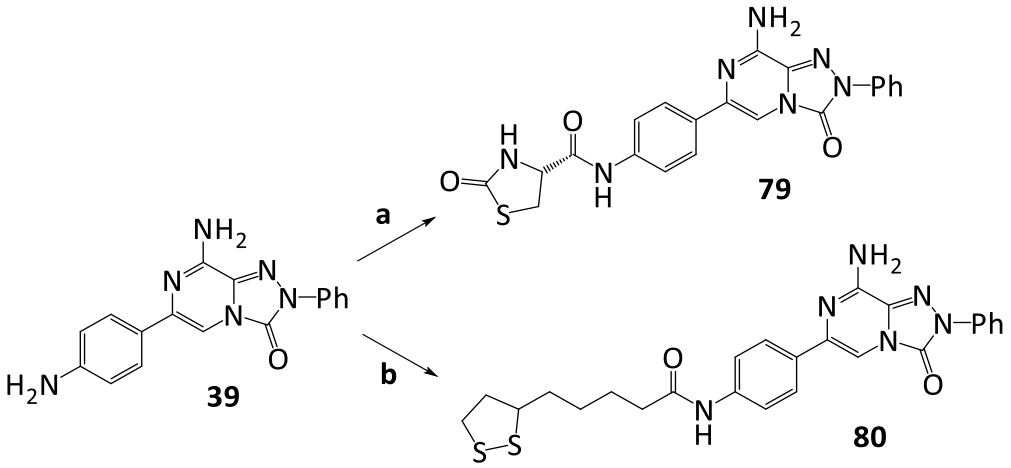

Scheme 11. a) (R) Oxothiazolidine-4-carboxylic acid, EDCI.HCl, DIPEA, HOBt.H_2O, anhydrous DMF, r.t.; **b)** (R, S) Lipoic acid, EDCI.HCl, DIPEA, HOBt.H_2O, anhydrous DMF, r.t.

Compounds **81-83** were synthesized by reacting the 4-(2-aminoethoxy)phenyl derivative **48** with the suitable carboxylic acids and in the same experimental conditions described above to prepare **79** and **80** from **39** (Scheme 12).

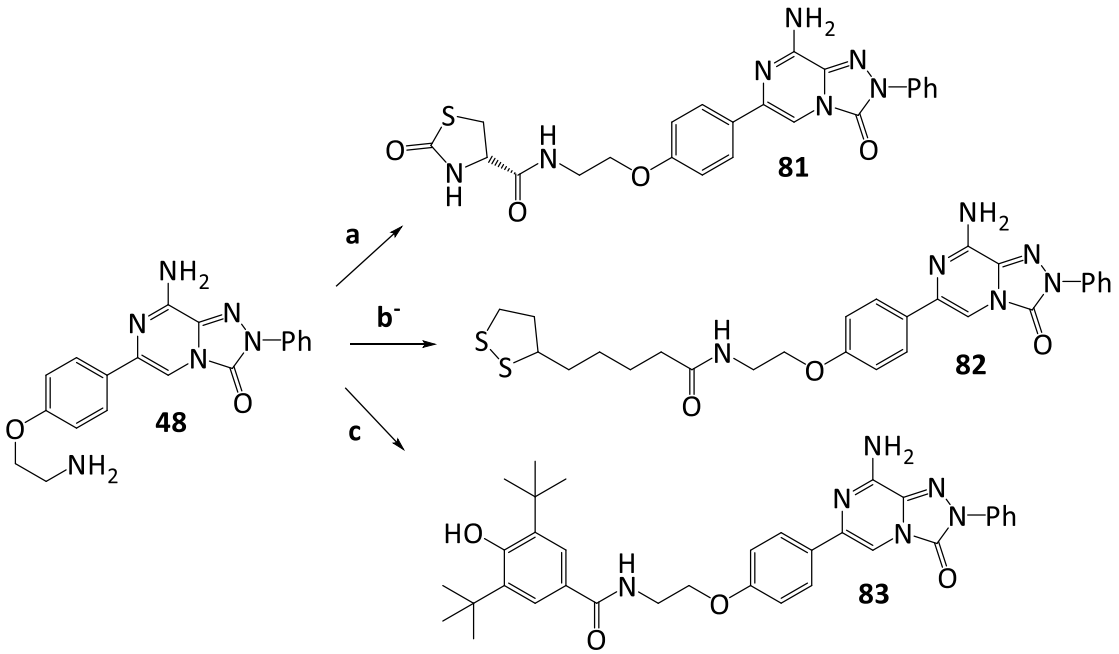

Scheme 12. a) (R) Oxothiazolidine-4-carboxylic acid, EDCI.HCl, DIPEA, HOBt.H_2O, anhydrous DMF, r.t.; **b)** (R, S) Lipoic acid, EDCI.HCl, DIPEA, HOBt.H_2O, anhydrous DMF, r.t.; **b)** 3,5-Di-tert-butyl-4-hydroxy-benzoic acid, EDCI.HCl, DIPEA, HOBt. H_2O, anhydrous DMF, r.t.

The same procedure was employed to prepare the novel 8-amino-1,2,4-triazolo[4,3-a]pyrazin-3-ones **84** and **85** (Scheme 13) starting from the amino derivative **51**.

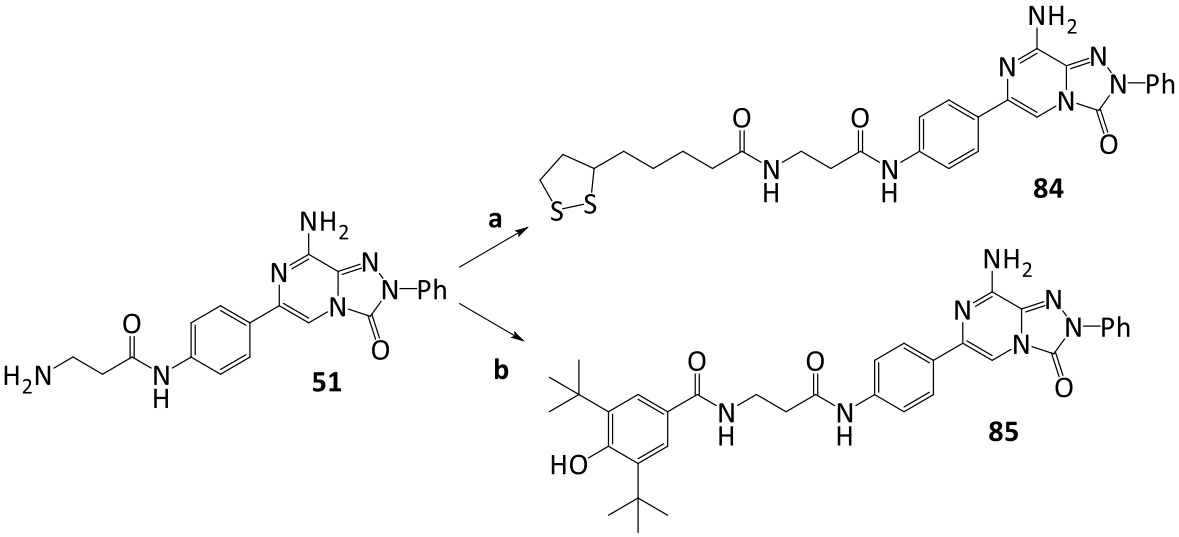

Scheme 13. a) (R, S) Lipoic acid, EDCI.HCl, DIPEA, HOBt.H_2O, anhydrous DMF, r.t.; **b)** 3,5-Di-tert-butyl-4-hydroxy-benzoic acid, EDCI.HCl, DIPEA, HOBt.H_2O, anhydrous DMF, r.t.

Compound **86**, bearing the 5-methyl-1,2-dihydro-3H-pyrazol-3-one ring on the lateral chain, was obtained starting from intermediate **194** which was reacted with hydrazine monohydrate in anhydrous THF at reflux to give the corresponding 3-hydrazinylpropanamide **197.** Cyclization of the latter with ethyl acetoacetate in ethanol at 60°C afforded the desired final compound (Scheme 14).

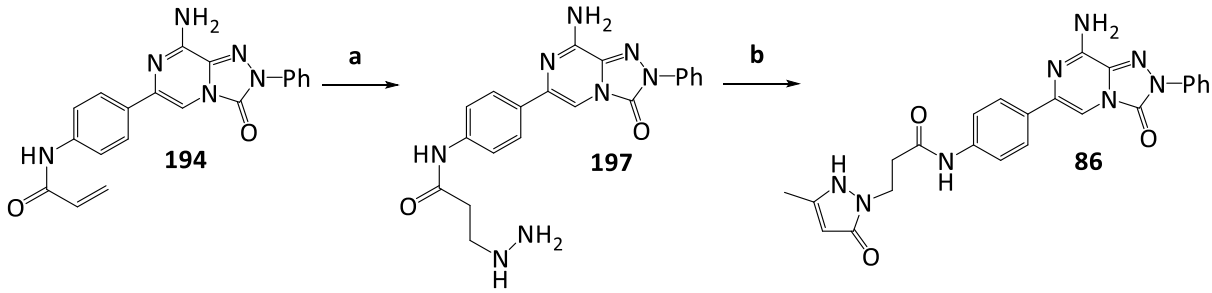

Scheme 14. a) Hydrazine.hydrate, anhydrous THF, reflux; **b)** Ethyl acetoacetate, EtOH, 60 °C

4. RESULTS AND DISCUSSION

The 8-amino-1,2,4-triazolo[4,3-a]pyrazin-3-ones **1-86** were evaluated for their affinity to hA_1, hA_{2A}, and hA_3 ARs, stably transfected in Chinese hamster ovary (CHO) cells, and were also tested at the hA_{2B} AR subtype by measuring their inhibitory effects on 5'-(N-ethyl-carboxamido)adenosine (NECA)-stimulated cAMP levels in hA_{2B} CHO cells. These studies were performed in collaboration with the group of Professor R. Volpini, from the University of Camerino. With the aim to rationalize the results obtained from pharmacological assays, the synthesized compounds were subjected to a molecular modeling investigation at the A_{2A}AR crystal structure. These studies were performed by the group of Professor Dal Ben, from the University of Camerino. As previously discussed in the "Aim of the Work", the synthesized compounds have been subdivided into four sets which reflect the different phases of the work. The same division was applied to SAR discussion.

4.1. Preliminary structure-affinity relationship investigations of 8-amino-2-aryl-1,2,4-triazolo[4,3-*a*]pyrazin-3-ones 1-10

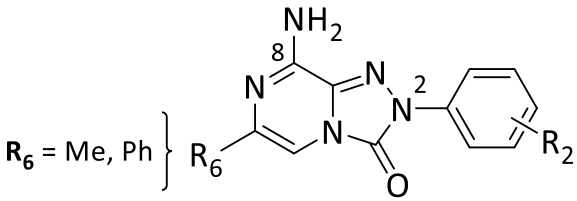

1-10

Table 4

			Binding experiments K_i (nM)[a]			cAMP assays IC_{50} (nM)[a]
	R_6	R_2	hA_1[b]	hA_{2A}[c]	hA_3[d]	hA_{2B}[e]
1	CH_3	H	67 ± 8	485 ± 39	4370 ± 355	>30000
2	C_6H_5	H	13 ± 1	10 ± 3	11 ± 2	>30000
3	CH_3	4-OCH_3	1743 ± 514	1038 ± 271	255 ± 21	>30000
4	C_6H_5	4-OCH_3	20 ± 5	78 ± 18	117 ± 26	>30000
5	C_6H_5	4-NO_2	8.1 ± 2.5	402 ± 91	>30000	>30000
6	C_6H_5	2-OCH_3	247 ± 31	309 ± 37	392 ± 60	>30000
7	CH_3	4-OH	1000 ± 128	1319 ± 184	5159 ± 752	>30000

8	C_6H_5	4-OH	18 ± 2	138 ± 28	429 ± 89	>30000
9	C_6H_5	2-OH	47 ± 9	232 ± 47	1558 ± 393	>30000
10	C_6H_5	4-NH_2	8.9 ± 1.1	3480 ± 398	650 ± 143	>30000
	DPCPX		2.8 ± 0.5	125 ± 21	3850 ± 762	989 ± 22[g] 73.24 ±2.0[f]
	NECA		4.6 ± 0.8	16 ± 3	12.8 ± 2.5	1510 ± 210[g] 1890[f]
	CCPA		1.2 ± 0.2	2050 ± 400	26 ± 5	16850 ± 320[g] 18800[f]

[a]Data (n = 3–5) are expressed as means ± standard errors. [b]Displacement of specific [^{3}H]-CCPA binding at hA_1 AR expressed in CHO cells. [c]Displacement of specific [^{3}H]-NECA binding at hA_{2A} AR expressed in CHO cells. [d]Displacement of specific [^{3}H]-HEMADO binding at hA_3 AR expressed in CHO cells. [e]IC_{50} values of the inhibition of NECA-stimulated adenylyl cyclase activity in CHO cells expressing hA_{2B}AR. [f]K_i values (nM) from radioligand binding assays, for DPCPX[417], for NECA[418] and CCPA. [g]EC_{50} value (nM) of the stimulation of adenylyl cyclase activity in CHO cells expressing hA_{2B} AR.

As anticipated above, the first purpose of the work was to perform a preliminary investigation of the SARs of this new series and to identify new hA_{2A} AR antagonists. In the early stage of the project, structural modifications were carried out to evaluate which group, between the methyl and the phenyl, was the better for the 6 position. Analyzing the binding data of the 8-amino-2-phenyl-1,2,4-triazolo[4,3-a]pyrazin-3-ones **1-10**, the 2,6-diphenyl-substituted derivative **2** turned out to be notable, showing high and comparable affinities at hA_1, hA_{2A} and hA_3 ARs (K_i = 10-13 nM). The 6-methyl-2-phenyl derivative **1** instead (K_i = 67-4370 nM) was significantly less active, in particular for the targeted hA_{2A} AR. The para-hydroxy substituent inserted on the 2-phenyl ring of **1** and **2** was chosen because in the TQX series[388] it was profitable for A_{2A} AR affinity. The 2-(4-hydroxyphenyl)-substituted derivatives **7** and **8** were less active at the hA_{2A}AR than the unsubstituted compounds **1** and **2** and also than their methoxy substituted synthetic precursors **3** and **4**. The last two derivatives showed, on the whole, lower affinities for both hA_1 and hA_{2A} ARs than their parent compounds **1** and **2**. The comparison of AR affinity data for the 6-phenyl derivatives **2** (K_i hA_{2A} = 10 nM), **4** (K_i hA_{2A} = 78 nM) and **8** (K_i hA_{2A} = 138 nM) with those of the corresponding 6-methyl derivatives **1** (K_i h A_{2A} = 485 nM), **3** (K_i hA_{2A} 1038 = nM) and **7** (K_i hA_{2A} = 1319 nM) highlighted that the 6-phenyl moiety is more advantageous than the methyl one, probably due to its higher lipophilicity and/or capability to enhance the structural complementarity of the whole molecule with the receptor binding site. Thus, subsequent investigations were carried out on the 6 phenyl

substituted compound **2** which was modified by introducing a *para*-amino group (compound **10**), as suggested by affinity data for the TQX series[388]. Compound **10** (K_i hA_{2A} = 3480 nM), as well as its synthetic precursor 2-(4-nitrophenyl) derivative **5** (K_i hA_{2A} = 402 nM) did not show enhanced affinity for the hA_{2A} AR with respect to the lead **2**. On the contrary, hA_1 AR affinities of **5** and **10** were very high (K_i = 8.1 and 8.9 nM) and similar to that of **2** (K_i hA_1 = 13 nM). The presence of a methoxy or hydroxy group at the ortho position of the 2-phenyl ring proved to be disadvantageous for the recognition of both hA_{2A} and hA_1 ARs. In fact, compounds **6** (K_i hA_{2A} = 309 nM) and **9** (K_i hA_{2A} = 232 nM) are significantly less active than **2** (K_i hA_{2A} = 10 nM).

4.1.1. Molecular modeling studies

The binding mode of the synthesized compounds at the hA_{2A} AR cavity was simulated with docking analysis by using the Molecular Operating Environment (MOE, 2014.09) docking tool and Gold and Autodock software[419-422]. For the docking tasks, two crystal structures of the hA_{2A} AR in complex with the antagonist/inverse agonist ZM241385 were employed (PDB 3EML, 2.6 Å resolution, and PDB 4EIY, 1.8 Å resolution)[423-425]. The MOE software analysis was made by selecting the induced fit docking and optimization protocol (schematically, a preliminary docking analysis provides a set of ligand conformations that are energy minimized, including inthis step the side chains of the receptor residues in proximity). The docking analysis was performed with different docking tools and two different crystal structures of the target to get an average prediction of the binding mode of the synthesized compounds at the binding cavity. The docking results at the hA_{2A} AR show that the molecules could bind to the pocket of this receptor with a preferred orientation ("type-one" conformations), presenting the substituent at the 2-position located in the depth of the cavity and the R_6 group at the entrance of the binding site (Figure 24, A).

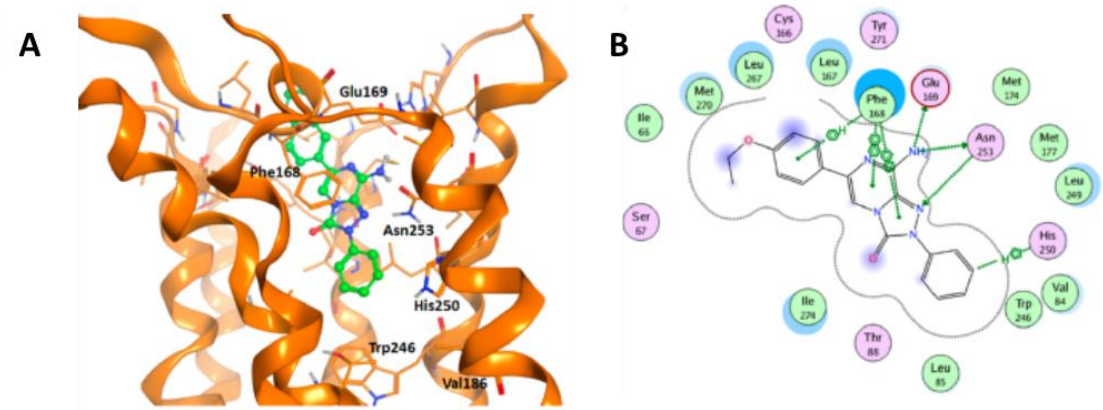

Figure 24. (A) General binding mode of the synthesized compounds atthe hA_{2A} AR (pdb 4EIY) binding cavity, with indication of some key receptor residues. (B) Schematic description of the ligand–target interaction (built with MOE software).

The scaffold adopts a position that makes it able to interact with Asn $253^{6.55}$ and Glu169 (EL2) through H-bond contacts, while a π–π interaction is present between the phenyl ring of Phe168 (EL2) and the bicyclic core of the compounds (Figure 24, B). This interaction is very similar to the one given by the cocrystallized hA_{2A} AR antagonist ZM241385[423-425] and by other structural classes of hA_{2A} AR ligands previously described[393,426]. A second binding mode ("type-two" conformations) simulated by docking experiments presents the scaffold oriented in the opposite way with respect to the conformations described above, the 6-substituent being located in the depth of the cavity and the 2-substituent pointing toward the extracellular environment. This second binding mode is generally not preferred at the hA_{2A} AR, being associated with lower docking scores than those of the above-described docking conformations, except for derivatives presenting ortho-substituent on the 2-phenyl ring (see below). Compound **2** can be considered the reference ligand of the series, as it bears two unsubstituted phenyl rings at the 2 and 6 positions. This derivative showed good affinity at the hA_1 AR, hA_{2A} AR, and hA_3 AR, and this makes it a sort of passe-partout for the three ARs. Docking results of compound **2** at the three AR structures showed that it may be inserted in the receptor cavities with the two binding modes, both associated with good docking scores (the "type-one" generally preferred). The possibility of making more than one complex with the same receptor could result in good affinity, and this feature could be applied at the three ARs. The substituents inserted on the 2-phenyl group modulate the interaction with the binding pocket. In detail, the presence of small groups at the para-position generally affords decreased hA_{2A} AR affinity with respect to the corresponding analogues with an

unsubstituted 2-phenyl ring (compare derivatives **3** and **7** with **1** and compounds **4, 5**, **8**, and **10** with **2**). This result was interpreted considering various parameters. The first is the topological complementarity of the ligand with the binding pocket (Figure 25, A).

The presence of a para-substituent on the 2-phenyl ring seems to cause a slight displacement of the ligand that decreases its ability in establishing some crucial interactions with the receptor (i.e., H-bonds with Asn253$^{6.55}$ and Glu169) with respect to the compounds with an unsubstituted 2-phenyl ring. Second, hA_{2A} AR affinities may be rationalized by docking results also considering that the depth of the binding cavity is mainly hydrophobic. Hence, a nonpolar group at the paraposition of the 2-phenyl ring, such as the methoxy group of **4** (K_i = 78 nM), would afford a slightly better interaction with the target when compared to a more polar group at the same position such as the OH group of **8** (K_i = 138 nM). On this basis, we conclude that a para-substituent on the 2-phenyl ring is fairly allowed for these compounds and, if present, should be a small hydrophobic function. Introduction of a substituent (OMe, OH) at the ortho position of the 2-phenyl ring of compound **2** afforded derivatives **6** and **9**, endowed with 20–30-fold reduced hA_{2A}AR affinity. Docking results suggest that these compounds preferentially adopt the "type-two" orientation with the 2-aryl pendant located at the entrance of the cavity and the R_6 group positioned in the depth of the pocket (Figure 25, B). In this way, the ortho-hydroxy group of derivative **9** could give some polar interaction with Glu169 (EL2).

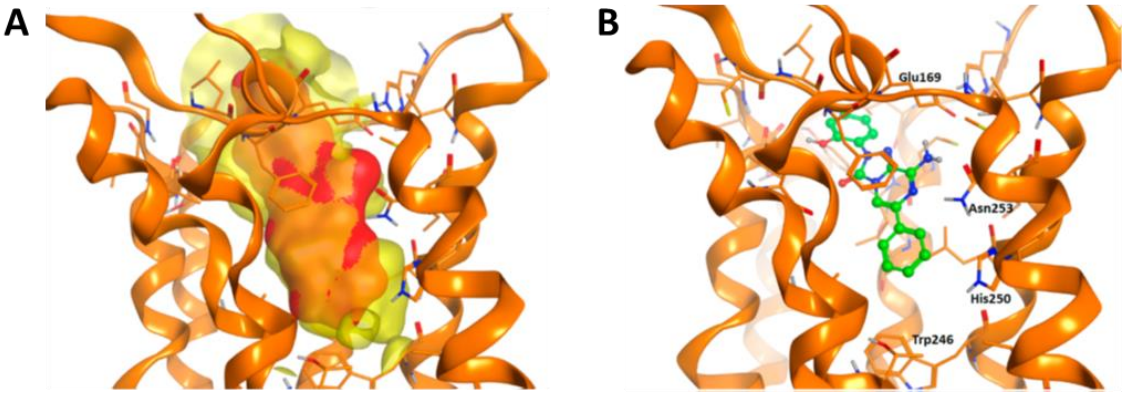

Figure 25. (A) Molecular surface representation of the A_{2A} hAR binding cavity (yellow) and the bound ligand (red) indicating the topological complementarity of the ligand and the cavity in the depth of the binding pocket. (B) Alternative binding mode of the synthesized compounds at the hA_{2A} AR (pdb 4EIY) binding cavity, with indication of some key receptor residues. This binding mode was particularly observed for compounds presenting an ortho-substituted phenyl ring at position 2.

4.2 Structural modifications on the 6-phenyl ring: 8-amino-6-aryl-2-phenyl-1,2,4-triazolo[4,3-*a*]pyrazin-3-ones 11-39

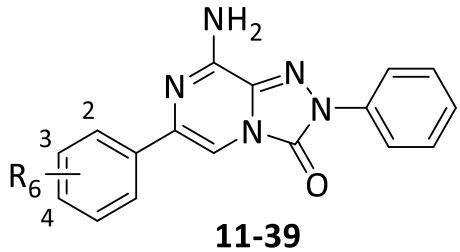

11-39

Table 5.

		Binding experiments K_i (nM)[a]			cAMP assays IC_{50} (nM)[a]
	R_6	hA_1[b]	hA_{2A}[c]	hA_3[d]	hA_{2B}[e]
2	C_6H_5	13 ± 1	10 ± 3	11 ± 2	>30000
11	2-OCH_3	40.8 ±7.1	2.0 ± 0.2	51.5 ± 3.5	>30000
12	3-OCH_3	44 ± 7	6.8 ± 0.7	42 ± 10	>30000
13	4-OCH_3	>30000	7.2 ± 1.8	>30000	>30000
14	2-OH	16.3 ± 0.3	2.4 ± 0.5	44.5±8.3	> 30000
15	3-OH	14 ± 2	3.5 ± 0.6	134 ± 13	>30000
16	4-OH	45 ± 10	45 ± 12	53 ± 13	>30000
17	4-CH_3	>30000	>30000	>30000	>30000
18	3-O-propargyl	45 ± 10	5.1 ± 1.5	67 ± 9	>30000
19	4-O-propargyl	>30000	10.6 ± 1.3	>30000	>30000
20	3-OCH_2Ph	>30000	>30000	>30000	>30000
21	4-OCH_2Ph	3704 ± 495	708 ± 160	>30000	>30000
22	4-OC_2H_5	>30000	2.9 ± 0.5	>30000	>30000
23	4-O-nC_3H_7	>30000	ND[f]	>30000	>30000
24	4-O-iC_3H_7	>30000	7.4 ± 0.9	>30000	>30000
25	4-OCH_2-iC_3H_7	ND[f]	ND[f]	ND[f]	>30000
26	4-$OCH_2cC_3H_5$	>30000	>30000	>30000	ND[f]
27	4-$OCH_2cC_4H_7$	>30000	>30000	>30000	>30000
28	4-OCH_2-$CH=CH_2$	ND[f]	ND[f]	ND[f]	>30000
29	3,4-OCH_2O	13 ± 2.5	7.4 ± 0.9	38 ± 6.7	>30000
30	3-Br	11±2	8±2.1	>30000	> 30000
31	4-Br	>30000	10.6 ± 2.5	705.4 ± 139.5	> 30000

32	3-Cl	4.7 ± 1.1	6.3 ± 1	>30000	> 30000
33	4-Cl	14.3 ± 3.6	10.9 ± 2.7	>30000	> 30000
34	2-NO_2	95 ± 18	43 ± 2.4	180 ± 34	>30000
35	3-NO_2	35.9 ± 7.8	ND[f]	38.6 ± 7.9	>30000
36	4-NO_2	7834 ± 597	7.2± 1.6	16421 ± 3505	> 30000
37	2-NH_2	191 ± 28	19.5 ± 1	321 ± 63	> 30000
38	3-NH_2	15.0 ± 3.0	10.9± 2.3	169 ± 13.5	> 30000
39	4-NH_2	33.5 ± 6.7	22.9 ± 0.2	253.7 ±67.6	> 30000

[a]Data (n = 3–5) are expressed as means ± standard errors. [b]Displacement of specific [^{3}H]-CCPA binding at hA_1 AR expressed in CHO cells. [c]Displacement of specific [^{3}H]-NECA binding at hA_{2A} AR expressed in CHO cells. [d]Displacement of specific [^{3}H]-HEMADO binding at hA_3 AR expressed in CHO cells. [e]IC_{50} values of the inhibition of NECA-stimulated adenylyl cyclase activity in CHO cells expressing hA_{2B} AR. [f]Not determined.

Affinity data of the first set of triazolopyrazines (**1-10**) indicated the unsubstituted phenyl ring as the best group for the 2-position. Thus, to enhance affinity and selectivity for the hA_{2A}AR and enlarge SAR studies, new derivatives (**11-39**) were synthesized by introduction of various substituents with different lipophilicity, electronic and steric properties (OR_1, NO_2, NH_2, Br, Cl, Me) at the 2, 3 and 4 positions of the 6-phenyl ring. The obtained results show that some of the probed substituents, such as para-alkoxy residues (derivatives **13, 19, 22, 24**), the para-bromo (compound **31**) and the para-nitro groups (compound **36**), afforded high hA_{2A} AR affinities and selectivities, the best group being the 4-ethoxy residue (**22**, K_i = 2.9 nM). Other compounds (**15, 30, 32, 33, 38, 39**) bind efficiently both hA_{2A} and hA_1 ARs. This result makes these derivatives interesting as well, because dual hA_1/A_{2A} AR antagonists have emerged as promising agents for the treatment of PD[107,109,384] since they are able to both relieve motor symptoms and ameliorate cognitive impairments associated to PD. In fact, hA_1 receptor antagonists facilitate DA release in the striatum and potentiates, like hA_{2A} AR antagonists, the DA-mediated responses. hA_1AR antagonists are also able to improve performance in an animal model of learning and memory[109,384] due to the high hA_1AR expression in brain areas (hippocamus, neocortex, limbic system) implicated in the control of cognitive and emotive functions. Analizing the affinity data in detail, introduction of a methoxy and hydroxy group at the ortho (**11** and **14**), meta (**12** and **15**) and para (**13** and **16**) positions on the 6-phenyl moiety achieved notable results, the most relevant being the

identification of the 6-(4 methoxyphenyl) derivative **13** possessing nanomolar affinity (K_i = 7.2 nM) and a complete selectivity for the hA_{2A} AR. Very interestingly, demethylation of compound **13** led to a completely change in the the affinity profile since the hydroxy derivative **16** shows a 6-fold reduced hA_{2A} AR affinity (K_i = 45 nM) and, above all, null selectivity, being able to bind also hA_1 and hA_3 ARs with similar K_i values. Moving the methoxy substituent from the para to the ortho (derivative **11**) or the meta position (derivative **12**) maintained a high hA_{2A} AR affinity (K_i = 2.0 and 6.8 nM) but lost selectivity since **11** and **12** displayed considerable and comparable affinity both for hA_1 AR (Ki = 40.8 and 44 nM) and hA_3 ARs (K_i = 51.5 and 42 nM). Demethylation of compounds **11** and **12** to the corresponding hydroxy derivatives **14** and **15** did not modify the affinity profile much, although they showed a higher affinity both to the hA_1 (K_i = 16.3 and 14 nM) and hA_{2A} ARs (K_i = 2.4 and 3.5 nM) and a quite good one to the hA_3 AR (K_i = 44.5 and 134 nM). On the contrary, replacement of the 4-methoxy group with a methyl elicited a detrimental effect, which was difficult to explain, since compound **17** being totally inactive. With the aim of enhancing the hA_{2A} AR affinity, compounds **12** and **13** were modified by replacing the 3- and 4-methoxy groups with the hindered propargiloxy (compound **18** and **19**) and benzyloxy moieties (compound **20** and **21**). In fact, it is well known that long and bulky side chain increase affinity and selectivity at the hA_{2A} AR.[380] Similarly, to the methoxy-substituted compounds **12** and **13**, the propargyloxy substituted derivatives **18** and **19** showed nanomolar affinity for the hA_{2A} AR (K_i = 5.1 and 10.6 nM) and **19** was also totally selective. On the contrary, the benzyloxy derivatives **20** (k_i hA_{2A} > 30000 nM) and **21** (k_i h A_{2A} = 708 nM) were significantly less active than **12** and **13,** in particular, the 3-benzyloxy derivative **20** was completely devoid of affinity for all the ARs. Other structural modifications were carried out by replacing the 4-methoxy group with small alchoxy residues containing either linear, unsaturated, branched or cyclic alkyl chains (derivatives **22**-**28**). Within this new set of ligands, the 4-ethoxyphenyl derivative **22** (K_i hA_{2A} = 2.9 nM) and the 4-isopropoxyphenyl derivative **24** (K_i hA_{2A} = 7.4 nM), bearing the smallest alkyl groups resulted in potent and completely selective hA_{2A} AR antagonists. Differently, compounds **26** and **27**, bearing the cyclopropylmethoxy and cyclobutylmethoxy moieties, were inactive at the hA_{2A} AR as well as at the other ARs. Disappointendly, no biological data are available for derivatives **25** and **28** since we met some difficulties in testing them, probably due to their scarce solubility in the assay medium. The same applies to **23** for

the assays at the hA_{2A} AR. Interestingly, the presence at 6 level of the 3,4-(methylendioxy)phenyl ring, (compound **29**), led to a potent and non selective hA_1 (Ki= 13 nM), hA_{2A} (K_i= 7.4 nM) and hA_3 (K_i= 38 nM) AR ligand.

To continue SAR investigations, other small substituents with different electronic, lipophilic and steric properties (Cl, Br, NO_2, NH_2) were probed on 6-phenyl ring (compounds **30-39**). Introduction of a 4-bromo and 4-nitro substituent resulted in potent and selective hA_{2A}AR ligands (compounds **31** and **36**, respectively, K_i= 10.6 and 7.2 nM). Insertion of the nitro group at the ortho position (derivative **34**) yielded to moderate affinity for the hA_1, hA_{2A} and hA_3 ARs. Good hA_1 and hA_3 AR affinities were achieved for the meta nitro-substituted derivative **35** (K_i= 35.9 and 38.6 nM, respectively) while it was not possible to obtain the hA_{2A} data. Its low solubility in the assay medium did not allow to test high enough concentrations to obtain the dose-response curve. Introduction of the lipophilic 3-bromo (**30**), 3-chloro (**32**) and 4-chloro (**33**) substituents on the 6-phenyl moiety led to dual potent hA_1 (K_i= 4.7-14.3 nM) and hA_{2A} ligands (K_i= 6.3-10.9 nM). The hydrophilic amino group inserted either in meta (**38**) or para (**39**) position gave compounds able to bind efficiently (K_i= 10.9-33.5 nM) both hA_1 and hA_{2A} ARs while the same group at the ortho position (**37**) preserved the hA_{2A} affinity (K_i= 19.5 nM) but worsened the hA_1 one (K_i= 191 nM). All the three amino-substituted compounds **37-39** showed also some ability to bind the hA_3 receptor subtype.

Concerning the hA_{2B} AR, all the compounds **11-39** were inactive (IC_{50}> 30000 nM) in inhibiting the NECA-stimulated cAMP levels in hA_{2B} CHO cells, thus suggesting that they lack affinity for the hA_{2B} AR.Derivative **32**, able to bind both hA_1 and hA_{2A} ARs with nanomolar affinity, and compounds **13**, **22** and **31**, highly selective for the hA_{2A} subtype, were selected to determine their antagonistic properties by evaluating their effect on cAMP production in CHO cells, stably expressing the hA_1 and hA_{2A} ARs. The obtained results (Table 6) showed that the compounds behaved as antagonists being able to counteract NECA-inhibited (A_1) or NECA-stimulated (A_{2A}) cAMP accumulation.

Table 6. Potencies of compounds **13**, **22, 31** and **32** at hA_1 and hA_{2A} ARs.

	hA_1 IC_{50} (nM)[a]	hA_{2A} IC_{50} (nM)[b]
13	ND[c]	180 ± 34
22	ND[c]	98 ± 19
31	ND[c]	694 ± 74
32	298 ± 58	374 ± 52

[a]IC_{50} values obtained counteracting the NECA-induced decrease of cAMP accumulation in CHO cells expressing hA_1R. [b]IC_{50} values obtained by inhibition of NECA-stimulated adenylyl cyclase activity in CHO cells expressing $hA_{2A}R$. [c]Not determined.

4.2.1. Molecular modeling studies

Docking results of compounds bearing an unsubstituted 2-phenyl ring and various aryl substituents at the R_6 position (**11**–**39**) again show a preferential binding mode with the 2- group located in the depths of the cavity and the 6-substituent pointing toward the external environment. Hence, the substituents on the 6-phenyl ring are generally located at the entrance of the cavity, providing different degrees of interaction with the receptor residues in proximity and modulating the affinity for the three ARs subtypes. The compounds featuring a small ortho-substituent (**11**, **14**, **34**, **37**) are generally endowed with low nanomolar hA_{2A} AR affinity. This substituent is oriented toward the N7 atom and in proximity of Glu169 (EL2) residue, with possibility to give polar interaction with the nitrogen atom of the compound scaffold or with the backbone or sidechain atoms of the above cited receptor residue (Figure 26).

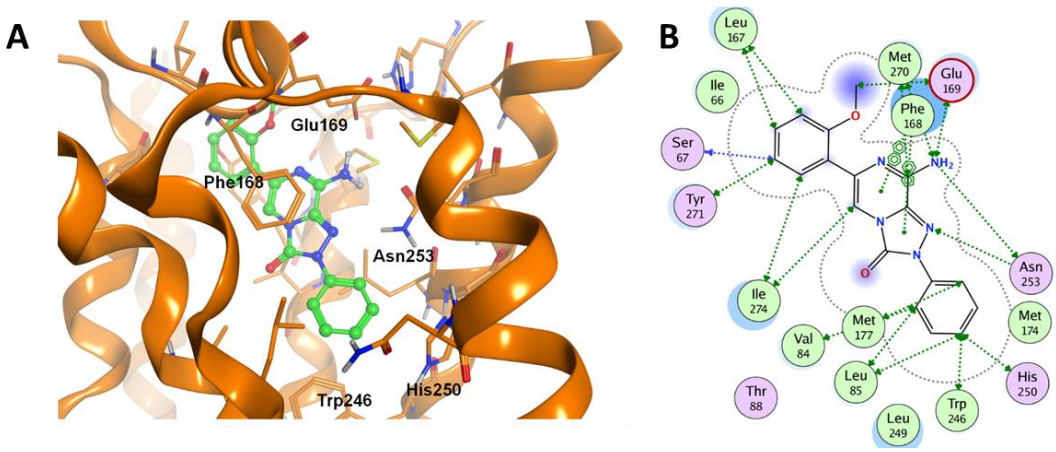

Figure 26. (A) The type-one docking conformation of the synthesized compounds at the hA_{2A} AR cavity, representing the preferred binding mode according to docking-scoring results; compound **11** is represented and key receptor residues are indicated. (B) Schematic description of the ligand-target interaction (built within MOE software).

However, the precence of a nitro group at the ortho position of the 6-phenyl ring (**34**) affords a lower hA_{2A} AR affinity, mainly due to higher hindrance of the substituent and consequent lower ability of the compound to maintain the co-planarity of the 6-phenyl ring with the heterocyclic scaffold. An electronic repulsion with the Glu169 (EL2) side chain is an additional factor at the basis of the lower affinity of this compound. According to the binding data, the presence of small substituent at the meta or para position of the 6-phenyl ring leads, excepting for **17**, **26** and **27**, to a high hA_{2A}AR affinity. Even these compounds appear to exclusively bind this receptor with the "type-one" docking conformation. These groups get located in proximity of H-bond donor functions of the receptor, such as the backbone NH groups of Phe168 and Glu169 (EL2) and the hydroxyl group of Tyr271$^{7.36}$. Even the side chains of (EL2) and Leu267 (EL3) are in proximity to these compound substituents, allowing non-polar interaction. Considering the effects of substituents at the para-position of the 6-phenyl ring, the introduction of a polar hydroxyl group led to a decrease in hA_{2A} AR affinity (**16**, K_i = 45 nM) with respect to the unsubstituted analogue **2**. Docking results suggest that this hydroxy group is inserted within a set of hydrophobic amino acid residues, such as Leu167 (EL2), Leu267 (EL3), and Tyr271$^{7.36}$, thus helping to explain the nonoptimal interaction of the 6-(4-phenol) group (**16**) with the receptor site with respect to the phenyl ring (**2**). On the same basis, we may interpret why the introduction of nonpolar groups at the para-position of the 6- phenyl ring is generally well tolerated, leading to compounds (**13**, **19**, **22**, and **24**) with similar affinity with respect to the corresponding analogue **2**, lacking a substituent on the 6-phenyl ring.

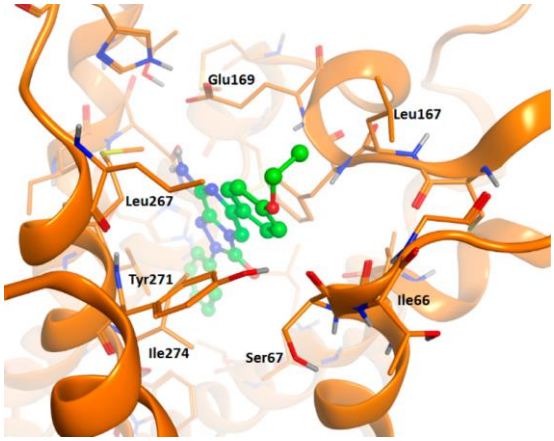

Figure 27. hA_{2A} AR residues located at the entrance of the binding cavity (pdb 4EIY) and able to provide interaction with substituents on the R6 aryl ring.

Figure 27 shows the binding mode of compound **22** with a focus on the residues located in proximity of the R_6 substituent. The para-ethoxy substituent of **22** appears inserted among the above cited hydrophobic residues Leu167 (EL2), Leu267 (EL3), and Tyr2717.36. In the case of derivatives with substituents at the meta position of the 6-phenyl ring, the affinity data show that the nature of the substituent does not significantly influence the receptor−ligand interaction because the presence of a polar hydroxyl group (**15**) or nonpolar functions, such as methoxy or propargyloxy groups (**12**, and **18**, respectively), leads to analogue affinities at the hA_{2A} AR. Figure 27 shows the presence on the receptor of nonpolar groups (i.e., the alkyl chain of Ile66$^{2.64}$) as well as polar functions (i.e., the carbonyl groups of Ile66$^{2.64}$ and Ser67$^{2.65}$) in proximity with the meta position of the 6-phenyl ring.

4.3. Structural refinement aimed at improving drug-like properties: 8-amino-6-(hetero)aryl-1,2,4-triazolo[4,3-a]pyrazin-3-ones 40-61 and 62-68

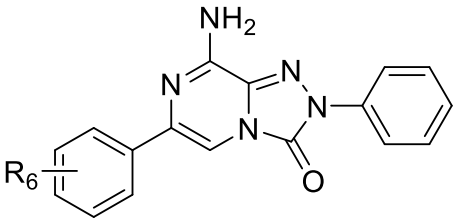

40-61

Table 7

		Binding experiments K_i (nM) [a]			cAMP assays IC_{50} (nM) [a]
	R_6	hA_1 [b]	hA_{2A} [c]	hA_3 [d]	hA_{2B} [e]
40	2-(piperazin-1-yl)	1640 ± 237	1528 ± 100	4465 ± 653	> 30000
41	3-(piperazin-1-yl)	36.1 ± 8.4	ND [f]	410.1 ± 89.2	>30000
42	4-(piperazin-1-yl)	265.1 ± 14.4	90.4 ± 8	1905 ± 314	> 30000
43	3-(N-dimethyl$^+$-piperazin-1-yl)	57.1 ± 2.9	89.8 ± 2.8	3783 ± 667	> 30000
44	3-(4-benzylpiperazin-1-il)-	235.7 ± 39.9	32.3± 7.5	298.1 ± 49.8	> 30000
45	4-(4-benzylpiperazin-1-yl)-	121 ± 28	29 ± 1.5	>30000	> 30000
46	C_6H_4-4-OCH_2-$CONH_2$	391.7 ± 104	26 ± 1.7	604 ± 94	> 30000

47	C_6H_4-4-OCH_2-CN	> 30000	8.2 ± 2.3	> 30000	> 30000
48	C_6H_4-4-O-$(CH_2)_2$-NH_2	288.7 ± 54	14.94 ± 0.1	2131 ± 173.5	> 30000
49	C_6H_4-4-O-$(CH_2)_2$-OH	510 ± 0.2	250 ± 24	>30000	>30000
50	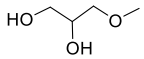	363.7 ± 58	355 ± 93	1774 ± 362	>30000
51	C_6H_4-4-NHCO-$(CH_2)_2$-NH_2	479.2 ± 89	0.59 ± 0.17	509 ± 90	9658 ± 1431
52	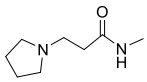	296 ± 36	4.31 ± 0.5	1016 ± 165	>30000
53	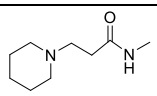	614.1 ± 145	5 ± 1.3	1169 ± 85	>30000
54	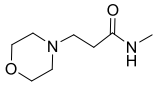	586 ± 164	3.6 ±1.1	1023 ± 76.7	>30000
55	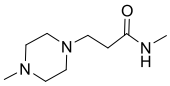	662.8 ± 178	1 ± 2.5	3104 ± 924	>30000
56	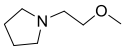	873.5 ± 171	230 ± 50	4303 ±968	>30000
57	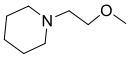	363.3 ± 52.8	45.4 ± 1.5	1062 ± 138	>30000
58	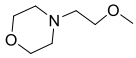	363.2 ± 61	174.4 ± 16	>30000	>30000
59	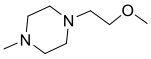	510.3 ± 86	85.2 ± 18	368.7 ± 90	>30000
60	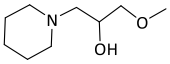	336.1 ± 87	91.7 ± 15	495 ± 112	>30000
61	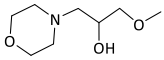	571 ± 47	197 ± 49	780 ± 149	>30000

[a]Data (n = 3–5) are expressed as means ± standard errors. [b]Displacement of specific [^{3}H]-CCPA binding at hA_1 AR expressed in CHO cells. [c]Displacement of specific [^{3}H]-NECA binding at hA_{2A} AR expressed in CHO cells. [d]Displacement of specific [^{3}H]-HEMADO binding at hA_3 AR expressed in CHO cells. [e]IC_{50} values of the inhibition of NECA-stimulated adenylyl cyclase activity in CHO cells expressing hA_{2B} AR.

The set of triazolopyrazines **40-68** (Tables 7 and 8) was designed to obtain derivatives endowed with enhanced water solubility and drug-like properties with respect to the compounds synthesized in the previuos phases of the work. Hence, the 6-phenyl ring was decorated with hydrophilic functions, some of which (substituted piperazines, morpholine, piperidine and pyrrolidine) are a common feature of known potent and selective hA_{2A} AR antagonists, structurally correlated to our series[380]. The selected substituents were attached both directly on the 6-phenyl ring (compounds **40-45**) or

through small alkoxy (derivatives **46-50, 56-61**) and amide (derivatives **51-55**) chains, both linked to the para position of the ring.

Analyzing the binding data**,** it can be observed that some derivatives (**46-48, 51-55**) are endowed with high affinity (K_i hA_{2A} = 0.59-26 nM) and good selectivity for the A_{2A} AR. The most relevant outcomes included derivatives **51-55** which showed hA_{2A} AR affinity values in the range 0.59-5 nM.

Compounds bearing piperazine moieties on the 6-phenyl group (**40-45**) did not showed the expected affinities. Insertion of an unsubstituted piperazine at the ortho position made the compound (**40**) a very weak ligand at all ARs, instead its presence at the para position (**42**) permit a quite good and selective interaction with the hA_{2A} AR (K_i= 90 nM). Unfortunately, we were not able to determine the hA_{2A} AR affinity of the meta- piperazine derivative **41**, for the problems described above for compounds **23**, **25**, **28** and **35**. Also the N,N-dimethylation of the meta-piperazine group afforded a quite good affinity for the hA_{2A} AR (**43**), and an even better substitution was the N-benzylation of the meta- (**44**) or para- (**45**) piperazine, giving rise to low nanomolar affinities at this receptor. In the subsequent modifications, small chains containing $CONH_2$ (**46**), CN (**47**), NH_2 (**48**, **51**) or OH (**49, 50**) as terminal group groups were inserted at the para position of the 6-phenyl ring by an –O- or NHCO linker. Very interestingly, compounds **46**-**48** and **51** were endowed with high affinity (K_i= 0.59-26 nM) and selectivity for the hA_{2A} AR, the most active being derivatives **47** (K_i= 8.2 nM) and **51** (K_i= 0.59 nM). On the contrary, compounds **49** and **50**, bearing, respectively, the 6-(4-(2-hydroxyethoxy)phenyl and 6-(4-(2,3-dihydroxypropoxy)phenyl pendants, emerged as weak hA_1 and hA_{2A} AR ligands. Concerning the set of compounds bearing cyclic amines (piperidine, pyrrolidine, morpholine or substituted piperazines) in the side chain (derivatives **52**-**61**), it can be observed that compounds **52**-**55** are highly potent (K_i = 3.6-11 nM) and selective hA_{2A}AR ligands while compounds **56-59** (K_i = 45-230 nM) are less active at the hA_{2A} subtype, as well as the other ARs. These data highlight that the propanamide linker is more profitable than the ethoxy or propoxy chain for hA_{2A} receptor-ligand interaction.

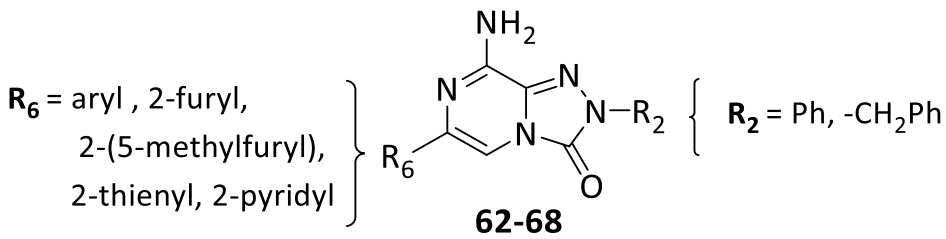

Table 8

			Binding experiments K_i (nM) [a]			cAMP assays IC_{50} (nM) [a]
	R_6	R_2	hA_1 [b]	hA_{2A} [c]	hA_3 [d]	hA_{2B} [e]
62	2-furyl	Ph	13 ± 2	8.4 ± 0.9	120 ± 18	> 30000
63	2-(5-methylfuryl)	Ph	10 ± 2.8	11 ± 1	77 ± 6.5	> 30000
64	2-thienyl	Ph	14.1 ± 3.2	9.0 ± 2.2	42 ± 10.2	> 30000
65	2-pyridyl	Ph	77.4 ± 5.2	13.2 ± 3.8	131.1 ± 30	> 30000
66	Ph	CH_2Ph	2.4 ± 0.5	4.4 ± 0.1	223.7 ± 4.8	> 30000
67	2-furyl	CH_2Ph	13.7 ± 0.3	2 ± 0.1	1131 ± 132	> 30000
68	2-(5-methylfuryl)	CH_2Ph	3.7 ± 0.2	4.6 ± 1.3	112 ± 2	> 30000

[a]Data (n = 3–5) are expressed as means ± standard errors. [b]Displacement of specific [^{3}H]-CCPA binding at hA_1 AR expressed in CHO cells. [c]Displacement of specific [^{3}H]-NECA binding at hA_{2A} AR expressed in CHO cells. [d]Displacement of specific [^{3}H]-HEMADO binding at hA_3 AR expressed in CHO cells. [e]IC_{50} values of the inhibition of NECA-stimulated adenylyl cyclase activity in CHO cells expressing hA_{2B} AR.

Other structural modifications, supposed to be advantageus for improving drug-like properties, were made by replacing the 6-phenyl ring of the reference ligand **2** with a heterocyclic moiety (2-furyl, 2-(5-methylfuryl), 2-thienyl, 2-pyridinyl). Compounds **62-65** maintained a high affinity for both hA_1 and hA_{2A} ARs (K_i= 8.4-13.2 nM) while showing an enhanced selectivity versus the hA_3 subtype (Table 8). Furthermore, derivatives bearing a benzyl chain at position 2, combined with a phenyl, 2-furyl and a 2-(5-methylfuryl) at position 6 (compounds **66-68,** Table 8), were synthesized because the 2-benzyl pendant, being more flexible than the 2-phenyl moiety, was thought to enhance the solubility of the compounds. This type of decoration was also suggested by the binding results previously obtained in our pyrazolopyrimidine series[393] in which combination of a benzyl moiety with a 2-furyl substituent shifted affinity toward the hA_{2A} AR. In the triazolopyrazine series, this modification enhanced both hA_1 and hA_{2A} AR affinities (compare the 2-benzyl derivative **66-68** with the relative 2-phenyl derivatives **2**, **62, 63**)

while reducing ability to bind the hA_3 AR. Compounds **66-68** are indeed dually potent hA_1 (K_i =2-4.6 nM) and hA_{2A} ligands (K_i= 2.4-13 nM).

Derivative **68,** able to bind both hA_1 (K_i= 3.7 nM) and hA_{2A} (K_i= 4.6 nM) ARs with nanomolar affinity, was selected to evaluate its antagonistic profile by measauring the effect on cAMP production in CHO cells, stably expressing hA_1 and hA_{2A} ARs. The obtained results (Table 9) showed that the compound behaved as antagonist being able to counteract NECA-inhibited (A_1) or NECA-stimulated (A_{2A}) cAMP accumulation.

Table 9. Potencies of compound **68** at hA_1 and hA_{2A} ARs.

	hA_1 IC_{50} (nM)[a]	hA_{2A} IC_{50} (nM)[b]
68	675 ± 123	521 ± 79

[a]IC_{50} values obtained counteracting the NECA-induced decrease of cAMP accumulation in CHO cells expressing hA_1R. [b]IC_{50} values obtained by inhibition of NECA-stimulated adenylyl cyclase activity in CHO cells expressing $hA_{2A}R$.

To verify if the performed modifications are effective or not in improving solubility and physicochemical properties of the compounds, further investigations are needed. However, we are confident about the successful outcome since for most of derivatives **40-68**, lower melting points (200-270 °C), a better solubility in the most common organic solvents (methanol, ethanol, nitromethane etc.), as well as less drastic recrystallization conditions, have been observed.

4.3.1. Molecular modeling studies

Molecular docking studies at the $A_{2A}AR$ crystal structure were carried out on compounds **42-45** (Table 7) to depict their hypothetical binding mode. The obtained results highlighted that derivatives **43** and **44** bearing large substituents at the meta position of the 6-phenyl ring adopt the "type-one" docking conformation, presenting the 2-phenyl-ring located in the depth of the cavity and the 6-aryl group at the entrance of the binding site. Compounds **42** and **45,** featuring a large substituent at the para position of the same ring, were also investigated, showing an upside-down conformation, where the 2-phenyl ring was inserted in the depth of the cavity while the scaffold was oppositely oriented with the 3-carbonyl group pointing toward the $Asn253^{6.55}$ amide function (Figure 28).

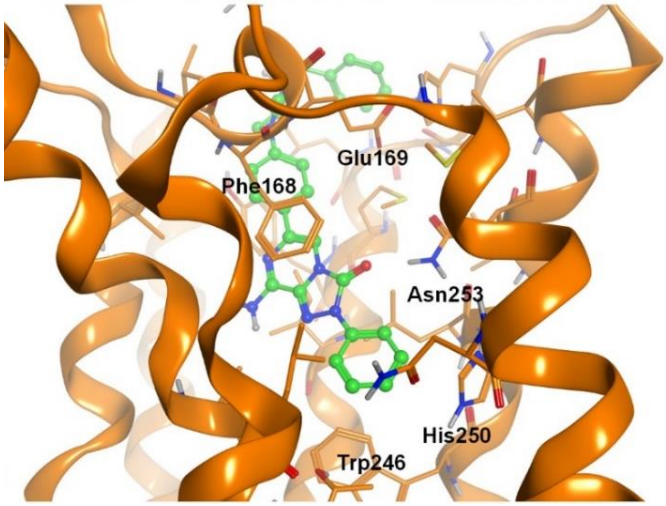

Figure 28. Alternative binding mode of the synthesized compounds presenting a large substituent in the para-position of the 6-phenyl ring (compound **45** is shown). The key ligand-target polar interaction is between the 3-carbonyl group of the compound and the Asn253$^{6.55}$ amide function.

Compounds **62-65**, bearing a heterocyclic moiety at the 6-position and a phenyl ring at the 2-position, may adopt both type-one and type-two docking conformations, like compound **2**, with a fair preference for the type-two conformation (the one pointing the 2-phenyl ring toward the extracellular environment). This behaviour may explain the high affinity of these derivatives for the hA_{2A} AR binding cavity, analogously to the reference compound **2**. When the 2-phenyl ring is replaced by a benzyl moiety and a heterocyclic ring is inserted at the 6-position (**66**-**68**), the compounds preferentially adopt a type-two docking conformation pointing the 2-substituent toward the extracellular environment. For both these sets (**62**-**65** and **66**-**68**) the steric and chemical-physical profile of the 6 substituent modulates the hA_{2A} AR affinity, with the 2-furyl providing the highest affinity data within each set, as expected.

4.4 Design of dual A_{2A} AR antagonist-antioxidant triazolopyrazines: 8-amino-6-aryl-2-phenyl-1,2,4-triazolo[4,3-*a*]pyrazin-3-ones 69-86

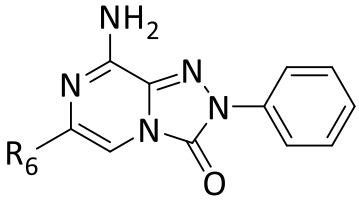

69-78

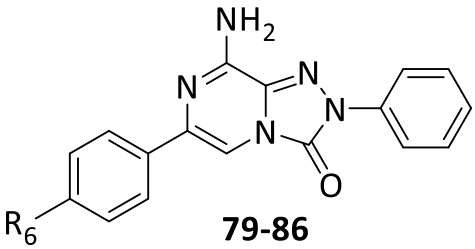

79-86

Table 10		Binding experiments K_i (nM) [a]			cAMP assays IC_{50} (nM) [a]
	R_6	hA_1 [b]	hA_{2A} [c]	hA_3 [d]	hA_{2B} [e]
69	C_6H_4-2,4-diOCH_3	28 ± 0.26	2.4 ± 0.48	118 ± 6.6	>30000
70	C_6H_4-3,4-diOCH_3	59.0 ± 12.7	5.68 ± 0.78	80.1±15.8	>30000
71	C_6H_4-3,4,5-triOCH_3	55 ± 16	3.5 ± 0.8	214 ± 4.4	>30000
72	C_6H_4-4-OCH_3-3,5-diCH_3	4.5 ± 1.4	0.17 ± 0.0046	8.6 ± 1.7	>30000
73	C_6H_4-4-OCH_3-3,5-ditBu	108.5 ± 17	141.6 ± 34	>30000	>30000
74	C_6H_4-2-OCH_3-4-OH	29.8 ± 1.6	16.8 ± 0.87	11130 ± 975	> 30000
75	C_6H_4-3,4-diOH	42.6 ±9.6	5.21 ± 0.5	950±200.4	>30000
76	C_6H_4-3,4,5-triOH	175.5 ± 3	94.5± 21	5575±989	17.330±3365
77	C_6H_4-4-OH-3,5-diCH_3	21.3 ± 7	2.5 ± 0.78	100 ± 0.7	>30000
78	C_6H_4-4-OH-3-tBu	>30000	8.47 ± 1.4	>30000	>30000
79	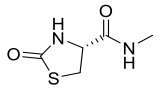	504 ± 129	8.1 ± 0.83	1140 ± 167	>30000
80	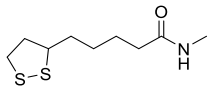	8.4 ± 0.39	5 ± 0.62	>30000	>30000
81	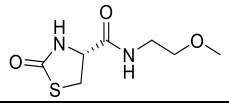	173.4 ± 37	1.7±1.4	868±169	>30000
82	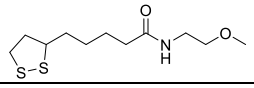	378.6	2.4±0.3	>30000	4097±812
83	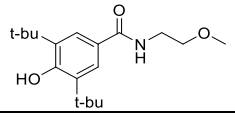	13670 ± 275	14750 ± 270	>30000	>30000
84	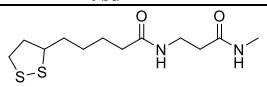	1359 ± 284	36.4 ± 8.2	>30000	>30000

85	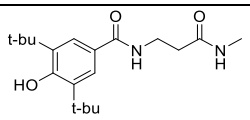	>30000	54.5 ± 7.1	>30000	>30000
86	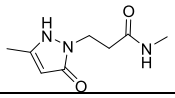	581.4±40.3	91±8.5	>30000	>30000

[a]Data (n = 3−5) are expressed as means ± standard errors. [b]Displacement of specific [^{3}H]-CCPA binding at hA_1 AR expressed in CHO cells. [c]Displacement of specific [^{3}H]-NECA binding at hA_{2A} AR expressed in CHO cells. [d]Displacement of specific [^{3}H]-HEMADO binding at hA_3 AR expressed in CHO cells. [e]IC_{50} values of the inhibition of NECA-stimulated adenylyl cyclase activity in CHO cells expressing hA_{2B} AR.

Finally, a new set of 8-amino-1,2,4-triazolo[4,3-a]pyrazin-3-ones (**74-86,** Table 10) bearing potential antioxidant moieties at the 6-position were synthesized and pharmacologically evaluated. These compounds can be divided into two sets: derivatives **74-78,** featuring substituted phenol rings at the 6-position, and compounds **79-86,** bearing antioxidant moieties on the lateral chain linked to the para position of the 6-phenyl ring. The affinity data**,** reported in Table 10, indicate that the presence of differently substituted phenols (compounds **74-78**) at the 6-position shifted affinity towards both the hA_1 (K_i = 21.3-175 nM) and A_{2A} (K_i = 2.5-94 nM) ARs. Within this set of compounds, the 6-(3-(tert-butyl)-4-hydroxyphenyl derivative **78** turned out to be a highly potent (K_i = 8.47 nM) and selective hA_{2A} AR ligand while compounds **74, 75** and **77** bind both hA_1 (K_i = 21.3-42.6 nM) and hA_{2A} (K_i = 2.5-16.8 nM) ARs with nanomolar affinity and different degrees of selectivity versus the hA_3 subtype. Among the latter derivatives, the best in terms of hA_{2A} affinity were **75** and **77**, displaying K_i values in the range of 2.5-5.21 nM. The methoxy derivatives **69-73,** synthetic precursors of the desired phenols **74-78**, were also tested to evaluate their affinity at ARs. The obtained binding data for this subset indicated that the contemporary presence of two or three methoxy groups on the 6-phenyl ring led to compounds (**69-71**) possessing high affinity for both hA_1 (K_i = 28-59 nM) and hA_{2A} (K_i = 2.4-5.68 nM) ARs, and also able to bind to the hA_3 AR subtype (K_i = 80.1-214 nM). Compound **72**, instead, bearing the 6-(3,5-dimethyl-4-methoxyphenyl) residue, showed subnanomolar hA_{2A} AR affinity (K_i = 0.17 nM) and was also able to bind efficiently the hA_1 and hA_3 ARs with K_i values of 4.5 and 8.6 nM respectively. Replacement of the methyl groups of **72** with t-butyl moieties (compound **73**) completely changed the affinity profile. In fact, the 6-(3,5-ditert-butyl-4-methoxyphenyl) derivative **73** shows a marked reduced affinity for both hA_1 (K_i = 108.5 nM) and hA_{2A} (K_i = 141.6 nM) ARs and completely lacks activity at the A_3 AR subtype. Other

groups supposed to exert antioxidant properties (see "Aim of the work") were introduced, by suitable spacers, at the para position of 6-phenyl ring. The (S)-2-oxothiazolidine-4-carboxylic acid (OTC) residue achieved good results since the triazolopyrazines **79**, **81** were endowed with high affinity (K_i = 8.1 and 1.7 nM respectively) and selectivity at the hA_{2A} AR. Also the lipoic acid residue, either directly appended on the para-amino function (compound **80**) or spaced by a chain (compounds **82**, **84**) was well tolerated by the hA_{2A} AR. In fact, compounds **82** and **84** emerged as highly potent and selective hA_{2A} AR ligands (K_i = 2.4 and 36.4 nM respectively) and derivative **80** also efficiently binds the hA_{2A} AR (K_i = 5 nM), even though showing high hA_1 AR affinity (K_i = 8.4 nM). It is worth noting that the presence of the ethoxy or propanamide spacer shifted the selectivity toward the A_{2A} AR (compounds **82** and **84**).

The presence of the 3,5-di-tert-butyl-4-hydroxybenzoic acid residue on the lateral chain of derivatives **83** and **85** led to opposite results in terms of AR affinity depending on the linker, -O- and -NHCO-, binding the chain to the 6-phenyl ring. The amide linker might confer more rigidity to the moiety, thus, probably, stabilizing the proper binding conformation of the triazolopyrazine **85**, which showed high affinity (K_i = 54 nM) and selectivity at the hA_{2A}AR. In contrast, compound **83**, featuring a more flexible pendant due to the –O- linker, completely lacks affinity towards all the ARs. Molecular docking studies are in progress to interpret these affinity data. The 5-methyl-1,2-dihydro-3H-pyrazol-3-one ring, appended on compound **86**, was chosen as potential antioxidant moiety because it plays a key role in the antioxidant mechanism of action[410] of edaravone, an approved anti-cerebral ischemia drug. This modification turned out to be advantageous since derivative **86** possesses good nanomolar affinity (K_i = 91 nM) toward the hA_{2A}AR and is also able to bind the hA_1 AR subtype with a 6-fold reduced activity.

The triazolopyrazines **75-80, 82**, bearing potential antioxidant functions, and endowed with high hA_{2A}AR affinity, were selected to evaluate their stability in human plasma, and in tris(hydroxymethyl)aminomethane/HCl (Tris/HCl) and phosphate buffer solutions (PBS). These tests are being performed by the research group of Prof. Gianluca Bartolucci, at the NEUROFARBA Department – Pharmaceutical and Nutraceutical Section, of the University of Florence. Preliminary results suggested that the tested compounds are, on the whole, stable in the assayed conditions (data not shown).

4.4.1 Molecular modeling studies

Molecular docking studies on compound **79** and **80** (Table 10), bearing antioxidant residues at 6-phenyl level**,** were carried out to determine the hypothetical binding mode at the A_{2A}AR crystal structure (PDB: 4EIY) and to gain useful information for the design of new hA_{2A} AR antagonists. The obtained results showed that these molecules bind to the receptor binding pocket with the preferred "type one" arrangement. The triazolopyrazinone scaffold has been demonstrated to be able to interact with Asn253$^{6.55}$ and Glu169 (EL2) through H-bond contacts and with the phenyl ring of Phe168 (EL2) through a π-π interaction[410]. Moreover, π-π interaction between Phe168 and the bicyclic core were evidenced, as well as hydrophobic interaction between Leu167, 267 and the lipoic and the (S)-2-oxothiazolidine-4-carboxylic acid moieties (Figure 29).

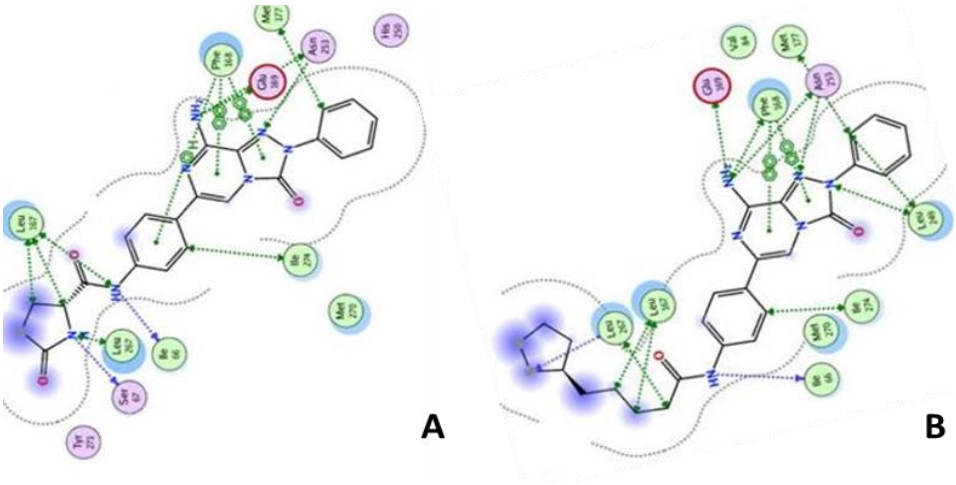

Figure 29. Schematic description of ligand–target interaction of derivatives **79** (A) and **80** (B) in the hA2A AR (built with MOE software).

4.5 Pharmacological studies

Based on their affinity and selectivity profile at ARs, some of the synthesized compounds (**13, 31, 32** and **68**) indentified in the second phase of the work (see "Aim of the work") were selected to investigate their in vitro neuroprotective properties in PD and AD models. The 6-(4-methoxyphenyl)-2-phenyl-triazolopyrazine derivative **13**, showing high affinity (K_i = 7.2 nM) and selectivity at the hA_{2A} AR, was evaluated for its ability in counteracting the MPP^+ induced neurotoxicity in cultured human neuroblastoma SH-SY5Y cell lines, a widely used cellular PD model[427,428]. Compound **31**, highly selective at the hA_{2A}

subtype, and derivatives **32** and **68**, able to bind both hA_1 and hA_{2A} ARs with nanomolar affinity, were profiled for their neuroprotective effect against the β-amyloid peptide (Aβ)-induced toxicity[429].

4.5.1 Neuroprotection Studies in MPP^+-induced toxicity in SH-SY5Y Cell Lines

As reported above (see "Introduction"), interest in the use of A_{2A} AR antagonists in PD has increased because they proved to be beneficial both in relieving motor symptoms and neuropsychiatric impairments of the disease[430,431] but, more importantly, because they might be helpful in counteracting neurodegeneration[190,432]. In fact, animal models of PD highlighted the A_{2A} AR antagonist ability to protect nigral dopaminergic neurons from death induced by 1-methyl-4-phenyl-1,2,3,6-tetrahydropyridine (MPTP)[190], thus slowing the deterioration of dopamine-producing cells and modifying the disease progression. Related to this, the A_{2A} AR antagonist protective effect against the MPTP-induced toxicity is probably associated to a mechanism counteracting neuroinflammation and involving A_{2A} AR on glial cells[190,433]. The aim of the herein reported study was to examine the efficacy of compound **13** in counteracting the 1-methyl-4-phenyl-pyridinium (MPP^+) induced neurotoxicity on SH-SY5Y cells in an in vitro model of PD. A large wide of evidence indicates that SH-SY5Y cells possess many features of dopaminergic neurons and have been widely employed for the study of neuroprotection against PD-related neurotoxins. MPP^+ is a well-recognized dopaminergic neurotoxin resulting from the metabolic transformation of MPTP and able to induce cell death through a series of processes such as oxidation, hydrogen peroxide formation, and direct inhibition of the mitochondrial respiratory chain[434]. These studies were carried out in collaboration with Dr. Teresa De Vita, from the Italian Institute of Technology (IIT) of Genova. First, a pilot study was conducted to evaluate the neurotoxic effect produced by MPP^+ on SH-SY5Y cells. Cells were treated for 24 h with increasing doses of MPP^+ (50 µM to 3 mM).

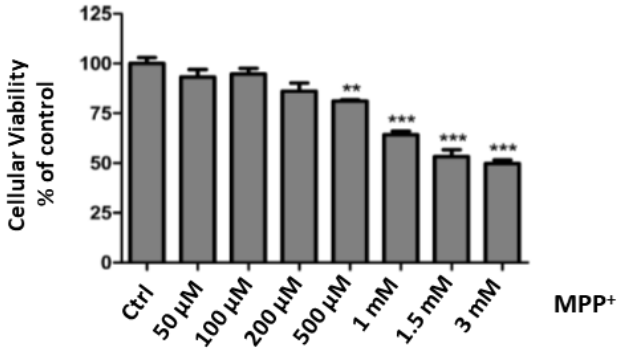

Figure 30. Dose dependency of MPP+ in SH-SY5Y cells. Cellular viability was carried out after 24 h of MPP+. Effect of MPP+ on cell viability was measured by CellTiter-Glo luminescent assay. Data are expressed as mean of three independent experiments. **P < 0.01 compared with control; ***P < 0.001 compared with control

The results in Figure 30 show that MPP+ produced a significant and concentration-dependent neurotoxic effect in this cell line. The dose of 1.5 mM, which caused 50% of cell death, was chosen for the subsequent neuroprotection studies. Compound **13**, when administered alone, did not modify cell viability (Figure 31, A) while at the concentration of 15 nM it was able to partially counteract MPP+-induced neurotoxicity (Figure 31, B).

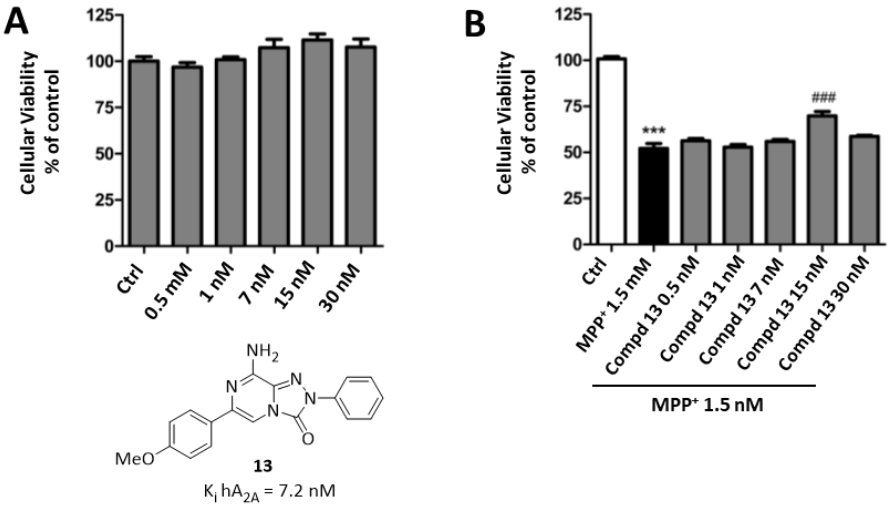

Figure 31. SH-SY5Y cells were treated for 24 h with different concentrations of compound **13** from 0.5 to 30 nM, alone (**A**) and inthe presence of MPP+ 1.5 mM (**B**). Compound **13** proved not to be toxic and neuroprotective against MPP+ in SH-SY5Y cells after CellTiter-Glo luminescent cell viability assay. Data are expressed asmean of three independent experiments. ***P < 0.001 compared withcontrol, ###P < 0.001 compared to MPP+ 1.5 mM.

To verify that the protective effect of **13** was due to the selective blockade of the A_{2A} AR, we compared the effects of the compound with those of the well-known selective hA_{2A}

AR antagonist 4-(2-[7-amino- 2-(2-furyl[1,2,4]-triazolo[2,3-a][1,3,5]triazin-5ylamino]ethyl)- phenol ZM241385[435] and we evaluated the effects of **13** in the presence of the selective hA_{2A} AR agonist 2-[p-(2-carboxyethyl)phenethylamino]-5'-N-ethylcarboxamido adenosine CGS21680[436]. As shown in Figure 32 A, the hA_{2A} AR antagonist ZM241385, used at the concentration of 0.5 nM[427], presented a neuroprotective effect on SH-SY5Y cells, thus counteracting MPP^+ toxicity. To validate the involvement of the A_{2A} AR in the neuroprotective activity of **13** against MPP^+ toxicity, we evaluated the ability of the hA_{2A} AR agonist CGS21680 to reverse the effects of compound **13**. SH-SY5Y cells were treated with **13** (15 nM) in the presence of different CGS21680 concentrations ranging from 10 to 100 nM. As shown in Figure 32 B, the hA_{2A} agonist CGS21680 was able to suppress the protective effects of **13**, thus confirming that the its effects may be attributed to the selective blockade of the A_{2A} AR.

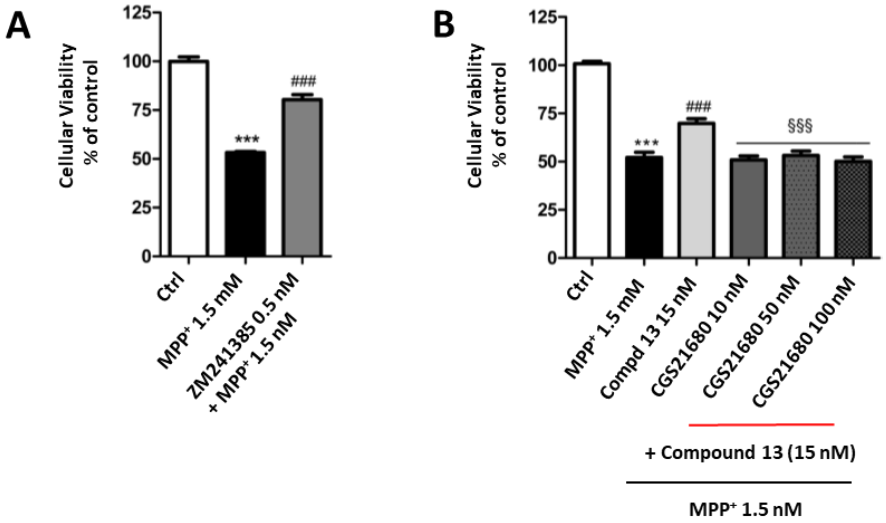

Figure 32. Reference hA_{2A} antagonist ZM241385-induced neuroprotection against MPP^+ toxicity in SH-SY5Y cells (A). Neuroprotection inducedby the hA_{2A} antagonist **13** is lost by the coadministration of the selective hA_{2A} agonist CGS21680. SH-SY5Y cells were treated for 24 h with 1.5 mM MPP^+ in absence and in the presence of 15 nM of compound 13 and different concentrations of the agonist CGS21680, from 10 to 100 nM (B). Cell viability was evaluated by using CellTiter-Glo luminescent assay. Data are expressed as mean of three independent experiments. ***P <0.001 compared with control, ###P < 0.001 compared to MPP^+ 1.5mM, §§§P < 0.001 compared with MPP^+ 1.5 mM + **13** 15 nM.

4.5.2 Neuroprotection studies in β-amyloid peptide (Aβ)-induced toxicity in SH-SY5Y cells

In the last decade, several human studies highlighted the beneficial effects of caffeine, a non-selective A_1 and A_{2A} AR antagonist, in reducing the risk of developing AD and PD[437-440]. The caffeine protective effect was also investigated in animal models of AD and PD turning out to be related, among other pathways, to antagonism of the A_{2A} AR subtype[140,441]. Moreover, in AD models, both caffeine and the potent A_{2A} AR antagonist ZM241385 proved to be effective in preventing cell death after exposure of rat cultured cerebellar granule neurons to Aβ-amyloid peptide (25-35)[140]. Recently, also the A_1 AR antagonism was recognized to afford neuroprotection in a model of combined neurotoxicity, in fact, the protective effect of dual A_1 and A_{2A} AR blockade in counteracting β-amyloid toxicity in neuroblastoma cells exposed to aluminium chloride has been demonstrated[429]. Within the synthesized compounds, the highly potent and selective hA_{2A} AR antagonist **31** togheter with the dual potent hA_1/A_{2A} AR ligands **32** and **68** were chosen to evaluate their ability in counteracting β-amyloid peptide (Aβ)-induced toxicity. For this purpose we used the neuronal cell line SH-SY5Y a widely emplyed catecholaminergic *in vitro* model for studies on pathologies or toxicities affecting the nervous system[429, 442-444]. The 25-35 aminoacids Aβ fragment was used for setting up a model of neurotoxicity[429]. It was previously incubated (at 2 and 10 µM) at 37 °C to allow peptide aggregation, 3 and 7 days were evaluated to establish the optimal timepoint. The obtained aggregates were incubated with cells for increasing times (24, 48 and 72 h), subsequently cell viability was assessed via the MTT assay. Results are shown in Table 11, we chose 48 h incubation with 7 days aggregated-Aβ as the most suitable, concentration-dependent condition for screening the new synthesized compounds (cell viability of control was arbitrarily set to 100%).

Table 11. Toxic effect induced by β-amyloid protein (Aβ fragment 25-35 aa)[a]

Time of incubation with cells	Cell viability %		Time of preventive aggregation of Aβ 25-35	
24 h			**3 days**	**7 days**
	Control	100 ± 4.2		
	Aβ 25-35, 2 μM		92.8 ± 1.9	69.6 ± 2.9**
	Aβ 25-35, 10 μM		80.3 ± 4.5*	64.4 ± 3.8**
48 h			**3 days**	**7 days**
	Control	100 ± 7.2		
	Aβ 25-35, 2 μM		80.5 ± 7.6	**73.3 ± 2.1***
	Aβ 25-35, 10 μM		69.8 ± 5.4**	**63.2 ± 4.6****
72 h			**3 days**	**7 days**
	Control	100 ± 8.9		
	Aβ 25-35, 2 μM		95.5 ± 15.1	108.1 ± 16.3
	Aβ 25-35, 10 μM		83.0 ± 11.4	68.7 ± 8.7**

[a]Aggregation of β-amyloid protein (Aβ fragment 25-35 aa; 2 and 10 μM) was allowed for 3 and 7 days at 37°C. The so obtained different proteins aggregates were tested in SH-SY5Y cell ($1x10^4$ cell/well) to evaluate the cytotoxic effect. Incubation was performed for increasing times (24, 48 and 72 h), subsequently cell viability was assessed via the MTT assay. Viability is expressed as % in comparison to the control cells (arbitrarily set 100 % of viable cells). Data are presented as mean ± SEM of 3 different experiments performed in quintuplicate. One-way ANOVA with a Bonferroni post-hoc test was used to compare different treatments. *P<0.05 and **P<0.01 *versus* control.

Derivatives **31**, **32** and **68** (0.1–1 μM) were co-incubated with SH-SY5Y cells ($1x10^4$ cell/well) for 48 h in the presence of Aβ 25-35 (2 and 10 μM). Figure 33 shows the decrease of cell viability induced by 2 μM Aβ up to 73.3 ± 2.1%. Compound **68** is able to significantly prevent Aβ toxicity starting from concentration 0.1 μM restoring the cell viability till to control level at 0.3 μM. Compound **31,** instead**,** proved to be effective in counteracting the Aβ induced neurotoxicity starting from 0.3 μM concetration. On the other hand, higher concentration of Aβ 25-35 (10 μM, previously aggregated for 7 days) decrease cell vitality to 63.2 ± 4.6% (Figure 34). Compound **31** was protective when co-incubated at 0.3 μM whereas **68** was able to significantly prevent cell mortality from 0.1 μM (Figure 34). In the concentration range 0.1-3 μM, caffeine was ineffective. These

studies were performed by Dr. Lorenzo Di Cesare Mannelli at the NEUROFARBA Department – Pharmacology and Toxicology section, of the University of Florence.

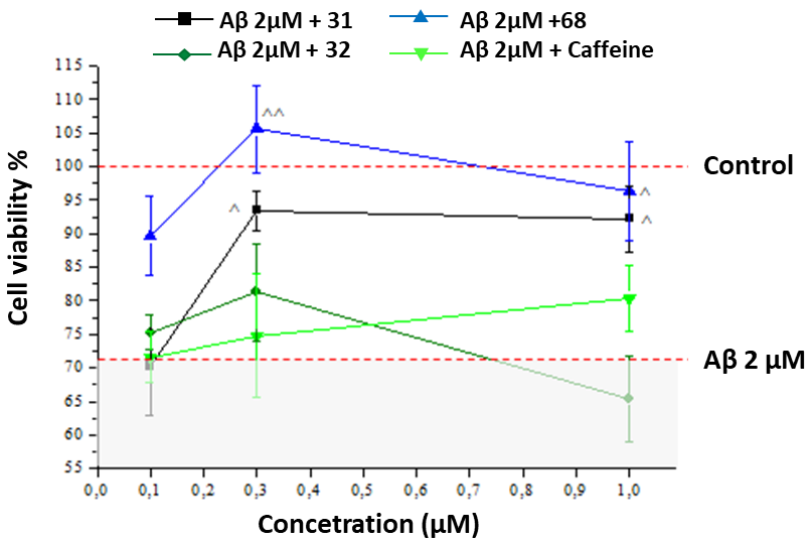

Figure 33. SH-SY5Y cell (1x10^4 cell/well) were incubated 48 h with compounds **31**, **32** and **68** (0.1, 0.3 and 3 μM) in the presence Aβ-amyloid peptide (Aβ fragment 25-35 aa; 2 μM following 7 days of 37 °C aggregation). Caffeine was used as reference compound. Cell vitality was assessed via MTT assay. Viability is expressed as % in comparison to the control cells (arbitrarily set 100 % of viable cells). Dashed lines represent values of control and Aβ-treated samples. Data are presented as mean ± SEM of 3 different experiments performed in quintuplicate. One-way ANOVA with a Bonferroni post-hoc test was used to compare different treatments. ^P<0.05 and ^^P<0.01 *versus* β-amyloid effect.

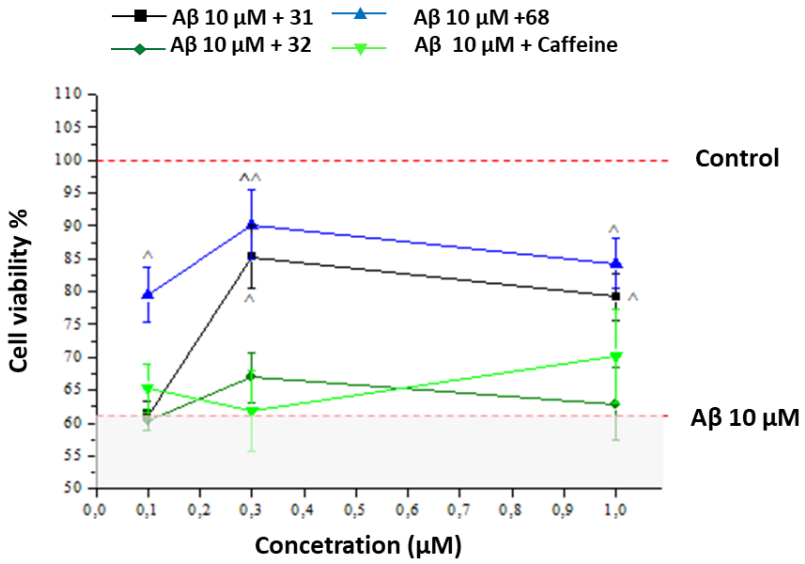

Figure 34. SH-SY5Y cell (1x10^4 cell/well) were incubated 48 h with compounds **31**, **32** and **68** (0.1, 0.3 and 3 μM) in the presence Aβ-amyloid peptide (Aβ fragment 25-35 aa; 10 μM following 7 days of 37 °C aggregation). Caffeine was used as reference compound. Cell vitality was assessed via MTT assay. Viability is expressed as % in comparison to the control cells (arbitrarily set 100 % of viable cells). Dashed lines represent values of control and Aβ-treated samples. Data are presented as mean ± SEM of 3 different experiments performed in quintuplicate. One-way ANOVA with a Bonferroni post-hoc test was used to compare different treatments. ^P<0.05 and ^^P<0.01 *versus* β-amyloid effect.

4.5.3 Neuroprotection studies in oxaliplatin-induced neurotoxicity in microglia cells

As previously reported in the "Introduction", the anticancer drug oxaliplatin leads to the development of neuropathic syndrome with paresthesia, dysesthesia, and pain. Despite informations about the molecular basis underlyng the neuropathy are unclear, some experimental evidences point toward a correlation between oxidative stress damage and neuropatic pain (NP) onset[374,445]. The aim of the current study was to determine the potential protective effects of the novel triazolopyrazines **47**, **78**, **82**, **84** and **85** against the oxaliplatin-induced neurotoxicity in rat microglia cells. These compounds were chosen taking into account their high affinity and selectivity toward the $hA_{2A}AR$ but also for the presence, in some of them (**78**, **82**, **84** and **85**), of antioxidant moieties which were envisaged to counteract the oxidative stress-neurotoxicity. Before to perform these studies, the antagonistic properties of the derivatives were preliminarly demonstrated in functional cAMP assays (data not shown).

Primary rat microglia cells have been obtained then they were treated with oxaliplatin in the absence or in the presence of the tested compounds. Oxaliplatin damage was evaluated as cell viability and oxidative stress as previously described as a main damage evoked by oxaliplatin[374,445]. The new synthesized compounds were tested at 10 µM, the maximum soluble concentration. Oxaliplatin, concentration-dependently, strongly reduced microglia viability (MTT test) after 24 h incubation (33% and 19% viability with 10 and 30 µM, respectively, in comparison to 100% of control condition).

This oxaliplatin-induced neurotoxicity assay was performed by Dr. Lorenzo Di Cesare Mannelli at the NEUROFARBA Department – Pharmacology and Toxicology section, of the University of Florence. The obtained results showed that derivative **82** was the most active in prevent the oxaliplatin damage also when incubated at the high concentration while **47** was effective against 10 µM oxaliplatin. With regard to the other tested compounds, only a partial activity has been observed for derivatives **78** and **85** whereas **84**, contrary to our expectations, turned out to be ineffective (Table 12).

Table 12	Cell viability (%)[a]		
	Oxa 0 µM	**Oxa 10 µM**	**Oxa 30 µM**
Control	100.0 ± 7	33.2 ± 1.3**	19.1 ± 0.8**
DMSO 0.75%	90.9 ± 8		
47 10 µM		**48.7 ± 0.8**^^**	23.0 ± 0.9
78 10 µM		46.4 ± 1.4^^	28.6 ± 1.21^
82 10 µM		**54.5 ± 1.9**^^**	**34.2 ± 0.60**^**
84 10 µM		38.9 ± 1.6	18.3 ± 0.3
85 10 µM		43.5 ± 1.8^	30.6 ± 2.2^

[a]Cell viability. Primary rat microglia cells were plated 4000 cells/well and 24 hours later cells were treated with oxaliplatin 10 and 30 µM in presence of **47, 78, 82, 84, 85** at 10 µM for 24 hours. Cell vitality was assessed via MTT assay. Viability is expressed as % in comparison to the control cells (arbitrarily set 100 % of viable cells). Data are presented as mean ± SEM. *P<0.05 and **P<0.01 versus control; ^P<0.05 and ^^P<0.01 versus oxaliplatin.

Further investigations were carried out these compounds by evaluating their ability to prevent the oxaliplatin-dependent increase of the SOD-inhibitable superoxide anion (cytochrome C assay). According to the obtained data, compounds **82** and **85** proved to be effective in significantly decrease the oxygen free radical level thus suggesting a direct antioxidant activity or, hypothetically, a protective property against mitochondrion (Figure 35).

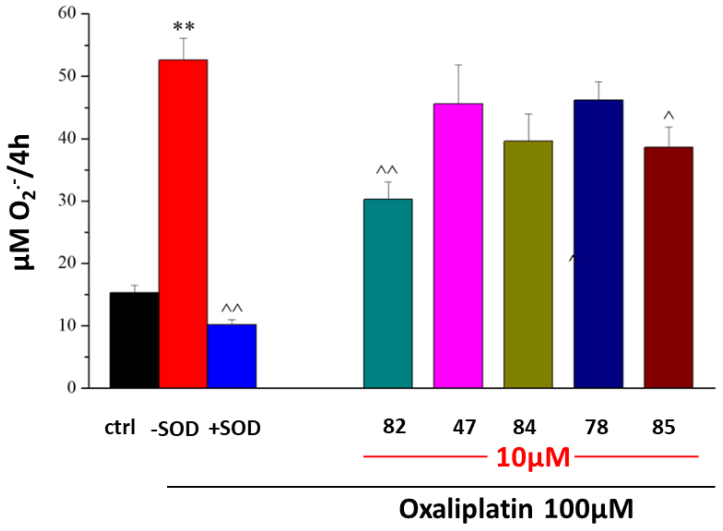

Figure 35. SOD-inhibitable $O_2^{\cdot-}$ concentrations. Microglia cells (5×10^5 cells/well) were exposed to 100 µM oxaliplatin for 4 h in the absence or presence of tested compounds (10 µM). $O_2^{\cdot-}$ concentration was evaluated by cytochrome *c* assay. The nonspecific absorbance was measured in the presence of SOD (300 mU/ml) and subtracted from the total value. Values are expressed as the mean ± SEM of three experiments. *P<0.05 and **P<0.01 versus control; ^P<0.05 and ^^P<0.01 versus oxaliplatin.

The activity of the detoxifying enzyme catalase was also measured to study the potential effect of new compounds on peroxisomes, the other intracellular organelle involved in the redox balance. As shown in Figure 36, oxaliplatin impaired peroxisome functionality reducing catalase activity while **82** and **85** significantly prevented the damage.

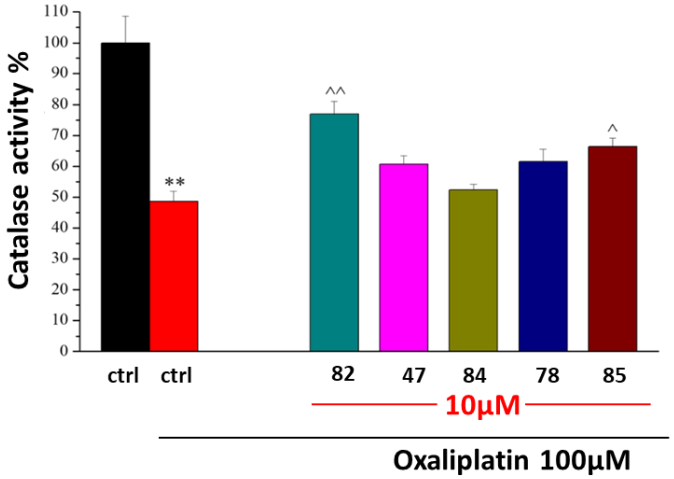

Figure 36. Activity of catalase. Microglia cells ($5 \cdot 10^5$ cells/well) were treated with oxaliplatin (10 µM) in the absence or in the presence of new compounds (10 µM). Activity was measured after 24h incubations. Values are expressed as the mean ± S.E.M. percent of control of three experiments. Control condition was arbitrarily set as 100%. *P<0.05 and **P<0.01 versus control; ^P<0.05 and ^^P<0.01 versus oxaliplatin.

5. CONCLUSIONS

The research activity accomplished in this PhD thesis led to the identification of the new and versatile 8-amino-1,2,4-triazolo[4,3-*a*]pyrazin-3-one scaffold which was successfully employed to obtain highly potent and selective antagonists for the hA_{2A} AR and compounds able to bind with high affinity both the hA_1 and the hA_{2A} ARs. These type of AR antagonists have attracted our attention for their therapeutic potential in neurodegenerative disorders, such as PD and AD.
Different sets of triazolopyrazines were designed and synthesized with diverse aims.

The first set of compounds (**1-10**) was prepared to carry out a preliminary SAR study, and point out the basic structural requirements to target the A_{2A} AR. The 2,6-diphenyl substituted compound **2** was the most notable within this set of ligands, possessing nanomolar affinity for hA_1, hA_{2A} and hA_3 ARs (K_i = 10-13 nM).

In the subsequent phase of the work a structural refinement was performed to enhance hA_{2A} AR affinity and selectivity and expand the SAR study. Within this set of AR ligands (**11-39**), some derivatives (**13, 19, 22, 24, 31** and **36**) turned out to be highly potent and selective hA_{2A} AR ligands (K_i = 2.9- 10.6 nM) while others (**15, 30, 32, 33, 38** and **39**) were able to efficiently bind both the hA_1 (K_i = 4.7-33.5 nM) and hA_{2A} ARs (K_i = 3.5-22.9 nM). Selected derivatives (**13, 31** and **32**), proved to be potent A_{2A} AR antagonists, were further investigated for their in vitro neuroprotective effects. Compound **13,** at 15 nM concentration, showed protective effect against the MPP^+ induced-neurotoxicity in SH-SY5Y cells, a widely used cellular PD model. Derivative **31,** at 0,3 µM concentration, demonstrated ability in counteracting the Aβ-amyloid peptide-induced toxicity in an AD model.

The set including the triazolopyrazines **40-68** was designed to improve the drug-like properties of the compounds. Within this set of ligands, compounds **46-48**, **51-55** emerged as potent and highly selective hA_{2A}AR antagonists (K_i = 0.59-26 nM) while derivatives **66-68** turned out to be dual potent hA_1 (K_i =2-4.6 nM) and hA_{2A} ligands (K_i= 2.4-13 nM). Derivative **68** was selected to be tested for the potential neuroprotective effect in the same *in vitro* model of AD used for **31** and **32.** The obtained results showed

that **68** was effective in preventing the cell mortality starting from concentration 0.1 µM and restoring the cell viability till to control level at 0.3 µM.

Further investigations are currently ongoing to understand if these structural modifications have been effective in improving the drug-like properties of these compounds.

The last purpose of the work was the synthesis of triazolopyrazines bearing, at position 6 of the scaffold, potential antioxidant functions (compounds **74-86**). These modifications were succesfull since compounds **78, 79, 81, 82, 84** and **85** showed high affinity and selectivity toward the hA_{2A} AR (K_i = 1.7-54.5 nM) while **74** and **80** were able to bind efficiently both the hA_1 (K_i = 8.4-29.8 nM) and hA_{2A} (K_i = 5-16.8 nM) ARs. The selected derivatives **78, 82, 84** and **85** were tested for their potential protective effects in microglia cells against oxaliplatin-induced neurotoxicity. The obtained results highlighted that compound **82** was effective in preventing the oxaliplatin damage at 10 and 30 µM concentrations whereas only a partial activity has been observed for derivatives **78** and **85.**

Further investigations are ongoing to confirm the stability of derivatives **75-80, 82** in human plasma, and in Tris/HCl and phosphate buffer solutions (PBS). These tests are being performed by the research group of Prof. Gianluca Bartolucci, at the NEUROFARBA Department – Pharmaceutical and Nutraceutical Section, of the University of Florence

Molecular modeling investigations were carried out on the synthesized compounds to gain informations about their hypothetical binding mode at the A_{2A}AR crystal structure and to provide useful indications for the design of new 8-amino-triazolo[4,3-a]pyrazin-3-one derivatives as hA_{2A} AR antagonists.

6. EXPERIMENTAL SECTION

The microwave-assisted syntheses were performed using an Initiator EXP Microwave Biotage instrument (frequency of irradiation: 2.45 GHz). Silica gel 60 (Merck, 70-230 mesh) was used for analytical TLC, and for column chromatog raphy, respectively. All melting points were determined on a Gallenkamp melting point apparatus and are uncorrected. Elemental analyses were performed with a Flash E1112 Thermofinnigan elemental analyzer for C, H, N and the results were within 0.4% of the theoretical values. All final compounds revealed purity not less than 95%. The IR spectra were recorded with a Perkin-Elmer Spectrum RX I spectrometer in Nujol mulls and are expressed in cm^{-1}. NMR spectra were recorded on a Bruker Avance 400 spectrometer (400 MHz). The chemical shifts are reported in δ (ppm) and are relative to the central peak of the solvent which was $CDCl_3$, MeOD or DMSO-d_6. The following abbreviations are used: s= singlet, d= doublet, dd = doublet of doublets, t= triplet, q= quartet, m= multiplet, br= broad and ar= aromatic protons. The following abbreviation are used for solvents and reactive products: AcOH = Acetic acid, $CDCl_3$ = Deuterated chloroform, $CHCl_3$ = Chloroform, DCM = Dichloromethane, DIPEA = N,N-Diisopropylethylamine, DMF = Dimethylformamide, DMSO-d_6 = Deuterated dimethyl sulfoxide, EtOAc = Ethyl acetate, EDCI.HCl = *N*-(3-Dimethylaminopropyl)-*N*'-ethylcarbodiimide hydrochloride, Et_2O = Diethyl ether, EtOH = Ethanol, HCl = Hydrochloric acid, HOBt = Hydroxybenzotriazole, MeOD = Deuterated methanol, MeOH = Methanol, THF = Tetrahydrofuran.

General procedure for the synthesis of Ethyl 2-amino-2-arylhydrazonoacetates (**94-97**).

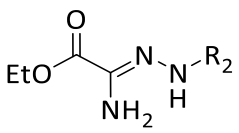

94-97

2-amino-2-arylhydrazonoacetates **95** (R_2= 4-OMe), **96** (R_2= 4-NO_2) and **97** (R_2= 2-OMe)[414] were prepared as previously described for **94** (R= H)[413] i.e. from the corresponding 2-chloro derivatives **90-93**.[392,411,412] Briefly, 33% aqueous ammonia (3 mL) in dioxane (5 mL) was added dropwise to a solution of the suitable chloro derivative **90-93** (13.3 mmol) in dioxane (15 mL) and the reaction mixture was stirred for 4 h at room temperature. The

white solid was filtered off and the mother liquor was concentrated at reduced pressure. The obtained precipitate was collected by filtration, washed with water (30 mL), dried and recristallized. The crude compound **51** was obtained as an oil residue which was purified on silica gel column chromatography (eluent Cyclohexane 7/EtOAc 3).

Ethyl 2-amino-2-(phenylhydrazono)acetate (**94**)**.** Yield 73% m.p. 129-130 °C (lit[413] 128 °C) (Cyclohexane/EtOAc). ^{1}H NMR (DMSO-d_6) 1.28 (t, 3H, ar, J = 7.1 Hz), 4.23 (q, 2H, CH_2, J = 7.1 Hz), 5.88 (br s, 2H, NH_2), 6.72 (t, 1H, ar, J = 7.3 Hz), 7.01 (d, 2H, ar, J = 7.6 Hz), 7.18 (t, 1H, ar, J = 8.2 Hz), 8.66 (br s, 1H, NH). Anal. Calcd. for $C_{10}H_{13}N_3O_2$

Ethyl 2-amino-2-(4-methoxyphenylhydrazono)acetate (95). Yield 55% brownish oil; ^{1}H NMR ($CDCl_3$) 1.42 (t, 3H, CH_3, J= 7.1 Hz), 3.87 (s, 3H, OCH_3), 4.38 (q, 2H, CH_2, J= 7.1 Hz), 4.69 (br s, 2H, NH_2), 6.45 (br s, 1H, NH), 6.88 (d, 2H, ar, J= 9.0 Hz), 7.11 (d, 2H, ar, J= 9.0 Hz), 8.27 (s, 1H, NH). Anal. Calcd. For $C_{11}H_{15}N_3O_3$.

Ethyl 2-amino-2-(4-nitrophenylhydrazono)acetate (96). Yield 65 % m.p. 192-193 °C (EtOH) (lit[414] 190-191 °C). ^{1}H NMR (DMSO-d_6) 1.29 (t, 3H, CH_3, J= 7.2 Hz), 4.27 (q, 2H, CH_2, J= 7.2 Hz), 6.39 (br,s, 2H, NH_2), 7.07 (d, 2H, ar, J= 9.2 Hz), 8.20 (d, 2H, ar, J= 9.2 Hz), 9.66 (br s, 1H, NH). Anal. Calcd. For $C_{10}H_{12}N_4O_4$.

Ethyl 2-amino-2-(2-methoxyphenylhydrazono)acetate (**97**)**.** Yield 95% m.p. 99-101 °C (Cyclohexane/EtOAc). ^{1}H- NMR (DMSO-d_6) 1.28 (t, 3H, ar, J= 7.1 Hz), 3.82 (s, 3H, OCH_3), 4.23 (q, 2H, CH_2, J= 7.1 Hz), 6.15 (br s, 2H, NH_2), 6.73 (t, 1H, ar, J= 7.6 Hz), 6.84-6.92 (m, 2H, ar), 7.28 (d, 1H, ar, J= 7.9 Hz), 7.86 (s, 1H, NH). Anal. Calcd. for $C_{11}H_{15}N_3O_3$.

Synthesis of ethyl (Z)-2-amino-2-(2-benzylhydrazono)acetate (98).

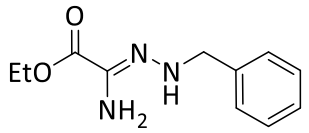

98

Ethyl thiooxamate (3.7 mmol) was added to a mixture of benzylhydrazine hydrochloride (3.7 mmol) and K_2CO_3 (3.7 mmol) in absolute ethanol (15 mL). The suspension was stirred at 25° C for 15 h then was treated with $NaHCO_3$ saturated solution (40 mL) and extracted with EtOAc (30 mL x 3). The organic layer was washed with brine (30 mL x 3), anhydrified (Na_2SO_4) and evaporated under reduced pressure to give a brown solid which was used

for the next step without further purification. Yield 88%. ^{1}H NMR (DMSO-d_6) 1.22 (t, 3H, CH_3, J = 7.1 Hz), 4.16 (q, 2H, CH_2, J = 7. 1 Hz), 4.25 (d, 2H, CH_2, J = 5.1 Hz), 5.49 (br s, 2H, NH_2), 5.88 (t, 1H, NH, J = 5.1 Hz), 7.24-7.35 (m, 5H, ar). Anal. Calcd. For $C_{11}H_{15}N_3O_2$.

General procedure for the synthesis of Ethyl 5-oxo-1-aryl-4,5-dihydro-1*H*-1,2,4-triazole-3-carboxylates (99-102).

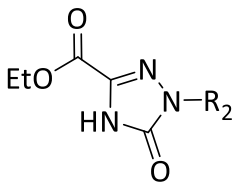

99-102

A solution of triphosgene (4.2 mmol) in anhydrous THF (10 mL) was added dropwise to a stirred solution of ethyl 2-amino-2-(arylhydrazono)acetate derivatives **94-97** (4.6 mmol) in anhydrous THF (15 mL) at 0 °C. After the addition was completed, the mixture was stirred 2-3 h at room temperature. Then, most of the solvent was removed at reduced pressure and water (20 mL) was added to the residue to give a solid wich was collected by filtration, washed with water (20 mL), dried and recrystallized.

Ethyl 5-oxo-1-phenyl-4,5-dihydro-1*H*-1,2,4-triazole-3-carboxylate (99). Yield 62%. m.p. 200-202 °C (lit.[415] 193-194 °C) (Cyclohexane/EtOAc). ^{1}H NMR (DMSO-d_6) 1.33 (t, 3H, CH_3, J = 7.1 Hz), 4.38 (q, 2H, CH_2, J = 7.1 Hz), 7.30 (t, 1H, ar, J = 7.4 Hz), 7.49 (t, 2H, ar, J = 7.4 Hz), 7.89 (d, 2H, ar, J = 7.6 Hz), 7.90 (s, 1H, H-9), 12.99 (br s, 1H, NH). Anal. Calcd. for $C_{11}H_{11}N_3O_3$.

Ethyl 1-(4-methoxyphenyl)-5-oxo-4,5-dihydro-1*H*-1,2,4-triazole-3-carboxylate (100). Yield 42%. m.p. 186-187 °C (lit[415] 179 °C) (EtOH). ^{1}H NMR ($CDCl_3$) 1.48 (t, 3H, CH_3, J= 7.2 Hz), 3.80 (s, 3H, OCH_3),4.50 (q, 2H, CH_2, J= 7.2 Hz), 6.98 (d, 2H, ar, J= 9.1 Hz), 7.87 (d, 2H, ar, J= 9.1 Hz), 10.65 (br s, 1H, NH). Anal. Calcd. for $C_{12}H_{13}N_3O_4$.

Ethyl 1-(4-nitrophenyl)-5-oxo-4,5-dihydro-1*H*-1,2,4-triazole-3-carboxylate (101). Yield 65%. m.p. 241-242 °C (Cyclohexane/EtOAc). ^{1}H NMR ($CDCl_3$) 1.50 (t, 3H, CH_3, J= 7.1 Hz,), 4.55 (q, 2H, CH_2, J= 7.1 Hz), 8.29-8.37 (m, 4H, ar), 10.31 (br s, 1H, NH). IR 3369, 1755, 1698, 1513, 1375. Anal. Calcd. for $C_{11}H_{10}N_4O_5$.

Ethyl 1-(2-methoxyphenyl)-5-oxo-4,5-dihydro-1*H*-1,2,4-triazole-3-carboxylate (102). Yield 79%. m.p. 131-133 °C (EtOAc). ^{1}H NMR (DMSO-d_6) 1.30 (t, 3H, CH_3, J = 7.1 Hz), 3.78

(s, 3H, OCH_3), 4.34 (q, 2H, CH_2, J= 7.1 Hz), 7.06 (t, 1H, ar, J= 7.6 Hz), 7.21 (d, 1H, ar, J= 8.3 Hz), 7.36 (d, 1H, J= 7.6 Hz), 7.49 (t, 1H, J= 7.6 Hz), 12.69 (br s, 1H, NH). Anal. Calcd. for $C_{12}H_{13}N_3O_4$.

Synthesis of Ethyl 5-oxo-1-benzyl-4,5-dihydro-1H-1,2,4-triazole-3-carboxylate (103).

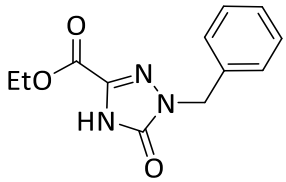

103

Carbonyldiimidazole (5.4 mmol) was portion wise added to a cold (T= 0° C) suspension of ethyl (Z)-2-amino-2-(2-benzylhydrazono)acetate **98** (2.7 mmol) in anhydrous DCM (20 mL). The mixture was stirred at room temperature for 15 h then was treated with a NH_4Cl saturated solution (30 mL) and extracted with DCM (30 mL x 3). The organic phase was anhydrified (Na_2SO_4) and the solvent evaporated under reduced pressure to afford a yellow solid which was purified by column chromatography (Cyclohexane 6/EtOAc 4/MeOH 1). Yield 35%. mp 154-156 °C. ^{1}H NMR (DMSO-d_6) 1.27 (t, 3H, CH_3, J = 7.1 Hz), 4.31 (q, 2H, CH_2, J = 7.1 Hz), 4.95 (s, 2H, CH_2), 7.26-7.38 (m, 5H, ar), 12.67 (br s, 1H, NH). Anal. Calc. for $C_{12}H_{13}N_3O_3$.

General procedure for the synthesis of ethyl 1-aryl- and 1-benzyl-substituted 5-oxo-4-(2-(hetero)aryl-2-oxoalkyl)-4,5-dihydro-1H-1,2,4-triazole-3-carboxylate derivatives (104-133).

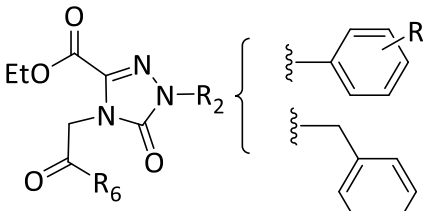

104-133

A solution of chloroacetone (1.2 mmol) or the suitable α-bromoketone (1.2 mmol), was added to a mixture of ethyl 1-aryl-5-oxo-1,2,4-triazole-3-carboxylate derivatives (**99-103**) (1 mmol) and potassium carbonate (2 mmol) in a mixture of DMF/acetonitrile (1:9, 10 mL). The suspension was stirred at room temperature until the disappearance of the

starting material (TLC monitoring, 2-24 h). The solvent was removed at reduced pressure and the residue was treated with water (50-70 mL). The precipitate was collected by filtration, washed with water (20 mL), then with Et_2O (10 mL). The crude compounds were purified by recrystallization except compound **129** which was purified by liquid chromatography.

Ethyl 5-oxo-4-(2-oxopropyl)-1-phenyl-4,5-dihydro-1*H*-1,2,4-triazole-3-carboxylate (104). Yield 58% m.p. 104-105 °C (EtOH). ^{1}H NMR (DMSO-d_6) 1.31 (t, 3H, CH_3, J = 7.1 Hz), 2.28 (s, 3H, CH_3), 4.35 (q, 2H, CH_2, J = 7.1 Hz), 4.92 (s, 2H, CH_2), 7.35 (t, 1H, ar, J = 7.4 Hz), 7.54 (t, 2H, ar, J = 7.4 Hz), 7.91 (d, 2H, ar, J = 7.7 Hz). Anal. Calc. for $C_{14}H_{15}N_3O_4$.

Ethyl 5-oxo-4-(2-oxo-2-phenylethyl)-1-phenyl-4,5-dihydro-1H-1,2,4-triazole-3-carboxylate (105). Yield 75%. m.p. 157-159 °C (EtOAc/EtOH). ^{1}H NMR (DMSO-d_6) 1.21 (t, 3H, ar, J = 7.1 Hz), 4.29 (q, 2H, CH_2, J = 7.1 Hz), 5.59 (s, 2H, CH_2), 7.37 (t, 1H, ar, J = 7.4 Hz), 7.55 (t, 2H, ar, J = 7.6 Hz), 7.63 (t, 2H, ar, J = 7.7 Hz), 7.76 (t, 1H, ar, J = 7.4 Hz), 7.95 (d, 2H, ar, J = 7.7 Hz), 8.11 (d, 2H, ar, J = 7.8 Hz). Anal. Calc. for $C_{19}H_{17}N_3O_4$.

Ethyl 1-(4-methoxyphenyl)-5-oxo-4-(2-oxopropyl)-4,5-dihydro-1H-1,2,4-triazole-3-carboxylate (106). Yield 92%. m.p. 98-100 °C (EtOH). ^{1}H NMR (DMSO-d_6) 1.30 (t, 3H, CH_3, J = 7.1 Hz), 3.80 (s, 3H, OMe), 4.34 (q, 2H, CH_2, J = 7.1 Hz), 4.91 (s, 2H, CH_2), 7.08 (d, 2H, ar, J = 9.1 Hz), 7.76 (d, 2H, ar, J = 9.1 Hz). Anal. Calc. for $C_{15}H_{17}N_3O_5$.

Ethyl 1-(4-methoxyphenyl)-5-oxo-4-(2-oxo-2-phenylethyl)-4,5-dihydro-1H-1,2,4-triazole-3-carboxylate (107). Yield 58%. m.p. 127-128 °C (Cyclohexane/EtOAc). ^{1}H NMR ($CDCl_3$) 1.38 (t, 3H, CH_3, J= 7.1), 3.86 (s, 3H, OCH_3), 4.40 (q, 2H, CH_2, J= 7.1 Hz), 5.57 (s, 2H, CH_2), 6.99 (d, 2H, ar, J= 9.1 Hz), 7.55 (t, 2H, ar, J = 7.5 Hz), 7.68 (t, 1H, ar, J = 7.4 Hz), 7.88 (d, 2H, ar, J = 9.1 Hz), 8.03 (d, 2H, ar, J = 7.4 Hz). IR 1732, 1711, 1694. Anal. Calc. for $C_{20}H_{19}N_3O_5$.

Ethyl 1-(4-nitrophenyl)-5-oxo-4-(2-oxo-2-phenylethyl)-4,5-dihydro-1H-1,2,4-triazole-3-carboxylate (108). Yield 92%. m.p. 147-148 °C (MeOH). ^{1}H NMR ($CDCl_3$) 1.40 (t, 3H, CH_3, J= 7.2 Hz), 4.44 (q, 2H, CH_2, J= 7.2 Hz), 5.59 (s, 2H, CH_2), 7.58 (t, 2H, ar, J = 7.2 Hz), 7.70 (t, 1H, ar, J = 8.4 Hz), 8.04 (d, 2H, ar, J = 7.2 Hz), 8.35-8.38 (m, 4H, ar). IR 1736, 1725, 1700, 1463, 1375. Anal. Calc. for $C_{19}H_{16}N_4O_6$.

Ethyl 1-(2-methoxyphenyl)-5-oxo-4-(2-oxo-2-phenylethyl)-4,5-dihydro-1H-1,2,4-triazole-3-carboxylate (109). Yield 65%. m.p. 88-90 °C (Cyclohexane/EtOAc). ^{1}H NMR

(DMSO-d_6) 1.18 (t, 3H, CH_3, J = 7.1 Hz), 3.81 (s, 3H, OMe), 4.24 (q, 2H, CH_2, J = 7.1 Hz), 5.55 (s, 2H, CH_2), 7.04-7.09 (m, 2H, ar), 7.42-7.48 (m, 2H, ar), 7.57 (t, 2H, ar, J = 7.5 Hz), 7.67 (t, 1H, ar, J = 7.4 Hz), 8.04 (d, 2H, ar, J = 7.1 Hz). Anal. Calc. for $C_{20}H_{19}N_3O_5$.

Ethyl 4-[2-(2-methoxyphenyl)-2-oxoethyl]-5-oxo-1-phenyl-4,5-dihydro-1H-1,2,4-triazole-3-carboxylate (110). Yield 53%. m.p. 155-157 °C (EtOH). ^{1}H NMR (DMSO-d_6) 1.21 (t, 3H, CH_3, J = 7.1 Hz), 4.02 (q, 2H, CH_2, J = 7.1 Hz), 4.31 (s, 3H, OCH_3), 5.37 (s, 2H, CH_2), 7.12 (t, 1H, ar, J = 7.5 Hz), 7.30 (d, 1H, ar, J = 8.6 Hz), 7.36 (t, 1H, ar, J = 7.4 Hz), 7.55 (t, 2H, ar, J = 7.6 Hz), 7.70 (t, 1H, ar, J = 7.8 Hz), 7.79 (d, 1H, ar, J = 7.8 Hz), 7.9 (d, 2H, ar, 7.9 Hz). $C_{20}H_{19}N_3O_5$

Ethyl 4-[2-(3-methoxyphenyl)-2-oxoethyl]-5-oxo-1-phenyl-4,5-dihydro-1H-1,2,4-triazole-3-carboxylate (111). Yield 80%. m.p. 123-125 °C (EtOH). ^{1}H NMR (DMSO-d_6) 1.20 (t, 3H, ar, J = 7.1 Hz), 3.86 (s, 3H, OCH_3), 4.29 (q, 2H, CH_2, J = 7.1 Hz), 5.59 (s, 2H, CH_2), 7.34-7.38 (m, 2H, ar), 7.52-7.57 (m, 4H, ar), 7.71 (d, 1H, ar, J = 7.7 Hz), 7.94 (d, 2H, ar, J = 8.0 Hz). Anal. Calc. for $C_{20}H_{19}N_3O_5$.

Ethyl 4-[2-(4-methoxyphenyl)-2-oxoethyl]-5-oxo-1-phenyl-4,5-dihydro-1H-1,2,4-triazole-3-carboxylate (112). Yield 85%. m.p. 149-151 °C (Cyclohexane/EtOAc). ^{1}H NMR ($CDCl_3$) 1.38 (t, 3H, CH_3, J = 6.9 Hz), 3.93 (s, 3H, CH_3), 4.41 (q, 2H, CH_2, J = 6.9 Hz), 5.53 (s, 2H, CH_2), 7.02 (d, 2H, CH_2, J = 7.6 Hz), 7.31 (t, 1H, ar, J = 7.4 Hz), 7.48 (t, 2H, ar, J = 7.4 Hz), 8.01-8.05 (m, 4H, ar). Anal. Calc. for $C_{20}H_{19}N_3O_5$.

Ethyl 4-[2-(4-methylphenyl)-2-oxoethyl]-5-oxo-1-phenyl-4,5-dihydro-1H-1,2,4-triazole-3-carboxylate (113). Yield 60%. m.p. 189-190 °C (EtOH). ^{1}H NMR (DMSO-d_6) 1.19 (t, 3H, CH_3, J = 6.9 Hz), 2.43 (s, 3H, CH_3) 4.28 (q, 2H, CH_2, J = 7.1 Hz), 5.55 (s, 2H, CH_2), 7.37 (t, 1H, ar, J = 7.4 Hz), 7.43 (d, 2H, ar, J = 7.7 Hz), 7.55 (t, 2H, ar, J = 7.7 Hz), 7.94 (d, 2H, ar., J = 8.3 Hz), 8.01 (d, 2H, ar, J = 7.6 Hz). Anal. Calc. for $C_{20}H_{19}N_3O_4$.

Ethyl 4-[2-(3,4-methylendioxyphenyl)-2-oxoethyl]-5-oxo-1-phenyl-4,5-dihydro-1H-1,2,4-triazole-3-carboxylate (114) Yield 77%. m.p. 179-181 °C (Cyclohexane/EtOAc). ^{1}H NMR ($CDCl_3$) 1.39 (t, 3H, CH_3, J = 7.1 Hz), 4.42 (q, 2H, CH_2, J = 7.1 Hz), 5.50 (s, 2H, CH_2), 6.11 (s, 2H, CH_2), 6.94 (d, 1H, ar, J = 8.2 Hz), 7.31 (t, 1H, ar, J = 7.6 Hz), 7.48 (t, 3H, ar, J = 8.0 Hz), 7.65 (d, 1H, ar, J = 8.2 Hz), 8.03 (d, 1H, ar, J = 8.0 Hz). Anal. Calc. for $C_{20}H_{17}N_3O_6$.

Ethyl 4-[2-(3-bromophenyl)-2-oxoethyl]-5-oxo-1-phenyl-4,5-dihydro-1H-1,2,4-triazole-3-carboxylate (115). Yield 62%. m.p. 200-202 °C (EtOH). ^{1}H NMR ($CDCl_3$) 1.40 (t, 3H, CH_3, J = 7.1 Hz), 4.42 (q, 2H, CH_2, J = 7.1 Hz), 5.54 (s, 2H, CH_2), 7.32 (t, 1H, ar, J = 7.5 Hz), 7.43-

7.5 (m, 3H, ar), 7.81 (d, 1H, ar, J = 8 Hz), 7.96 (d, 1H, ar, J = 7.8 Hz), 8.02 (d, 2H, ar, J = 8.2 Hz), 8.16 (t, 1H, ar, J = 1.8 Hz). Anal. Calc. for $C_{19}H_{16}BrN_3O_4$.

Ethyl 4-[2-(4-bromophenyl)-2-oxoethyl]-ethyl-5-oxo-1-phenyl-4,5-dihydro-1H-1,2,4-triazole-3-carboxylate (116). Yield 77%. m.p. 167-169 °C (EtOH). ^{1}H NMR ($CDCl_3$) 1.39 (t, 3H, CH_3, J = 7.1 Hz), 4.42 (q, 2H, CH_2, J = 7.1 Hz), 5.53 (s, 2H, CH_2), 7.32 (t, 1H, ar, J = 7.5 Hz), 7.48 (t, 2H, ar, J = 8.4) Hz), 7.71 (d, 2H, ar, J = 6.7 Hz), 7.9 (d, 2H, ar, J = 8.6 Hz), 8.02 (d, 2H, ar, J = 7.8 Hz). Anal. Calc. for $C_{19}H_{16}BrN_3O_4$.

Ethyl 4-[2-(3-chlorophenyl)-2-oxoethyl]-5-oxo-1-phenyl-4,5-dihydro-1H-1,2,4-triazole-3-carboxylate (117). Yield 47%. m.p. 141-143 °C (EtOH). ^{1}H NMR (DMSO-d_6) 1.20 (t, 3H, CH_3, J = 7.1 Hz), 4.30 (q, 2H, CH_2, J = 7.1 Hz), 5.61 (s, 2H, CH_2), 7.37 (t, 1H, ar, J = 7.6 Hz), 7.56 (t, 2H, ar, J = 7.6 Hz), 7.67 (t, 1H, ar, J = 7.9 Hz), 7.83-7.85 (dd, 1H, ar, J = 1.2 Hz, J = 6.7 Hz), 7.94 (d, 2H, ar, J = 7.7 Hz), 8.08 (d, 1H, ar, J = 7. 8 Hz), 8.14 (t, 1H, ar, J = 1.8 Hz) (C, H, N). Anal.Calc. for $C_{19}H_{16}ClN_3O_4$.

Ethyl 4-[2-(4-chlorophenyl)-2-oxoethyl]-ethyl-5-oxo-1-phenyl-4,5-dihydro-1H-1,2,4-triazole-3-carboxylate (118). Yield 60%. m.p. 194-196 °C (MeOH). ^{1}H NMR (DMSO-d_6) 1.20 (t, 3H, CH_3, J = 7.1 Hz), 4.30 (q, 2H, CH_2, J = 7.1 Hz), 5.59 (s, 2H, CH_2), 7.37 (t, 1H, ar, J = 7. 4 Hz), 7.55 (t, 2H, ar, J = 7.5 Hz), 7.70 (d, 2H, ar, J = 8.6 Hz), 7.94 (d, 2H, ar, J = 7.9 Hz), 8.13 (d, 2H, ar, J = 8.7 Hz). Anal. Calc. for $C_{19}H_{16}ClN_3O_4$.

Ethyl 4-[2-(2-nitrophenyl)-2-oxoethyl]-5-oxo-1-phenyl-4,5-dihydro-1H-1,2,4-triazole-3-carboxylate (119). Yield 92%. m.p. 171-173 °C (EtOH). ^{1}H NMR ($CDCl_3$) 1.49 (t, 3H, CH_3, J = 7.1 Hz), 4.52 (q, 2H, CH_2, J = 7.1 Hz), 5.44 (s, 2H, CH_2), 7.32 (t, 1H, ar, J = 7.4 Hz), 7.48 (t, 2H, ar, J = 7.8 Hz), 7.70-7.77 (m, 2H, ar), 7.84 (t, 1H, ar, J = 7.3 Hz), 8.04 (d, 2H, ar, J = 7.9 Hz), 8.22 (d, 1H, ar, J = 8.2 Hz). Anal. Calc. for $C_{19}H_{16}N_4O_6$.

Ethyl 4-[2-(3-nitrophenyl)-2-oxoethyl]-5-oxo-1-phenyl-4,5-dihydro-1H-1,2,4-triazole-3-carboxylate (120). Yield 89%. m.p. 134-136 °C (Cyclohexane/EtOAc). ^{1}H NMR (DMSO-d_6) 1.20 (t, 3H, CH_3, J = 7.1 Hz), 4.30 (q, 2H, CH_2, J = 7.3 Hz), 5.71 (s, 2H, CH_2), 7.39 (t, 1H, ar, J = 7.4 Hz), 7.56 (t, 2H, ar, J = 8.1 Hz), 7.91-7.95 (m, 3H, ar), 8.57 (t, 2H, ar, J = 8. 6 Hz), 8.78 (s, 1H, ar). Anal. Calc. for $C_{19}H_{16}N_4O_6$.

Ethyl-4-[2-(4-nitrophenyl)-2-oxoethyl]-5-oxo-1-phenyl-4,5-dihydro-1H-1,2,4-triazole-3-carboxylate (121). Yield 97%. m.p. 180-182 °C (EtOH/Nitromethane). ^{1}H NMR (DMSO-d_6) 1.21 (t, 3H, CH_3, J = 7.1 Hz), 4.30 (q, 2H, CH_2, J = 7.1 Hz), 5.67 (s, 2H, CH_2), 7.37 (t, 1H, ar,

J = 7.5 Hz), 7.56 (t, 2H, ar, J = 8.3 Hz), 7.94 (d, 2H, ar, J = 7.8 Hz), 8.35 (d, 2H, ar, J = 8.8 Hz), 8.43 (d, 2H, ar, J = 8.8 Hz). Anal. Calc. for $C_{19}H_{16}N_4O_6$.

Ethyl 4-[2-(furan-2-yl)-2-oxoethyl]-5-oxo-1-phenyl-4,5-dihydro-1H-1,2,4-triazole-3-carboxylate (122). Yield 72%. m.p. 170-172 °C (EtOH). ^{1}H NMR (DMSO-d_6) 1.22 (t, 3H, CH_3, J= 7.1 Hz), 4.31 (q, 2H, CH_2, J= 7.1 Hz), 5.37 (s, 2H, CH_2), 6.84 (d, 1H, furan proton, J= 2.0 Hz),7.35-7.38 (m, 1H, ar), 7.53-7.57 (m, 2H, ar),7.75 (d, 1H, furan proton, J= 2.0 Hz), 7.93 (d, 2H, ar, J= 7.4 Hz), 8.15 (m, 1H, furan proton). Anal. Calc. for $C_{17}H_{15}N_3O_5$.

Ethyl 4-[2-(5-methylfuran-2-yl)-2-oxoethyl]-5-oxo-1-phenyl-4,5-dihydro-1H-1,2,4-triazole-3-carboxylate (123). Yield 58%. m.p. 142-144 °C (Cyclohexane/AcOEt). ^{1}H NMR ($CDCl_3$) 1.40 (t, 3H, CH_3, J = 7.1 Hz), 2.46 (s, 3H, CH_3), 4.42 (q, 2H, CH_2, J = 7.1 Hz), 5.40 (s, 2H, CH_2), 6.26 (d, 1H, furan proton, J = 2.8 Hz), 7.31-7.33 (m, 2H, 1 ar, 1 furan proton), 7.47 (t, 2H, ar, J = 7.7 Hz), 8.03 (d, 2H, ar, J = 8.4 Hz). Anal. Calc. for $C_{18}H_{17}N_3O_5$.

Ethyl 4-[2-(thiophen-2-yl)-2-oxoethyl]-5-oxo-1-phenyl-4,5-dihydro-1H-1,2,4-triazole-3-carboxylate (124). Yield 80%. m.p. 167-168 °C (EtOH). ^{1}H-NMR (DMSO-d_6) 1.21 (t, 3H, CH_3, J = 7.1 Hz), 4.31 (q, 2H, CH_2, J = 7.1 Hz), 5.52 (s, 2H, CH_2), 7.35-7.39 (m, 2H, CH_2), 7.55 (t, 2H, ar, J = 7.8 Hz), 7.94 (d, 2H, ar, J = 7.7 Hz), 8.18 (d, 1H, ar, J = 4.0 Hz), 8.28 (d, 1H, ar, J = 2.9 Hz). Anal. Calc. for $C_{17}H_{15}N_3O_4S$.

Ethyl 4-[2-(pyrid-2-yl)-2-oxoethyl]-5-oxo-1-phenyl-4,5-dihydro-1H-1,2,4-triazole-3-carboxylate (125). Yield 30%. m.p. 153-155 °C (EtOH). ^{1}H-NMR (DMSO-d_6) 1.29 (t, 3H, CH_3, J = 7.0 Hz), 4.29 (q, 2H, CH_2, J = 7.0 Hz), 5.67 (s, 2H, CH_2), 7.37 (t, 1H, ar, J = 7.4 Hz), 7.55 (t, 2H, ar, J = 7.8 Hz), 7.80 (t, 1H, ar, J = 3.1 Hz), 7.82 (d, 1H, ar, J = 4.8 Hz), 7.95 (d, 1H, ar, J = 8.5 Hz), 8.05 (d, 1H, ar, J = 7.8 Hz), 8.11 (t, 1H, ar, J = 7.7 Hz), 8.85 (d, 1H, ar, J = 4.7 Hz). Anal. Calc. for $C_{18}H_{16}N_4O_4$.

Ethyl 1-benzyl-5-oxo-4-[2-oxo-2-phenylethyl]-4,5-dihydro-1H-1,2,4-triazole-3-carboxylate (126). Yield 34%. m.p. 90-92 °C. ^{1}H NMR ($CDCl_3$) 1.34 (t, 3H, CH_3, J = 7.1 Hz), 4.36 (q, 2H, CH_2, J = 7.1 Hz), 5.15 (s, 2H. CH_2), 5.51 (s, 2H. CH_2), 7.32-7.42 (m, 5H, ar), 7.54 (t, 2H, ar, J = 7.7 Hz), 7.67 (t, 1H, ar, J = 7.5 Hz), 8.01 (d, 2H, J =7.7 Hz). Anal. Calc. for $C_{20}H_{19}N_3O_4$.

Ethyl 1-benzyl-4-[2-(furan-2-yl)-2-oxoethyl]-5-oxo-4,5-dihydro-1H-1,2,4-triazole-3-carboxylate (127). Yield 68%. m.p. 104-106 °C. ^{1}H NMR ($CDCl_3$) 1.34 (t, 3H, CH_3, J = 7.1 Hz), 4.36 (q, 2H, CH_2, J = 7.1 Hz), 5.13 (s, 2H. CH_2), 5.37 (s, 2H. CH_2), 6.63 (dd, 1H, furan

proton, J = 1.6 Hz, J = 1.9 Hz), 7.32-7.41 (m, 6H, 5ar + 1 furan proton), 7.67 (s, 1H, furan proton). Anal. Calc. for $C_{18}H_{17}N_3O_5$.

Ethyl 1-benzyl-4-[2-(5-methylfuran-2-yl)-2-oxoethyl]-5-oxo-4,5-dihydro-1H-1,2,4-triazole-3-carboxylate (128). Yield 93%. Oily compound. ^{1}H NMR ($CDCl_3$) 1.35 (t, 3H, CH_3, J = 7.1 Hz), 2.44 (s, 3H, CH_3), 4.37 (q, 2H, CH_2, J = 7.1 Hz), 5.13 (s, 2H, CH_2), 5.33 (s, 2H, CH_2), 6.24 (d, 1H, furan proton, J = 3.3 Hz), 7.25 (d, 1H, 1 furan proton, J = 3.4 Hz), 7.41-7.31 (m, 5H, ar). $C_{19}H_{19}N_3O_5$.

Ethyl 4-[2-(2,4-dimethoxyphenyl)-2-oxoethyl]-5-oxo-1-phenyl-4,5-dihydro-1H-1,2,4-triazole-3-carboxylate (129). Yield 85%. m.p. 150-152 °C. Purified by column chromatography (Cyclohexane 6/EtOAc 4). ^{1}H NMR (CDCl3-d_6) 1.38 (t, 3H, CH_3, J = 7.1 Hz), 3.96 (s, 3H, CH_3), 3.98 (s, 3H, CH_3), 4.41 (q, 2H, CH_2, J = 7.1 Hz), 5.45 (s, 2H, CH_2), 6.53 (d, 1H, ar, J = 1.8 Hz), 6.61 (dd, 1H, ar, J = 1.9 Hz, J = 6.8 Hz), 7.30 (t, 1H, ar, J = 7.3 Hz), 7.47 (t, 2H, ar, J = 7.8 Hz), 7.99-8.07 (m, 3H, ar). Anal. Calc. for $C_{22}H_{23}N_3O_6$.

Ethyl 4-[2-(3,4-dimethoxyphenyl)-2-oxoethyl]-5-oxo-1-phenyl-4,5-dihydro-1H-1,2,4-triazole-3-carboxylate (130). Yield 76%. m.p. 159-161 °C (EtOH). ^{1}H NMR ($CDCl_3$) 1.39 (t, 3H, CH_3, J= 7.1 Hz), 3.96 (s, 3H, OCH_3), 4.00 (s, 3H, OCH_3), 5.55 (s, 2H, CH_2), 6.97 (d, 1H, ar, J= 8.4 Hz), 7.31 (t, 1H, ar, J= 7.4 Hz), 7.48 (t, 2H, ar, J= 8.3 Hz), 7.54 (d, 1H, J= 1.7 Hz), 7.68 (d, 1H, ar, J= 8.4 Hz), 8.02 (d, 2H, ar, J= 8.2 Hz). Anal. Calc. for $C_{21}H_{21}N_3O_6$. $C_{22}H_{23}N_3O_6$.

Ethyl 4-[2-(3,4,5-trimethoxyphenyl)-2-oxoethyl]-5-oxo-1-phenyl-4,5-dihydro-1H-1,2,4-triazole-3-carboxylate (131). Yield 95%. m.p. 131-133 °C (Cyclohexane/EtOAc). ^{1}H NMR ($CDCl_3$) 1.41 (t, 3H, CH_3, J = 7.1 Hz), 4.43 (q, 2H, CH_2, J = 7.1 Hz), 5.55 (s, 2H, CH_2), 7.27-7.34 (m, 4H, ar), 7.49 (t, 2H, ar, J = 7.4 Hz), 8.04 (d, 2H, ar, J = 8.6 Hz). Anal. Calc. for $C_{23}H_{25}N_3O_7$

Ethyl 4-(2-(4-methoxy-3,5-dimethylphenyl)-2-oxoethyl)-5-oxo-1-phenyl-4,5-dihydro-1H-1,2,4-triazole-3-carboxylate (132). Yield 70%. m.p. 140-142 °C (EtOH). ^{1}H-NMR ($CDCl_3$) 1.39 (t, 3H, CH_3, J = 7.1 Hz), 2.38 (s, 6H, CH_3), 3.81 (s, 3H, CH_3), 4.41 (q, 2H, CH_2, J = 7.1 Hz), 5.52 (s, 2H, CH_2), 7.31 (t, 1H, ar, J = 7.2 Hz), 7.48 (t, 2H, ar, J = 7.9 Hz), 7.71 (s, 2H, ar), 8.04 (d, 2H, ar, J = 8.1 Hz). Anal. Calc. for $C_{23}H_{25}N_3O_5$.

Ethyl 4-(2-(3,5-di-tert-butyl-4-methoxyphenyl)-2-oxoethyl)-5-oxo-1-phenyl-4,5-dihydro-1H-1,2,4-triazole-3-carboxylate (133). Yield 60%. m.p. 196-198 °C (EtOH). ^{1}H-NMR (CDCl3-d) 1.40 (t, 3H, CH_3, J = 7.1 Hz), 1.48 (s, 18H, $(CH_3)_3$), 3.76 (s, 3H, CH_3), 4.42 (q, 2H, CH_2, J = 7.1 Hz), 5.56 (s, 2H, CH_2), 7.32 (t, 1H, ar, J = 7.5 Hz), 7.48 (t, 2H, ar, J = 7.7 Hz), 7.94 (s, 2H, ar), 8.04 (d, 2H, ar, J = 7.8 Hz). Anal. Calc. for $C_{29}H_{37}N_3O_5$.

General procedure for the synthesis of 1,2,4-triazolo[4,3-a]pyrazine-3,8(2H,7H)-dione derivatives (134-163).

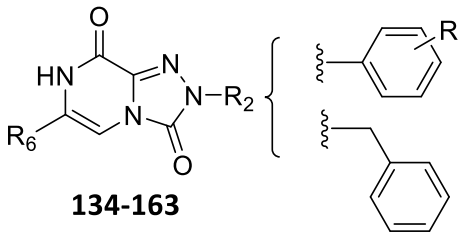

134-163

A mixture of the suitable ethyl 1,2,4-triazole-3-carboxylate derivatives **104-133** (0.87 mmol) and ammonium acetate (3.48 mmol) was heated under microwave irradiation at 140 °C otherwise in a sealed tube at 130°C (compound **139**) or 190 °C (compounds **136**, **137**) until the disappearance of starting material (TLC monitoring, 3-24 h). The residue was taken up with EtOH (1 mL) and Et_2O (5 mL), collected by filtration and washed with water (20 mL). All the crude compounds were purified by recrystallization.

6-Methyl-2-phenyl-1,2,4-triazolo[4,3-*a*]pyrazine-3,8(2*H*,7*H*)-dione (134). Yield 85%. m.p. 288-289 °C (2-Methoxyethanol). ^{1}H NMR (DMSO-d_6) 2.04 (s, 3H, CH_3), 6.88 (s, 1H, H-5), 7.34 (t, 1H, ar, J = 7.4 Hz), 7.54 (t, 2H, ar, J = 7.8 Hz), 7.98 (d, 2H, ar, J = 8.3 Hz), 11.32 (br s, 1H, NH). Anal. Calc. for $C_{12}H_{10}N_4O_2$.

2,6-Diphenyl-1,2,4-triazolo[4,3-*a*]pyrazine-3,8(2*H*,7*H*)-dione (135). Yield 65%. m.p. 290-291 °C (2-Methoxyethanol). ^{1}H NMR (DMSO-d_6) 7.28 (s, 1H, H-5), 7.37 (t, 1H, ar, J = 7.4 Hz), 7.46-7.51 (m, 2H, ar,), 7.57 (t, 2H, ar, J = 7.7 Hz), 7.72 (d, 2H, ar, J = 8.0 Hz), 8.02 (d, 2H, ar, J = 7.9 Hz), 11.63 (br s, 1H, NH). Anal. Calc. for $C_{17}H_{12}N_4O_2$.

6-Methyl-2-(4-methoxyphenyl)-1,2,4-triazolo[4,3-*a*]pyrazine-3,8(2*H*,7*H*)-dione (136). Yield 78%. m.p. > 300 °C (DMF). ^{1}H NMR (DMSO-d_6) 2.04 (s, 3H, CH_3), 3.80 (s, 3H, OCH_3), 6.87 (s, 1H, H-5), 7.09 (d, 2H, ar, J= 9.1 Hz), 7.85 (d, 2H, ar, J= 9.1 Hz), 11.30 (br s, 1H, NH). Anal. Calc. for $C_{13}H_{12}N_4O_3$.

2-(4-Methoxyphenyl)-6-phenyl-1,2,4-triazolo[4,3-*a*]pyrazine-3,8(2*H*,7*H*)-dione (137). Yield 75% m.p. >300 °C (DMF). ^{1}H NMR (DMSO-d_6) 3.82 (s, 3H, CH_3), 7.14 (d, 2H, ar, J= 9.0 Hz), 7.26 (s, 1H, H-5) 7.46-7.51 (m, 3H, ar), 7.71 (d, 2H, ar, J= 6.2 Hz), 7.88 (d, 2H, ar, J= 9.0 Hz), 11.60 (br s, 1H, NH). IR 3218, 1688. Anal. Calc. for $C_{18}H_{14}N_4O_3$

2-(4-Nitrophenyl)-6-phenyl-1,2,4-triazolo[4,3-*a*]pyrazine-3,8(2*H*,7*H*)-dione (138). Yield 92%. m.p. > 300 °C (DMF). ^{1}H NMR (DMSO-d_6) 7.32 (s, 1H, H-5), 7.47-7.50 (m, 3H, ar), 7.72-7.74 (m, 2H, ar), 8.34 (d, 2H, ar, J = 9.2 Hz), 8.46 (d, 2H, ar, J = 9.2 Hz), 11.71 (br s, 1H, NH). IR 3260, 1686. Anal. Calc. for $C_{17}H_{11}N_5O_4$

2-(2-Methoxyphenyl)-6-phenyl-1,2,4-triazolo[4,3-*a*]pyrazine-3,8(2*H*,7*H*)-dione (139). Yield 85%. m.p. > 300 °C (2-Methoxyethanol). ^{1}H NMR (DMSO-d_6) 3.99 (s, 3H, OMe), 7.12 (t, 1H, ar, J= 7.1 Hz), 7.23 (s, 1H, H-5), 7.27 (d, 1H, ar, J = 7.7 Hz), 7.44-7.50 (m, 4H, ar), 7.53 (t, 1H, ar, J = 8.5 Hz), 7.71 (s, 2H, ar, J = 8.2 Hz), 11.60 (br s, 1H, NH). IR 3259, 1714, 1689. Anal. Calc. for $C_{18}H_{14}N_4O_3$.

6-(2-Methoxyphenyl)-2-phenyl-1,2,4-triazolo[4,3-a]pyrazine-3,8(2H,7H)-dione (140). Yield 77%. m.p. 279-281 °C (2-Methoxyethanol/DMF). ^{1}H NMR (DMSO-d_6) 3.84 (s, 3H, CH_3), 7.02 (s, 1H, H-5), 7.05 (t, 1H, ar, J = 8.3 Hz), 7.15 (d, 1H, ar, J = 8.00 Hz), 7.36 (t, 1H, ar, J = 7.4 Hz), 7.41-7.49 (m, 2H, ar), 7.56 (t, 2H, ar, J = 8.4 Hz), 8.01 (d, 2H, ar, J =7.6 Hz) 11.39 (br s, 1H, NH). Anal. Calc. for $C_{18}H_{14}N_4O_3$.

6-(3-Methoxyphenyl)-2-phenyl-1,2,4-triazolo[4,3-*a*]pyrazine-3,8(2*H*,7*H*)-dione (141). Yield 79%. m.p.> 300 °C (2-Methoxyethanol). ^{1}H NMR (DMSO-d_6) 3.85 (s, 3H, CH_3), 6.99-7.02 (m, 1H, ar), 7.27-7.30 (m, 2H, ar), 7.35-7.40 (m, 2H, 1 ar + H-5), 7.57 (t, 2H, ar, J = 7.1 Hz), 8.02 (d, 2H, ar, J = 8.6 Hz), 11.60 (s, 1H, NH). Anal. Calc. for $C_{18}H_{14}N_4O_3$.

6-(4-Methoxyphenyl)-2-phenyl-1,2,4-triazolo[4,3-*a*]pyrazine-3,8(2*H*,7*H*)-dione (142). Yield 70%. m.p. 290-291 °C (2-Methoxyethanol). ^{1}H NMR (DMSO-d_6) 3.82 (s, 3H, CH_3), 7.03 (d, 2H, ar., J = 8.8 Hz), 7.19 (s, 1H, H_5), 7.36 (t, 1H, ar, J = 7.4 Hz), 7.56 (t, 2H, ar, J = 8.0 Hz), 7.66 (d, 2H, ar., J = 8.8 Hz), 8.02 (d, 2H, ar, J = 7.8 Hz), 11.55 (br s, 1H, NH). IR 3229, 1682 cm^{-1}. Anal. Calc. for $C_{18}H_{14}N_4O_3$.

6-(4-Methylphenyl)-2-phenyl-1,2,4-triazolo[4,3-*a*]pyrazine-3,8(2*H*,7*H*)-dione (143) . Yield 80%. m.p. > 300 °C (EtOH/2-Methoxyethanol). ^{1}H NMR (DMSO-d_6) 2.36 (s, 3H, CH_3), 7.23 (s, 1H, H-5), 7.29 (d, 2H, ar, J = 8.0 Hz), 7.37 (t, 1H, ar, J = 7.1 Hz), 7.54-7.62 (m, 4H,

ar.), 8.02 (d, 2H, ar, J = 8.5 Hz), 11.59 (br s, 1H, NH). IR 3387, 1688. Anal. Calc. For $C_{18}H_{14}N_4O_2$.

6-(3,4-methylendioxyphenyl)-2-phenyl-1,2,4-triazolo[4,3-*a*]pyrazine-3,8(2*H*,7*H*)-dione (144). Yield 78%. m.p. 279-281 °C (AcOH/DMF). ^{1}H NMR (DMSO-d_6) 6.10 (s, 2H, CH_2), 7.01 (d, 1H, ar, J = 8.16 Hz), 7.20-7.23 (m, 2H, 1 ar, H-5), 7.30 (d, 1H, ar, J = 1.6 Hz), 7.36 (t, 1H, ar, J = 7.4 Hz), 7.56 (t, 2H, ar, J = 7.7 Hz), 8.01 (d, 2H, ar, J = 7.8 Hz) 11.53 (br s, 1H, NH). Anal. Calc. For $C_{18}H_{12}N_4O_4$.

6-(3-Bromophenyl)-2-phenyl-1,2,4-triazolo[4,3-a]pyrazine-3,8(2H,7H)-dione (145). Yield 47%. m.p. > 300 °C (2-Methoxyethanol). ^{1}H NMR (DMSO-d_6) 7.37 (t, 1H, ar, J = 7.4 Hz), 7.41-7.45 (m, 2H, 1 ar, H-5), 7.56 (t, 2H, ar, J = 8.4 Hz), 7.64 (d, 1H, ar, J = 8.0 Hz), 7.74 (d, 1H, ar, J = 8.6 Hz), 7.96 (s, 1H, ar), 8.02 (d, 2H, ar, J = 8.8 Hz), 11.67 (br s, 1H, NH). Anal. Calc. For $C_{17}H_{11}BrN_4O_2$.

6-(4-Bromophenyl)-2-phenyl-1,2,4-triazolo[4,3-a]pyrazine-3,8(2H,7H)-dione (146). Yield 49%. m.p. > 300 °C (AcOH/DMF). ^{1}H NMR (DMSO-d_6) 7.35-7.38 (m, 2H, 1 ar, H-5), 7.56 (t, 2H, ar, J = 7.7 Hz), 7.67 (s, 4H, ar), 8.01 (d, 2H, ar, J = 7.7 Hz), 11.62 (br s, 1H, ar). Anal. Calc. For $C_{17}H_{11}BrN_4O_2$.

6-(3-Chlorophenyl)-2-phenyl-1,2,4-triazolo[4,3-a]pyrazine-3,8(2H,7H)-dione (147). Yield 76%. m.p. > 300 °C (2-Methoxyethanol). ^{1}H NMR (DMSO-d_6) 7.37 (t, 1H, ar, J = 7.3 Hz), 7.44 (s, 1H, H-5), 7.50-7.54 (m, 2H, ar), 7.56 (t, 2H, ar, J = 7.8 Hz), 7.69-7.71 (m, 1H, ar), 7.83 (s, 1H, ar), 8.01 (d, 2H, ar, J = 7.80 Hz) 11.65 (br s, 1H, NH). Anal. Calc. For $C_{17}H_{11}ClN_4O_2$.

6-(4-Chlorophenyl)-2-phenyl-1,2,4-triazolo[4,3-a]pyrazine-3,8(2H,7H)-dione (148). Yield 81%. m.p. > 300 °C (2-Methoxyethanol/DMF). ^{1}H NMR (DMSO-d_6) 7.35-7.38 (m, 2H, 1 ar, H-5), 7.53-7.58 (m, 4H, ar), 7.74 (d, 2H, ar, J = 8.6 Hz), 8.01 (d, 2H, ar, J = 8.00 Hz), 11.66 (br s, 1H, ar). ^{13}C NMR (DMSO-d_6) 100.92, 119.58, 126.98, 127.27, 128.77, 129.22, 129.81, 130.31, 134.37, 135.96, 137.67, 147.67, 153.47. Anal. Calc. For $C_{17}H_{11}ClN_4O_2$.

6-(2-Nitrophenyl)-2-phenyl-1,2,4-triazolo[4,3-a]pyrazine-3,8(2H,7H)-dione (149). Yield 66%. m.p. > 300 °C (2-Methoxyethanol). ^{1}H NMR (DMSO-d_6), 7.20 (s, 1H, H-5), 7.41 (t, 1H, ar, J = 7.4 Hz), 7.60 (t, 2H, ar, J = 7.6 Hz), 7.75 (d, 1H, ar, J = 6.1 Hz), 7.84 (t, 1H, ar, J = 7.6 Hz), 7. 93 (t, 1H, ar, J = 7.5 Hz), 8.02 (d, 2H, ar, J = 8.5 Hz), 8.31 (d, 1H, ar, J = 8.1 Hz), 11.8 (br s, 1H, NH). Anal. Calc. For $C_{17}H_{11}N_5O_4$.

6-(3-Nitrophenyl)-2-phenyl-1,2,4-triazolo[4,3-a]pyrazine-3,8(2H,7H)-dione (150). Yield 62%. m.p. > 300 °C (AcOH). ^{1}H NMR (DMSO-d_6), 7.37 (t, 1H, ar, J = 7.4 Hz), 7.55-7-59 (m, 3H, 2 ar, H-5), 7.77 (t, 1H, ar, J = 8. 00 Hz), 8.02 (d, 2H, ar, J = 7.8 Hz), 8.19 (d, 1H, ar, J = 7.7 Hz), 8.29 (d,1H, ar, J =) 8.57 (s, 1H, ar) 11. 87 (br s, 1H, NH). Anal. Calc. For $C_{17}H_{11}N_5O_4$.

6-(4-Nitrophenyl)-2-phenyl-1,2,4-triazolo[4,3-a]pyrazine-3,8(2H,7H)-dione (151). Yield 88%. m.p. > 300 °C (2-Methoxyethanol/DMF). ^{1}H NMR (DMSO-d_6) 7.37 (t, 1H, ar, J = 7.4 Hz), 7.57 (m, 3H, 2 ar, H-5), 8.00-8.03 (m, 4H, ar), 8.29 (d, 2H, ar, J = 8.7 Hz), 11.83 (br s, 1H, NH). Anal. Calc. For $C_{17}H_{11}N_5O_4$.

6-(2-Furan-2-yl)-2-phenyl-1,2,4-triazolo[4,3-a]pyrazine-3,8(2H,7H)-dione (**152**). Yield 73%. m.p. 298-299 °C (EtOH). ^{1}H NMR (DMSO-d_6) 6.65-6.67 (m, 1H, furan proton), 7.16 (s, 1H, H-5), 7.21 (d, 1H, furan proton, J= 1.8 Hz),7.35-7.38 (m, 1H, ar), 7.54-7.58 (m, 2H, ar), 7.80-7.82 (m, 1H, furan proton), 7.99-8.01 (m, 2H, ar), 11.71 (br s, 1H, NH). IR 3187, 3123, 1691. Anal. Calc. For $C_{15}H_{10}N_4O_3$.

6-(5-Methylfuran-2-yl)-2-phenyl-1,2,4-triazolo[4,3-a]pyrazine-3,8(2H,7H)-dione (**153**). Yield 75%. m.p. 281-283 °C (AcOH). ^{1}H NMR (DMSO-d_6) 2.35 (s, 3H, CH_3), 6.26 (d, 1H, furan proton, J = 2.3 Hz), 7.07- 7.08 (m, 2H, H-5 + furan proton), 7.36 (t, 1H, ar, J = 7.5 Hz), 7.56 (t, 2H, ar, J = 7.7 Hz), 8.00 (d, 2H, ar, J = 7.6 Hz) 11.63 (br s, 1H, NH). Anal. Calc. For $C_{16}H_{12}N_4O_3$.

2-Phenyl-6-(2-thienyl)-1,2,4-triazolo[4,3-a]pyrazine-3,8(2H,7H)-dione (154). Yield 55% m.p. > 300 °C (2-Methoxyethanol). ^{1}H NMR (DMSO-d_6) 7.17 (q, 2H, ar, J = 3.6 Hz), 7.36 (t, 1H, ar, J = 7.4 Hz), 7.56 (t, 2H, ar, J = 7.9 Hz), 7.67 (d, 2H, ar + H-5, J = 4.4 Hz), 8.00 (d, 2H, ar, J = 7.9 Hz), 11.70 (br. s, 1H, NH). Anal. Calc. For $C_{15}H_{10}N_4O_2S$.

2-Phenyl-6-(2-pyridyl)-1,2,4-triazolo[4,3-a]pyrazine-3,8(2H,7H)-dione (155). Yield 70%. m.p. 264-265 °C (EtOH/2-Methoxyethanol). ^{1}H NMR (DMSO-d_6) 7.38 (t, 1H, ar, J = 7.4 Hz), 7.46 (t, 1H, ar, J = 4.1 Hz), 7.57 (t, 2H, ar, J = 8.0 Hz), 7.92-7.97 (m, 2H, ar + H-5), 8.02 (d, 2H, ar, J = 8.4 Hz), 8.19 (d, 1H, ar, J = 8.1 Hz), 8.68 (d, 1H, pyridine proton, J = 4.8 Hz), 11.02 (br s, 1H, NH). IR 3254, 1688. Anal. Calc. For $C_{16}H_{11}N_5O_2$.

2-Benzyl-6-phenyl-1,2,4-triazolo[4,3-a]pyrazine-3,8(2H,7H)-dione (156). Yield 32%. m.p. 278-279 °C (2-Methoxyethanol). ^{1}H NMR (DMSO-d_6) 5.13 (s, 2H, CH_2), 7.20 (s, 1H, H-5), 7.35-7.38 (m, 5H, ar), 7.45-7.47 (m, 3H, ar), 7.68-7.69 (m, 2H, ar), 11.49 (br s, 1H, NH). . Anal. Calc. For $C_{18}H_{14}N_4O_2$.

2-Benzyl-6-(furan-2-yl)-1,2,4-triazolo[4,3-a]pyrazine-3,8(2H,7H)-dione (**157**). Yield 81%. m.p. 280-282 °C (AcOH). ^{1}H NMR (DMSO-d_6) 5.11 (s, 2H, CH_2), 6.63 (dd, 1H, furan proton, J = 1.6 Hz, J = 1.8 Hz), 7.11 (s, 1H, H-5), 7.16 (d, 1H, ar, J = 3. 4 Hz), 7.32-7.39 (m, 5H, 4ar + 1 furan proton), 7.8 (s, 1H, furan proton), 11.56 (br s, 1H, NH). Anal. Calc. For $C_{16}H_{12}N_4O_3$.

2-Benzyl-6-(5-methylfuran-2-yl)-1,2,4-triazolo[4,3-a]pyrazine-3,8(2H,7H)-dione (158). Yield 28%. m.p. 286-288 °C (AcOH). ^{1}H NMR (DMSO-d_6) 2.32 (s, 3H, CH_3), 5.11 (s, 2H, CH_2), 6.22 (s, 1H, furan proton), 7.01 (s, 1H, furan proton), 7.03 (s, 1H, H-5), 7.34-7.37 (m, 5H, ar), 11.46 (br s, 1H, NH). Anal. Calc. For $C_{17}H_{14}N_4O_3$.

6-(2,4-Dimethoxyphenyl)-2-phenyl-1,2,4-triazolo[4,3-*a*]pyrazine-3,8(2*H*,7*H*)-dione (159). Yield 64%. mp 252-254 °C (AcOH). ^{1}H NMR (DMSO-d_6) 3.84 (s, 6H, CH_3), 6.60 (dd, 1H, ar, J = 2.4 Hz, J = 6.1 Hz), 6.67 (d, 1H, ar, J = 2.3 Hz), 6.93 (s, 1H, H-5), 7.33-7.37 (m, 2H, ar), 7.55 (t, 2H, ar, J = 7.60 Hz), 8.00 (d, 2H, ar, J = 7.7 Hz), 11.34 (br s, 1H, NH). Anal. Calc. For $C_{19}H_{16}N_4O_4$.

6-(3,4-Dimethoxyphenyl)-2-phenyl-1,2,4-triazolo[4,3-*a*]pyrazine-3,8(2*H*,7*H*)-dione (160). Yield 53%. m.p. >300 °C (EtOH/2-Methoxyethanol). ^{1}H NMR (DMSO-d_6) 3.81 (s, 3H, OCH_3), 3.87 (s, 3H, OCH_3), 7.03 (d, 2H, ar, J = 9.0 Hz), 7.27-7.29 (m, 3H, 2 ar + H-5), 7.36 (t, 1H, ar, J = 7.4 Hz), 7.56 (t, 2H, ar, J = 7.7 Hz), 8.02 (d, 2H, ar, J = 7.9 Hz), 11.54 (br s, 1H, NH). Anal. Calc. for $C_{19}H_{16}N_4O_4$.

6-(3,4,5-Trimethoxyphenyl)-2-phenyl-1,2,4-triazolo[4,3-*a*]pyrazine-3,8(2*H*,7*H*)-dione (161). Yield 25%. m.p. > 300 °C (AcOH/DMF). ^{1}H NMR (DMSO-d_6) 3.70 (s, 3H, CH_3), 3.89 (s, 6H, CH_3), 7.02 (s, 2H, ar), 7.37 (t, 1H, ar, J = 7.4 Hz), 7.49 (s, 1H, H-5), 7.57 (t, 2H, ar, J = 7.7 Hz), 8.02 (d, 2H, ar, J = 7.7 Hz), 11.59 (br s, 1H, NH). Anal. Calc. For $C_{20}H_{18}N_4O_5$.

6-(4-Methoxy-3,5-dimethylphenyl)-2-phenyl-[1,2,4]triazolo[4,3-a]pyrazine-3,8(2H,7H)-dione (162). Yield 70%. m.p. > 300 °C (2-Methoxyethanol/DMF). ^{1}H-NMR (DMSO-d_6) 2.28 (s, 6H, CH_3), 3.70 (s, 3H, CH_3), 7.21 (s, 1H, ar), 7.36 (t, 1H, ar, J = 7.4 Hz), 7.44 (s, 2H, ar), 7.56 (t, 2H, ar, J = 7.9 Hz), 8.01 (d, 2H, ar, J = 7.9 Hz), 11.48 (br. s, 1H, NH). Anal. Calc. For $C_{20}H_{18}N_4O_3$.

6-(3,5-di-tert-butyl-4-methoxyphenyl)-2-phenyl-[1,2,4]triazolo[4,3-a]pyrazine-3,8(2H,7H)-dione (163). Yield 75%. m.p. > 300°C (AcOH/DMF). ^{1}H-NMR (DMSO-d_6) 1.44 (s, 18H, $(CH_3)_3$), 3.67 (s, 3H, CH_3), 7.24 (s, 1H, ar), 7.36 (t, 1H, ar, J = 7.4 Hz), 7.49 (s,

2H, ar), 7.56 (t, 2H, ar, J = 7.4 Hz), 8.02 (d, 2H, ar, J = 8.2 Hz), 11.63 (br. s, 1H, NH). Anal. Calc. For $C_{26}H_{30}N_4O_3$.

General procedure for the synthesis of 8-chloro-1,2,4-triazolo[4,3-a]pyrazin-3-(2H)-one derivatives (164-193).

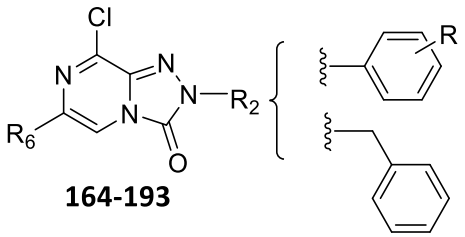

164-193

A suspension of the suitable 8-oxo-triazolopyrazine derivatives **134-163** (2 mmol) in phosphorus oxychloride (10 mL) was heated in the following conditions: microwave irradiation at 160 °C for 90 min otherwise at 160 °C for 20 min (compound **165**), 1 h (compound **168**) and 3.5 h (compound **169**) or at 170 °C for 30 min (compound **171**) and 1.5 h (compounds **172** and **173**); sealed tube in a bath oil at 140 °C for 16 h (compounds **164, 166**) or at 180 °C for 3 h (compound **167**). The excess of phosphorus oxychloride was distilled off and the residue was treated with water (about 5−10 mL). The obtained solid was collected by filtration. These intermediates were pure enough (NMR, TLC) to be used for the next step without further purification.

8-Chloro-6-methyl-2-phenyl-1,2,4-triazolo[4,3-*a*]pyrazin-3(2*H*)-one (164). Yield 81%. ^{1}H NMR (DMSO-d_6) 2.21 (s, 3H, CH_3), 7.36-7.40 (m, 1H, ar), 7.47 (s, 1H, H-5), 7.55-7.58 (m, 1H, ar), 7.54 (t, 2H, ar, J = 7.7 Hz), 8.01-8.3 (m, 2H, ar). Anal. Calc. For $C_{12}H_9ClN_4O$.

8-Chloro-2,6-diphenyl-1,2,4-triazolo[4,3-*a*]pyrazin-3(2*H*)-one (165). Yield 78%. ^{1}H NMR (DMSO-d_6) 7.41-7.43 (m, 2H, ar), 7.50 (t, 2H, ar, J = 7.3 Hz), 7.60 (t, 2H, ar, J = 8.0 Hz), 8.04-8.09 (m, 4H, ar), 8.61 (s, 1H, H-5). Anal. Calc. For $C_{17}H_{11}ClN_4O$.

8-Chloro-6-methyl-2-(4-methoxyphenyl)-1,2,4-triazolo[4,3-*a*]pyrazin-3(2*H*)-one (166). Yield 80%. ^{1}H NMR (DMSO-d_6) 2.31 (s, 3H, CH_3), 3.82 (s, 3H, OCH_3), 7.12 (d, 2H, ar, J = 8.0 Hz), 7.90-7.93 (m, 3H, 2 ar + H-5). Anal. Calc. For $C_{13}H_{11}ClN_4O_2$.

8-Chloro-2-(4-methoxyphenyl)-6-phenyl-1,2,4-triazolo[4,3-*a*]pyrazin-3(2*H*)one (167). Yield 96%. ^{1}H NMR (DMSO-d_6) 3.84 (s, 3H, CH_3), 7.15 (d, 2H, ar, J= 9.1 Hz), 7.04-7.63 (m, 3H, ar), 7.94 (d, 2H, ar, J= 9.1 Hz), 8.05 (d, 2H, ar, J= 7.5 Hz), 8.61 (s, 1H, H-5). Anal. Calc. For $C_{18}H_{13}ClN_4O_2$.

8-Chloro-2-(4-nitrophenyl)-6-phenyl-1,2,4-triazolo[4,3-*a*]pyrazin-3(2*H*)one (168). Yield 72%. ^{1}H NMR (DMSO-d_6) 7.42 (t, 1H, ar, J= 7.4 Hz), 7.51 (d, 2H, ar, J= 7.4 Hz), 8.07 (d, 2H, ar, J= 7.4 Hz), 8.39 (d, 2H, ar, J= 7.1 Hz), 8.47 (d, 2H, ar, J= 7.1 Hz), 8.67 (s, 1H, H-5). Anal. Calc. For $C_{17}H_{10}ClN_5O_3$.

8-Chloro-2-(2-methoxyphenyl)-6-phenyl-1,2,4-triazolo[4,3-*a*]pyrazin-3(2*H*)one (169). Yield 96%. ^{1}H NMR (DMSO-d_6) 3.83 (s, 3H, OCH_3), 7.14 (t, 1H, ar, J= 7.6 Hz), 7.30 (d, 1H, ar, J= 8.4 Hz), 7.42 (t, 1H, ar, J= 7.3 Hz), 7.46-7.55 (m, 1H; ar), 7.57 (t, 1H, ar), 8.02 (d, 2H, ar, J= 7.3 Hz), 8.56 (s, 1H, H-5). Anal. Calc. For $C_{18}H_{13}ClN_4O_2$.

8-Chloro-6-(2-methoxyphenyl)-2-phenyl-1,2,4-triazolo[4,3-a]pyrazin-3-(2H)-one (170). Yield 81%. ^{1}H NMR (DMSO-d_6) 3.98 (s, 3H, OCH_3), 7.13 (t, 1H, ar, 7.5 Hz), 7.21 (d, 1H, ar, J= 8.3 Hz), 7.38-7.45 (m, 2H, ar), 7.59 (t, 2H, ar, J= 7.8 Hz), 8.00 (d, 1H; ar, J= 7.8 Hz), 8.06 (d, 2H, ar, J= 8.2 Hz), 8.46 (s, 1H, H-5). Anal. Calc. For $C_{18}H_{13}ClN_4O_2$.

8-Chloro-6-(3-methoxyphenyl)-2-phenyl-1,2,4-triazolo[4,3-*a*]pyrazin-3 (2*H*)-one (171). Yield 87%. ^{1}H NMR (DMSO-d_6) 3.85 (s, 3H, OCH_3), 6.98 (d, 1H, ar, J = 7.6 Hz), 7.38-7.42 (m, 2H, ar), 7.57-7.63 (m, 4H, ar), 8.07 (d, 2H, ar, J = 7.7 Hz), 8.68 (s, 1H, H-5). Anal. Calc. For $C_{18}H_{13}ClN_4O_2$.

8-Chloro-6-(4-methoxyphenyl)-2-phenyl-1,2,4-triazolo[4,3-*a*]pyrazin-3 (2*H*)-one (172). Yield 92%. ^{1}H NMR (DMSO-d_6) 3.82 (s, 3H, CH_3), 7.05 (d, 2H, ar, J = 8.8 Hz), 7.40 (t, 1H, ar, J = 7.4 Hz), 7.59 (t, 2H, ar, J = 7.9 Hz), 7.98 (d, 2H, ar, J = 8.8 Hz), 8.07 (d, 2H, ar, J = 7.9 Hz), 8.49 (s, 1H, H_5). Anal. Calc. For $C_{18}H_{13}ClN_4O_2$.

8-Chloro-6-(4-methylphenyl)-2-phenyl-1,2,4-triazolo[4,3-*a*]pyrazin-3 (2*H*)-one (173). Yield 90%. ^{1}H NMR (DMSO-d_6) 2.36 (s, 3H, CH_3), 7.30 (d, 2H, ar, J = 8.1 Hz), 7.40 (t, 1H, ar, J = 7.8 Hz), 7.59 (t, 2H, ar, J = 7.8 Hz), 7.94 (d, 2H, ar, J = 8.1 Hz), 8. 07 (d, 2H, ar, J = 8.5 Hz), 8.55 (s, 1H, H-5). Anal. Calc. For $C_{18}H_{13}ClN_4O$.

8-Chloro-6-(3,4-methylendioxyxyphenyl)-2-phenyl-1,2,4-triazolo[4,3-*a*]pyrazin-3 (2*H*)-one (174). Yield 64%. ^{1}H NMR (DMSO-d_6) 6.10 (s, 2H, CH_2), 7.03 (d, 1H, ar, J = 8.1 Hz), 7.40 (t, 1H, ar, J = 7.3 Hz), 7.57-7.59 (m, 3H, ar), 7.65 (s, 1H, ar), 8.07 (d, 2H, ar, J = 8.00 Hz), 8.55 (s, 1H, H-5). Anal. Calc. For $C_{18}H_{11}ClN_4O_3$.

6-(3-Bromophenyl)-8-chloro-2-phenyl-1,2,4-triazolo[4,3-a]pyrazin-3-(2H)-one (175). Yield 82%. ^{1}H NMR (DMSO-d_6) 7.36-7.41 (m, 2H, ar), 7.53-7.59 (m, 3H, ar), 7.82 (d, 1H, ar, J = 7.9 Hz), 7.09-7.11 (m, 2H, 1 ar + H-5), 8. 15 (d, 2H, ar, J = 7.7 Hz). Anal. Calc. For $C_{17}H_{10}BrClN_4O$.

6-(4-Bromophenyl)-8-chloro-2-phenyl-1,2,4-triazolo[4,3-a]pyrazin-3-(2H)-one (176). Yield 93%. ^{1}H NMR (DMSO-d_6) 7.41 (t, 1H, ar, J = 7.3 Hz), 7.60 (t, 2H, ar, J = 8.1 Hz), 7.68 (d, 2H, ar, J = 8.5 Hz), 8.02 (d, 2H, ar, J = 8.5 Hz), 8.07 (d, 2H, ar, J = 8.6 Hz), 8.71 (s, 1H, H-5). Anal. Calc. For $C_{17}H_{10}BrClN_4O$.

8-Chloro-6-(3-chlorophenyl)-2-phenyl-1,2,4-triazolo[4,3-a]pyrazin-3-(2H)-one (177). Yield 77%. ^{1}H NMR (DMSO-d_6) 7.41 (t, 1H, ar, J = 7.3 Hz), 7.47-7.54 (m, 2H, ar), 7.60 (t, 2H, ar, J = 7.4 Hz), 8.03-8.08 (m, 3H, ar), 8.13 (s, 1H, ar) 8.80 (s, 1H, H-5). Anal. Calc. For $C_{17}H_{10}Cl_2N_4O$.

8-Chloro-6-(4-chlorophenyl)-2-phenyl-1,2,4-triazolo[4,3-a]pyrazin-3-(2H)-one (178). Yield 75%. ^{1}H NMR (DMSO-d_6) 7.40 (t, 1H, ar, J = 7.3 Hz), 7.53-7.61 (m, 4H, ar), 8.05-8.09 (m, 4H, ar), 8.69 (s, 1H, H-5). Anal. Calc. For $C_{17}H_{10}Cl_2N_4O$.

8-Chloro-6-(2-nitrophenyl)-2-phenyl-1,2,4-triazolo[4,3-a]pyrazin-3 (2H)-one (179). Yield 93%. ^{1}H NMR (DMSO-d_6) 7.45 (t, 1H, ar, J = 7.4 Hz), 7.63 (t, 2H, ar, J = 7.5 Hz), 7.76-7.75 (m, 1H, ar), 7.86-7.89 (m, 2H, ar), 8.06-8.08 (m, 3H, ar), 8.63 (s, 1H, H-5). Anal. Calc. For $C_{17}H_{10}ClN_5O_3$.

8-Chloro-6-(3-nitrophenyl)-2-phenyl-1,2,4-triazolo[4,3-a]pyrazin-3 (2H)-one (180). Yield 95%. ^{1}H NMR (DMSO-d_6) 7.42 (t, 1H, ar, J = 7.1 Hz), 7.60 (t, 2H, ar, J = 7.6 Hz), 7.79 (t, 1H, ar, J = 7.8 Hz), 8.07 (d, 2H, ar, J = 7.8 Hz), 8.26 (d, 1H, ar, J = 7.7 Hz), 8.54 (d, 1H, ar, J = 7.8 Hz), 8.82 (s, 1H, ar), 8.98 (s, 1H, H-5). Anal. Calc. For $C_{17}H_{10}ClN_5O_3$.

8-Chloro-6-(4-nitrophenyl)-2-phenyl-1,2,4-triazolo[4,3-a]pyrazin-3 (2H)-one (181). Yield 89%. ^{1}H NMR (DMSO-d_6) 7.42 (t, 1H, ar, J = 7.4 Hz), 7.61 (t, 2H, ar, J = 7.7 Hz), 8.07 (d, 2H, ar, J = 7.7 Hz), 8.32 (d, 2H, ar, J = 9.2 Hz), 8.36 (d, 2H, ar, J = 9.2 Hz), 8.95 (s, 1H, H-5). Anal. Calc. For $C_{17}H_{10}ClN_5O_3$.

8-Chloro-6-(2-furyl)-2-phenyl[1,2,4]triazolo[4,3-a]pyrazin-3-(2H)-one (182). Yield 90%. ^{1}H NMR (DMSO-d_6) 6.65-6.66 (d, 1H, furan proton), 6.98 (d, 1H, furan proton, J = 1.8 Hz), 7.39 (t, 1H, ar, J = 7.3 Hz), 7.58 (t, 2H, ar, J = 7.3 Hz), 7.83 (s, 1H, furan proton), 8.03 (d, 2H, ar, J= 7.1 Hz), 8.07 (s, 1H, H-5). Anal. Calc. For $C_{15}H_9ClN_4O_2$.

8-Chloro-6-(5-methylfuran-2-yl)-2-phenyl[1,2,4]triazolo[4,3-a]pyrazin-3-(2H)-one (183). Yield 92%. ^{1}H NMR (DMSO-d_6) 2.38 (s, 3H, CH_3), 6.28 (s, 1H, furan proton), 6.86 (s, 1H, furan proton), 7.41 (t, 1H, ar, J = 7.4 Hz), 7.59 (t, 2H, ar, J = 7.4 Hz), 7.96 (s, 1H, H-5), 8.05 (d, 2H, ar, J = 8.3 Hz). Anal. Calc. For $C_{16}H_{11}ClN_4O_2$.

8-Chloro-6-(2-thienyl)-2-phenyl[1,2,4]triazolo[4,3-a]pyrazin-3-(2H)-one (184). Yield 72%. ^{1}H NMR (DMSO-d_6) 7.18 (t, 1H, ar, J = 4.3 Hz), 7.41 (t, 1H, ar, J = 7.4 Hz), 7.58-7.65 (m, 3H, ar), 7.89 (d, 1H, thiophene proton, J = 3.6 Hz), 8.07 (d, 2H, ar, J = 8.3 Hz), 8.62 (s, 1H, H_5). $C_{15}H_9ClN_4OS$.

8-Chloro-2-phenyl-6-(2-pyridyl)[1,2,4]triazolo[4,3-a]pyrazin-3-(2H)-one (185). Yield 87%. ^{1}H NMR (DMSO-d_6) 7.42 (t, 1H, ar, J = 7.1 Hz), 7.50 (t, 1H, ar, J = 6.1 Hz), 7.60 (t, 2H, ar, J = 7.8 Hz), 8.01-8.14 (m, 4H, ar), 8.62 (d, 1H, pyridine proton, J = 4.5 Hz), 8.71 (s, 1H, H_5). Anal. Calc. For $C_{16}H_{10}ClN_5O$.

2-Benzyl-8-chloro-6-phenyl-1,2,4-triazolo[4,3-a]pyrazin-3-(2H)-one (186). Yield 68%. ^{1}H NMR (DMSO-d_6) 5.24 (s, 2H, CH_2), 7.33-7.42 (m, 6H, ar), 7.48 (t, 2H, ar, J = 7.1), 8.01 (d, 2H, ar, J = 7.2 Hz), 8.53 (s, 1H, H-5). Anal. Calc. For $C_{18}H_{13}ClN_4O$.

2-Benzyl-8-chloro-6-(furan-2-yl)-1,2,4-triazolo[4,3-a]pyrazin-3-(2H)-one (187). Yield 85%. ^{1}H NMR (DMSO-d_6) 5.22 (s, 2H, CH_2), 6.65 (dd, 1H, furan proton, J = 1.7 Hz, J = 1.5 Hz), 6.95 (d, 1H, furan proton, J = 3.2 Hz), 7.36-7.41 (m, 5H, ar), 7.82 (s, 1H, furan proton), 8.02 (s, 1H, H-5). Anal. Calc. For $C_{16}H_{11}ClN_4O_2$.

2-Benzyl-8-chloro-6-(5-methylfuran-2-yl)-1,2,4-triazolo[4,3-a]pyrazin-3-(2H)-one (188). Yield 95%. ^{1}H NMR (DMSO-d_6) 2.36 (s, 3H, CH_3), 5.22 (s, 2H, CH_2), 6.25 (d, 1H, furan proton, J = 2.1 Hz), 6.81 (d, 1H, furan proton, J = 2.8 Hz), 7.33-7.38 (m, 5H, ar), 7.89 (s, 1H, H-5). Anal. Calc. For $C_{17}H_{13}ClN_4O_2$.

8-Chloro-6-(2,4-dimethoxyphenyl)-2-phenyl-1,2,4-triazolo[4,3-*a*]pyrazin-3 (2*H*)-one (189). Yield 96 % ^{1}H NMR (DMSO-d_6) 3.90 (s, 3H, CH_3), 3.97 (s, 3H, CH_3), 6.71-6.75 (m, 2H, ar), 7.39 (t, 1H, ar, J = 7.4 Hz), 7.58 (t, 2H, ar, J = 7.6 Hz), 7.92 (d, 1H, ar, J = 8.6 Hz), 8.06 (d, 2H. ar, J = 7.8 Hz), 8.34 (s, 1H, H-5). Anal. Calc. For $C_{19}H_{15}ClN_4O_3$.

8-chloro-6-(3,4-dimethoxyphenyl)-2-phenyl-[1,2,4]triazolo[4,3-a]pyrazin-3(2H)-one (190). Yield 85 % ^{1}H NMR (DMSO-d_6) 3.81 (s, 3H, CH_3), 3.88 (s, 3H, CH_3), 7.06 (d, 1H, ar, J = 8.2 Hz), 7.41 (t, 1H, ar, J = 7.4 Hz), 7.62-7.58 (m, 4H, ar), 8.08 (d, 2H, ar, J = 8.1 Hz), 8.63 (s, 1H, H-5). Anal. Calc. For $C_{19}H_{15}ClN_4O_3$.

8-Chloro-6-(3,4,5-trimethoxyphenyl)-2-phenyl-1,2,4-triazolo[4,3-*a*]pyrazin-3 (2*H*)-one (191). Yield 96 % ^{1}H NMR (DMSO-d_6) 3.71 (s, 3H, CH_3), 3.89 (s, 6H, CH_3), 7.33 (s, 2H, ar), 7.41 (t, 1H, ar, J = 7.6 Hz), 7.62 (t, 2H, ar, J = 7.8 Hz), 8.07 (d, 2H, ar, J = 7.9 Hz), 8.79 (s, 1H, H-5). Anal. Calc. For $C_{20}H_{17}ClN_4O_4$.

8-Chloro-6-(4-methoxy-3,5-dimethylphenyl)-2-phenyl-[1,2,4]triazolo[4,3-a]pyrazin-3(2H)-one (192). Yield 82 % ^{1}H-NMR (DMSO-d_6) 2.30 (s, 6H, CH_3), 3.70 (s, 3H, CH_3), 7.41 (t, 1H, ar, J = 7.5 Hz), 7.59 (t, 2H, ar, J = 7.9 Hz), 7.73 (s, 2H, ar), 8.07 (d, 2H, ar, J = 8.1 Hz), 8.48 (s, 1H, ar). Anal. Calc. For $C_{20}H_{17}ClN_4O_2$.

8-Chloro-6-(3,5-di-tert-butyl-4-methoxyphenyl)-2-phenyl-[1,2,4]triazolo[4,3-a]pyrazin-3(2H)-one (193). Yield 90 % ^{1}H-NMR (DMSO-d_6) 1.45 (s, 18H, tBu), 3.67 (s, 3H, CH_3), 7.41 (t, 1H, ar, J = 7.56 Hz), 7.60 (t, 2H, ar, J = 7.80 Hz), 7.85 (s, 2H, ar), 8.07 (d, 2H, ar, J = 7.92 Hz), 8.65 (s, 1H, ar). Anal. Calc. For $C_{26}H_{29}ClN_4O_2$.

General procedure for the synthesis of 8-amino-1,2,4-triazolo[4,3-*a*]pyrazin-3(2*H*)-one derivatives (1-6, 11-13, 17, 29-36, 62-73).

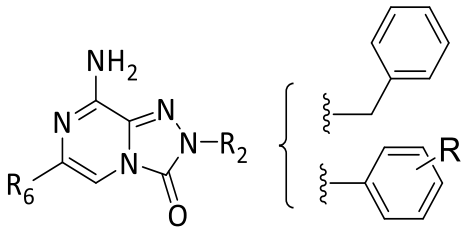

1-6, 11-13, 17, 29-36, 62-73

A suspension of the 8-chloro-triazolopirazine derivatives **164-193** (1 mmol) in a saturated ethanolic solution of NH_3 (30 mL) was heated at 130 °C in a sealed tube overnight with the exception of the 6-(2-furyl) derivative **182** that was reacted at 100 °C for 4 h. After cooling the mixture at room temperature, the solid was collected by filtration, washed with water (about 5-10 mL), dried and recrystallized. Derivatives **63, 67, 68** and **71** were purified by column chromatography.

8-Amino-6-methyl-2-phenyl-1,2,4-triazolo[4,3-*a*]pyrazin-3(2*H*)-one (1). Yield 92%. m.p. 258-259 °C (Toluene). ^{1}H NMR (DMSO-d_6) 2.11 (s, 3H, CH_3), 7.09 (s, 1H, H-5), 7.35 (t, 1H, ar, J = 6.6 Hz), 7.40 (br s, 2H, NH_2), 7.54 (t, 2H, ar, J = 7.7 Hz), 8.05 (d, 2H, ar, J = 7.7 Hz). Anal. Calc. for $C_{12}H_{11}N_5O$.

8-Amino-2,6-diphenyl-1,2,4-triazolo[4,3-*a*]pyrazin-3(2*H*)-one (2). Yield 50%. m.p. 276-277 °C (Nitromethane). ^{1}H NMR (DMSO-d_6) 7.33-7.38 (m, 2H, ar), 7.43 (t, 2H, ar, J = 7.4 Hz), 7.55-7.59 (m, 4H, 2 ar + NH_2), 7.77 (s, 1H, H-5), 7.98 (d, 2H, ar, J = 7.5 Hz), 8.08 (d, 2H, ar, J = 7.9 Hz). Anal. Calc. for $C_{17}H_{13}N_5O$.

8-Amino-6-methyl-2-(4-methoxyphenyl)-1,2,4-triazolo[4,3-*a*]pyrazin-3(2*H*)-one (3). Yield 83%. m.p. 243-244 °C (EtOH/2-Methoxyethanol). ^{1}H NMR (DMSO-d_6) 2.11 (s, 3H, CH_3), 3.81 (s, 3H, OCH_3), 7.07 (s, 1H, H-5), 7.09 (d, 2H, ar, J = 9.1 Hz), 7.36 (br s, 2H, NH_2), 7.90 (d, 2H, ar, J = 9.1 Hz). Anal. Calc. for $C_{13}H_{13}N_5O_2$.

8-Amino-2-(4-methoxyphenyl)-6-phenyl-1,2,4-triazolo[4,3-*a*]pyrazin-3(2*H*)-one (4). Yield 84%. m.p. 254-255 °C (Nitromethane). ^{1}H NMR (DMSO-d_6) 3.82 (s, 3H, OCH_3), 7.13 (d, 2H, ar, J= 8.8 Hz), 7.33-7.45 (m, 3H, ar), 7.56 (br s, 2H, NH_2), 7.75 (s, 1H, H-5), 7.92-7.99 (m, 4H, ar). IR 3366, 3311, 1644. Anal. Calc. for $C_{18}H_{15}N_5O_2$.

8-Amino-2-(4-nitrophenyl)-6-phenyl-1,2,4-triazolo[4,3-*a*]pyrazin-3(2*H*)-one (5). Yield 62%. m.p. 290-291 °C (Cyclohexane/EtOAc). ^{1}H NMR (DMSO-d_6) 7.13 (t, 1H, ar, J= 8.8 Hz), 7.35 (t, 2H, ar, J = 7.5 Hz), 7.69 (br s, 2H, NH_2), 7.79 (s, 1H, H-5), 7.99 (d, 2H, ar, J = 7.5 Hz), 8.38 (d, 2H, ar, J = 9.3 Hz), 8.48 (d, 2H, ar, J = 9.3 Hz). IR 3366, 3311, 1644. Anal. Calc. for $C_{17}H_{12}N_6O_3$.

8-Amino-2-(2-methoxyphenyl)-6-phenyl-1,2,4-triazolo[4,3-*a*]pyrazin-3(2*H*)-one (6). Yield 74%. m.p. 257-258 °C (Nitromethane). ^{1}H NMR (DMSO-d_6) 3.80 (s, 3H, OCH_3), 7.11 (t, 1H, ar, J= 7.6 Hz), 7.26 (d, 1H, ar, J= 8.3 Hz), 7.35 (t, 1H, ar, J= 7.3 Hz), 7.43 (t, 2H, ar, J= 7.3 Hz), 7.49-7.56 (m, 4H, 2ar + NH_2), 7.73 (s, 1H, H-5), 7.97 (d, 2H, ar, J= 7.5 Hz). Anal. Calc. for $C_{18}H_{15}N_5O_2$.

8-Amino-6-(2-methoxyphenyl)-2-phenyl-1,2,4-triazolo[4,3-a]pyrazin-3(2H)-one (11). Yield 68%. m.p. 249-251 °C (EtOH). ^{1}H NMR (DMSO-d_6) 3.93 (s, 3H, OCH_3), 7.06 (t, 1H, ar, J = 8.1 Hz), 7.14 (d, 1H, ar, J = 8.1 Hz), 7.34-7.37 (m, 2H, ar), 7.48 (br s, 2H, NH_2), 7.56 (t, 2H, ar, J = 7.8 Hz), 7.9 (s, 1H, H-5), 8.06-8.09 (m, 3H, ar). Anal. Calc. for $C_{18}H_{15}N_5O_2$.

8-Amino-6-(3-methoxyphenyl)-2-phenyl-1,2,4-triazolo[4,3-*a*]pyrazin-3(2*H*)-one (12). Yield 66%. m.p. 249-251 °C (EtOH). ^{1}H NMR (DMSO-d_6) 3.83 (s, 3H, CH_3), 6.90-6.93 (m, 1H, ar), 7.31-7.37 (m, 2H, ar), 7.53-7.58 (m, 6H, 4 ar + NH_2), 7.81 (s, 1H, H-5), 8.07 (d, 2H, ar, J = 7.5 Hz). IR = 3358, 3312, 1703, 1645 cm^{-1}. Anal. Calc. for $C_{18}H_{15}N_5O_2$.

8-Amino-6-(4-methoxyphenyl)-2-phenyl-1,2,4-triazolo[4,3-*a*]pyrazin-3(2*H*)-one (13). Yield 94%. m.p. 251-252 °C (EtOH/2-Methoxyethanol). ^{1}H NMR (DMSO-d_6) 3.80 (s, 3H, CH_3), 6.99 (d, 2H, ar, J = 8.7Hz), 7.36 (t, 1H, ar, J = 7.5 Hz), 7.54-7.58 (m 4H, 2ar + NH_2), 7.67 (s, 1H, H_5), 7.92 (d, 2H, ar, J = 8.7 Hz), 8.08 (d, 2H, ar, J = 8.5 Hz). IR 3381, 3308, 1697, 1649. Anal. Calc. for $C_{18}H_{15}N_5O_2$.

8-Amino-6-(4-methylphenyl)-2-phenyl-1,2,4-triazolo[4,3-*a*]pyrazin-3(2*H*)-one (17). Yield 75%. m.p. 287-288 °C (2-Methoxyethanol). ^{1}H NMR (DMSO-d_6) 2.34 (s, 3H, CH_3), 7.24 (d, 2H, ar., J = 7.9 Hz), 7.36 (t, 1H, ar, J = 7.4 Hz), 7.54-7.58 (m, 4H, 2 ar + NH_2), 7.70 (s, 1H, H_5), 7.87 (d, 2H, ar, J = 7.9 Hz), 8.07 (d, 2H, ar, J = 7.6 Hz). IR 3366, 3310, 1701, 1651. Anal. Calc. for $C_{18}H_{15}N_5O$.

8-Amino-6-(3,4-methylendioxyxyphenyl)-2-phenyl-1,2,4-triazolo[4,3-a]pyrazin-3 (2H)-one (29). Yield 96%. m.p. > 300 °C (AcOH/DMF). ^{1}H NMR (DMSO-d_6) 6.06 (s, 2H, CH_2), 6.96 (d, 1H, ar, J = 7.9 Hz), 7.35 (t, 1H, ar, J = 7.4 Hz), 7.54-7.58 (m, 6H, 4 ar + NH_2), 7.72 (s, 1H, H-5), 8.07 (d, 2H, ar, J = 7.8 Hz). Anal. Calc. for $C_{18}H_{13}N_5O_3$.

8-Amino-6-(3-bromophenyl)-2-phenyl-1,2,4-triazolo[4,3-a]pyrazin-3(2H)-one (30). Yield 87%. m.p. 281-283 °C (2-Methoxyethanol). ^{1}H NMR (DMSO-d_6) 7.35-7.40 (m, 2H, ar), 7.52-7.59 (m, 3H, ar), 7.66 (br s, 2H, NH_2), 7.93 (s, 1H, H-5), 8.02 (d, 1H, ar, J = 7.8 Hz), 8.07 (d, 2H, ar, J = 8.0 Hz), 8.23 (s, 1H, ar). ^{13}C NMR (DMSO-d_6) 102.93, 119.90, 122.57, 124.64, 126.83, 128.65, 129.68, 131.04, 131.09, 131.60, 134.18, 137.89, 139.26, 147.63, 147.94. Anal. Calc. for $C_{17}H_{12}BrN_5O$.

8-Amino-6-(4-bromophenyl)-2-phenyl-1,2,4-triazolo[4,3-a]pyrazin-3(2H)-one (31). Yield 92%. m.p. 266-268 °C (2-Methoxyethanol). ^{1}H NMR (DMSO-d_6) 7.36 (t, 1H, ar, J = 7.4 Hz), 7.57 (t, 2H, ar, J = 7.8 Hz), 7.63-7.61 (m, 4H, 2 ar + NH_2), 7.85 (s, 1H, H-5), 7.96 (d, 2H, ar, J = 8.6 Hz), 8.07 (d, 2H, ar, J = 7.8 Hz). ^{13}C NMR (DMSO-d_6) 102.35, 119.89, 121.63, 126.79, 128.01, 129.66, 131.57, 131.81, 134.82, 136.15, 137.93, 147.63, 147.94. Anal. Calc. for $C_{17}H_{12}BrN_5O$.

8-Amino-6-(3-chlorophenyl)-2-phenyl-1,2,4-triazolo[4,3-a]pyrazin-3(2H)-one (32). Yield 85%. m.p. 279-281 °C (EtOH/2-Methoxyethanol). ^{1}H NMR (DMSO-d_6) 7.34-7.47 (m, 3H, ar), 7.57 (t, 2H, ar, J = 7.7 Hz), 7.65 (br s, 2H, NH_2), 7.92 (s, 1H, H-5), 7.98 (d, 1H, ar, J = 7. 7 Hz), 8.06-8.08 (m, 3H, ar). ^{13}C NMR (DMSO-d_6) 102.96, 119.92, 124.30, 125.78, 126.82, 128.14, 129.67, 130.78, 131.62, 133.96, 134.33, 137.91, 139.09, 147.64, 147.95. Anal. Calc. for $C_{17}H_{12}ClN_5O$.

8-Amino-6-(4-chlorophenyl)-2-phenyl-1,2,4-triazolo[4,3-a]pyrazin-3(2H)-one (33). Yield 87%. m.p. 256-258 °C (2-Methoxyethanol). ^{1}H NMR (DMSO-d_6) 7.36 (t, 1H, ar, J = 7.4 Hz), 7.48 (d, 2H, ar, J = 8.6 Hz), 7.56 (t, 2H, ar, J = 7.6 Hz), 7.63 (br s, 2H, NH_2), 7.84 (s, 1H, H-5), 8.02 (d, 2H, ar, J = 8.5 Hz), 8.07 (d, 2H, ar, J = 7.6 Hz). ^{13}C NMR (DMSO-d_6) 102.40, 119.88,

127.70, 128.97, 129.57, 129.72, 131.55, 132.99, 134.75, 135.76, 137.92, 147.62, 147.92. Anal. Calc. for $C_{17}H_{12}ClN_5O$.

8-Amino-6-(2-nitrophenyl)-2-phenyl-1,2,4-triazolo[4,3-a]pyrazin-3 (2H)-one (34). Yield 83%. m.p. 281-283 °C (AcOH). ^{1}H NMR (DMSO-d_6) 7. 40 (t, 1H, ar, J = 7. 4 Hz), 7.58- 7.69 (m, 6H, 4ar + NH_2), 7.76-7.80 (m, 2H, 1 ar + H-5), 7.98 (d, 1H, ar, J = 7. 8 Hz), 8.09 (d, 2H, ar, J = 7.7 Hz). Anal. Calc. for $C_{17}H_{12}N_6O_3$.

8-Amino-6-(3-nitrophenyl)-2-phenyl-1,2,4-triazolo[4,3-a]pyrazin-3 (2H)-one (35). Yield 72%. m.p. 280-281 °C (AcOH). ^{1}H NMR (DMSO-d_6) 7.37 (t, 1H, ar, J = 7.2 Hz), 7.57 (t, 2H, ar, J = 7.6 Hz), 7.71 (t, 1H, ar, J = 7.7 Hz), 7.77 (br s, 2H, NH_2), 8.07-8.09 (m, 3H, 2 ar + H-5), 8.19 (d, 1H, ar, J = 7.6 Hz), 8.48 (d, 1H, ar, J = 7.6 Hz), 8.85 (s, 1H, ar). Anal. Calc. for $C_{17}H_{12}N_6O_3$.

8-Amino-6-(4-nitrophenyl)-2-phenyl-1,2,4-triazolo[4,3-a]pyrazin-3 (2H)-one (36). Yield 69%. m.p. 297-299 °C (2-Methoxyethanol/DMF). ^{1}H NMR (DMSO-d_6) 7.36 (t, 1H, ar, J = 7.4 Hz), 7.57 (t, 2H, ar, J = 7.7 Hz), 7.73 (br s, 2H, NH_2), 8.06-8.08 (m, 3H, 2 ar + H-5), 8.28 (s , 4H, ar). ^{13}C-NMR (DMSO-d_6) 104.87, 119.91, 124.19, 126.80, 126.87, 129.69, 131.56, 133.78, 137.85, 143.48, 147.17, 147.64, 148.08. IR = 1713, 3373, 3485 cm^{-1}. Anal. Calc. for $C_{17}H_{12}N_6O_3$.

8-Amino-6-(2-furyl)-2-phenyl-1,2,4-triazolo[4,3-a]pyrazin-3-(2H)-one (62). Yield 25%. ^{1}H NMR (DMSO-d_6) 6.59-6.60 (m, 1H, furan ptoton), 6.78 (d, 1H, furan proton, J = 1.8 Hz), 7.38 (t, 1H, ar, J = 7.4 Hz), 7.41 (s, 1H, H-5), 7.58 (t, 2H, ar, J = 7.8 Hz), 7.65 (br s, 2H, NH_2), 7.74 (s, 1H, furan proton), 8.06 (d, 2H, ar, J= 7.8 Hz). Anal. Calc. for $C_{15}H_{11}N_5O_2$.

8-Amino-6-(5-methylfuran-2-yl)-2-phenyl-1,2,4-triazolo[4,3-a]pyrazin-3-(2H)-one (63). Yield 52%. m.p. 263-265 °C Purified by column chromatography. (Cyclohexane 6/EtOAc 4). ^{1}H NMR (DMSO-d_6) 2.34 (s, 3H, CH_3), 6.20 (s, 1H, furan proton), 6.66 (s, 1H, furan proton), 7.33-7.37 (m, 2H, 1ar + 1 furan proton), 7.56 (t, 2H, ar, J= 7.8 Hz), 7.63 (br s, 2H, NH_2), 8.06 (d, 2H, ar, J= 7.8 Hz). ^{13}C NMR (DMSO-d_6) 13.89, 99.15, 108.39, 108.79, 119.81, 126.78, 129.58, 129.65, 131.47, 137.88, 147.51, 148.27, 150.06, 152.30. Anal. Calc. for $C_{16}H_{13}N_5O_2$.

8-Amino-2-phenyl-6-(2-thienyl)-1,2,4-triazolo[4,3-a]pyrazin-3(2H)-one (**64**). Yield 58%. m.p. 283-284 °C (EtOH/2-Methoxyethanol). ^{1}H NMR (DMSO-d_6) 7.11 (t, 1H, ar, J = 4.4 Hz), 7.36 (t, 1H, ar, J = 7.5 Hz), 7.51-7.71 (m, 6H, 4ar + NH_2), 7.80 (s, 1H, H_5), 8.07 (d, 2H, ar, J = 7.8 Hz).^{13}C NMR (DMSO-d_6) 100.20, 119.85, 123.09, 126.50, 126.79, 128.62, 129.67,

131.52, 132.25, 137.92, 142.42, 147.53, 147.92. IR = 3318, 3223, 1715, 1643 cm^{-1}. Anal. Calc. for $C_{15}H_{11}N_5OS$.

8-Amino-2-phenyl-6-(2-pyridyl)- 1,2,4-triazolo[4,3-a]pyrazin-3(2H)-one (**65**). Yield 62%. m.p. 251-252 °C (EtOH). ^1H NMR (DMSO-d_6) 7.36 (t, 2H, ar, J = 5.9 Hz), 7.57 (t, 2H, ar, J = 8.0 Hz), 7.65 (br s, 2H, NH_2), 7.90 (t, 1H, pyridine proton, J = 3.9 Hz), 7.92-8.10 (m, 4H, 3ar + H_5), 8.62 (d, 1H, ar, J = 3.8 Hz). IR = 3217, 3167, 1715, 1634 cm^{-1}. Anal. Calc. for $C_{16}H_{12}N_6O$.

8-Amino-2-benzyl-6-phenyl-1,2,4-triazolo[4,3-a]pyrazin-3(2H)-one (**66**). Yield 79%. m.p. 288-290 °C (DMF). ^1H NMR (DMSO-d_6) 5.18 (s, 2H, CH_2), 7.31-7.45 (m, 10H, 8 ar + NH_2), 7.72 (s, 1H, H-5), 7.95 (d, 2H, ar, J = 7.2 Hz). Anal. Calc. for $C_{18}H_{15}N_5O$.

8-Amino-2-benzyl-6-(furan-2-yl)-1,2,4-triazolo[4,3-a]pyrazin-3(2H)-one (**67**). Yield 38%. m.p. 185-187 °C. Purified by column chromatography (n-Hexane 7/EtOAc 3 / MeOH 0.1). ^1H NMR (DMSO-d_6) 5.16 (s, 2H, CH_2), 6.58 (dd, 1H, furan proton, J = 1.6 Hz, J = 1.8 Hz), 6.75 (d, 1H, furan proton, J = 3.1 Hz), 7.31-7.37 (m, 6H, 5 ar + H-5), 7.51 (br s, 2H, NH_2), 7.72 (s, 1H, furan proton). Anal. Calc. for $C_{16}H_{13}N_5O_2$.

8-Amino-2-benzyl-6-(5-methylfuran-2-yl)-1,2,4-triazolo[4,3-a]pyrazin-3-(2H)-one (**68**). Yield 54%. m.p. 215-217 °C Purified by column chromatography. (Cyclohexane 5 /EtOAc 4 /MeOH 1). ^1H NMR (DMSO-d_6) 2.33 (s, 3H, CH_3), 5.15 (s, 2H, CH_2), 6.17-6.18 (m, 1H, furan proton), 6.61 (d, 1H, furan proton, J = 3.0 Hz), 7.30-7.39 (m, 6H, ar + H-5), 7.47 (br s, 2H, NH_2). Anal. Calc. for $C_{17}H_{15}N_5O_2$.

8-Amino-6-(2,4-dimethoxyphenyl)-2-phenyl-1,2,4-triazolo[4,3-a]pyrazin-3 (2H)-one (**69**). Yield 43%. m.p. 255-257 °C (EtOH/2-Methoxyethanol). ^1H NMR (DMSO-d_6) 3.82 (s, 3H, CH_3), 3.92 (s, 3H, CH_3), 6.64-6.68 (m, 2H, ar), 7.35 (t, 1H, ar, J = 7.4 Hz), 7.43 (br s, 2H, NH_2), 7.57 (t, 2H, ar, J = 8.4 Hz), 7.80 (s, 1H, H-5), 8.02 (d, 1H, ar, J = 8.6 Hz), 8.07 (d, 2H, ar, J = 8.4 Hz). Anal. Calc. for $C_{19}H_{17}N_5O_3$.

8-Amino-6-(3,4-dimethoxyphenyl)-2-phenyl-1,2,4-triazolo[4,3-a]pyrazin-3(2H)-one (**70**). Yield 65%. m.p. 212-214 °C (EtOH/2-Methoxyethanol). ^1H NMR (DMSO-d_6) 3.80 (s, 3H, OCH_3), 3.86 (s, 3H, OCH_3), 7.00 (d, 2H, ar, J = 8.4 Hz), 7.36 (t, 1H, ar, J = 7.4 Hz), 7.52-7.58 (m, 6H, 4 ar + NH_2), 7.76 (s, 1H, H-5), 8.08 (d, 2H, ar, J = 7.7 Hz).^{13}C-NMR (DMSO-d_6) 55.98, 56.09, 100.99, 109.59, 112.05, 118.63, 119.85, 126.72, 129.57, 129.64, 131.54, 135.92, 137.99, 147.63, 149.20, 149.42. IR = 3348.42, 3340.00-3300.00, 1714.72, 1699.29 cm^{-1}. Anal. Calc. for $C_{19}H_{17}N_5O_3$.

8-Amino-6-(3,4,5-trimethoxyphenyl)-2-phenyl-1,2,4-triazolo[4,3-a]pyrazin-3 (2H)-one (**71**). Yield 95%. m.p. 231-232 °C. Purified by liquid chromatography ($CHCl_3$ 9.5/MeOH 0.4). ^{1}H NMR (DMSO-d_6) 3.70 (s, 3H, CH_3), 3.87 (s, 6H, CH_3), 7.28 (s, 2H, ar), 7.35 (t, 1H, ar, J = 7.4 Hz), 7.56-7.58 (m, 4H, ar + NH_2), 7.90 (s, 1H, H-5), 8.08 (d, 2H, ar, J = 7.7 Hz). Anal. Calc. for $C_{20}H_{19}N_5O_4$.

8-Amino-6-(4-methoxy-3,5-dimethylphenyl)-2-phenyl-[1,2,4]triazolo[4,3-a]pyrazin-3(2H)-one (**72**)**.** Yield 70%. m.p. 228-229°C (EtOH). ^{1}H-NMR (DMSO-d_6) 2.27 (s, 6H, CH_3), 3.68 (s, 3H, CH_3), 7.35 (t, 1H, ar, J = 7.4 Hz), 7.58-7.54 (m, 4H, ar + NH_2), 7.71-7.66 (m, 3H, ar), 8.07 (d, 2H, ar, J = 7.8 Hz).^{13}C-NMR (DMSO-d_6) 16.43, 59.79, 101.15, 119.91, 126.38, 126.76, 129.66, 130.67, 131.51, 132.02, 135.79, 137.96, 147.62, 147.75, 157.12. IR = 3400.50, 3298.28, 1699.29 cm^{-1}. Anal. Calc. for $C_{20}H_{19}N_5O_2$.

8-Amino-6-(3,5-di-tert-butyl-4-methoxyphenyl)-2-phenyl-[1,2,4]triazolo[4,3-a]pyrazin-3(2H)-one (**73**). Yield 75%. m.p. 263-264°C (2-Methoxyethanol). ^{1}H-NMR (DMSO-d_6) 1.44 (s, 18H, tBu), 3.66 (s, 3H, CH_3), 7.35 (t, 1H, ar, J = 7.4 Hz), 7.54 (br. s, 2H, NH_2), 7.56 (t, 2H, ar, J = 7.7 Hz), 7.68 (s, 1H, ar), 7.78 (s, 2H, ar), 8.08 (d, 2H, ar, J = 7.7 Hz).IR = 3473.80, 3296.35, 1716.65 cm^{-1}. Anal. Calc. for $C_{26}H_{31}N_5O_2$.

General procedure for the Synthesis of Hydroxy-substituted 8-amino-1,2,4-triazolo[4,3-*a*]pyrazin-3(2*H*)-one derivatives (7-9, 14-16, 74-77).

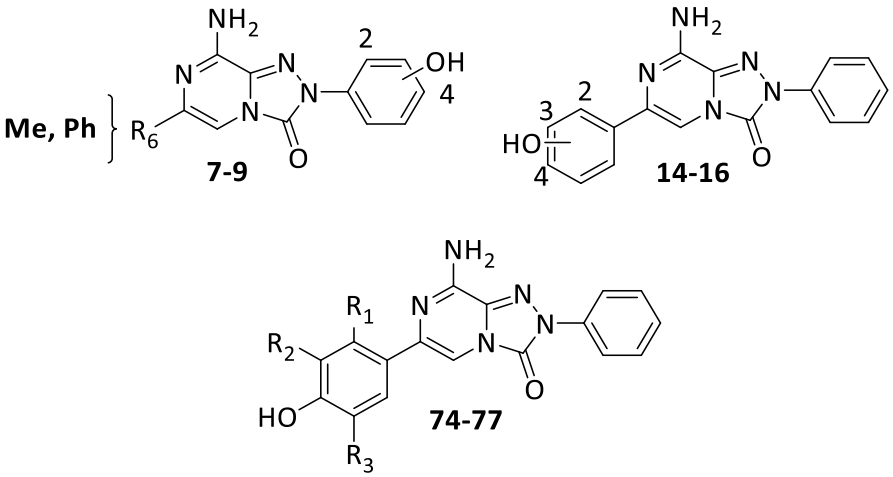

74, $\mathbf{R_1}$ = OMe; $\mathbf{R_2}$,$\mathbf{R_3}$ = H
75, $\mathbf{R_1}$, $\mathbf{R_3}$ = H ; $\mathbf{R_2}$ = OH
76, $\mathbf{R_1}$ = H; $\mathbf{R_2}$,$\mathbf{R_3}$ = OH
77, $\mathbf{R_1}$ = H; $\mathbf{R_2}$, $\mathbf{R_3}$ = Me

1 M solution of BBr_3 in DCM (5.1 mL) was slowly added at 0 °C, under nitrogen atmosphere, to a suspension of the methoxy-substituted triazolopirazines **3,4,6, 11-13**, **69-72** (1.02 mmol) in anhydrous DCM (20 mL). The mixture was stirred at room temperature until the disappearance of the starting material (TLC monitoring, 5-16 h), then was diluted with water (10 mL) and neutralized with a $NaHCO_3$ saturated solution. The organic solvent was removed by evaporation at reduced pressure and the solid was collected by filtration. The crude compounds were dried and purified by recrystallization (compounds **7-9**, **14-16, 75**) or liquid chromatography (compounds **74**, **76**, **77**).

8-Amino-2-(4-hydroxyphenyl)-6-methyl-1,2,4-triazolo[4,3-*a*]pyrazin-3(2*H*)-one (7). Yield 65%. m.p. > 300 °C (EtOH/2-Methoxyethanol). ^{1}H NMR (DMSO-d_6) 2.11 (s, 3H, CH_3), 6.88 (d, 2H, ar, J = 6.8 Hz), 7.06 (s, 1H, H-5), 7.33 (br s, 2H, NH_2), 7.75 (d, 2H, ar, J = 6.8 Hz). 9.69 (br s, 1H, OH). Anal. Calc. for $C_{12}H_{11}N_5O_2$.

8-Amino-2-(4-hydroxyphenyl)-6-phenyl-1,2,4-triazolo[4,3-*a*]pyrazin-3(2*H*)-one (8). Yield 72%. m.p. > 300 °C (EtOH). ^{1}H NMR (DMSO-d_6) 6.91 (d, 2H, ar, J = 8.5 Hz), 7.34 (t, 1H, ar, J = 7.5 Hz), 7.43 (t, 3H, ar, J = 7.5 Hz), 7.53 (br s, 2H, NH_2), 7.74 (s, 1H, H-5), 7.78 (d, 2H, ar, J = 8.5 Hz), 7.97 (d, 2H, ar, J = 7.8 Hz), 9.72 (s, 1H, OH). IR = 3393-3122, 1642, 1667 cm^{-1}. Anal. Calc. for $C_{17}H_{13}N_5O_2$.

8-Amino-2-(2-hydroxyphenyl)-6-phenyl-1,2,4-triazolo[4,3-*a*]pyrazin-3(2*H*)-one (9). Yield 67%. m.p. 271-273 °C (2-Methoxyethanol). ^{1}H NMR (DMSO-d_6) 6.95 (t, 1H, ar, J = 7.5 Hz), 7.03 (d, 1H, ar, J = 8.1 Hz), 7.33-7.44 (m, 5H ar), 7.55 (br s, 2H, NH_2), 7.75 (s, H, H-5), 7.98 (d, 2H, ar, J = 7.5 Hz), 9.88 (s, 1H, OH). Anal. Calc. for $C_{17}H_{13}N_5O_2$.

8-Amino-6-(2-hydroxyphenyl)-2-phenyl-1,2,4-triazolo[4,3-a]pyrazin-3(2H)-one (14). Yield 88%. m.p. 274-276 °C (EtOH). ^{1}H NMR (DMSO-d_6) 6.83-6.87 (m, 2H, ar), 7.18 (t, 1H, ar, J = 8.1 Hz), 7.37 (t, 1H, ar, J = 7.8 Hz), 7.57 (t, 2H, ar, J = 8.0 Hz), 7.91- 7.93 (m, 4H, 1ar + H-5 + NH_2), 8.07 (d, 2H, ar, J = 8. 0 Hz). 11.93 (s, 1H, OH). ^{13}C NMR (DMSO-d_6) 102.57, 117.76, 119.46, 119.61, 119.90, 126.87, 127.18, 129.70, 129.87, 131.27, 134.75, 137.88, 147.12, 147.59, 157.06. Anal. Calc. for $C_{17}H_{13}N_5O_2$.

8-Amino-6-(3-hydroxyphenyl)-2-phenyl-1,2,4-triazolo[4,3-*a*]pyrazin-3(2*H*)-one (15). Yield 93%. m.p. > 300 °C (EtOH/2-Methoxyethanol). ^{1}H NMR (DMSO-d_6) 6.75 (d, 1H, ar J = 7.3 Hz), 7.21 (t, 1H, ar, J = 7.4 Hz), 7.36-7.38 (m, 3H, ar), 7.55-7.61 (m, 5H, 3 ar + NH_2), 7.61 (s, 1H, H-5), 8.08 (d, 2H, ar, J = 8.1 Hz), 9.45 (s, 1H, OH). Anal. Calc. for $C_{17}H_{13}N_5O_2$.

8-Amino-6-(4-hydroxyphenyl)-2-phenyl-1,2,4-triazolo[4,3-*a*]pyrazin-3(2*H*)-one (16). Yield 85%. m.p. 285-286 °C (EtOH/2-Methoxyethanol). ^{1}H NMR (DMSO-d_6) 6.81 (d, 2H, ar., J = 6.8 Hz), 7.35 (t, 1H, ar, J = 7.4 Hz), 7.40 (t, 2H, ar, J= 7.6 Hz), 7.53 (br s, 2H, NH_2), 7.73 (s, 1H, H-5), 7.79 (d, 2H, ar, J = 6.8 Hz), 8.08 (d, 2H, ar, J = 7.6 Hz), 9.58 (s, 1H, OH). IR = 3379-3294, 1694, 1643 cm^{-1}. Anal. Calc. for $C_{17}H_{13}N_5O_2$.

8-Amino-6-(4-hydroxy-2-methoxyphenyl)-2-phenyl-[1,2,4]triazolo[4,3-a]pyrazin-3(2H)-one (74) . Yield 90%. m.p. 282-284 °C. Purified by liquid chromatography (Cyclohexane 5/EtOAc 5/MeOH 1). ^{1}H-NMR (DMSO-d_6) 9.67 (br. s, 1H, OH), 8.07 (d, 2H, ar, J = 7.8 Hz), 7.91 (d, 1H, ar, J = 8.6 Hz), 7.77 (s, 1H, H-5), 7.56 (t, 2H, ar, J = 7.7 Hz), 7.39-7.33 (m, 3H, NH_2+ ar), 6.53 (s, 1H, ar), 6.47 (d, 1H, ar, J = 8.5 Hz), 3.87 (s, 3H, CH_3). Anal. Calc. for $C_{18}H_{15}N_5O_3$.

8-Amino-6-(3,4-dihydroxyphenyl)-2-phenyl-1,2,4-triazolo[4,3-*a*]pyrazin-3(2H)-one (75). Yield 88%. m.p. 256-258 °C (EtOH). ^{1}H NMR (DMSO-d_6) 6.77 (d, 1H, ar, J = 8.1 Hz), 7.23 (dd, 1H, ar, J = 8.1, 1.5 Hz), 7.38-7.36 (m, 2H, ar), 7.43-7.53 (s + br s, H-5 + NH_2), 7.55 (t, 2H, ar, J = 7.5 Hz), 8.08 (d, 2H, ar, J = 8.6 Hz), 9.00 (br s, 2H, 2 OH). ^{13}C-NMR (DMSO-d_6) 99.83, 113.69, 116.06, 117.26, 119.81, 126.71, 128.23, 129.65, 131.51, 136.46, 137.99, 145.66, 146.14, 147.56, 147.59, IR = 3417.86-3091.89, 1693.50, 1681.93 cm^{-1}. Anal. Calc. for $C_{17}H_{13}N_5O_3$.

8-Amino-6-(3,4,5-trihydroxyphenyl)-2-phenyl-1,2,4-triazolo[4,3-*a*]pyrazin-3(2*H*)-one (76). Yield 79%. m.p. 281-283 °C. Purified by liquid chromatography ($CHCl_3$ 9/MeOH 1). ^{1}H-NMR (DMSO-d_6) 6.85 (s, 2H, ar), 7.30 (s, 1H, H-5), 7.35 (t, 1H, ar, J = 7.4 Hz), 7.46 (br. S, 2H, NH_2), 7.56 (t, 2H, ar, J = 7.6 Hz), 8.07 (d, 2H, ar, J = 7.8 Hz), 8.29 (br s, 1H, OH), 8.91 (br. s, 2H, OH). Anal. Calc. for $C_{17}H_{13}N_5O_4$.

8-amino-6-(4-hydroxy-3,5-dimethylphenyl)-2-phenyl-[1,2,4]triazolo[4,3-a]pyrazin-3(2H)-one (77). Yield 90%. m.p. 236 °C. Purified by liquid chromatography (Cyclohexane 1 /EtOAc 1). ^{1}H-NMR (DMSO-d_6) 2.21 (s, 6H, CH_3), 7.35 (t, 1H, ar, J = 7.3 Hz), 7.45 (s, 2H, ar), 7.54 (s, 1H, ar), 7.55-7.52 (m, 7H, ar + NH_2), 8.07 (d, 2H, ar, J = 7.9 Hz) 8.40 (br. s, 1H, OH). ^{13}C-NMR (DMSO-d_6) 17.21, 99.91, 119.85, 124.54, 126.04, 126.71, 127.54, 129.65, 131.49, 136.39, 137.99, 147.59, 147.64, 153.94. IR = 3550-3450, 3363.86, 3323.35, 1699.29 cm^{-1}. Anal. Calc. for $C_{19}H_{17}N_5O_2$.

Synthesis of 8-amino-6-(3-(tert-butyl)-4-hydroxyphenyl)-2-phenyl-[1,2,4]triazolo[4,3-a]pyrazin-3(2H)-one (78).

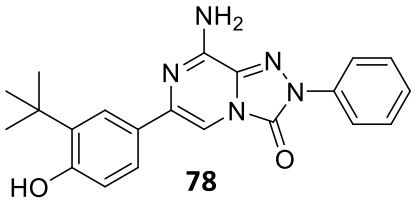

78

A solution of 48% aqueous HBr (2.5 mL) was added to a mixture of 8-amino-6-(3,5-di-tert-butyl-4-methoxyphenyl)-2-phenyl-[1,2,4]triazolo[4,3-a]pyrazin-3(2H)-one (**73**) (0.50 mmol) in glacial AcOH (2 mL). The mixture was refluxed 24 h, then the cooled suspension was treated with ice and water (30 mL) and the solid was collected by filtration and rinsed with Et_2O. The crude product was purified by column chromatography ($CHCl_3$ 9.5/MeOH 0.5). Yield 89%. m.p. > 300 °C ^{1}H-NMR (DMSO-d_6) ^{1}H NMR (400 MHz, DMSO) δ 9.54 (s, 1H, OH), 8.08 (d, 2H, ar, J = 7.7 Hz), 7.72 (d, 1H, ar, J = 2.0 Hz), 7.58-7.54 (m, 3H, ar + H-5), 7.50 (s, 3H, ar + NH_2), 7.35 (t, 1H, ar, J = 7.4 Hz), 6.82 (d, 1H, ar, J = 8.3 Hz), 1.40 (s, 9H, $(CH_3)_3$). ^{13}C NMR (DMSO-d_6) 37.26, 45.14, 52.50, 101.01, 119.35, 119.85, 126.02, 126.33, 126.74, 128.73, 129.65, 131.45, 131.56, 135.74, 137.97, 139.58, 142.94, 144.95, 145.36, 147.61, 147.79, 170.84. Anal. Calc. for $C_{21}H_{21}N_5O_2$.

General procedure for the synthesis of 8-amino-6-(alkyloxyphenyl)-2-phenyl-1,2,4-triazolo[4,3-*a*]pyrazin-3(2*H*)-ones (18-28).

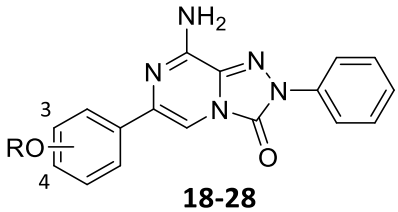

18-28

	R		R
18	3-O-propargyl	**24**	4-O-iC_3H_7
19	4-O-propargyl	**25**	4-OCH_2-iC_3H_7
20	3-OCH_2Ph	**26**	4-$OCH_2cC_3H_5$
21	4-OCH_2Ph	**27**	4-$OCH_2cC_4H_7$
22	4-OC_2H_5	**28**	4-OCH_2-CH=CH_2
23	4-O-nC_3H_7		

A solution of the suitable alkyl bromide (1.2 mmol) in butan-2-one (3 mL) was added dropwise to a mixture of the hydroxyphenyl- derivative **15** or **16** (1 mmol) and K_2CO_3 (2 mmol) in butan-2-one (5 mL). The mixture was heated at reflux until the disappearance of the starting hydroxy-derivative (TLC monitoring, 7-58 h). After cooling at room temperature, the solid was collected by filtration, washed with water and recrystallized.

8-Amino-2-phenyl-6-(3-propargyloxyphenyl)-1,2,4-triazolo[4,3-*a*]pyrazin-3(2*H*)-one (18). Yield 58%. m.p. 217-219 °C (EtOH/2-Methoxyethanol). ^{1}H NMR (DMSO-d_6) 3.58 (t, 1H, CH, J = 2.3 Hz), 4.89 (d, 2H, CH_2, J = 2.3 Hz), 6.97 (d, 1H, ar, J = 6.5 Hz), 7.36 (t, 2H, ar, J = 7.6 Hz), 7.55-7.63 (m, 6H, 4ar + NH_2), 7.84 (s, 1H, H-5), 8.08 (d, 2H, ar, J = 7.6 Hz). IR = 3443, 3298, 1721, 1643 cm^{-1}. Anal. Calc. for $C_{20}H_{15}N_5O_2$.

8-Amino-2-phenyl-6-(4-propargyloxy)phenyl-1,2,4-triazolo[4,3-*a*]pyrazin-3(2*H*)-one (19). Yield 56%. m.p. 244-245 °C (AcOH). ^{1}H NMR (DMSO-d_6) 3.59 (t, 1H, CH, J = 2.3 Hz), 4.85 (d, 2H, CH_2, J = 2.4 Hz), 7.04 (d, 2H, ar, J = 6.9 Hz), 7.36 (t, 1H, ar, J = 7.4 Hz), 7.54-7.59 (m, 4H, 2ar + NH_2), 7.69 (s, 1H, H-5), 7.93 (d, 2H, ar, J = 6.9 Hz), 8.08 (d, 2H, ar, J = 7.6 Hz). IR = 3458, 3331, 3219, 1695, 1620 cm^{-1}. Anal. Calc. for $C_{20}H_{15}N_5O_2$.

8-Amino-6-(3-benzyloxyphenyl)-2-phenyl-1,2,4-triazolo[4,3-*a*]pyrazin-3(2*H*)-one (20). Yield 78%. m.p. 264-266 °C (2-Methoxyethanol). ^{1}H NMR (DMSO-d_6) 5.19 (s, 2H, CH_2), 6.99 (d, 1H, ar, J = 8.3 Hz), 7.32-7.65 (m, 13H, 11ar + NH_2), 7.84 (s, 1H, H-5), 8.07 (d, 2H, ar, J = 8.0 Hz). Anal. Calc. for $C_{24}H_{19}N_5O_2$.

8-Amino-6-(4-benzyloxyphenyl)-2-phenyl-1,2,4-triazolo[4,3-*a*]pyrazin-3(2*H*)-one (21). Yield 78%. m.p. 284-285 °C (2-Methoxyethanol). ^{1}H NMR (DMSO-d_6) 5.16 (s, 2H, CH_2), 7.07 (d, 2H, ar, J = 8.9 Hz), 7.34-7.48 (m, 6H, ar), 7.51-7.58 (m, 4H, 2ar + NH_2), 7.67 (s, 1H, H-5), 7.92 (d, 2H, ar, J = 8.9 Hz), 8.08 (d, 2H,ar, J = 7.6 Hz). IR = 3362, 3310, 1697, 1647 cm^{-1}. Anal. Calc. for $C_{24}H_{19}N_5O_2$.

8-Amino-6-(4-ethoxyphenyl)-2-phenyl-1,2,4-triazolo[4,3-*a*]pyrazin-3(2*H*)-one (22). Yield 72%. m.p. 267-268 °C (EtOH/2-Methoxyethanol). ^{1}H NMR (DMSO-d_6) 1.35 (t, 3H, CH_3, J = 7.0 Hz), 4.07 (q, 2H, CH_2, J = 7.0 Hz), 6.96 (d, 2H, ar, J = 6.8 Hz), 7.36 (t, 1H, ar, J = 8.8 Hz), 7.53-7.58 (m, 4H, 2ar + NH_2), 7.65 (s, 1H, H-5), 7.90 (d, 2H, ar, J = 6.8 Hz), 8.08 (d, 2H, ar, J = 8.8 Hz). IR = 3119, 3102, 1697, 1647 cm^{-1}. Anal. Calc. for $C_{19}H_{17}N_5O_2$.

8-Amino-6-(4-n-propyloxyphenyl)-2-phenyl-1,2,4-triazolo[4,3-*a*]pyrazin-3(2*H*)-one (23). Yield 67%. m.p. 266-267 °C (2-Methoxyethanol). ^{1}H NMR (DMSO-d_6) 0.99 (t, 3H, CH_3, J = 7.4 Hz), 1.72-1.77 (m, 2H, CH_2), 3.97 (t, 2H, CH_2, J = 6.5 Hz), 6.97 (d, 2H, ar, J = 8.8 Hz),

7.35 (t, 1H, ar, J = 7.3 Hz), 7.54-7.58 (m, 2ar + NH_2), 7.65 (s, 1H, H-5), 7.89 (d, 2H, ar, J = 8.8 Hz), 8.07 (d, 2H, ar, J = 7.9 Hz). Anal. Calc. for $C_{20}H_{19}N_5O_2$.

8-Amino-6-(4-isopropyloxyphenyl)-2-phenyl-1,2,4-triazolo[4,3-*a*]pyrazin-3(2*H*)-one (24). Yield 70%. m.p. 240-241 °C (EtOH/2-Methoxyethanol). ^{1}H NMR (DMSO-d_6) 1.30 (d, 6H, $2CH_3$, J = 6.0 Hz), 4.63-4.69 (m, 1H, CH), 6.96 (d, 2H, ar, J = 8.7 Hz), 7.36 (t, 1H, ar, J = 7.4 Hz), 7.52 (br s, 2H, NH_2), 7.58 (m, 2H, ar, J = 7.7 Hz), 7.64 (s, 1H, H_5), 7.88 (d, 2H, ar, J = 8.7 Hz), 8.08 (d, 2H, ar, J = 7.9 Hz). IR = 3385, 3310, 1701, 1638 cm^{-1}. Anal. Calc. for $C_{20}H_{19}N_5O_2$.

8-Amino-6-(4-isobutyloxyphenyl)-2-phenyl-1,2,4-triazolo[4,3-*a*]pyrazin-3(2*H*)-one (25). Yield 64%. m.p. 249-251 °C (2-Methoxyethanol). ^{1}H NMR (DMSO-d_6) 1.00 (d, 6H, $2CH_3$, J= 6.5 Hz), 1.99-2.06 (m, 1H, CH), 3.78 (d, 2H, CH_2, J = 6.5 Hz), 6.97 (d, 2H, J = 8.7 Hz), 7.35 (t, 1H, ar, J = 7.3 Hz), 7.54-7.57 (m, 2ar + NH_2), 7.65 (s, 1H, H-5), 7.98 (d, 2H, ar, J = 8.7 Hz), 8.07 (d, 2H, ar, J = 7.9 Hz). Anal. Calc. for $C_{21}H_{21}N_5O_2$.

8-Amino-6-[(4-cyclopropylmethoxy)phenyl]-2-phenyl-1,2,4-triazolo[4,3-*a*]pyrazin-3(2*H*)-one (26). Yield 86%. m.p. 276-278 °C (EtOH/2-Methoxyethanol). ^{1}H NMR (DMSO-d_6) 0.32-0.36 (m, 2H, 2CH), 0.57-0.60 (m, 2H, 2CH), 1.21-1.24 (m, 1H, CH), 3.85 (d, 2H, CH_2, J = 7.0 Hz), 6.97 (d, 2H, ar, J = 8.9 Hz), 7.36 (t, 1H, ar, J = 7.4 Hz), 7.54 (br s, 2H, NH_2), 7.56 (t, 2H, ar, J = 7.4 Hz), 7.65 (s, 1H, H-5), 7.91 (d, 2H, ar, J = 8.9 Hz), 8.08 (d, 2H, ar, J = 7.4 Hz). IR = 3362, 3316, 1669, 1649 cm^{-1}. Anal. Calc. for $C_{21}H_{19}N_5O_2$.

8-Amino-6-[(4-cyclobutylmethoxy)phenyl]-2-phenyl-1,2,4-triazolo[4,3-*a*]pyrazin-3(2*H*)-one (27). Yield 45%. m.p. 266-268 °C (EtOH/2-Methoxyethanol). ^{1}H NMR (DMSO-d_6) 1.88-1.96 (m, 4H, 4CH), 2.06-2.13 (m, 2H, 2CH), 2.72-2.75 (m, 1H, CH), 3.99 (d, 2H, CH_2, J = 6.7 Hz), 6.98 (d, 2H, ar, J = 8.8 Hz), 7.36 (t, 1H, ar, J = 7.4 Hz), 7.56 (br s, 2H, NH_2), (t, 2H, ar, J = 7.8 Hz), 7.65 (s, 1H, H-5), 7.90 (d, 2H, ar, J = 8.8 Hz), 8.08 (d, 2H, ar, J = 7.8 Hz). IR = 3354, 3312, 1699, 1647 cm^{-1}. Anal. Calc. for $C_{22}H_{21}N_5O_2$.

8-Amino-2-phenyl-6-(4-allyloxy)phenyl-1,2,4-triazolo[4,3-*a*]pyrazin-3(2*H*)-one (28). Yield 75%. m.p. 260-261 °C (2-Methoxyethanol). ^{1}H NMR (DMSO-d_6) 4.60 (d, 2H, CH_2), 5.27 (d, 1H, geminal CH, J = 10.4 Hz), 5.42 (d, 1H, geminal CH=, J = 17.4 Hz), 6.02-6.11 (m, 1H, CH=), 7.00 (d, 2H, ar, J = 8.8 Hz), 7.35 (t, 1H, ar, J = 7.9 Hz), 7.54-7.58 (m, 2ar + NH_2), 7.66 (s, 1H, H-5), 7.90 (d, 2H, ar, J = 8.8 Hz), 8.07 (d, 2H, ar, J = 7.9 Hz). Anal. Calc. for $C_{20}H_{17}N_5O_2$.

General procedure for the synthesis of amino-substituted 8-amino-1,2,4-triazolo[4,3-*a*]pyrazin-3(2*H*)-one derivatives (10, 37-39).

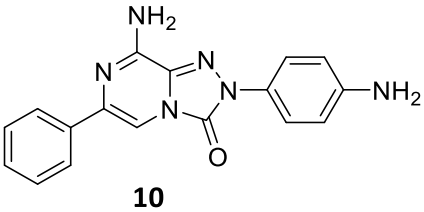

10

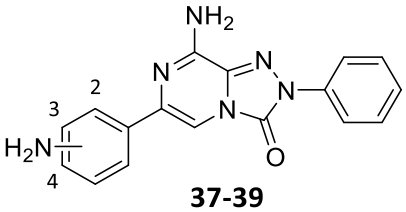

37-39

10% Pd/C (10% w/w with respect to the nitro derivative) was added to a solution of the 6-(nitrophenyl) derivatives **5, 34-36** (1.2 mmol) in DMF (10 mL). The mixture was hydrogenated in a Parr apparatus at 40 psi for 24 h (TLC, monitoring). Then the catalyst was filtered off and the clear solution was diluted with water (about 50 mL) to obtain a solid that was collected by filtration, washed with water and Et_2O, dried and recrystallized.

8-Amino-2-(4-aminophenyl)-6-phenyl-1,2,4-triazolo[4,3-*a*]pyrazin-3-(2*H*)one (10). . Yield 39%. m.p. >300 °C (2-Methoxyethanol). ^{1}H NMR (DMSO-d_6) 5.33 (br s, 2H, NH_2), 6.68 (d, 2H, ar, J = 8.7 Hz), 7.34 (t, 1H, ar, J = 7.2 Hz), 7.42 (t, 2H, J = 7.4 Hz), 7.49 (br s, 2H, NH_2), 7.57 (d, 2H, J= 8.7 Hz), 7.72 (s, 1H, H-5), 7.96 (d, 2H, ar, J = 7.4 Hz). Anal. Calc. for. $C_{17}H_{14}N_6O$.

8-Amino-6-(2-aminophenyl)-2-phenyl-1,2,4-triazolo[4,3-a]pyrazin-3 (2H)-one (37). Yield 59%. m.p. 256-258 °C (2-Methoxyethanol). ^{1}H NMR (DMSO-d_6) 5.78 (br s , 2H, NH_2), 6.58 (t, 1H, ar, J = 7.4 Hz), 6.72 (d, 1H, ar, J = 8. 00 Hz), 7.05 (t, 1H, ar, J = 7.2 Hz), 7.30-7.38 (m, 3H, 2 ar + H-5), 7.56 (t, 2H, ar, J = 7.9 Hz), 7.62 (br s, 2H, NH_2), 8.07 (d, 2H, ar, J = 7.9 Hz). Anal. Calc. for. $C_{17}H_{14}N_6O$.

8-Amino-6-(3-aminophenyl)-2-phenyl-1,2,4-triazolo[4,3-a]pyrazin-3 (2H)-one (38). Yield 75%. m.p. 280-282 °C (2-Methoxyethanol). ^{1}H NMR (DMSO-d_6) 5.10 (br s , 2H, NH_2), 6.54-6.57 (m, 1H, ar), 7.04-7.10 (m, 2H, ar), 7.16 (s, 1H, ar), 7.36 (t, 1H, ar, J = 7.4 Hz), 7.50 (s, 1H, H-5), 7.51 (br s, 2H, NH_2), 7.56 (t, 2H, ar, J = 7.7 Hz), 8.08 (d, 2H, ar, J = 7.7 Hz). Anal. Calc. for. $C_{17}H_{14}N_6O$.

8-Amino-6-(4-aminophenyl)-2-phenyl-1,2,4-triazolo[4,3-a]pyrazin-3 (2H)-one (39). Yield 78%. m.p. 294-296 °C (Nitromethane/DMF). ^{1}H NMR (DMSO-d_6) 5.27 (br s, 2H, NH_2), 6.59 (d, 2H, ar, J = 8.6 Hz), 7.35 (t, 1H, ar, J = 7.4 Hz), 7.44 (br s , 2H, NH_2), 7.46 (s, 1H, H-5), 7.56 (t, 2H, ar, J = 8. 5 Hz), 7.64 (d, 2H, ar, J = 8.6 Hz), 8.08 (d, 2H, ar, J = 7. 6 Hz). ^{13}C-NMR

(DMSO-d_6) 98.70, 114.1 119.83, 124.15, 126.68, 126.89, 129.64, 131.50, 136.93, 138.03, 147.54, 147.56, 149.40. IR = 1703, 3292-3115, 3350, 3435 cm^{-1}. Anal. Calc. for. $C_{17}H_{14}N_6O$.

General procedure for the synthesis of 8-amino-2-phenyl-6-(piperazinylphenyl)-1,2,4-triazolo[4,3-a]pyrazin-3-(2H)one (40-42).

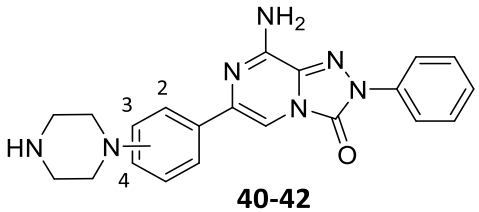

40-42

A suspension of the 8-amino-6-(aminophenyl) derivatives **37-39** (1.1 mmol) and bis-(2-chloroethyl)amine hydrochloride in sulfolane (5 mL) was heated at 150 °C until the disappearance of starting material (TLC-monitoring 16-24 h). After cooling at 0-5 °C, the mixture was treated with acetone (30 mL) and the obtained ammonium salts were collected by filtration and dissolved in water (50 mL). The solution was neutralized with a $NaHCO_3$ saturated solution and extracted with EtOAc (40 mL x 5). The organic phase was anhydrified (Na_2SO_4) and reduced to dryness under vacuum to give a yellow solid. All the crude derivatives were purified by recrystallization.

8-Amino-2-phenyl-6-(2-piperazin-1-yl-phenyl)-1,2,4-triazolo[4,3-a]pyrazin-3-(2H)one (40). Yield 52%. m.p. 214-216 °C (Nitromethane). ^{1}H NMR (DMSO-d_6) 2.82 (s , 8H, 4 CH_2), 7.08-7.11 (m, 2H, ar), 7.28 (t, 1H, ar, J = 7.6 Hz), 7.36 (t, 1H, ar, J = 7.4 Hz), 7.51 (br s, 2H, NH_2), 7.56 (t, 2H, ar, J = 7.7 Hz), 7.84 (d, 1H, ar, J = 6.6 Hz), 8.09 (d, 2H, ar, J = 7.8 Hz), 8.40 (s, 1H, H-5). Anal. Calc. for. $C_{21}H_{21}N_7O$.

8-Amino-2-phenyl-6-(3-piperazin-1-yl-phenyl)-1,2,4-triazolo[4,3-a]pyrazin-3-(2H)one (41). Yield 47%. m.p. 234-235 °C (Nitromethane). ^{1}H NMR (DMSO-d_6) 2.86 (t, 4H, 2 CH_2, J = 4. 9 Hz), 3.11 (t, 4H, 2 CH_2, J = 5.1 Hz), 6. 90 (dd, 1H, ar, J = 6.3 Hz, J = 1.9 Hz), 7.25 (t, 1H, ar), 7.34-7.39 (m, 2H, ar), 7.51-7.58 (m, 5H, 3 ar + NH_2), 7.77 (s, 1H, H-5), 8.08 (d, 2H, ar, J = 8.6 Hz). Anal. Calc. for. $C_{21}H_{21}N_7O$.

8-Amino-2-phenyl-6-(4-(piperazin-1-yl-)phenyl)-1,2,4-triazolo[4,3-a]pyrazin-3-(2H)one (42). Yield 56%. m.p. 255-257 °C (Nitromethane). ^{1}H NMR (DMSO-d_6) ^{1}H NMR (DMSO-d_6) 2.84 (t, 4H, 2 CH_2, J = 4.9 Hz), 3.11 (t, 4H, 2 CH_2, J = 5.1 Hz), 7. 96 (d, 2H, ar, J = 8.9 Hz),

7.36 (t, 1H, ar, J = 7.4 Hz), 7. 50 (br s, 2H, NH_2), 7. 54- 7.59 (m, 2H, 1 ar + H-5), 7.82 (d, 2H, ar, J = 8.8 Hz), 8.08 (d, 2H, ar, J = 7.7 Hz). Anal. Calc. for. $C_{21}H_{21}N_7O$.

Synthesis of 4-(3-(8-amino-3-oxo-2-phenyl-2,3-dihydro-1,2,4-triazolo[4,3-a]pyrazin-6-yl)phenyl)-1,1-dimethyl-piperazin-1-ium (**43**).

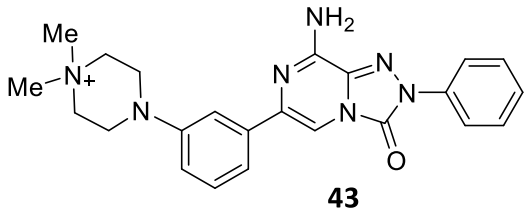

43

A mixture of compound **41** (0.4 mmol), methyl iodide (0.7 mmol) and potassium carbonate in anhydrous DMF (0.5 mL) was stirred at room temperature for 7 h, then it was diluted with H_2O (about 50 mL) and EtOAc (about 40 mL). The obtained solid was collected by filtration and recrystallized. Yield 35%. m.p. > 300 °C (DMF). ^{1}H NMR (DMSO-d_6) 3.23 (s, 6H, $2CH_3$), 3.61 (br s, 8H, piperazine protons), 7.02 (d, 1H, ar, J = 7.6 Hz), 7.32-7.38 (m, 2H, ar), 7.52-7.59 (m, 6H, 4 ar + NH_2), 7.87 (s, 1H, H-5), 8.07 (d, 2H, ar, J = 8.2 Hz).). Anal. Calc. for $C_{23}H_{26}N_7O^+$.

General procedure for the synthesis of 8-amino-6-((4-benzylpiperazin-1-yl)-phenyl)-2-phenyl-1,2,4-triazolo[4,3-a]pyrazin-3-(2H)one (44, 45).

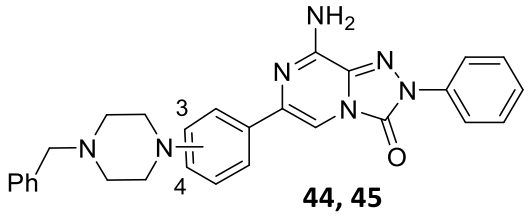

44, 45

A suspension of the 8-amino-6-(piperazinyl)phenyl derivative **41** or **42** (0.7 mmol), anhydrous triethylamine (0.9 mmol) and benzylchloride (0.9 mmol) in anhydrous dioxane (10 mL) was refluxed until the disappearance of starting material (TLC monitoring, 24-48 h). In case of compound **44**, the organic solvent was removed by evaporation at reduced pressure and the residue treated with EtOAc (50 mL). The organic phase was washed with water (30 mL x 3), anhydrified (Na_2SO_4) and reduced to dryness under vacuum to give a solid. To isolate compound **45**, the solvent was evaporated under vacuum and the residue was treated with water (30 mL). The resulting solid was collected by filtration and washed

with diethyl ether (about 20 mL). The crude products were purified by recrystallization (**44**) or column chromatography (**45**).

8-Amino-6-[3-(4-benzylpiperazin-1-yl)phenyl]-2-phenyl-1,2,4-triazolo[4,3-a]pyrazin-3-(2H)one (44). Yield 34%. m.p. 208-210 °C (EtOH). ^{1}H NMR (DMSO-d_6) 2.55 (t, 4H, 2 CH_2, J = 4. 8 Hz), 3.22 (t, 4H, 2 CH_2, J = 4.9 Hz), 6.91 (dd, 1H, ar, J = 6.2, J = 2.00 Hz), 7.24-7.30 (m, 2H, ar), 7.34-7.31 (m, 6H, ar), 7.52-7.59 (m, 5H, 3 ar + NH_2), 7.77 (s, 1H, H-5), 8.08 (d, 2H, ar, J = 7.6 Hz). Anal. Calc. for. $C_{28}H_{27}N_7O$.

8-Amino-6-[4-(4-benzylpiperazin-1-yl)phenyl]-2-phenyl-1,2,4-triazolo[4,3-a]pyrazin-3-(2H)one (45). Purified by liquid chromatography (Cyclohexane 5.5 /EtOAc 4.5/ MeOH 0.1). Yield 63%. m.p. 244-246 °C (EtOH). ^{1}H NMR ($CDCl_3$-d_6) 2.65 (t, 4H, 2 CH_2, J = 4. 8 Hz), 3.30 (t, 4H, 2 CH_2, J = 4.9 Hz), 5.54 (br s, 2H, NH_2), 6.98 (d, 2H, ar, J = 8.8 Hz), 7.30-7.40 (m, 6H, ar), 7.52 (t, 2H, ar, J = 7.7 Hz), 7.60 (s, 1H, H-5), 7.76 (d, 2H, ar, J = 8.8 Hz), 8.12 (d, 2H, ar, J = 7.8 Hz). ^{13}C NMR (DMSO-d_6) 48.63, 52.95, 63.07, 101.56, 110.64, 119.84, 126.64, 126.85, 127.21, 128.32, 129.19, 129.24, 130.81, 136.62, 137.58, 146.38, 147.47, 151.50. Anal. Calc. for. $C_{28}H_{27}N_7O$.

General procedure for the synthesis 2-(4-(8-amino-3-oxo-2-phenyl-2,3-dihydro-[1,2,4]triazolo[4,3-a]pyrazin-6-yl)phenoxy)acetonitrile/acetamide (46-47).

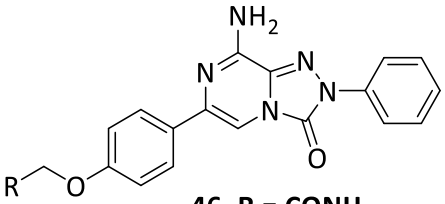

46, R = $CONH_2$
47, R = CN

2-Chloroacetamide (7.05 mmol, **46**) or 2-chloroacetonitrile (6.28 mmol, **47**) was added to a suspension of 8-amino-6-(4-hydroxyphenyl)-2-phenyl-[1,2,4]triazolo[4,3-a]pyrazin-3(2H)-one (**16**) (1.57 mmol) and K_2CO_3 (3.14 mmol) in anhydrous acetone (20 mL) . The mixture was stirred at room temperature overnight (TLC monitoring). The resulting solid was collected by filtration, rinsed with water (20 mL) and petroleum ether, dried and purified by recrystallization.

2-(4-(8-amino-3-oxo-2-phenyl-2,3-dihydro-[1,2,4]triazolo[4,3-a]pyrazin-6-yl)phenoxy)acetamide (46).

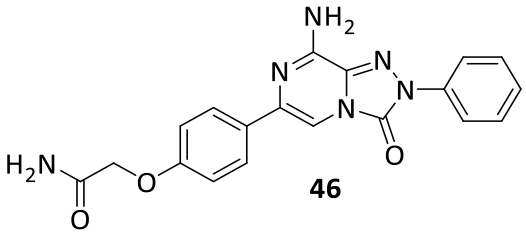

46

Yield 51%. m.p. 260-263 °C (EtOH/ 2-Methoxyethanol). ^{1}H NMR (DMSO-d_6) 8.08 (d, 2H, ar, J = 7.8 Hz), 7.92 (d, 2H, ar, J = 8.3 Hz), 7.68 (s, 1H, H-5), 7.56-7-55 (m, 4H, ar + NH_2), 7.41 (br s, 1H, NH_2), 7.34 (t, 1H, ar, J = 7.2 Hz), 7.01 (d, 2H, ar, J = 8.3 Hz), 4.47 (s, 2H, CH_2). ^{13}C NMR (DMSO-d_6) 39.39, 39.59, 39.8, 40.01, 40.22, 40.43, 40.64, 43.05, 67.25, 100.73, 102.92, 115.12, 119.87, 126.74, 127.22, 129.64, 129.88, 131.53, 135.75, 137.98, 147.62, 147.78, 158.26, 170.32. IR = 3458, 3371, 3284, 3209, 2671, 1707, 1377 cm^{-1}). Anal. Calc. for $C_{19}H_{16}N_6O_3$.

2-(4-(8-amino-3-oxo-2-phenyl-2,3-dihydro-[1,2,4]triazolo[4,3-a]pyrazin-6 yl)phenoxy)acetonitrile (47).

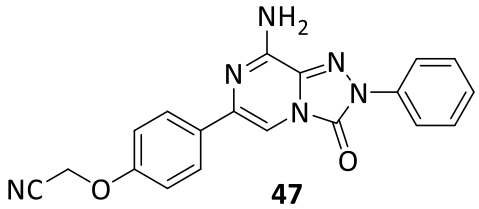

47

Yield 89%. m.p. 249-250 °C (EtOH). ^{1}H NMR (DMSO d_6) 8.08 (d, 2H, ar, J = 7.7 Hz), 8.00 (d, 2H, ar, J = 8.8 Hz), 7.75 (s, 1H, H-5), 7.63–7.50 (m, 4H, ar + NH_2), 7.36 (t, 1H, ar, J = 7.4 Hz), 7.13 (d, 2H, ar, J = 8.9 Hz), 5.22 (s, 2H). ^{13}C NMR (DMSO-d_6) 39.39, 39.60, 39.81, 40.02, 40.23, 40.44, 40.65, 54.01, 101.21, 115.28, 117.11, 119.87, 126.74, 127.46, 129.64, 131.23, 131.54, 135.42, 137.97, 147.63, 147.83, 156.74. IR = 3406, 3311, 3169, 1701, 1643, 1460 cm^{-1}. Anal. Calc. for. $C_{19}H_{14}N_6O_2$.

Synthesis of 8-amino-6-(4-(2-aminoethoxy)phenyl)-2-phenyl-[1,2,4]triazolo[4,3-a]pyrazin-3(2H)-one (48).

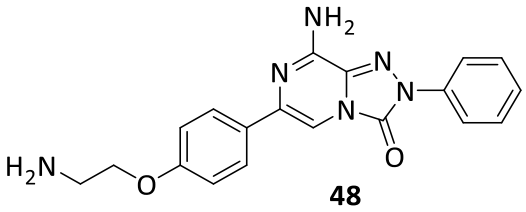

48

2-(4-(8-Amino-3-oxo-2-phenyl-2,3-dihydro-[1,2,4]triazolo[4,3-a]pyrazin-yl)phenoxy)acetonitrile (**47**) (0.78 mmol) was added portionwise to a suspension of $LiAlH_4$ (1.95 mmol) in anhydrous THF (20 mL) at 0 °C. The mixture was stirred at room temperature for 2 h, then treated with ice and water (15 mL) and extracetd with EtOAc (20 mL x 3). The organic phase was washed with water (20 mL x 3) and anhydrified (Na_2SO_4), then the solvent eliminated under reduced pressure. The resulting residue was treated with water (20 mL) and collected by filtration. The crude was purified by column chromatography ($CHCl_3$ 9.5/MeOH 0.5). Yield 78%. m.p. 239-241 °C ^{1}H NMR (DMSO-d_6) 2.89 (t, 2H, CH_2, J = 5.3 Hz), 3.96 (t, 2H, CH_2, J = 5.4 Hz), 6.98 (d, 2H, ar, J = 8.5 Hz), 7.35 (t, 1H, ar, J = 7.3 Hz), 7.45 – 7.60 (m, 4H, ar + NH_2), 7.65 (s, 1H, H-5), 7.90 (d, 2H, ar, J = 8.5 Hz), 8.07 (d, 2H, ar, J = 7.9 Hz). IR: 3391, 3329, 3215, 3111, 2677, 1705, 1655, 1547, 1510, 1456, 1360, 1246 cm^{-1}. Anal.Calc. for $C_{19}H_{18}N_6O_2$.

Synthesis of 8-amino-6-(4-(2-hydroxyethoxy)phenyl)-2-phenyl-[1,2,4]triazolo[4,3-a]pyrazin-3(2H)-one (49).

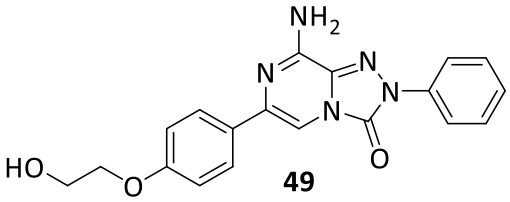

49

Ethylene carbonate (2.96 mmol) was added to a suspension of 8-amino-6-(4-hydroxyphenyl)-2-phenyl-[1,2,4]triazolo[4,3-a]pyrazin-3(2H)-one (**16**) (1.41 mmol) and K_2CO_3 (1.41 mmol) in anhydrous DMF (1.5 mL), The mixture was heated at 110 °C for 6h then treated with water (20 mL). The solid was collected by filtration, rinsed with petroleum ether, dried and recrystallized. Yield 88 %. m.p. 269-269 °C (2-Methoxyethanol).^{1}H NMR (DMSO-d_6) 3.73 (dd, 2H, *J* = 10.1, 5.2 Hz), 4.03 (t, 2H, *J* = 5.0 Hz),

4.88 (t, 1H, OH, *J* = 5.5 Hz), 6.99 (d, 2H, ar, *J* = 8.8 Hz), 7.35 (t, 1H, ar, *J* = 7.4 Hz), 7.54 – 7.58 (m, 4H, ar + NH_2), 7.65 (s, 1H, H-5), 7.90 (d, 2H, ar, *J* = 8.8 Hz), 8.08 (d, 2H, ar, *J* = 7.9 Hz). ^{13}C NMR (DMSO-d_6) 59.20, 152.15, 147.76, 140.65, 137.99, 137.05, 135.88, 129.65, 129.19, 127.28, 126.73, 125.19, 119.85, 119.12, 114.85, 70.02, 61.53, 60.04. Anal. Calc. for

Synthesis of 8-amino-6-(4-(2,3-dihydroxypropoxy)phenyl)-2-phenyl-[1,2,4]triazolo[4,3-a]pyrazin-3(2H)-one (50).

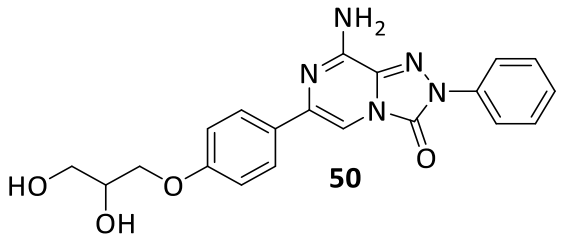

50

A solution of 3-chloropropane-1,2-diol in anhyrous acetonitrile (2 mL) was added to a suspension of 8-amino-6-(4-hydroxyphenyl)-2-phenyl-[1,2,4]triazolo[4,3-a]pyrazin-3(2H)-one (**16**) (0.626 mmol) and anhydrous K_2CO_3 (3.13 mmol) in acetonitrile (5 mL). The mixture was refluxed for 36 h (TLC monitoring). The solvent was eliminated under reduced pressure and the residue was treated with water (20 mL). The solid was collected by filtration, rinsed with Et_2O/acetone (20 + 10 mL), dried and recrystallized. Yield 73%. m.p. 237-239 °C. (2-Methoxyethanol) ^1H NMR (DMSO-d_6) 3.47 (t, 2H, J = 5.5 Hz), 3.81 (dd, 1H, J = 11.1, 4.2 Hz), 3.91 (dd, 1H, J = 9.8, 6.1 Hz), 4.05 (dd, 1H, J = 9.8, 4.2 Hz), 4.65 (t, 1H, OH, J = 5.6 Hz), 4.93 (d, 1H, OH, J = 5.1 Hz), 6.99 (d, 2H, ar, J = 8.9 Hz), 7.36 (t, 1H, ar, J = 7.4 Hz), 7.56 (7, 4 H, J =), 7.65 (s, 1H, H-5), 7.90 (d, 2H, J = 8.8 Hz), 8.08 (d, 2H, J = 7.8 Hz).). Anal. Calc. for. $C_{20}H_{19}N_5O_4$.

Synthesis of N-(4-(8-amino-3-oxo-2-phenyl-2,3-dihydro-[1,2,4]triazolo[4,3-a]pyrazin-6-yl)phenyl)acrylamide (194).

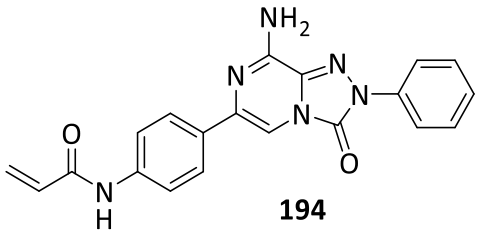

194

A mixture of 8-amino-6-(4-aminophenyl)-2-phenyl-[1,2,4]triazolo[4,3-a]pyrazin-3(2H)-one **(39)** (1.00 mmol), 3-chloropropionic acid (1.2 mmol), EDCI. HCl (1.2 mmol), DIPEA (1.2 mmol) in anhydrous DMF (3 mL) was stirred at room temperature for 2h. The mixture was treated with water (30 mL). The resulting solid was collected by filtration washed with Et_2O and recrystallized. Yield 99%. m.p. > 300 °C (Nitromethane) ^{1}H-NMR (DMSO-d_6) 5.76 (m, 1H, CH), 6.28 (m, 1H, CH), 6.50 (m, 1H, CH), 7.33 (t, 1H, ar, J = 7.2 Hz), 7.52-7.54 (m, 4H, ar + NH_2), 7.69 (s, 1H, H-5), 7.75 (d, 2H, ar, J = 8.5 Hz), 7.93 (d, 2H, ar, J = 8.9 Hz), 8.07 (d, 2H, ar, J = 7.9 Hz), 10.33 (br. s, 1H, NH). ^{13}C-NMR (DMSO-d_6) 101.15, 119.65, 119.82, 126.37, 126.69, 127.28, 129.60, 131.54, 131.91, 132.36, 135.70, 137.96, 139.40, 147.59, 147.79, 163.63. IR = 3375.43, 3331.07, 3296.35, 3205.69, 3180.62, 1693.50, 1681.93, 1643.35, 1633.71 cm^{-1}. Anal. Calc. for $C_{20}H_{16}N_6O_2$.

Synthesis of 3-amino-N-(4-(8-amino-3-oxo-2-phenyl-2,3-dihydro-[1,2,4]triazolo[4,3-a]pyrazin-6-yl)phenyl)propenamide(51).

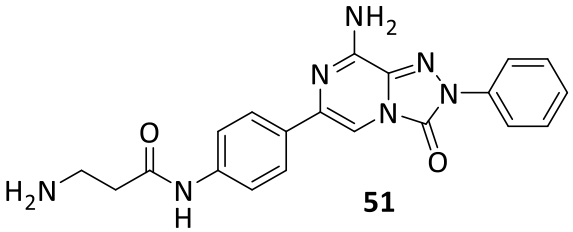

51

A suspension of N-(4-(8-amino-3-oxo-2-phenyl-2,3-dihydro-[1,2,4]triazolo[4,3-a]pyrazin-6-yl)phenyl)acrylamide (**194**) (0.13 mmol) in a saturated ethanolic solution of NH_3 (15 mL) was heated at 130 °C in a sealed tube for 3 h. The mixture was cooled at room temperature, the solid was collected by filtration and washed with water (about 5-10 mL) and petroleum ether. Purified by liquid chromatography (DCM 8/MeOH 2/NH_3 0.2). Yield 89%. m.p. 239-241 °C. ^{1}H-NMR (DMSO-d_6) 2.43 (t, 2H, CH_2, J = 6.4 Hz), 2.87 (t, 2H, CH_2, J

= 6.2 Hz), 7.35 (t, 1H, ar, J = 7.4 Hz), 7.54-7.58 (m, 4H, ar + NH_2, J = 7.8 Hz), 7.65 – 7.69 (m, 3H, ar + H-5), 7.91 (d, 2H, ar, J = 8.7 Hz), 8.08 (d, 2H, ar, J = 7.9 Hz), 10.18 (br s, 1H, NH). ^{13}C-NMR (DMSO-d_6) 38.45, 39.37, 100.98, 119.33, 119.85, 126.31, 126.74, 129.65, 131.40, 131.56, 135.76, 137.98, 139.63, 147.61, 147.79, 170.98. Anal. Calc. for. $C_{20}H_{19}N_7O_2$.

General procedure for the Synthesis of N-(4-(8-amino-3-oxo-2-phenyl-2,3-dihydro-[1,2,4]triazolo[4,3-a]pyrazin-6-yl)phenyl)-3-propanamide derivatives (52-55).

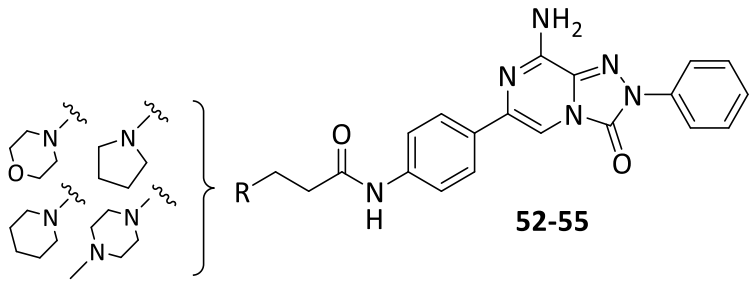

A suspension of N-(4-(8-amino-3-oxo-2-phenyl-2,3-dihydro-[1,2,4]triazolo[4,3-a]pyrazin-6-yl)phenyl)acrylamide **194** (1 mmol) and the suitable amine (pyrrolidine, 5 mmol; piperidine and morpholine, 4 mmol; N-methylpiperazine, 3 mmol) in anhydrous THF (20 mL) was refluxed for 2-16 h (TLC monitoring). The solvent was removed under reduced pressure and the resulting solid was collected bt filtration. The crude product was dryed and purified by recrystallization (**52**, **54**, **55**) or column chromatography (**53**).

N-(4-(8-amino-3-oxo-2-phenyl-2,3-dihydro-[1,2,4]triazolo[4,3-a]pyrazin-6-yl)phenyl)-3-(pyrrolidin-1-yl)propenamide (52). Yield 59%. m.p. 212-214 °C. (EtOH) ^{1}H-NMR (DMSO-d_6) 1.70 (m, 4H), 2.74 (t, 2H, CH_2, J = 7.0 Hz), 7.35 (t, 1H, ar, J = 7.4 Hz), 7.56-7.55 (m, 2H, ar), 7.56 (s, 2H, NH_2), 7.64 (d, 2H, ar, J = 7.9 Hz), 7.69 (s, 1H, ar), 7.91 (d, 2H, ar, J = 7.9 Hz), 8.08 (d, J = 7.9 Hz, 2H, ar), 10.20 (br. S, 1H, NH). ^{13}C NMR (DMSO-d_6) 23.62, 36.53, 51.98, 53.89, 100.99, 119.24, 119.85, 126.37, 126.74, 129.65, 131.44, 131.56, 135.74, 137.97, 139.63, 147.61, 147.79, 170.62. Anal. Calc. for $C_{24}H_{25}N_7O_2$.

N-(4-(8-amino-3-oxo-2-phenyl-2,3-dihydro-[1,2,4]triazolo[4,3-a]pyrazin-6-yl)phenyl)-3-(piperidin-1-yl)propenamide (53). Purified by column chromatography ($CHCl_3$ 9/MeOH 1). Yield 60%. m.p. > 300 °C. ^{1}H-NMR (DMSO-d_6) 1.40 (m, 2H), 1.53 (m, 4H), 2.45 (m, 4H), 2.66 (m, 2H), 3.37 (m, 2H), 7.35 (t, 1H, ar, J = 7.36 Hz), 7.56 (t, 2H, ar, J = 8.00 Hz), 7.56 (br. s, 2H, NH_2), 7.63 (d, 2H, ar, J = 8.50 Hz), 7.69 (s, 1H, ar), 7.91 (d, 2H, ar, J = 8.50 Hz), 8.08

(d, 2H, ar, J = 7.96 Hz), 10.27 (br. s, 1H, NH). ^{13}C-NMR (DMSO-d_6) 24.28, 25.84, 34.27, 54.02, 54.72, 101.0, 119.23, 119.83, 126.37, 126.74, 129.66, 131.46, 131.55, 135.70, 137.96, 139.58, 147.61, 147.79, 170.62. IR = 3360.00, 3305.99, 1681.93, 1651.07 cm^{-1}. Anal. Calc. for $C_{25}H_{27}N_7O_2$.

N-(4-(8-amino-3-oxo-2-phenyl-2,3-dihydro-[1,2,4]triazolo[4,3-a]pyrazin-6-yl)phenyl)-3-morpholinopropanamide (54).

Yield 65%. m.p. 267-268 °C (EtOH /2-methoxyethanol) ^{1}H-NMR (DMSO-d_6) 2.41 (m, 4H), 2.50 (m, 2H), 2.63 (m, 2H), 3.58 (m, 4H), 7.35 (t, 1H, ar, J = 6.94 Hz), 7.54-7.56 (m, 4H, ar + NH_2), 7.64 (d, 2H, ar, J = 8.04 Hz), 7.69 (s, 1H, ar), 7.91 (d, 2H, ar, J = 7.96 Hz), 8.07 (d, 2H, ar, J = 7.92 Hz), 10.13 (br. s, 1H, NH). ^{13}C-NMR (DMSO-d_6) 34.39, 53.51, 54.64, 66.65, 101.0, 119.28, 119.83, 126.36, 126.75, 129.66, 131.55, 135.69, 137.97, 139.58, 147.61, 147.79, 170.60. IR = 3437.15, 3358.07, 3331.07, 1693.50, 1622.13, 1593.20 cm^{-1}. Anal. Calc. for $C_{24}H_{25}N_7O_3$.

N-(4-(8-amino-3-oxo-2-phenyl-2,3-dihydro-[1,2,4]triazolo[4,3-a]pyrazin-6-yl)phenyl)-3-(4-methylpiperazin-1-yl)propanamide (55). Yield 70%. m.p. 246-248°C (Nitromethane). ^{1}H-NMR (DMSO-d_6) 2.15 (s, 3H, CH_3), 2.33 (m, 2H), 2.48 (m, 8H), 2.62 (m, 2H), 7.35 (t, 1H, ar, J = 7.08 Hz), 7.56 (m, 4H, ar + NH_2), 7.63 (d, 2H, ar, J = 8.34 Hz), 7.69 (s, 1H, ar), 7.91 (d, 2H, ar, J = 8.34 Hz), 8.08 (d, 2H, ar, J = 7.80 Hz), 10.18 (br. s, 1H, NH). ^{13}C-NMR (DMSO-d_6) 34.62, 46.21, 52.83, 54.19, 55.22, 100.99, 119.24, 119.83, 126.36, 126.74, 129.66, 131.46, 131.55, 135.70, 137.97, 139.59, 147.61, 147.79, 170.68. IR = 3371.57, 3336.85, 3201.83, 1712.79, 1674.21 cm^{-1}. Anal. Calc. for $C_{25}H_{28}N_8O_2$.

Synthesis of 8-amino-6-(4-(2-chloroethoxy)phenyl)-2-phenyl-[1,2,4]triazolo[4,3-a]pyrazin-3(2H)-one (195).

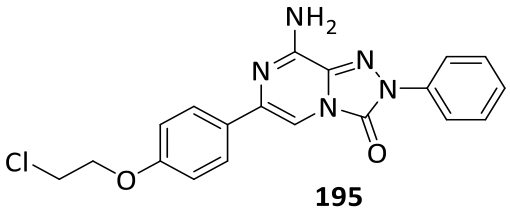

195

Thionyl chloride (0.66 mmol) was slowly added at 10-15 °C to a suspension of 8-amino-6-(4-(2-hydroxyethoxy)phenyl)-2-phenyl-[1,2,4]triazolo[4,3-a]pyrazin-3(2H)-one (**49**) (0.44 mmol) and pyridine (0.66 mmol) in anhydrous toluene (20 mL). The mixture was stirred

at the same temperature for 15 minutes and then refluxed for 2h (TLC monitoring). The mixture was treated with water (20 mL), the solid was collected by filtration and rinsed with petroleum ether. The crude product was purified by column chromatography (Cyclohexane 5/EtOAc 5). Yield 65%. m.p. 270-272 °C. ^{1}H NMR (DMSO-d_6) 4.03 - 3.91 (m, 2H), 4.36 – 4.27 (m, 2H), 7.02 (d, 2H, *J* = 8.8 Hz), 7.36 (t, 1H, *J* = 7.4 Hz), 7.60 - 7.51 (m, 4H), 7.68 (s, 1H), 7.93 (d, 2H, *J* = 8.8 Hz), 8.08 (d, 2H, *J* = 7.7 Hz). ^{13}C NMR (DMSO-d_6) 158.97, 148.29, 147.40, 137.63, 131.58, 129.78, 127.66, 127.15, 119.92, 115.26, 68.51, 43.52. Anal. Calc. for. $C_{19}H_{16}ClN_5O_2$.

General procedure for the Synthesis of 8-amino-2-phenyl-6-(4-ethoxy)phenyl)-[1,2,4]triazolo[4,3-a]pyrazin-3(2H)-one derivatives (56-59).

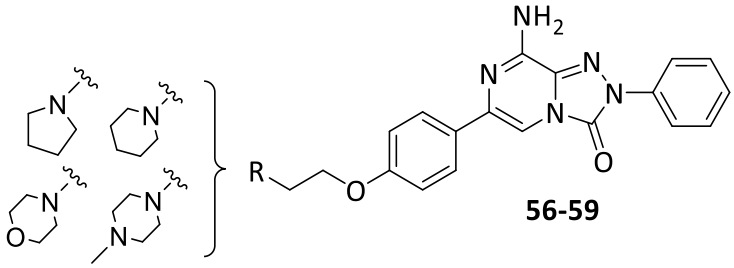

56-59

To a suspension of 8-amino-6-(4-(2-chloroethoxy)phenyl)-2-phenyl-[1,2,4]triazolo[4,3-a]pyrazin-3(2H)-one (**195**) (0.37 mmol), anhydrous K_2CO_3 (0.74 mmol), KI (catalytic amount) in anhydrous DMF (3 mL), the suitable amine (pyrrolidine, 1.85 mmol; morpholine, 6.76 mmol; piperidine, 6.24 mmol; N-methylpiperazine, 1.84 mmol) was added. The mixture was refluxed for 8 h (TLC monitoring) and then diluted with water (20 mL). The resulting solid was collected by filtration, rinsed with water (20 mL), petroleum ether and purified by column chromatography.

8-amino-2-phenyl-6-(4-(2-(pyrrolidin-1-yl)ethoxy)phenyl)-[1,2,4]triazolo[4,3-a]pyrazin-3(2H)-one (56). Purified by column chromatography (DCM3 8/MeOH 2). Yield 35%. m.p. 213-214 °C ^{1}H NMR (DMSO-d_6) 1.72 (s, 4H), 2.61 (s, 4H), 2.88 (s, 2H, CH_2), 4.13 (t, 2H, CH_2, J = 5.7 Hz), 6.99 (d, 2H, ar, J = 8.8 Hz), 7.35 (t, 1H, ar, J = 7.4 Hz), 7.54 – 7.58 (m, 4H, ar +$_{NH2}$), 7.66 (s, 1H, H-5), 7.91 (d, 2H, ar, J = 8.8 Hz), 8.08 (d, 2H, ar, J = 7.8 Hz). Anal. Calc. for $C_{23}H_{24}N_6O_2$.

8-amino-2-phenyl-6-(4-(2-(piperidin-1-yl)ethoxy)phenyl)-[1,2,4]triazolo[4,3-a]pyrazin-3(2H)-one (57). Purified by column chromatography (Cyclohexane 2/ EtOAc 8; $CHCl_3$ 9/

MeOH 1). Yield 20%. m.p. 220-222 °C ^{1}H NMR (DMSO-d_6) 1.38 -1.48 (m, 2H), 1.53 (dt, 4H, J = 10.9, 5.6 Hz), 2.44 (m, 4H), 2.67 (t, 2H, J = 5.9 Hz), 4.10 (t, CH_2, 2H, J = 5.9 Hz), 6.99 (d, 2H, ar, J = 8.9 Hz), 7.35 (t, 1H, ar, J = 7.4 Hz), 7.58 – 7.50 (m, 4H, ar + NH_2), 7.65 (s, 1H, H-5), 7.90 (d, 2H, ar, J = 8.8 Hz), 8.08 (dd, 2H, ar, J = 8.5, 0.9 Hz). IR = 3356, 1707, 1458 cm^{-1}. Anal. Calc. for. $C_{24}H_{26}N_6O_2$.

8-amino-6-(4-(2-morpholinoethoxy)phenyl)-2-phenyl-[1,2,4]triazolo[4,3-a]pyrazin-3(2H)-one (58). Purified by column chromatography (Cyclohexane 2/EtOAc 8; Cyclohexane 6/EtOAc 6/MeOH 1) Yield 52%. m.p. 219-221 °C ^{1}H NMR (DMSO-d_6) 2.50 (d, 4H, J = 1.5 Hz), 2.71 (t, 2H, CH_2, J = 5.7 Hz), 3.58-3.62(m, 4H), 4.13 (t, 2H, CH_2, J = 5.7 Hz), 6.99 (d, 2H, ar, J = 8.8 Hz), 7.36 (t, 1H, ar, J = 7.4 Hz), 7.54-7.58 (m, 4H, ar + NH_2), 7.66 (s, 1H, 5-H), 7.90 (d, 2H, ar, J = 8.7 Hz), 8.08 (d, 2H, ar, J = 8.0 Hz). ^{13}C NMR (DMSO-d_6) 45.50, 53.98, 56.42, 57.36, 62.40, 66.45, 100.57, 107.83, 114.92, 119.87, 126.76, 127.28, 129.34, 129.65, 131.53, 133.85, 135.84, 137.97, 144.80, 147.62, 147.76, 155.66, 158.90. IR = 3462, 3367, 2795, 1707, 1614, 1454, 1114 cm^{-1}. Anal. Calc. for $C_{23}H_{24}N_6O_3$.

8-amino-6-(4-(2-(4-methylpiperazin-1-yl)ethoxy)phenyl)-2-phenyl-[1,2,4]triazolo[4,3-a]pyrazin-3(2H)-one (59). Purified by column chromatography (Cyclohexane 2/EtOAc 6/ MeOH 2; $CHCl_3$ 9/MeOH 1). Yield 43 % m.p. 242-244 °C. ^{1}H NMR ($CDCl_3$) 2.33 (s, 3H, CH_3), 2.52 (m, 4H), 2.67 (m, 4H), 2.87 (t, 2H, CH_2, J = 5.8 Hz), 4.18 (t, 2H, CH_2, J = 5.8 Hz), 5.53 (br s, 2H, NH_2), 6.99 (d, 2H, ar, J = 8.8 Hz), 7.34 (t, 1H, ar, J = 7.4 Hz), 7.52 (t, 2H, ar, J = 7.9 Hz), 7.61 (s, 1H, H-5), 7.79 (d, 2H, ar, J = 8.8 Hz), 8.13 (d, 2H, ar, J = 7.8 Hz). ^{13}C NMR (DMSO-d_6) 39.33, 39.54, 39.75, 39.96, 40.17, 40.38, 40.59, 45.95, 53.24, 55.02, 114.90, 118.38, 119.87, 122.64, 127.28, 129.26, 129.66. IR = 3312, 2727, 1714, 1456, 1377, 1163 cm^{-1}. Anal. Calc. for $C_{24}H_{27}N_7O_2$.

Synthesis of 8-amino-6-(4-(oxiran-2-ylmethoxy)phenyl)-2-phenyl-[1,2,4]triazolo[4,3-a]pyrazin-3(2H)-one (196).

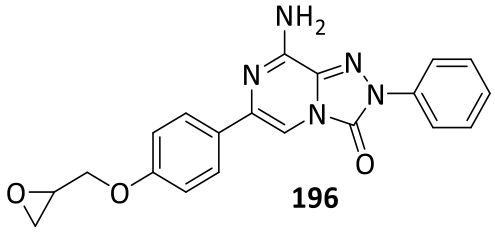

Epichlorohydrin (6.90 mmol) was added to a suspension of 8-amino-6-(4-hydroxyphenyl)-2-phenyl-[1,2,4]triazolo[4,3-a]pyrazin-3(2H)-one (**16**) (0.627 mmol) and K_2CO_3 (1.25 mmol) in anhydrous acetone (10 mL). The mixture was refluxed for 24 h. The solvent was evaporated under reduced pressure and the resulting residue was treated with water (20-25 mL). The solid was collected by filtration, rinsed with diethyl ether (25-30 mL) and petroleum ether (20 mL), dried and recrystallized. Yield 68 % m.p. > 300°C (EtOH). ^{1}H NMR (DMSO-d_6) 2.72 (s, 1H), 2.85 (t, 1H, J = 4.5 Hz), 3.83 (dd, 2H, J = 11.2, 6.5 Hz), 4.37 (d, 1H, J = 11.6 Hz), 7.01 (d, 2H, J = 8.7 Hz), 7.35 (t, 1H, J = 7.3 Hz), 7.55 (t, 3H, J = 7.7 Hz), 7.63 (s, 1H), 7.87 (d, 2H, J = 8.5 Hz), 8.04 (d, 2H, J = 8.1 Hz). Anal. Calc. for. $C_{20}H_{17}N_5O_3$.

General procedure for the synthesis of 8-amino-6-(4-(2-hydroxy-3-morpholino/(piperidin-1-yl)propoxy)phenyl)-2-phenyl-[1,2,4]triazolo[4,3-a]pyrazin-3(2H)-one (60-61).

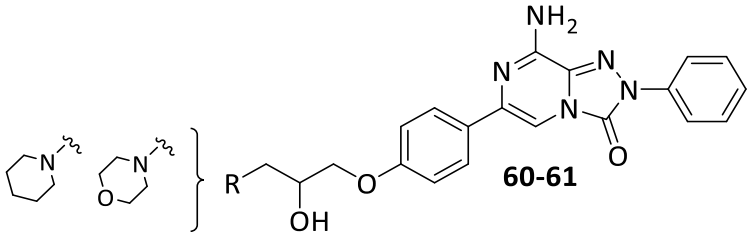

Piperidine (10.60 mmol, **60**) or morpholine (14.4 mmol, **61**) was added to a suspension of 8-amino-6-(4-(oxiran-2-ylmethoxy)phenyl)-2-phenyl-[1,2,4]triazolo[4,3-a]pyrazin-3(2H)-one **(196)** (0.533 mmol) and K_2CO_3 (1.066 mmol) in absolute EtOH (5 mL). The mixture was refluxed for 24 h (TLC monitoring). The solvent was evaporated under reduced pressure to dryness and the resulting residue was treated with water (20-25 mL). The solid was collected by filtration, rinsed with diethyl ether and petroleum ether, dried and recrystallized.

8-amino-6-(4-(2-hydroxy-3-(piperidin-1-yl)propoxy)phenyl)-2-phenyl-[1,2,4]triazolo[4,3-a]pyrazin-3(2H)-one (60). Yield 65%. m.p. 202-204 °C (2-Methoxyethanol). ^{1}H NMR (DMSO-d_6) 1.57 – 1.42 (m, 2H), 1.65 (dd, 4H, *J* = 10.3, 5.5 Hz), 2.46 (s, 2H), 2.56 (d,2H, *J* = 6.8 Hz), 2.68 (s, 2H), 4.04 (dd, 2H, *J* = 9.8, 4.9 Hz), 4.14 (dd, *J* = 12.5, 5.7 Hz, 1H), 5.54 (s, 1H), 7.01 (d, 2H, *J* = 8.7 Hz), 7.34 (t, 1H, *J* = 7.3 Hz), 7.52 (t,2H, *J* = 7.9 Hz), 7.61 (s, 1H), 7.79 (d, 2H, *J* = 8.7 Hz), 8.13 (d, 2H, *J* = 8.1 Hz). Anal. Calc. for. $C_{25}H_{28}N_6O_3$.

8-amino-6-(4-(2-hydroxy-3-morpholinopropoxy)phenyl)-2-phenyl-[1,2,4]triazolo[4,3-a]pyrazin-3(2H)-one (61). Yield 65%. m.p. 231-233 °C (2-Methoxyethanol). ^{1}H NMR (DMSO-d_6) 2.47 (d, 4H, *J* = 22.9 Hz), 3.58 (s, 4H), 4.13 – 3.73 (m, 3H), 4.88 (s, 1H), 6.99 (d, 2H, *J* = 5.9 Hz), 7.36 (s, 1H), 7.55 (d, 4H, *J* = 9.0 Hz), 7.66 (s, 1H), 7.90 (d, 2H, *J* = 5.7 Hz), 8.08 (d, 2H, *J* = 5.7 Hz). Anal. Calc. for $C_{24}H_{26}N_6O_4$.

General procedure for the synthesis of (R)-2-oxothiazolidine-4-carboxamide-substituted 8-amino-1,2,4-triazolo[4,3-*a*]pyrazin-3(2*H*)-one derivatives (**79, 81**)

A mixture of the suitable triazolopirazine (**39, 48**) (1 mmol), (R)-2-oxothiazolidine-4-carboxylic acid (2 mmol), EDCI. HCl (2 mmol), HOBt monohydrate (2 mmol), DIPEA (2 mmol) in anhydrous DMF (3 ml) was heated at 60 °C per 18 h (TLC monitoring). The mixture was treated with water (20 mL) and the solid was collected by filtration and rinsed with Et_2O and petroleum ether. The crude product was purified by recrystallization (**79**) or column chromatography (**80**).

(R)-N-(4-(8-amino-3-oxo-2-phenyl-2,3-dihydro-[1,2,4]triazolo[4,3-a]pyrazin-6-yl)phenyl)-2-oxothiazolidine-4-carboxamide (79)

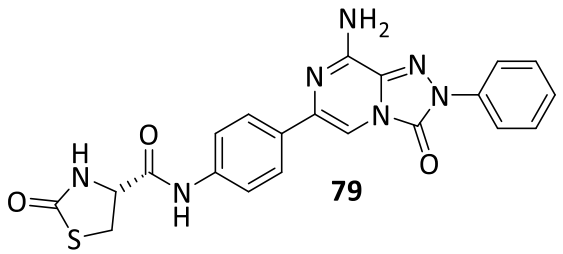

79

Yield 99%. m.p. > 300 °C. Purified by column chromatography ($CHCl_3$ 9.4/MeOH 0.6). ^{1}H-NMR (DMSO-d_6) 3.51 (m, 1H, CH), 3.78 (m, 1H, CH), 4.50 (m, 1H, CH), 7.35 (t, 1H, ar, J

= 7.3 Hz), 7.56 (t, 2H, ar, J = 8.00 Hz), 7.65 (br. s, 2H, NH_2), 7.68 (d, 2H, ar, J = 8.6 Hz), 7.73 (s, 1H, ar), 7.96 (d, 2H, ar, J = 8.6 Hz), 8.08 (d, 2H, ar, J = 8.00 Hz), 8.37 (s, 1H, NH), 10.26 (s, 1H, NH). ^{13}C-NMR (DMSO-d_6) 32.79, 57.49, 101.26, 119.71, 119.84, 126.44, 126.76, 129.66, 131.56, 132.18, 135.56, 137.96, 138.90, 147.62, 147.83, 169.11, 174.06. Anal.Calc. for $C_{21}H_{17}N_7O_3S$.

(R)-N-(2-(4-(8-amino-3-oxo-2-phenyl-2,3-dihydro-[1,2,4]triazolo[4,3-a]pyrazin-6-yl)phenoxy)ethyl)-2-oxothiazolidine-4-carboxamide (81).

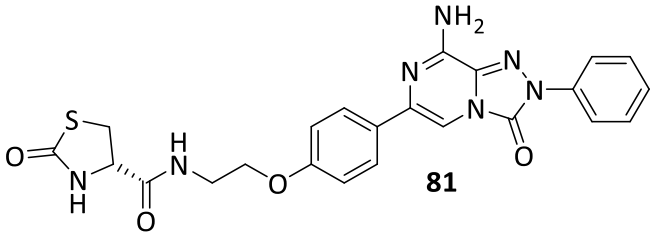

Yield 100%. m.p. 255-257 °C (EtOH/2-Methoxyethanol). ^{1}H-NMR (DMSO-d_6) 3.51 (q, 2H, CH_2, J = 5.5 Hz), 3.67 (m, 1H, CH), 4.07 (t, 2H, CH_2, J = 5.5 Hz), 4.32 (m, 1H, CH), 7.00 (d, 2H, ar, J = 8.9 Hz), 7.35 (t, 1H, ar, J = 7.4 Hz), 7.56 (m, 4H, ar + NH_2), 7.67 (s, 1H, H-5), 7.92 (d, 2H, ar, J = 8.8 Hz), 8.07 (d, 2H, ar, J = 7.8 Hz), 8.32 (br s, 1H, NH), 8.37 (t, 1H, NH, J = 5.4 Hz). Anal. Calc. for $C_{23}H_{21}N_7O_4S$.

General procedure for the synthesis of the 5-(1,2-dithiolan-3-yl)pentanamide substituted 8-amino-1,2,4-triazolo[4,3-*a*]pyrazin-3(2*H*)-one derivatives (80, 82, 84).

A mixture of the suitable triazolopirazine (**39, 48, 51**) (1.00 mmol), racemic lipoic acid (1.35 mmol), EDCI.HCl (1.35 mmol), HOBt monohydrate (1.35 mmol) and DIPEA (1.70 mmol) in anhydrous DMF (3mL) was stirred at room temperature 24 h (TLC monitoring). The mixture was treated with water (20 mL). The obtained solid was collected by filtration, rinsed with Et_2O and petroleum ether. The crude product was purified by recrystallization (**80**) or column chromatography (**82**, **84**)

N-(4-(8-amino-3-oxo-2-phenyl-2,3-dihydro-[1,2,4]triazolo[4,3-a]pyrazin-6-yl)phenyl)-5-(1,2-dithiolan-3-yl)pentanamide (80).

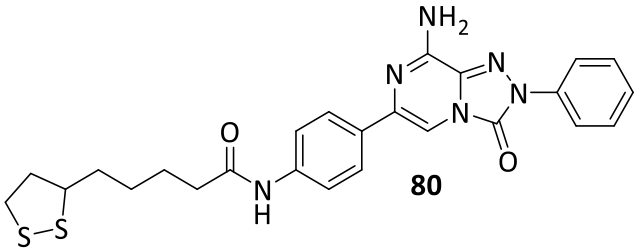

80

Yield 99%. m.p. 229-233 °C (Nitromethane). ^{1}H-NMR (DMSO-d_6) 1.43 (m, 2H), 1.63 (m, 2H), 1.71 (m, 2H), 1.88 (m, 1H, J = 6.6 Hz), 2.34 (t, 2H, J = 7.3 Hz), 2.43 (m, 1H, J = 6.3 Hz), 3.14 (m, 1H), 3.19 (m, 1H), 3.64 (m, 1H, J = 6.2 Hz), 7.35 (t, 1H, ar, J = 7.4 Hz), 7.54 (br s, 2H, NH_2), 7.56 (t, 2H, ar, J = 8.1 Hz), 7.65 (d, 2H, ar, J = 8.7 Hz), 7.69 (s, 1H, H-5), 7.91 (d, 2H, ar, J = 8.9 Hz), 8.08 (d, 2H, ar, J = 7.9 Hz), 9.96 (br s, 1H, NH). ^{13}C-NMR (DMSO-d_6) 25.35, 28.82, 34.64, 36.74, 38.58, 56.58, 100.98, 119.30, 120.00, 126.31, 126.75, 129.67, 131.39, 131.56, 135.75, 137.98, 139.68, 147.61, 147.79, 171.60. IR = 3431.36, 3311.78, 3207.62, 1693.50, 1681.93 cm^{-1}. Anal.Calc. for $C_{25}H_{26}N_6O_2S_2$.

N-(2-(4-(8-amino-3-oxo-2-phenyl-2,3-dihydro-[1,2,4]triazolo[4,3-a]pyrazin-6-yl)phenoxy)ethyl)-5-(1,2-dithiolan-3-yl)pentanamide (82).

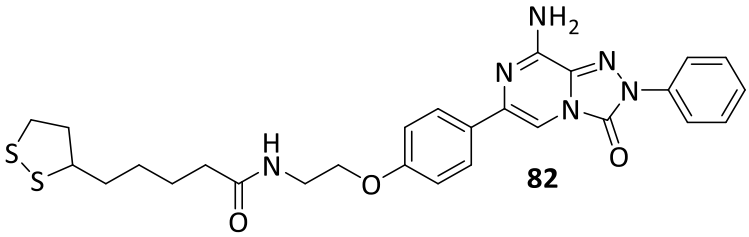

82

Yield 82%. m.p. 202-204 °C. Purified by liquid chromatography (Cyclohexane 2/EtOAc 8). ^{1}H NMR (DMSO-d_6) 1.35 (dd, 2H, J = 14.7, 7.5 Hz), 1.53 (dd, 3H, J = 15.1, 7.4 Hz), 1.64 (dd, 1H, J = 13.5, 7.5 Hz), 1.75 – 1.90 (m, 1H), 2.11 (t, 2H, J = 7.1 Hz), 2.38 (dd, 1H, J = 12.5, 6.2 Hz), 3.02 – 3.21 (m, 2H), 3.43 (d, 2H, J = 5.2 Hz), 3.53 – 3.64 (m, 1H), 4.02 (d, 2H, J = 5.0 Hz), 6.99 (d, 2H, ar, J = 8.2 Hz), 7.36 (t, 1H, ar, J = 7.3 Hz), 7.49– 7.63 (m, 4H, ar + NH_2), 7.66 (s, 1H, H-5), 7.91 (d, 2H, ar, J = 8.1 Hz), 8.08 (m, 3H, ar + NH, J = 8.4 Hz). IR = 3358, 3285, 3179, 1709,1628, 1541, 1462 cm^{-1}. Anal. Calc. for $C_{27}H_{30}N_6O_3S_2$.

N-(3-((4-(8-amino-3-oxo-2-phenyl-2,3-dihydro-[1,2,4]triazolo[4,3-a]pyrazin-6-yl)phenyl)amino)-3-oxopropyl)-5-(1,2-dithiolan-3-yl)pentanamide (84).

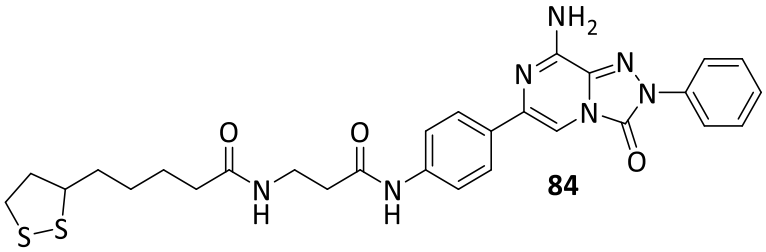

Yield 89%. m.p. 250-251 °C. Purified by column chromatography (DCM 9.7/MeOH 0.3). ^{1}H NMR (DMSO-d_6) 1.29-1.36 (m, 2H), 1.47-1.54 (m, 3H), 1.59-1.66 (m, 1H), 1.83 (m, 1H), 2.07 (t, 2H, J = 7.2 Hz), 2.36 (m, 1H, J = 6.2 Hz), 3.04-3.11 (m, 1H), 3.12-3.19 (m, 1H), 3.52-3.59 (m, 1H), 7.35 (t, 1H, ar, J = 7.4 Hz), 7.54-7.58 (m, 4H, ar + NH_2), 7.65-7.69 (m, 3H, ar + H-5), 7.92 (m, 3H, ar + NH), 8.08 (d, 2H, ar, J = 7.9 Hz), 10.03 (br s, 1H, NH). Anal. Calc. for $C_{28}H_{31}N_7O_3S_2$.

General procedure for the Synthesis of substituted the 3,5-di-tert-butyl-4-hydroxybenzamide 8-amino-1,2,4-triazolo[4,3-*a*]pyrazin-3(2*H*)-one derivatives (83, 85). A mixture of the suitable triazolopirazine (**48, 51**), 3,5-di-tert-butyl-4-hydroxybenzoic acid (2 mmol), EDCI. HCl (2 mmol), HOBt monohydrate (2 mmol), DIPEA (2 mmol) in anhydrous DMF (3 mL) was heated at 60 °C per 18 h. The mixture was treated with water (20 mL). The solid was collected by filtration, rinsed with Et_2O and petroleum ether. The crude product was purified by recrystallization **(83)** or column chromatography **(85)**.

N-(3-((4-(8-amino-3-oxo-2-phenyl-2,3-dihydro-[1,2,4]triazolo[4,3-a]pyrazin-6-yl)phenyl)amino)-3-oxopropyl)-3,5-di-tert-butyl-4-hydroxybenzamide (83).

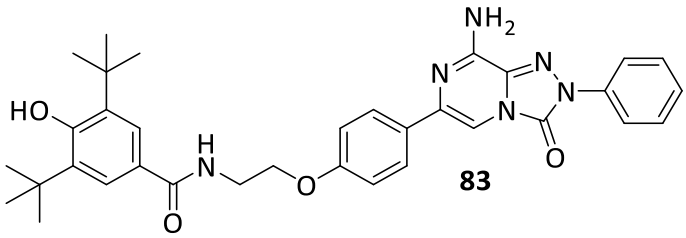

Yield 90%. m.p. 250-252 °C (Nitromethane). ^{1}H NMR (DMSO-d6) 1.41 (s, 18H, $(CH_3)_3$), 3.62 (m, 2H, CH_2), 4.15 (t, 2H, CH_2, J = 5.8 Hz), 7.02 (d, 2H, ar, J = 8.8 Hz) 7.36 (t, 1H, ar, J = 7.4 Hz) 7.39 (s, 1H, ar), 7.50-7.59 (m, 4H, ar + NH_2), 7.63 (s, 2H, ar), 7.66 (s, 1H, ar, H-5), 7.91

(d, 2H, ar, J = 8.6 Hz), 8.08 (d, 2H, ar, J = 7.9 Hz), 8.51 (t, 1H, NH, J = 5.5 Hz).^{13}C NMR (DMSO-d6) 30.68, 35.03, 36.38, 37.19, 101.02, 119.45, 119.88, 124.47, 126.29, 126.75, 129.64, 131.52, 131.57, 135.77, 137.99, 138.66, 139.58, 147.62, 147.80, 157.02, 167.64, 170.19. Anal. Calc. for $C_{35}H_{39}N_7O_4$.

N-(2-(4-(8-amino-3-oxo-2-phenyl-2,3-dihydro-[1,2,4]triazolo[4,3-a]pyrazin-6-yl)phenoxy)ethyl)-3,5-di-tert-butyl-4-hydroxybenzamide (85).

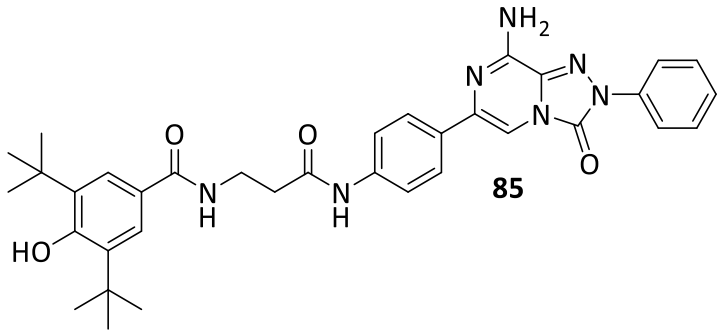

Yield 78%. m.p. 259-260°C. Purified by column chromatography (Cyclohexane 6/EtOAc 4). ^{1}H NMR (DMSO-d6) 1.41 (s, 18H, $(CH_3)_3$), 3.62 (d, 2H, CH_2, J = 5.6 Hz), 4.15 (t, 2H, CH_2, J = 5.8 Hz), 7.02 (d, 2H, ar, J = 8.8 Hz), 7.36 (t, 1H, ar, J = 7.4 Hz), 7.39 (s, 1H, OH), 7.54–7.59 (m, 4H, ar + NH_2), 7.63 (s, 2H, ar), 7.66 (s, 1H, H-5), 7.91 (d, 2H, ar, J = 8.7 Hz), 8.08 (d, 2H, ar, J = 7.9 Hz), 8.51 (t, 1H, NH, J = 5.5 Hz). ^{13}C NMR (DMSO-d6) 30.68, 35.05, 66.69, 114.90, 119.87, 124.54, 125.97, 126.75, 127.33, 129.39, 129.64, 131.53, 135.84, 137.34, 137.98, 138.69, 144.69, 147.61, 147.77, 157.14, 158.99, 167.75. IR = 3315, 3213, 1699, 1616, 1456 1377, 1315, 1248, 1178 cm^{-1}. Anal. Calc. for $C_{34}H_{38}N_6O_4$.

Synthesys of N-(4-(8-amino-3-oxo-2-phenyl-2,3-dihydro-[1,2,4]triazolo[4,3-a]pyrazin-6-yl)phenyl)-3-hydrazinylpropanamide (197).

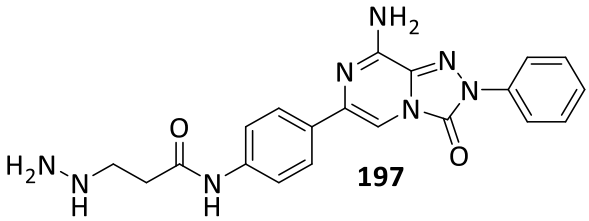

Hydrazine monohydrate (13.425 mmol) was added to a suspension of N-(4-(8-amino-3-oxo-2-phenyl-2,3-dihydro-[1,2,4]triazolo[4,3-a]pyrazin-6-yl)phenyl)acrylamide **194** (0.537 mmol) in anhydrous THF and the resulting mixture was refluxed for 21 h (TLC

monitoring, $CHCl_3$ 9/MeOH 1). The solvent was eliminated under reduced pressure and the residue was treated with Et_2O (20 mL). The obtained solid was collected by filtration and rinsed with pethroleum ether (20 mL). Yield 78%. (Nitromethane). ^1H NMR (DMSO-d6) 2.48 (t, 2H, CH_2, J = 6.7 Hz), 2.91 (t, 2H, CH_2, J = 6.7 Hz), 7.35 (t, 1H, ar, J =7.4 Hz), 7.54-7.58 (m, 4H, ar + NH_2), 7.63-7.69 (m, 3H, ar + H-5), 7.91 (d, 2H, ar, J = 8.7 Hz), 8.08 (d, 2H, ar, J = 7.6 Hz), 8.93 (br s, 1H, NH), 10.17 (s, 1H, NH), Anal. Calc. for $C_{20}H_{20}N_8O_2$.

N-(4-(8-amino-3-oxo-2-phenyl-2,3-dihydro-[1,2,4]triazolo[4,3-a]pyrazin-6-yl)phenyl)-3-(3-methyl-5-oxo-2,5-dihydro-1H-pyrazol-1-yl)propenamide (86).

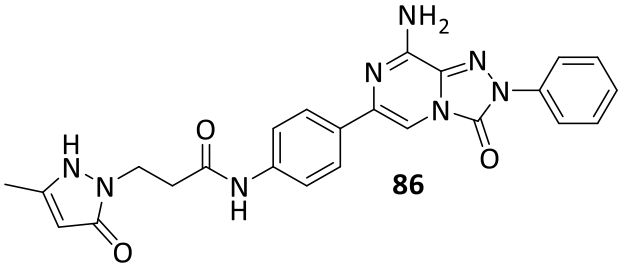

To a suspension of N-(4-(8-amino-3-oxo-2-phenyl-2,3-dihydro-[1,2,4]triazolo[4,3-a]pyrazin-6-yl)phenyl)-3-hydrazinylpropanamide (**197**) (0.42 mmol) in EtOH (20 mL) ethyl acetoacetate (0.42 mmol) was added. The resulting mixture was heated at 60 °C for 2h (TLC monitoring). The solid was filtered off and the ethanolic organic layer was evaporated under reduced pressure. The obtained residue was taken up with Et_2O (20 mL) and the solid was collected by filtration. The crude product was purified by column chromatography ($CHCl_3$/MeOH 1). Yield 56%. m.p. 226-228 °C. ^1H NMR (DMSO-d6) 2.01 (s, 3H, CH_3), 2.77 (m, 2H, CH_2), 4.05 (m, 2H, CH_2), 5.14 (s, 1H), 7.35 (t, 1H, ar, J = 7.4 Hz), 7.54-7.59 (m, 4H, ar + NH_2), 7.63 (d, 2H, ar, J = 8.7 Hz), 7.70 (s, 1H, H-5), 7.90 (d, 2H, ar, J = 8.7 Hz), 8.06 (d, 2H, ar, J =7.6 Hz), 10.10 (s, 1H, NH), 10.69 (br s, 1H, NH). Anal. Calc. for $C_{24}H_{22}N_8O_3$.

7. VISITING PERIOD AT THE LEIDEN CENTRE OF DRUG RESEARCH (LACDR)

7.1 Introduction

Between the second and third year of my PhD course, I spent six months (September 2017-March 2018) at the Leiden Academic Centre for Drug Research (LACDR) in Netherlands, where I joined the research group of Prof. A.P. IJzerman, Professor of Medicinal Chemistry and Head of the Medicinal Chemistry group at the Division of Drug Discovery & Safety. The research topic assigned to me was the synthesis of non-adenosine-like compounds designed to target the hA_{2A}AR and based on the structure of **LUF5833** (Figure 37).

As largely anticipated in the "Introduction" chapter, A_{2A}ARs play an important role in a variety of physiopathogical conditions including both neurodegenerative disorders and inflammatory tissue damage. At present, it is well known the beneficial application of selective A_{2A}ARantagonists in the treatment of neurodegenerative disorders such as Parkinson's disease[379] (PD), Huntington's disease[378], and Alzheimer's disease [382,383]. However, several animal models of neurodegenerative disorders have given evidence that also the A_{2A} AR agonists are able to exert neuroprotective effect through the reduction of the excitatory neurotransmitter release, apoptosis, and inflammatory responses[280,437]. Also in the cardiovascular field a number of A_{2A}AR agonists have been tested as candidate for myocardial perfusion since they are able to modulate the coronary arterial vasodilation[446,447]. A_{2A} AR agonists could be also beneficial in the treatment of neuropathic pain, being capable of modulating the production of glial cytokines[448]. Moreover, a large body of evidence has clearly show that A_{2A}AR agonists exert anti-inflammatory properties modulating the activity of neutrophils, macrophages, and T lymphocytes[446,449]. A_{2A}AR stimulation also inhibits neutrophil adherence to the endothelium, degranulation of neutrophils and monocytes, and superoxide anion generation[280], thus indicating that A_{2A}ARs are involved in inflammation processes and selective agonists could be developed as potential therapeutic agents in the treatment allergic rhinitis, asthma, and chronic obstructive pulmonary disease[446,450].

In the past, adenosine receptor agonists were usually associated to a adenosine-like structure where the ribose moiety was tought to play a crucial role for the agonistic functional activty[451]. Several studies, in fact, highlighted that in the agonist-bound crystal structure, the ribose moiety of the ligands inserts deeply into a predominantly hydrophilic region of the binding cavity and enganges contacts or hydrogen bonds with important amicnoacid residues at this level[452-454]. However, progress has been made and novel non-nucleoside AR ligands belonging to the amino-3,5-dicyanopyridine series were identified. These compounds possessed both a significant affinity and efficacy toward different adenosine receptor subtypes[275,276,455,456] and, among these derivatives, the 2-amino-4-(phenyl/4-hydroxyphenyl)-6-(1H-imidazol-2-yl-methylsulfanyl)-pyridine-3,5-dicarbonitrile (**LUF5833,** and **LUF5834** Figure 37) turned out to be a high-affinity non-adenosine partial agonists at the $A_{2A}AR$[276].

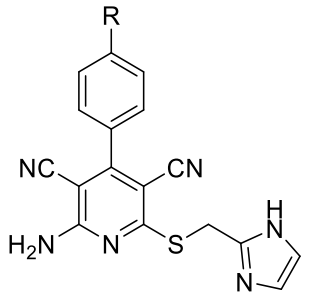

R = H, LUF5833
R = OH, LUF5834

Figure 37. Structure of the hA_{2A} AR partial agonists **LUF5833** and **LUF5834**

Table 13. [a]Interaction of compounds **LUF5833** and **LUF5834** with the hA_{2A} adenosine receptor, [b]Stimulation (A_{2A}) of cAMP production by the compounds **LUF5833** and **LUF5834** compared to reference Agonist[276].

	[a]hA_{2A} K_i (nM)	[c]Efficacy
LUF5833	8.13 ± 0.05	55 ± 20
LUF5834	6.25 ± 0.08	55 ± 12

[a] Radioligand binding experiments were carried out on membranes made from HEK_{293} cells stably expressing the A_{2A} with [^{3}H]ZM241385 as radio ligand. [b]Production of cAMP was studied in CHO cells stably expressing the hA_{2A} adenosine receptor (n = 3). [c]Efficacy is expressed with respect to reference agonist CGS21680, compounds were tested at 100 times their K_i values.

7.2 Aim of the work

Recently, a crystal structure of the $hA_{2A}AR$ containing the 2-((1H-imidazol-2-yl)methylthio)-6-amino-4-phenylpyridine-3,5-dicarbonitrile (**LUF5833,** Figure 37) in the binding pocket has been obtained. Since the structural determinants involved in the functional activity of these compounds are largely unknown, the design and synthesis of compounds structurally related to **LUF5833** have been undertaken to shed light on the hypothetical binding mode of these ligands at the $A_{2A}AR$ crystal structure. The project I worked on concerned the synthesis of the non-nucleoside compounds **LUF7760**, **LUF7762** and **LUF7763** (**87-89**) which were designed together with the pyrimidine derivatives **LUF7724** and **LUF7740** to target the $hA_{2A}AR$ (Figure 38). The triazine derivative **87** ensued from the replacement of the two CN groups of **LUF5833** with endocyclic nitrogen atoms, while the pyridine derivatives **88-89** derived from removal of the CN group(s) of the lead. Hopefully, combination of the synthetic and computational studies will led to valuable information about the role of the substituents and scaffold properties on the functional profile of $A_{2A}AR$ non-adenosine-like agonists.

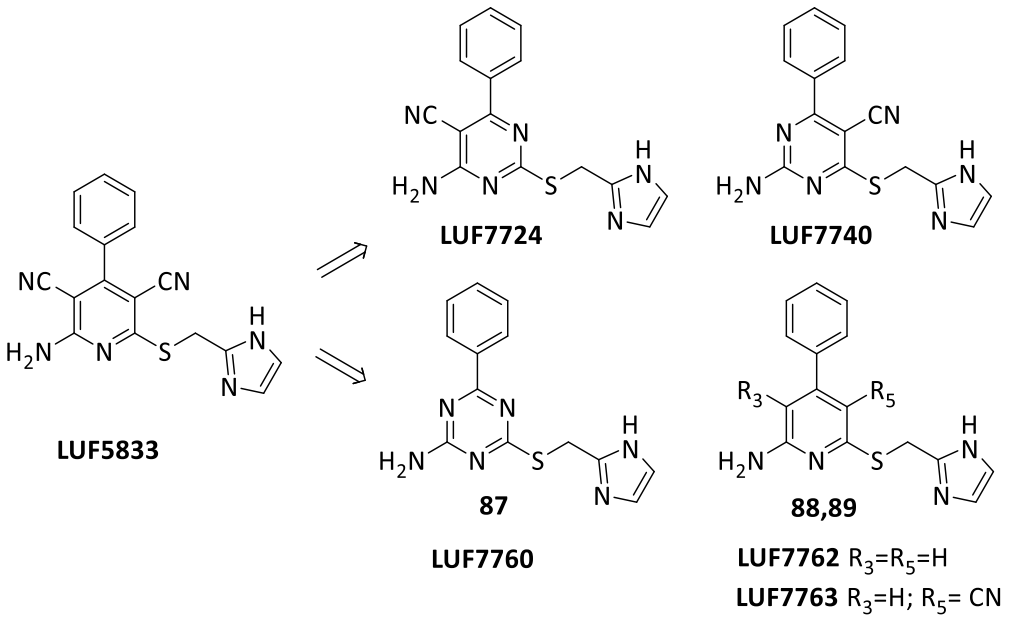

Figure 38. **LUF5833**-based structures of the newly synthetized derivatives**.**

It has to be pointed that compounds **LUF7724** and **LUF7740,** were already synthesized and tested before I joined Professor's IJzerman group and are herein reported as reference compounds.

7.3 Chemistry

Synthesis of the 4-(((1H-imidazol-2-yl)methyl)thio)-6-phenyl-1,3,5-triazin-2-amine 1 (LUF7760).

The synthesis of the 4-(((1H-imidazol-2-yl)methyl)thio)-6-phenyl-1,3,5-triazin-2-amine **87** (**LUF7760**), depicted in Scheme 15, started from the commercial cyanuric chloride which was reacted with phenylmagnesium bromide at room temperature in anhydrous THF to give the 2,6-dichloro-4-phenyl-1,3,5-triazine (**198**). Treatment of **198** with 25% aqueous ammonia in dichloromethane yielded the amino derivative **199** which was reacted with anhydrous sodium sulfide in DMF at 80 °C to give the corresponding 4-amino-6-phenyl-1,3,5-triazine-2-thiol **200**. Reaction of intermediate **200** with the properly synthesized 2-(bromomethyl)-1H-imidazole[276] in anhydrous DMF and in the presence of $NaHCO_3$, at room temperature, afforded the desired triazine **87** (**LUF7760)**.

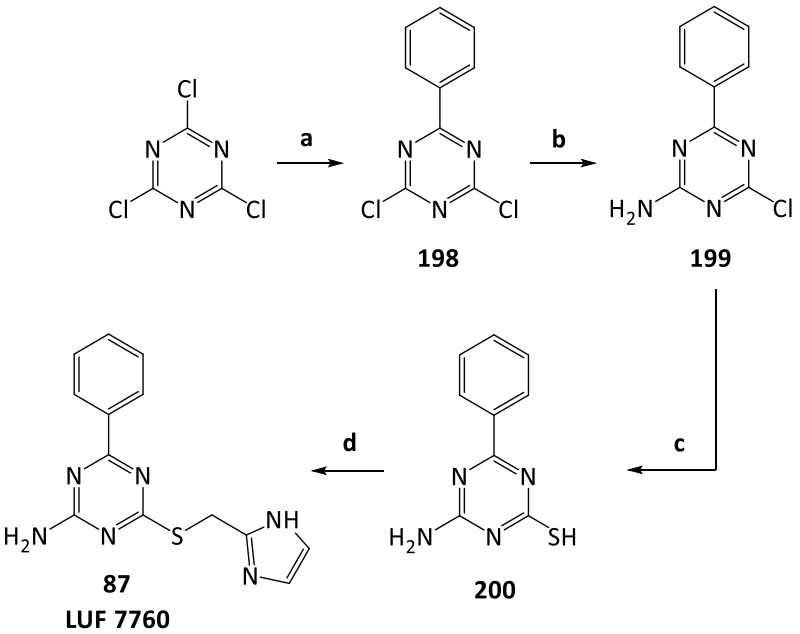

Scheme 15: **a)** Phenylmagnesium bromide, anhydrous THF, r.t.; **b)** NH_3 25% in H_2O, dichloromethane, r.t.; **c)** anhydrous Na_2S, DMF, 80 °C; **d)** 2-Bromomethyl-(1H)-imidazole, $NaHCO_3$, anhydrous DMF, r.t.

Synthesis of 6-(((1H-imidazol-2-yl)methyl)thio)-4-phenylpyridin-2-amine 2 (LUF7762).

Scheme 16 shows the synthesis of 6-(((1H-imidazol-2-yl)methyl)thio)-4-phenylpyridin-2-amine **88** (**LUF7762**). The 2,6-dichloro-4-phenylpyridine **201** was obtained from the commercial 2,6-dichloro-4-iodopyridine which was reacted with phenylboronic acid pinacol esther, $Pd(PPh_3)Cl_2$, Na_2CO_3 in H_2O/MeCN at 70 °C, under Suzuki-Miyaura conditions. Treatment of **201** with 2-methyl-propanethiol, and Cs_2CO_3, in DMF at 80 °C afforded **202** intermediate whose reaction with t-butyl carbamate in anhydrous 1,4-dioxane at 110 °C, and in presence of the couple $Pd(OA)_2$, Xantphos and Cs_2CO_3, gave the tert-butyl-(6-(tert-butylthio)-4-phenylpyridin-2-yl)-carbamate **203**. Deprotection of its amino-group, performed with TFA in dichloromethane at room temperature, yielded compound **204** which was allowed to react with boiling 37% hydrochloric acid to give the 6-amino-4-phenylpyridine-2-thiol **205.** Finally, the desired product **LUF7762** was achieved by alkylating compound **205** with 2-(bromomethyl)-1H-imidazole, in presence of $NaHCO_3$ in anhydrous DMF.

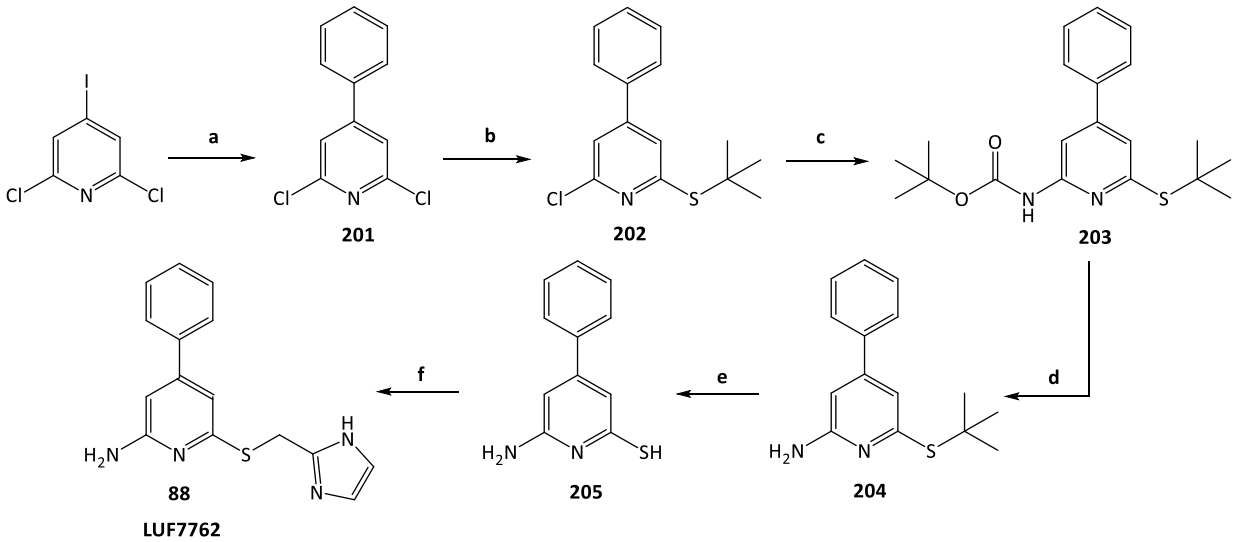

Scheme 16. a) Phenylboronic acid pinacol esther, $Pd(PPh_3)Cl_2$,Na_2CO_3, H_2O/acetonitrile, 70 °C; **b)** 2-Methyl-propanethiol, Cs_2CO_3, DMF, 80 °C; **c)** $Pd(OA)_2$, xantphos, Cs_2CO_3, t-butyl carbamate, anydrous 1,4-dioxane, 110 °C; **d)** TFA, dichloromethane, reflux; **e)** 37% HCl, 100 °C; **f)** Bromomethyl-(1H)-imidazole, $NaHCO_3$, anydrous DMF, r.t.

Synthesis of (2)6-(((1H-imidazol-2-yl)methyl)thio)-2(6)-amino-4-phenylnicotinonitrile 3 (LUF7763).

The synthetic pathway yielding the novel compound **89** (**LUF7763)** is outlined in Scheme 17. The commercial ethyl benzoyl acetate, 2-cyanoacetamide and KOH were refluxed in EtOH to give the 2,6-dihydroxy-4-phenylnicotinonitrile **206** which was chlorinated to the corresponding 2,6-dichloro-4-phenylnicotinonitrile **207** with phosphorus oxychloride in autoclave at 130 °C. Treatment of **207** with t-butyl carbamate, under Buchwald-Hartwig conditions, i.e. in presence of $Pd(OA)_2$/Xantphos, and Cs_2CO_3, in anhydrous 1,4-dioxane at 110 °C, gave the tert-butyl-(6-chloro-5-cyano-4-phenylpyridin-2-yl)-carbamate **208**. Reaction of **208** with 2-methyl-propanethiol, Cs_2CO_3 in DMF at 80 °C afforded derivative **209** which was deprotected with boiling 37% hydrochloric acid to give the intermediate 6-amino-2-mercapto-4-phenylnicotinonitrile **210**. The latter was alkylated with 2-(bromomethyl)-1H-imidazole, $NaHCO_3$, in anhydrous DMF to give the desired compound **89** (**LUF7763**).

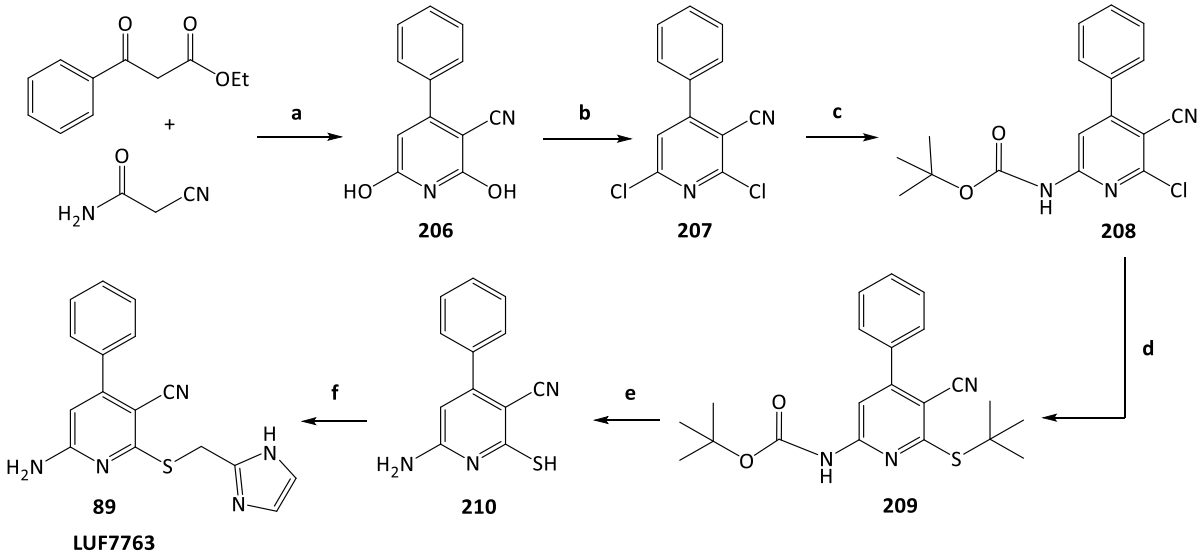

Scheme 17: **a)** NaOH, EtOH, 80 °C, reflux; **b)** $POCl_3$, in autoclave, 180 °C; **c)** $Pd(OA)_2$, xantphos, Cs_2CO_3, t-butyl carbamate, anhydrous 1,4-dioxane 40 °C; **d)** 2-Methyl-propanethiol, Cs_2CO_3, DMF, 90 °C; **e)** 37% HCl, 100 °C; **f)** 2-Bromomethyl-(1H)-imidazole, $NaHCO_3$, anhydrous DMF, r.t.

7.4 Structure affinity study

All the synthesized compounds **LUF7760 (87)**, **LUF7762 (88)** and **LUF7763 (89)** were investigated to determine their affinity at the human ARs. In particular, the affinity of these compounds for the A_1, A_{2A}, and A_3 receptors stably expressed on Chinese hamster

ovary cells (CHO) (A_1, A_3) or Human embryonic kidney 293 cells (HEK_{293}) (A_{2A}) was determined in radioligand binding studies with [^{3}H]DPCPX (K_D) 1.6 nM), [^{3}H]ZM241385 (K_D) 1.0 nM), and [^{3}H]PSB11 (17.3 nM) as radioligands, respectively.

Analyzing the binding data (Table 14), the newly synthesized **LUF7760 (87,** pK_i = 6.25**)** and **LUF7763** (**89,** pK_i = 5.99) showed a decreased binding activity at the hA_{2A} AR, in comparison with those of the reference compounds **LUF5833** (pK_i = 8.13), **LUF7724** and **LUF7740** (pK_i =7.17 and 8.00, respectively). A similar behavior can also be observed for the binding at the hA_1 subtype, indeed, both**LUF7760** (pK_i = 6.54) and **LUF7763** (pK_i = 6.95) showed lower affinity than the pyrimidine derivatives **LUF7724**, **LUF7740** (pK_i = 7.07 and pK_i = 7.16 respectively) and were much less potent than the reference ligand (**LUF5833,** pK_i = 8.54). With regard to the hA_3 AR, all the synthesized compounds were endowed with very low affinity at this receptor showing a 8-91 fold reduced binding capability than **LUF5833**. These findings suggest that, in **LUF5833,** the two cyano groups are actively involved in binding to ARs so much so that their replacement with nitrogen atoms (**LUF7724**, **LUF7760**) or their partial removal (**LUF7763, 89**) result in much lower affinities towards the targeted proteins. The only exception was represented by the pyrimidine derivative **LUF7740** which showed high affinity for the hA_{2A} AR and a pK_i value comparable with those of **LUF5833**. The absence of both the cyano moieties led to a completely lack of affinity for both the hA_1 and hA_{2A} ARs. In fact, the pyridine compound **LUF7762 (88)** was inactive at the investigated ARs (no displacement curves were performed).

Table 14. Affinities of Synthesized Ligands for the Human Adenosine Receptors[a].

Compound	hA_1 pK_i[b]	hA_{2A} pK_i[c]	hA_3 pK_i[d]
LUF5833	8.52±0.04	8.13±0.05	7.38±0.01
LUF7724	7.07±0.01	7.17±0.08	6.46±0.06
LUF7740	7.16±0.02	8.00±0.05	5.94±0.05
LUF7760	6.54±0.05	6.25±0.08	5.42±0.06
LUF7763	6.95±0.08	5.99±0.12	5.87±0.10

[a]Data are expressed as means ± SEM of three separate experiments. [b]Affinity expressed as pK_i value, determined from displacement of specific [^{3}H]DPCPX binding from the hA_1R at 25 °C incubation. [c]Affinity expressed as pK_i value, determined from displacement of specific [^{3}H]ZM241385 binding from the $hA_{2A}R$ at 25 °C incubation. [d]Affinity expressed as pK_i value, determined from displacement of specific [^{3}H]PSB11 binding from the hA_3R at 25 °C incubation.

7.5 Conclusion

To summarize, during the six months I worked at LACDR, the syntheses of new suitably substituted triazine and pyridines (**LUF7760**, **LUF7762** and **LUF7763**) structurally related to the $hA_{2A}AR$ partial agonist **LUF5833** were successfully achieved. **LUF7760** and **LUF7763** emerged as very weak ligands for the $hA_{2A}AR$ subtype while derivative **LUF7762** turned out to be completely inactive at this receptor. Molecular modeling studies are currently ongoing to rationalize these binding data and shed light on the hypothetical binding mode of these derivatives at the $hA_{2A}AR$. Moreover, with the aim to expand the SAR studies new compounds will be synthesized by introducing hydroxy or methoxy moieties at the meta or para position of the phenyl ring.

7.6 Experimental section

All solvents and reagents were purchased from commercial sources and were of analytical grade. TLC analysis was performed to monitor the reactions, using Merck silica gel F_{254} plates. Grace Davison Davisil silica column material (LC60A, 30−200 µm) was used to perform column chromatography. Microwave reactions were performed in an Emrys Optimizer (Biotage AB, formerly Personal Chemistry). ^{1}H and ^{13}C NMR spectra were recorded on a Bruker DMX-400 (400 MHz) spectrometer, using tetramethylsilane as internal standard. Chemical shifts are reported in δ (ppm) and the following abbreviations are used: br = broad, s = singlet, d = doublet, dd = doublet of doublets, dt = doublet of triplets t = triplet, m = multiplet, tt = triplet of triplets. The analytical purity of the final compounds is 95% or higher and was determined by high-performance liquid chromatography (HPLC) with a Phenomenex Gemini 3 µm C18 110A column (50 mm × 4.6 mm, 3 µm), measuring UV absorbance at 254 nm. The sample preparation and HPLC method was as follows: 0.3−0.6 mg of compound was dissolved in 1 mL of a 1:1:1 mixture of CH_3CN/H_2O/t-BuOH and eluted from the column within 15 min at a flow rate of 1.3 mL/min. The elution method was set up as follows: 1−4 min isocratic system of H_2O/CH_3CN/1% TFA in H_2O, 80:10:10; from the fourth min, a gradient was applied from 80:10:10 to 0:90:10 within 9 min, followed by 1 min of equilibration at 0:90:10 and 1 min at 80:10:10. Liquid chromatography−mass spectrometry (LC−MS) analyses were performed using a Thermo Finnigan Surveyor-LCQ Advantage Max LC−MS system and a

Gemini C18 Phenomenex column (50 mm × 4.6 mm, 3 µm). The elution method was set up as follows: 1−4 min isocratic system of H_2O/CH_3CN/1% TFA in H_2O, 80:10:10; from the fourth min, a gradient was applied from 80:10:10 to 0:90:10 within 9 min, followed by 1 min of equilibration at 0:90:10 and 1 min at 80:10:10**.** The following abbreviation are used for solvents and reactive products: AcOH = Acetic acid, $CDCl_3$ = Deuterated chloroform, DCM = Dichloromethane, DMF = Dimethylformamide, DMSO-d_6 = Deuterated dimethyl sulfoxide, EtOAc = Ethyl acetate, Et_2O = Diethyl ether, EtOH = Ethanol, HCl = Hydrochloric acid, MeOD = Deuterated methanol, MeOH = Methanol, TFA = Trifluoroacetic acid, THF = Tetrahydrofuran.

Synthesis of 2,6-Dichloro-4-phenyl-1,3,5-triazine (198)

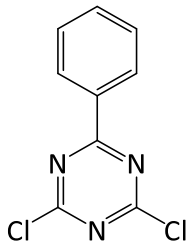

198

To a stirred suspension of cyanuric chloride (7.5 g, 40.7 mmol), in anhydrous THF (20 mL) at 0°C under nitrogen atmosphere, a 3M solution of phenylmagnesium bromide (0.993 mL, 2.98 mmol) in THF (10 mL) was added dropwise (over 30 min). The mixture was stirred at room temperature for 6h (TLC monitoring, Petroleum ether 8/EtOAc 2) then it was treated with 10 % aqueous HCl (50 mL) and extracted with EtOAc (40 mL x 3). The combined organic layers were washed with water (30 mL), dried on $MgSO_4$ and evaporated under reduced pressure to give a brown solid. The product was used for the next step without further purification. Yield 52,3 %. ^{1}H NMR (400 MHz, $CDCl_3$) 7.54 (t, J = 7.8 Hz, 2H), 7.66 (dd, 1H, J = 11.7, 4.3 Hz,), 8.51 (m, 2H). Anal. Calc. for $C_9H_5Cl_2N_3$

Synthesis of 2-amino-6-chloro-4-phenyl-1,3,5-triazine (199)

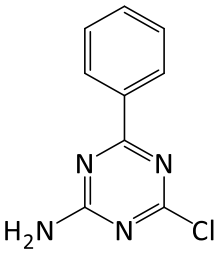

199

To a stirred solution of 2,6-dichloro-4-phenyl-triazine **198** (0.3 g, 1.327 mmol) in DCM (5 mL), 25% aqueous ammonia was added dropwise (0.09 mL, 1.327 mmol). The resulting mixture was stirred at room temperature for 8h. (TLC monitoring, Petroleum Ether 8/ AcOEt 2). The suspended solid was filtered and rinsed wit DCM (30 mL). The combined mother liquors were evaporated under pressure to afford a pale orange solid (180 mg). The compound has been used in the next reaction without further purification. Yield 65.6%. ^{1}H NMR (400 MHz, $CDCl_3$) 5.75 (br s, 2H, NH_2), 7.51 (t, 2H, ar, J = 7.6 Hz), 7.61 (t, 1H, ar, J = 7.3 Hz), 8.43 (d, 2H, ar, J = 7.5 Hz). LC-MS (ESI): 207.1 $[M + H]^+$. Anal. Calc. for $C_9H_7ClN_4$.

Synthesis of 4-amino-6-phenyl-1,3,5-triazine-2-thiol (200)

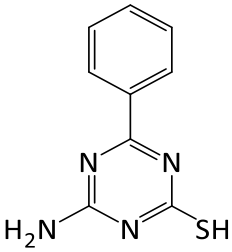

200

A suspension of 4-amino-6-phenyl-2-phenylthio-1,3,5-triazine **199** (0.68 g, 3.29 mmol), and sodium sulfide monohydrate (1.185 g, 4.93 mmol) in DMF (3 mL) was heated at 80 °C for 3h (TLC monitoring, EtOAc 8/Petroleum ether 2). The solvent was eliminated under reduced pressure (water bath 80 °C) and the residue was treated carefully with HCl 1M solution in EtOAc (10 mL). The resulting solid was collected by filtration and extracted with boiling EtOH (20 mL x 5). The collected organic layers were evaporated at reduced pressure to afford a pale yellow solid (240 mg) which was purified by recrystallization. Yield 28 %. (DCM) ^{1}H NMR (400 MHz, DMSO-d_6) 7.53 (m, 2H, ar), 7.60 (m, 1H, ar), 8.24 (m, 2H, ar), 12.83 (s, 1H, SH). LC-MS (ESI): 205.1 $[M + H]^+$. Anal. Calc. for $C_9H_8N_4S$.

Synthesis of 4-(((1H-imidazol-2-yl)methyl)thio)-6-phenyl-1,3,5-triazin-2-amine (87) LUF7760.

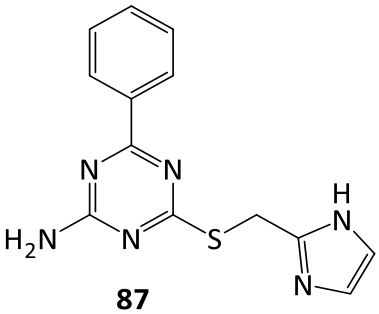

87

LUF7760

A suspension of 4-amino-6-phenyl-1,3,5-triazine-2-thiol **200** (0.148 g, 0.725 mmol), $NaHCO_3$ (0.061 g, 0.725 mmol) and 2-(bromomethyl)-1H-imidazole (0.263 g, 1.087 mmol) in DMF (1.5 mL) was stirred at room temperature for 3 h (TLC monitoring DCM 9/ MeOH 1). Then the solvent was evaporated under reduced pressure (water bath 60 °C) and the resulting residue was treated with water (15 mL) and extracted with EtOAc (30 mL x 4). The combined organic layers were dried on $MgSO_4$ and evaporated to afford a pale brown oil. (93 mg). Purification of the crude product by recrystallization afforded the pure compound as a white solid (7 mg). Yield 3 %. (Petroleum ether/MeOH). ^{1}H NMR (400 MHz, MeOD) 4.49 (s, 2H, CH_2), 6.97 (br s, 2H, imidazole protons), 7.45 (t, 2H, ar, J= 8.0 Hz), 7.53 (tt, 1H, ar, J = 7.6, 1.2 Hz), 8.34 (d, 2H, ar, J = 8.0 Hz). HPLC: 97,2 %, RT 4.56 min, LC-MS (ESI): 285.1 $[M + H]^+$ Anal. Calc. for $C_{13}H_{12}N_6S$.

Synthesis of 2,6-dichloro-4-phenylpyridine (201)

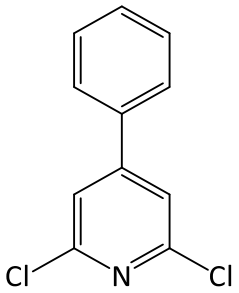

201

A suspension of 2,6-dichlo-4-iodopyridine (1 g, 3.65 mmol), Na_2CO_3 (1.16 g, 10.95 mmol), phenylboronic acid pinacol esther (0.745 g, 3.65 mmol) and $Pd(PPh_3)_2Cl_2$ (0.128 g, 0.183 mmol) in a mixture of acetonitrile (12 mL) and water (8 mL) under N_2 atmosphere was heated at 70 °C for 16 h (TLC monitoring, Petroleum ether 9.8/EtOAc 0.2). The obtained mixture was diluted with EtOAc (50 mL) and washed with brine (30 mL x 3). The organic layer was dried on $MgSO_4$ and evaporated under reduced pressure to afford a brown oil which was purified by column chromatography (Petroleum ether 9.8/EtOAc 0.2). Yield 92 %. ^{1}H NMR (400 MHz, $CDCl_3$) 7.50 (s, 2H, pyridine protons), 7.52-7.55 (m, 3H, ar), 7.60-7.63 (m, 2H, ar). Anal. Calc. for $C_{11}H_7Cl_2N$.

Synthesis of 2-(tert-butylthio)-6-chloro-4-phenylpyridine (202)

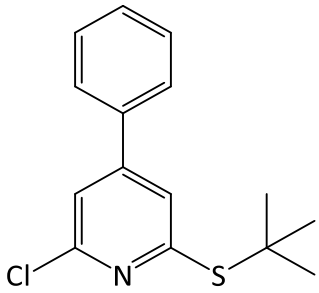

202

A suspension of 2,6-dichloro-4-phenylpyridine (0.2 g, 0.89 mmol), Cs_2CO_3 (0.58 g, 1.78 mmol), and 2-methyl-propanethiol (0.0846 mg, 0.93 mmol) in DMF was heated at 80 °C overnight (TLC monitoring, Petroleum ether 9/EtOAc 1 and HPLC). The mixture was diluted with EtOAc (50 mL) and washed with brine (30 mL x 5). The organic phase was dried on $MgSO_4$ and evaporated to afford a pale yellow oil (249 mg) which was used for the next step without purification. Quantitative yield. ^{1}H NMR (400 MHz, $CDCl_3$) 1.62 (s, 9H, $(CH_3)_3$), 7.30 (d, 1H, pyridine proton, J = 1.3 Hz), 7.40 (d, 1H, pyridine proton, J = 1.3

Hz), 7.46 -7.54 (m, 3H, ar), 7.58-7.61 (m, 2H, ar). LC-MS (ESI): 277.9 [M + H] $^{+}$. Anal. Calc. for $C_{15}H_{16}ClNS$.

Synthesis of Tert-butyl-(6-(tert-butylthio)-4-phenylpyridin-2-yl)-carbamate (203)

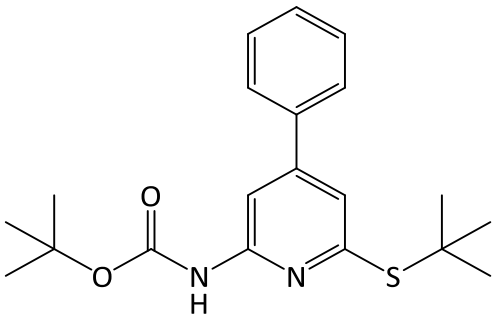

203

A suspension of 2-(tert-butylthio)-6-chloro-4-phenylpyridine **202** (0.23 g, 0.83 mmol), Cs_2CO_3 (0.54 g, 1.66 mmol), Xantphos (0,144 g, 0,25 mmol), $Pd(OAc)_2$ (0,028 g, 0,124 mmol), t-butylcarbamate (0,097 g, 0,83 mmol) in anhydrous 1,4-Dioxane (2,8 mL) under N_2 atmosphere was heated at 110 °C overnight. The reaction progress was monitored by TLC (Petroleum ether 9.8/AcOEt 0.2) and HPLC. The mixture was treated with boiling acetone (25 mL) and filtered. The organic layer was evaporated to afford a red oil (478 mg) which was purified by liquid chromatography (Petroleum ether 9.8/AcOEt 0.2). (80 mg of a yellow solid). Yield 26.9 %. ^{1}H NMR (400 MHz, DMSO-d_6) 1.51 (s, 9H, $(CH_3)_3$), 1.55 (s, 9H, $(CH_3)_3$), 7.17 (d, 1H, pyridine proton, J = 1.3 Hz), 7.46–7.54 (m, 3H, ar), 7.67-7.69 (m, 2H, ar), 7.86 (d, 1H, pyridine proton, J = 1.3 Hz), 9.97 (br s, 1H, NH). LC-MS (ESI): 358.9 [M + H] $^{+}$. Anal. Calc. for $C_{20}H_{26}N_2O_2S$.

Synthesis of 6-(tert-butylthio)-4-phenylpyridin-2-amine (204)

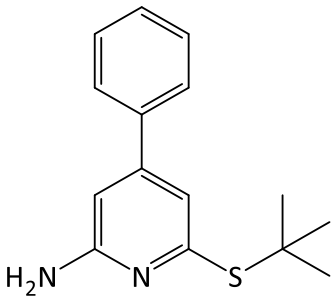

204

To a solution of tert-butyl (6-(tert-butylthio)-4-phenylpyridin-2-yl)-carbamate **203** (0.25 g, 0.697 mmol) in DCM (5 mL) TFA (0,266 mL, 3,48 mmol) was added. The mixture was

refluxed overnight (TLC monitoring, DCM 9.4/MeOH 0.6 and HPLC). The mixture was diluted with EtOAc (50 mL) and washed with water (25 mL x 4). The organic phase was dried on $MgSO_4$ and evaporated to afford a brown oil. The crude compound was purified by liquid chromatography (Petroleum ether 5/EtOAc 5) to yield a pale yellow oil (135 mg). Yield 75%. ^{1}H NMR (400 MHz, DMSO-d_6) 1.47 (s, 9H, $C(CH_3)_3$), 6.78 (s, 1H, pyridine proton), 6.96 (s, 1H, pyridine proton), 7.51-7.54 (m, 3H, ar), 7.68 (d, 2H, ar, J = 6.4 Hz). LC-MS (ESI): 259.0 $[M + H]^+$. Anal. Calc. for $C_{15}H_{18}N_2S$.

Synthesis of 6-amino-4-phenylpyridine-2-thiol (205)

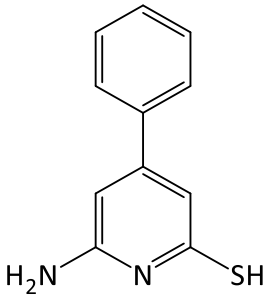

205

A stirred solution of 6-(tert-butylthio)-4-phenylpyridin-2-amine **204** (0.445 g, 1.722 mmol) in 37 % HCl (15 mL) was heated at 100 °C for 10 h (HPLC monitoring). The mixture was cooled to 0 °C and carefully neutralized to pH = 7 with $NaHCO_3$ saturated solution. The resulting solution was extracted with EtOAc (40 mL x 5). The combined organic phases were dried on $MgSO_4$ and evaporated to afford 135 mg of orange solid. The compound was used for the next reaction without further purification. Yield 39 %.^{1}H NMR (400 MHz, DMSO-d_6) 6.42 (s, 1H, pyridine proton), 6.87 (s, 1H, pyridine proton), 7.47-7.48 (m, 3H, ar), 7.57-7.59 (m, 2H, ar), 12.07 (br s, 1H, SH). LC-MS (ESI): 203.1 $[M + H]^+$. Anal. Calc. for $C_{11}H_{10}N_2S$.

Synthesis of 6-(((1H-imidazol-2-yl)methyl)thio)-4-phenylpyridin-2-amine (88) LUF7762

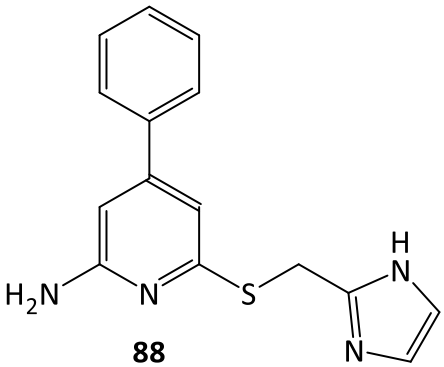

88

LUF7762

To a suspension of 6-amino-4-phenylpyridine-2-thiol (0.145 g, 0.716 mmol) and $NaHCO_3$ (0.0602 g, 0,57 mmol) in anhydrous DMF (2 mL) was added bromo-methyl-(1H)-imidazole (0.225 g, 0.931 mmol). The mixture was stirred at room temperature for 23 h (HPLC monitoring). The solvent was evaporated under reduced pressure (water bath, 70 °C). The resulting residue was treated with water (20 mL) and extracted with EtOAc (30 mL x 4). The organic phase was dried on $MgSO_4$ and evaporated to afford 282 mg of an orange oil. The compound was purified by liquid chromatography (DCM 9/MeOH 1). Yield 33 %. ^{1}H NMR (400 MHz, MeOD) 4.39 (s, 2H, CH_2), 6.50 (d, 1H, pyridine proton, J = 1.2 Hz), 6.70 (d, 1H, pyridine proton, J = 1.2 Hz), 6.94 (s, 2H, imidazole protons), 7.32-7.46 (m, 3H, ar), 7.54 (dd, 2H, ar, J = 8.0, 1.4 Hz). HPLC: 96,52 %, RT 4.30 min, LC-MS (ESI): 283.1 $[M + H]^+$. Anal. Calc. for $C_{15}H_{14}N_4S$.

Synthesis of 2,6-dihydroxy-4-phenylnicotinonitrile (206)[457]

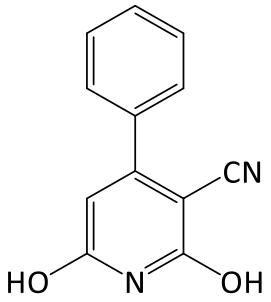

206

A suspension of ethyl benzoyl acetate (3 g, 15.6 mmol), 2-cyanoacetamide (1.31 g, 15.6 mmol) and KOH (0.96 g, 15.6 mmol) in EtOH (20 mL) was refluxed for 24 h (TLC monitoring, DCM 8/MeOH 2). The mixture was cooled to 0°C. The resulting solid was collected by

filtration and then dissolved in warm water (60 mL/60 °C). The alkaline solution was carefully treated with 37% HCl solution to pH = 1. The precipitate was collected by filtration and dried (1.3 g). Yield 33.6 %. ^{1}H NMR (400 MHz, DMSO-d_6) 5.81 (s, 1H, nicotinonitrile proton), 7.53 (s, 5H, ar). LC-MS (ESI): 213.1 [M + H] $^+$. Anal. Calc. for $C_{12}H_8N_2O_2$.

Synthesis of 2,6-dichloro-4-phenylnicotinonitrile (207)

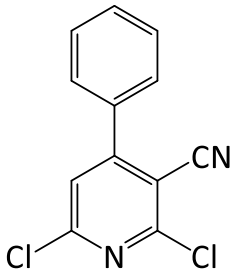

207

A suspension of 2,6-dihydroxy-4-phenylnicotinonitrile **206** (1.2 g, 5.657 mmol) in $POCl_3$ (5.3 mL, 56.6 mmol) was heated at 180 °C in autoclave for 16 h (HPLC monitoring). The mixture was cooled to 0 °C and treated with crushed ice. The suspended solid was collected by filtration, rinsed with Petroleum ether (30 mL) and dried (990 mg). The product has been used for the next step without further purification. Yield 70 %. ^{1}H NMR (400 MHz, $CDCl_3$) 7.47 (s, 1H, nicotinonitrile proton), δ 7.60–7.63 (m, 5H, ar). $^+$. Anal. Calc. for $C_{12}H_6Cl_2N_2$.

Synthesis of tert-butyl-(6-chloro-5-cyano-4-phenylpyridin-2-yl)-carbamate (208)

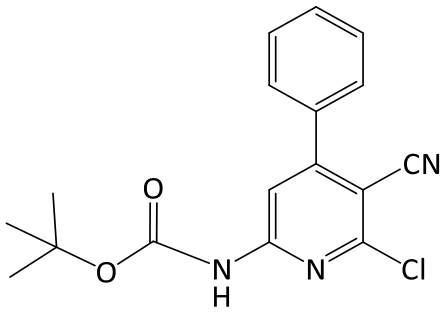

208

To a suspension of 2,6-dichloro-4-phenylnicotinonitrile **207** (0.2 g, 0.806 mmol), t-butylcarbamate (0.0944 g, 0.806 mmol), Cs_2CO_3 (0.54 g, 1.66 mmol) and Xantphos (0.139 g, 0.242 mmol) in anhydrous 1,4-dioxane (2.7 mL) under N_2 atmosphere was added

$Pd(OAc)_2$ (0.027 g, 0.121 mmol). The mixture was heated at 40 °C for 23 h (TLC monitoring, Petroleum ether 9.8/EtOAc 0.2). The mixture was treated with boiling acetone (25 mL) and filtered. The collected organic layer was evaporated to afford 90 mg of a pale brown solid. The product was used for the next reaction without further purification. Yield 33%. ^{1}H NMR (300 MHz, $CDCl_3$) 1.55 (s, 9H, $C(CH_3)_3$), 7. 50 (br s, 1H, NH), 7.52-7.55 (m 3H, ar), 7.62 – 7.65 (m, 2H, ar), 8.09 (s, 1H, 5-cyano-pyridine proton). LC-MS (ESI): 329.92 $[M + H]^+$. Anal. Calc. for $C_{17}H_{16}ClN_3O_2$.

Synthesis of tert-butyl (6-(tert-butylthio)-5-cyano-4-phenylpyridin-2-yl)-carbamate (209)

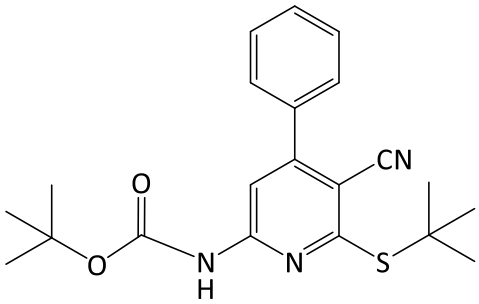

209

A suspension of tert-butyl (6-chloro-5-cyano-4-phenylpyridin-2-yl)-carbamate **208** (0.09 g, 0.273 mmol), 2-methyl-propanethiol (0.03 mL, 0.273 mmol) and Cs_2CO_3 (0.546 mmol) in DMF (2 mL) was heated at 90 °C for 20 h (HPLC monitoring). The mixture was cooled to room temperature, diluted with EtOAc (50 mL) and washed with brine (25 mL x 5). The organic layer was dried on $MgSO_4$ and evaporated to afford an orange oil (93 mg). The compound was used for the next reaction without further purification. Yield: 89 %. ^{1}H NMR (400 MHz, $CDCl_3$) 1.56 (s, 9H, $(CH_3)_3$), 1.67 (s, 9H, $(CH_3)_3$), 7.34 (br s, 1H, NH), 7.46–7.50 (m, 3H, ar), 7.58–7.61 (m, 2H, ar), 7.82 (s, 1H, 5-cyano-pyridine proton). LC-MS (ESI): 384.00 $[M + H]^+$. Anal. Calc. for $C_{21}H_{25}N_3O_2S$.

Synthesis of 6-amino-2-mercapto-4-phenylnicotinonitrile (210).

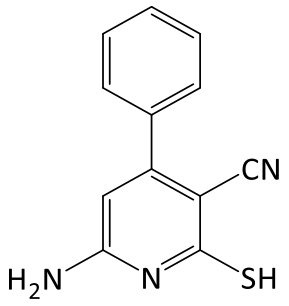

210

A suspension of tert-butyl (6-(tert-butylthio)-5-cyano-4-phenylpyridin-2-yl)-carbamate **209** (0.7 g, 1.825 mmol) in 37% HCl (7 mL) was heated at 100 °C for 2 h (HPLC monitoring). The mixture was cooled to room temperature and diluted with $NaHCO_3$ saturated solution (7 mL). The resulting suspension carefully treated with solid $NaHCO_3$ to pH = 7 and extracted with EtOAc (30 mL x 5). The combined organic phases were dried on $MgSO_4$ and evaporated to afford an orange solid which was purified by column chromatography (Petroleum ether 6/EtOAc 4) and (DCM 9/MeOH 1). Pale yellow solid (156 mg). Yield 37%.^{1}H NMR (300 MHz, MeOD) 6.07 (s, 1H, 5-cyano-pyridine proton), 7.51-7.57 (m, 5H, ar). LC-MS (ESI): 228.08 $[M + H]^+$. Anal. Calc. for $C_{12}H_9N_3S$.

Synthesis of 2-(((1H-imidazol-2-yl)methyl)thio)-6-amino-4-phenylnicotinonitrile (89) (LUF7763)

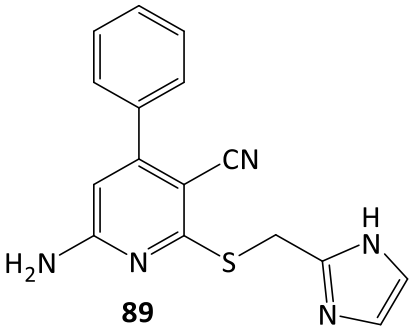

89

LUF7763

A suspension 6-amino-2-mercapto-4-phenylnicotinonitrile **210** (0.096 g, 0.422 mmol), $NaHCO_3$ (0.0202 g, 0.422 mmol), bromo-methyl-(1H)-imidazole (0.153 g, 0.633 mmol) in anhydrous DMF (2,5 mL) was stirred at room temperature for 4 h (TLC monitoring, DCM 9 /MeOH 1). The solvent was evaporated under reduced pressure (water bath 70 °C). The resulting residue was treated with water (10 mL) and extracted with EtOAc (30 mL x 5).

The organic layer was dried on $MgSO_4$ and evaporated to afford a pale brown oil (116 mg). First, the crude product was purified by column chromatography (Petroleum ether 1/ AcOEt 7.8/MeOH 1.2) and then recrystallized (Et_2O/MeOH) to give a yellow solid (10 mg). Yield 7.7 %. ^{1}H NMR (400 MHz, MeOD) 4.53 (s, 2H, CH_2), 6.28 (s, 1H, nicotinonitrile proton), 6.97 (s, 2H, imidazole protons) 7.48 (dt, 5H, ar, J = 6.8, 4.0 Hz). HPLC: 98,2 %, RT 5.52 min, LC-MS (ESI): 308.1 $[M + H]^+$. Anal. Calc. for $C_{16}H_{13}N_5S$.

7.7 Materials and method

7.7.1 Chemicals and Reagents

Chinese hamster ovary cells stably expressing the human adenosine A_1 receptor ($CHOhA_1R$) were kindly provided by Prof. Steve hill (University of Nottingham, UK); Human embryonic kidney 293 cells stably expressing the human adenosine A_{2A} receptor ($HEK_{293}hA_{2A}R$) were kindly provided by Dr. J Wang (Biogen/IDEC, Cambridge, MA); Chinese hamster ovary (CHO) cells stably expressing the human adenosine A_3 receptor ($CHOhA_3$) were a gift from Dr. K-N Klotz (University of Würzburg, Germany). [^{3}H]-1,3-dipropyl-8-cyclopentyl-xanthine([^{3}H]DPCPX, specific activity 120 Ci/mmol) was purchased from ARC. (St.Louis, USA); [^{3}H 4-(-2-[7-amino-2-{2-furyl}{1,2,4}triazolo{2,3-a} {1,3,5}triazin-5-yl-amino]ethyl) phenol ([^{3}H]- ZM241385, specific activity 50 Ci/mmol) was purchased from ARC, Inc. (St. Louis, MO); [^{3}H]8-Ethyl-4-methyl-2-phenyl-(8R)-4,5,7,8-tetrahydro-1H-imidazo[2,1-i]-purin-5-one ([^{3}H]PSB-11, specific activity 56 Ci/mmol) was obtained with the kind help of Prof. C.E. Müller (University of Bonn, Germany). 5'-N-ethylcarboxamidoadenosine (NECA), N^6-Cyclopentyladenosine (CPA) and Adenosine deaminase (ADA) were purchased from Sigma-Aldrich (Steinheim, Germany). Pierce Bicinchoninic acid (BCA) protein assay reagents were obtained from Pierce Chemical Company (Rockford, IL, USA). All other chemicals were of analytical grade and obtained from standard commercial sources.

7.7.2 Cell Culture and Membrane Preparation

$CHOhA_1R$ and $CHOhA_3R$ were Dulbecco's Modified Eagles Medium (DMEM) and Ham's F12 medium (1:1) supplemented with 10% (v/v) 10% newborn calf serum, 50 $\mu g.mL^{-1}$

streptomycin, 50 IU.mL^{-1} penicillin, and 200 µg.mL^{-1} G418 at 37 °C and 5% CO_2. CHOhA$_1$R cells were subcultured twice a week at a ratio of 1:20 on 10 cm Ø plates and 15 cm Ø plates. CHOhA$_3$ cells were subcultured twice a week at a ratio of 1:8 on 10 cm Ø plates and 15 cm Ø plates. HEK$_{293}$hA$_{2A}$R cells were grown in culture medium consisting of Dulbecco's Modified Eagles Medium (DMEM) supplemented with 10% newborn calf serum, 50 µg.mL^{-1} streptomycin, 50 IU.mL^{-1} penicillin, and 500 µg.mL^{-1} G418 at 37 °C and 7% CO_2. Cells were subcultured twice a week at a ratio of 1:8 on 10 cm Ø plates and 15 cm Ø plates. All cells were grown to 80-90% confluency and detached from plates by scraping them into 5 mL PBS. Detached cells were collected and centrifuged at 0.2 x g for 5 min. Pellets derived from 100 15 cm Ø plates were pooled and resuspended in 70 mL of Ice-cold 50 mM Tris-HCl buffer, pH = 7.4. A Heidolph Diax 900 homogenizer was used to homogenize the cell suspension. Membranes and the cytosolic fraction were separated by centrifugation at 100 000x *g* in a Beckman Optima LE-80 K ultracentrifuge (Beckman Coulter, Fullerton, CA) at 4 °C for 20 min. The pellet was resuspended in 35 mL of the Tris-HCl buffer, and the homogenization and centrifugation steps were repeated. Tris-HCl buffer (25 mL) was used to resuspend the pellet, and ADA was added (0.8 U/mL) to break down endogenous adenosine. Membranes were stored in 250 µL and 500 µL aliquots at 80 °C. Total protein concentrations were measured using the BCA method[458]

7.7.3 Radioligand Displacement Assay

Membrane aliquots containing 5 µg (CHOhA$_1$R), or 30 µg (HEK$_{293}$hA$_{2A}$R) or 15 µg (CHOhA$_3$R) were incubated in a total volume of 100 µL assay buffer (50 mM Tris-HCl, pH = 7.4) for CHOhA$_1$R and HEK$_{293}$hA$_{2A}$R; and assay buffer (50 mM Tris-HCl, pH = 8.0, supplemented with 10 mM $MgCl_2$, 1 mM EDTA and 0.01% (w/v) CHAPS) for CHOhA$_3$R at 25 °C for 1 h (CHOhA$_1$R and HEK$_{293}$hA$_{2A}$R) and 2 h (CHOhA$_3$R). Radioligand displacement experiments were performed using 6 concentrations of competing ligand in the presence of 1.6nM [^{3}H]DPCPX for CHOhA$_1$R, 5.5 nM [^{3}H]ZM241385 for HEK$_{293}$hA$_{2A}$R and 10 nM [^{3}H]PSB11 for CHOhA$_3$R**.** At these concentrations total radioligand binding did not exceed 10% of that added to prevent ligand depletion. Nonspecific binding was determined in the presence of 100 µM CPA for CHOhA$_1$R, 100 µM NECA for CHOhA$_1$R and CHOhA$_3$R. Incubations were terminated by rapid vacuum filtration to separate the bound and free

radioligand through prewetted 96-well GF/B filter plates using a PerkinElmer Filtermate-harvester (Perkin Elmer, Groningen, the Netherlands). Filters were subsequently washed 12 times with ice-cold wash buffer (50 mM Tris-HCl, pH = 7.4) for $CHOhA_1R$ and $HEK_{293}hA_{2A}R$; and wash buffer for $CHOhA_3R$ (50 mM Tris-HCl supplemented with 10 mM $MgCl_2$, 1mM EDTA, pH = 8.0). The plates were dried at 55 ^oC after which Microscint^{TM}-20 cocktail was added (Perkin Elmer, Groningen, The Netherlands). After 3 h the filter-bound radioactivity was determined by scintillation spectrometry using a 2450 MicroBeta Microplate Counter (Perkin Elmer, Groningen, The Netherlands).

7.7.4 Data analysis

All experimental data was analyzed by using GraphPad Prism 7.0 (GraphPad Software Inc., San Diego, CA). IC_{50} values obtained from competition displacement binding data were converted into K_i values using the Cheng-Prusoff equation[459]. The K_D value of [^{3}H]DPCPX at $CHOhA_1R$ membrane was taken from Kourounakis, A. et al. Biochem. Pharmacol. G1 (2001) 137-144. The K_D value (1.0 nM) of [^{3}H]ZM241385 at $hA_{2A}R$ membranes and the K_D value (17.3nM) of [^{3}H]PSB11 at $CHOhA_3R$ membranes were taken from in-house determination.

8. ACRONYMS AND ABBREVIATIONS

The following acronyms and abbreviations are used for the NMR spectra:

ar = Aromatic protons

br = Broad

d = Doublet

dd = Doublet of doublets

dt = Doublet of triplets

m = Multiplet

q = Quartet

s = Singlet

t = Triplet

tt = Triplet of triplets

The following acronyms and abbreviations are used for solvents and chemical reagents:

AcOH = Acetic acid

$CDCl_3$ = Deuterated chloroform

DIPEA = N,N-Diisopropylethylamine

DCM = Dichloromethane

DMF = Dimethylformamide

DMSO-d_6 = Deuterated dimethyl sulfoxide

EDCI.HCl = *N*-(3-Dimethylaminopropyl)-*N*'-ethylcarbodiimide hydrochloride

EDTA = Ethylenediaminetetraacetic acid

EtOAc = Ethyl acetate

Et_2O = Diethyl ether

EtOH = Ethanol

HCl = Hydrochloric acid

HOBt = Hydroxybenzotriazole

MeOH = Methanol

MeOD = Deuterated methanol

TFA = Trifluoroacetic acid

THF = Tetrahydrofuran

t-BuOH = *Tert*-butanol

Other acronyms and abbreviations:

ADP = Adenosine diphosphate

AMP = Adenosine monophosphate

cAMP = Cyclic adenosine monophosphate

ATP = Adenosine triphosphate

EC_{50} = Half maximal effective concentration

g = Gram

mg = Milligram

µg = Micrograms

HPLC = high-performance liquid chromatography

Hz = Hertz

IC_{50} = Half maximal inhibitory concentration

IR = Infrared radiation

IU = International Unit

LC-MS = Liquid chromatography–mass spectrometry

mL = Milliliter

µL = Microliter

mM = Millimolar

µM = Micromolar

nM = Nanomolar

m.p. = Melting point

mw = Microwave

NMR = Nuclear magnetic resonance

PBS = Phosphate-buffered saline

ppm = Parts per million

r.t. = Room temperature

TLC = Thin layer chromatography

9.REFERENCES

1.Yacoubian, Y.A. Neurodegenerative disorders: why do we need new therapies? *Drug Discovery Approaches for the Treatment of Neurodegenerative Disorders.* **2017.**

2.Stockwell, J., et al. Adenosine A_1 and A_{2A} Receptors in the Brain: Current Research and Their Role in Neurodegeneration. *Molec.* **2017**, 22, 676.

3. Drury, A.N., et al. The physiological activity of adenine compounds with special reference to their action upon the mammalian heart. *J. Physiol.* **1929**, 68, 213–237.

4. Belhassen, B., et al. Electrophysiologic effects of adenosine triphosphate and adenosine on the mammalian heart: clinical and experimental aspects. *J. Am. Coll. Cardiol.* **1984,** 4, 414–424.

5. Delacrétaz, E., et al. Clinical practice. Supraventricular tachycardia. *N. Engl. J. Med.* **2006**, 354, 1039–1051

6. Fredholm, B.B., et al. International Union of Pharmacology. XXV. Nomenclature and classification of adenosine receptors. *Pharmacol. Rev.* **2001,** 53, 527–552.

7. Fredholm, B.B., et al. International Union of Basic and Clinical Pharmacology. LXXXI. Nomenclature and classification of adenosine receptors — an update. *Pharmacol. Rev.* **2011**, 63, 1–34.

8. Eltzschig, H.K., et al. Purinergic signaling during inflammation. *N. Engl. J. Med.* **2012,** 367, 2322–2333.

9. Eltzschig, H.K., et al. Adenosine: an old drug newly discovered. *Anesthesiology.* **2009,** 111, 904–915.

10 Johansson, S. M., et al. Eliminating the antilipolytic adenosine A_1 receptor does not lead to compensator changes in the antilipolytic actions of PGE2 and nicotinic acid. *Acta. Physiol.* **2007**, 190, 87–96.

11. Grenz, A. et al. Equilibrative nucleoside transporter 1 (ENT1) regulates postischemic blood flow during acute kidney injury in mice. *J. Clin. Invest.* **2012,** 122, 693–710.

12. Sun, D., et al. Mediation of tubuloglomerular feedback by adenosine: evidence from mice lacking adenosine 1 receptors. *Proc. Natl. Acad. Sci.* **2001,** 98, 9983–9988.

13. Rosenberger, P. et al. Hypoxia-inducible factor-dependent induction of netrin-1 dampens inflammation caused by hypoxia. *Nature. Immunol.* **2009,** 10, 195–202.

14. Huang, Z. L. et al. Adenosine A_{2A}, but not A_1, receptors mediate the arousal effect of caffeine. *Nature Neurosci.* **2005,** 8, 858–859.

15. Lazarus, M. et al. Arousal effect of caffeine depends on adenosine A_{2A} receptors in the shell of the nucleus accumbens. *J. Neurosci.* **2011,** 31, 10067–10075.

16. Liu, X. L. *et al.* Genetic inactivation of the adenosine A_{2A} receptor attenuates pathologic but not developmental angiogenesis in the mouse retina. *Invest. Ophthalmol. Vis. Sci.* **2010**, 51, 6625–6632.

17. **Hasko, G., et al**. Adenosine receptors: therapeutic aspects for inflammatory and immune diseases. *Nature Rev. Drug Discov.* **2008,** 7, 759–770.

18. Eltzschig, H. K., et al. Hypoxia and inflammation. *N. Engl. J. Med.* **2011,** 364, 656–665.

19. Eltzschig, H. K., et al. Ischemia and reperfusion — from mechanism to translation. *Nature Med.* **2011,** 17, 1391–1401.

20. Fredholm, B. B., et al. Adenosine, an endogenous distress signal, modulates tissue damage and repair. *Cell Death Differ.* **2007,** 14, 1315–1323.

21.Borea, P.A., et al. Pharmacology of adenosine receptors: the state of art. *Physiol. Rev.* **2018,** 98, 1591-1625.

22. **MacDonald, P., et al.** Release of small transmitters through kiss-and-run fusion pores in rat pancreatic β cells. *Cell Metab.* **2006,** 4, 283–290.

23. Zhang, Z., *et al.* Regulated ATP release from astrocytes through lysosome exocytosis. *Nature Cell Biol.* **2007,** 9, 945–953.

24. Chekeni, F. B., *et al.* Pannexin 1 channels mediate 'find-me' signal release and membrane permeability during apoptosis. *Nature.* **2010,** 467, 863–867.

25. Elliott, M., R. *et al.* Nucleotides released by apoptotic cells act as a find-me signal to promote phagocytic clearance. *Nature.* **2009,** 461, 282–286.

26. Anselmi, F., *et al.* ATP release through connexin hemichannels and gap junction transfer of second messengers propagate Ca^{2+} signals across the inner ear. *Proc. Natl. Acad. Sci.* **2008,** 105, 18770–18775.

27. Kanneganti, T. D., *et al.* Pannexin-1-mediated recognition of bacterial molecules activates the cryopyrin inflammasome independent of Toll-like receptor signaling. *Immunity.* **2007,** 26, 433–443.

28. Faigle, M., et al. ATP release from vascular endotheliaoccurs across Cx43 hemichannels and is attenuated during hypoxia. *PLoS ONE* 3, e2801 (2008).

29. Chen, JF., et al. Adenosine receptors as drug targets–what are the challenges? *Nat. Rev. Drug. Discov.* **2013,** 12, 265–286.

30. Deussen, A., et al. Metabolic flux rates of adenosine in the heart. *Naunyn. Schmiedebergs. Arch. Pharmacol.* **2000,** 362, 351–363.

31. Deussen, A., et al. Formation and salvage of adenosine by macrovascular endothelial cells. *Am. J. Physiol. Heart Circ Physiol.* **1993,** 264, H692–H700.

32 Deussen, A., et al. Quantification of extracellular and intracellular adenosine production: understanding the transmembranous concentration gradient. *Circulation.* **1999,** 99, 2041–2047.

33. Antonioli, L., et al. Immunity, inflammation and cancer: a leading role for adenosine. *Nat. rev. canc*. **2013**, 13, 842-857.

34. Peleli, M., et al. Pharmacological targeting of adenosine receptor signaling. *Mol Aspects Med.* **2017,** 55, 4–8.

35. Fredholm, B.B., et al. International Union of Pharmacology. XXV. Nomenclature and classification of adenosine receptors. *Pharmacol. Rev.* **2001,** 53, 527–552.

36. Fredholm, B.B., et al. Structure and function of adenosine receptors and their genes. *Naunyn Schmiedebergs Arch. Pharmacol.* **2000,** 362, 364–374.

37. Klotz K.N. Adenosine Receptors and Their Ligands. *Naunyn. Schmiedebergs. Arch. Pharmacol.* **2000**, 362, 382–391.

38. Van Calker D., et al. Adenosine regulates, via two different types ofreceptors, the accumulation of cyclic AMP in cultured brain cells.,33,. *J. Neurochem.* **1979**, 33, 999-1005.

39. Londos C., et al. Subclasses of external adenosine receptors. *Biochem.* **1979**, 77, 2551-2554.

40. Daly J.W., et al. Subclasses of adenosine receptors in the central nervous system: interaction with caffeine and related methylxanthines. *Cell. Mol. Neurobiol.* **1983**, 3, 69-80.

41. Zhou Q.Y., et al. Molecular cloning and characterization of an adenosine receptor: the A_3 adenosine receptor. *Proc. Natl. Acad. Sci. USA.* **1992**, 89, 7432-7436.

42. Brugarolas, M., et al. G-protein-coupled receptor heteromers as key players in the molecular architecture of the central nervous system. *CNS. Neurosci. Ther.* **2014,** 20, 703–709.

43. Ferré, S., et al. Adenosine-cannabinoid receptor interactions. Implications for striatal function. *Br. J. Pharmacol.* **2010,** 16, 443–453.

44. Ferré, S., et al. G protein-coupled receptor heteromers as new targets for drug development. *Prog Mol Biol Transl Sci.* **2010,** 91, 41–52.

45. Navarro, G., et al. Quaternary structure of a G-protein-coupled receptor heterotetramer in complex with Gi and Gs. *BMC Biol.* 14, 26, 2016,

46. Navarro, G., et al. Interactions between intracellular domains as key determinants of the quaternary structure and function of receptor heteromers. *J Biol Chem.* **2010,** 285, 27346–27359.

47. Navarro, G., et al. Direct involvement of sigma-1 receptors in the dopamine D_1 receptor-mediated effects of cocaine. *Proc Natl Acad Sci USA.* **2010,** 107, 18676–18681.

48. Cristóvão-Ferreira, S., et al.. A_1R-$A_{2A}R$ heteromers coupled to Gs and $G_{i/0}$ proteins modulate GABA transport into astrocytes. *Purinergic Signal.* **2013,** 9, 433–449.

49. Hill, S.J., et al. Allosteric interactions at adenosine $A(_1)$ and $A(_3)$ receptors: new insights into the role of small molecules and receptor dimerization. *Br. J. Pharmacol.* **2014,** 171, 1102–1113.

50. Kim, S-K., et al. Computational prediction of homodimerization of the A_3 adenosine receptor. *J Mol. Graph. Model.* **2006,** 25, 549–561.

51 Fuxe, K., et al. Adenosine A_{2A} and dopamine D_2 heteromeric receptor complexes and their function. *J Mol Neurosci.* **2005,** 26, 209–220.

52. Fuxe, K., et al. Adenosine receptor-dopamine receptor interactions in the basal ganglia and their relevance for brain function. *Physiol. Behav.* **2007,** 92, 210–217.

5**3. Navarro, G., et al**. Purinergic signaling in Parkinson's disease. Relevance for treatment. *Neuropharmacology.* **2016,** 104, 161–168.

54. **Gessi, S., et al**. Adenosine receptor targeting in health and disease. *Expert. Opin. Investig. Drugs.* **2011,** 20, 1591–1609,

55. Sawynok, J., et al. Adenosine receptor targets for pain. *Neuroscience.* **2016,** 338, 1–18.

56. Stenberg, D., et al. Sleep and its homeostatic regulation in mice lacking the adenosine A_1 receptor. *J. Sleep Res.* **2003,** 12, 283–290.

57. Dhalla, A.K., et al. A_1 adenosine receptor: role in diabetes and obesity. *Handb Exp Pharmacol.* **2009,** 193, 271–295.

58. Merighi, S., et al. Adenosine receptors and diabetes: Focus on the $A(_{2B})$ adenosine receptor subtype. *Pharmacol. Res.* **2015,** 99, 229–236.

59. Prystowsky, E.N., et al. Termination of paroxysmal supraventricular tachycardia by tecadenoson (CVT-510), a novel A_1-adenosine receptor agonist. *J. Am. Coll. Cardiol.* **2003,** 42, 1098–1102.

60. Rabadi, M.M., et al. Adenosine receptors and renal ischaemia reperfusion injury. *Acta Physiol (Oxf).* **2015,** 213, 222–231.

61. Sun, D., et al. Mediation of tubuloglomerular feedback by adenosine: evidence from mice lacking adenosine 1 receptors. *Proc. Natl. Acad. Sci. USA.* **2001,** 98, 9983–9988.

62. Vallon, V., et al. Adenosine and kidney function. *Physiol. Rev.* **2006,** 86, 901–940.

63. Vincenzi, F., et al. The anti-tumor effect of A_3 adenosine receptors is potentiated by pulsed electromagnetic fields in cultured neural cancer cells. *PLoS One.* **2012,** 7, e39317.

64. Hua, X., et al. Involvement of A_1 adenosine receptors and neural pathways in adenosine-induced bronchoconstriction in mice. *Am. J. Physiol. Lung. Cell. Mol. Physiol.* **2007,** 293, L25–L32.

65. Ponnoth, D.S., et al. Involvement of A_1 adenosine receptors in altered vascular responses and inflammation in an allergic mouse model of asthma. *Am. J. Physiol. Heart. Circ. Physiol.* **2010,** 299, H81–H87

66. Wilson, C.N., et al. Adenosine receptors and asthma. *Handb Exp Pharmacol.* **2009,** 193, 329–362.

67. Schulte, G., et al. Human adenosine $A(_1)$, $A(_{2A})$, $A(_{2B})$, and $A(_3)$ receptors expressed in Chinese hamster ovary cells all mediate the phosphorylation of extracellular- regulated kinase 1/2. *Mol. Pharmacol.* **2000,** 58, 477–482.

68. Schulte G., et al. Signalling from adenosine receptors to mitogen-activated protein kinases. *Cell. Signal.* **2003,** 15, 813–827.

69. Gundlfinger, A., et al. Adenosine modulates transmission at the hippocampal mossy fibre synapse via direct inhibition of presynaptic calcium channels. *J. Physiol.* **2007,** 582, 263–277.

70. Wu, L.G., et al. Adenosine inhibits evoked synaptic transmission primarily by reducing presynaptic calcium influx in area CA1 of hippocampus. *Neuron.* **1994,** 12, 1139– 1148.

71. **Von Lubitz, D.K., et al**. Chronic administration of selective adenosine A_1 receptor agonist or antagonist in cerebral ischemia. *Eur. J. Pharmacol.* **1994,** 256, 161–16.

72. Von Lubitz, D.K., et al. Chronic adenosine A_1 receptor agonist and antagonist: effect on receptor density and *N*-methyl-D-aspartate induced seizures in mice. *Eur. J. Pharmacol.* **1994,** 253, 95–99.

73. Yoon, K.W., et al. Adenosine inhibits excitatory but not inhibitory synaptic transmission in the hippocampus. *J. Neurosci.* **1991**, 11, 1375–1380.

74. Borea, P.A., et al. Adenosine as a Multi-Signalling Guardian Ange in Human Diseases: When, Where and How Does it Exert its Protective Effects? *Trends. Pharmacol. Sci.* **2016,** 37, 419–434.

75. Hargus, N.J., et al. Enhanced actions of adenosine in medial entorhinal cortex layer II stellate neurons in temporal lobe epilepsy are mediated via $A(_1)$-receptor activation. *Epilepsia.* **2012,** 53, 168–176.

76. Masino, S.A., et al. A ketogenic diet suppresses seizures in mice through adenosine A_1 receptors. *J. Clin. Invest.* **2011,** 121, 2679–2683.

77. Lusardi, T.A., et al. Ketogenic diet prevents epileptogenesis and disease progression in adult mice and rats. *Neuropharmacology.* **2015,** 99, 500–509.

78. Boison, D., et al. Adenosine kinase: exploitation for therapeutic gain. *Pharmacol. Rev.* **2013,** 65, 906–943.

79. **Williams-Karnesky, R.L., et al**. Epigenetic changes induced by adenosine augmentation therapy prevent epileptogenesis. *J. Clin. Invest.* **2013,** 123, 3552–3563.

80. Kashfi, S., et al. A_1 Adenosine Receptor Activation Modulates Central Nervous System Development and Repair. *Mol. Neurobiol.* **2017,** 54, 8128–8139.

81. Constantino, L.C., et al. Adenosine A_1 receptor activation modulates *N*methyl- D-aspartate (NMDA) preconditioning phenotype in the brain. *Behav Brain Res.* **2015,** 282, 103–110.

82. Fredholm, B.B., et al. How does adenosine inhibit transmitter release? *Trends. Pharmacol. Sci*. **1988,** 9, 130-134.

83. Corradetti, R., et al. Adenosine decreases aspartate and glutamate release from rat hippocampal slices. *Eur. J. Pharmacol.* **1984,** 104, 19-26.

84. Dunwiddie, T.V., et al. Adenosine A_1 receptors inhibit adenyl cyclase activity and neurotransmitter release and hyperpolarize pyramidal neurons in rat hippocampus. *J. Pharmacol. Exp. Ther.* **1989***,* 249, 31-37.

85. Cotman, C.W., et al. N-Methyl-D-aspartate receptors and Alzheimer's disease. *Neurobiol. Aging.* **1989,** 10, 603-605.

86 **Greenamyre, J.T., et al**. Excitatory amino acids and Alzheimer's disease. *Neurobiol. Aging.* **1989***,* 10, 593-602.

87. de Mendonça, A., et al. 2-Chloroadenosine decreases long-term potentiation in the hippocampal CA1 area of the rat. *Neurosci. Lett.* **1990**, 118, 107-111.

88. de Mendonça, A., et al. Endogenous adenosine attenuates long-term depression and depotentiation in the CA1 region of the rat hippocampus. *Neuropharmacology.* **1997,**36, 161-167.

89. Bliss, T.V., et al. A synaptic model of memory: long-term potentiation in the hippocampus. *Nature*. **1993**, 361, 31-39.

90. de Mendonca, A., et al. Adenosine and synaptic plasticity. *Drug. Dev. Res.* **2001,** 52, 283-290.

91. Corodimas, K.P., et al. Adenosine A_1 receptor activation selectively impairs the acquisition of contextual fear conditioning in rats. *Neuroscience.* **2001***,* 115, 1283-1290.

92. Hauber, W., et al. Facilitative effects of an adenosine A_1/A_2 receptors blockade on spatial memory performance of rats: selective enhacements of reference memory retention during the light period. *Behav. Brain Res.* **2001***,* 118, 43-52.

93. Kopf, S.R., et al. Adenosine and memory storage: effect of $A(_1)$ and $A(_2)$ receptor antagonist. *Psychopharmacology. (Berl).* **1999***,* 146, 214-219.

94. Fastbom, J., et al. Adenosine A_1 receptors in the human brain: a quantitative autoradiographic study. *Neuroscience.* **1987**, 22, 827-839.

95. Angulo, E., et al. A_1 adenosine receptors accumulate in neurogenerative structures in Alzheimer disease and mediate both amyloid precursor protein processing and tau phosphorylation and translocation. *Brain. Pathol.* **2003***,* 13, 440-451.

96. Ikeda, M., et al. Differential alterations in adenosine A_1 and Kappa 1 opioid receptors in the striatum in Alzheimer's disease. *Brain. Res.* **1993**, 616, 211-217.

97. Ułas, J., et al. Reduced density of adenosine A_1 receptors and preserved coupling of adenosine A_1 receptors to G proteins in Alzheimer hippocampus: a quantitative autoradiographic study. *Neuroscience.* **1993**, 52, 843-854.

98. **Kalaria, R.N., et al**. Hippocampal adenosine A_1 receptors are decreased in Alzheimer's disease. *Neurosci. Lett.* **1990**, 118, 257-260.

99. **Hyman, B.T., et al**. Perforant pathway changes and the memory impairment of Alzheimer's disease. *Ann. Neurol.* **1986***,* 20, 472-481.

100. Albasanz, J.L., et al. Up-regulation of adenosine receptors in the frontal cortex in Alzheimer's disease. *Brain Pathol.* **2008***,* 18, 211-219.

101. Arendash, G.W., et al. Caffeine protects Alzheimer's mice against cognitive impairment and reduce brain β−amyloid production. *Neuroscience.* **2006**, 142, 941-952.

102. Sveningsson, P., et al. Distribution of adenosine receptors in the postmortem human brain: an extended autoradiographic study. *Synapse*. **1997**, 27, 322−335.

103. Kimura, Y., et al. Quantitative analysis of adenosine A_1 receptors in human brain using positron emission tomography and [1-methyl-11C]8-dicyclopropylmethyl-1-methyl-3-propylxanthine. *Nuclear Med. Biol*. **2004**, 31, 975−981.

104. Ballarin, M., et al. Effect of locally infused 2-cholroadenosine, an A_1 receptor agonist, on spontaneous and evoked dopamine release in rat neostriatum. *Neurosci. Lett*. **1995**, 185, 29−32.

105. Rebola, N., et al. Subcellular localization of adenosine A_1 receptors in nerve terminal and synapses of the rat hippocampus. *Brain. Res*. **2003**, 987, 49−58.

106. Maemoto, T., et al. Pharmacological characterization of FR194921, a new potent, selective, orally active antagonist for central adenosine A_1 receptors. *J. Pharmacol. Sci.* **2004**, 96, 42−52.

107. Yonishi, S., et al. A. Preparation of pyrazines as adenosine A_1 and A_{2A} receptor antagonists and their pharmaceutical compositions. PCT Int. Appl. WO 2005040151, **2005**.

108. Mihara, T., et al. A novel adenosine A_1 and A_{2A} receptor antagonist ASP5854 ameliorates motor impairment in MPTP-treated marmosets: Comparison with existing anti- Parkinson's disease drugs. *Behav. Brain Res*. **2008**, 194, 152−161.

109. Mihara, T., et al. Brain adenosine A_{2A} receptor occupancy by a novel A_1/A_{2A} receptor antagonist, ASP5854, in rhesus monkeys: Relationship to anticataleptic effect. *J. Nucl. Med*. **2008**, 49, 1183−1188.

110 Mihara, T., et al. Pharmacological characterization of a novel, potent adenosine A_1 and A_{2A} receptor dual antagonist, 5-[5-amino-3-(4-fluorophenyl)pyrazin-2- yl]-1-isopropylpyridine-2(1H)-one (ASP5854), in models of Parkinson's disease and cognition. *J. Pharmacol. Exp. Ther*. **2007**, 323, 708− 719.

111 Bjorklund, O., et al. Adenosine $A(_1)$ and $A(_3)$ receptors protect astrocytes from hypoxic damage. *Eur J Pharmacol*. **2008**, 596, 6–13.

112 Ciccarelli, R., et al. Molecular signalling mediating the protective effect of A_1 adenosine and mGlu3 metabotropic glutamate receptor activation against apoptosis by oxygen/glucose deprivation in cultured astrocytes*. Mol. Pharmacol*. **2007,** 71, 1369–1380.

113. D'Alimonte, I., et al. Staurosporine induced apoptosis in astrocytes is prevented by A_1 adenosine receptor activation. *Neurosci. Lett*. **2007**, 418, 66–71.

114. Tsutsui, S., et al. A_1 adenosine receptor upregulation and activation attenuates neuroinflammation and demyelination in a model of multiple sclerosis. *J. Neurosci*. **2004**, 24, 1521–1529.

115. Synowitz, M., et al. A_1 adenosine receptors in microglia control glioblastoma–host interaction. *Cancer. Res*. **2006**, 66, 8550–8557.

116. Martin, E.D., et al. Adenosine released by astrocytes contributes to hypoxia-induced modulation of synaptic transmission. *Glia*. **2007**, 55, 36–45.

117. Halassa, M.M., et al. Astrocytic modulation of sleep homeostasis and cognitive consequences of sleep loss. *Neuron*. 2009, 61, 213–219.

118. Day, Y-J., et al. Renal protection from ischemia mediated by A_{2A} adenosine receptors on bone marrow-derived cells. *J. Clin. Invest.* **2003**, 112, 883-891.

119. Kull, B., et al. Adenosine A_{2A} receptors are colocalized with and activate g_{olf} in rat striatum. *Mol. Pharmacol.* **2000**, 58, 771–777.

120. Preti. D., et al. History and perspectives of A_{2A} adenosine receptor antagonists as potential therapeutic agents. *Med Res Rev.* **2015**, 35, 790-848.

121. Baraldi P.G., et al. Adenosine receptor antagonists: translating medicinal chemistry and pharmacology into clinical utility. *Chem. Rev.* **2008**, 108, 238–263.

122 Chen, J.F., et al. Adenosine receptors as drug targets–what are the challenges? *Nat. Rev. Drug. Discov.* **2013**, 12, 265–286.

123 Burgueño, J., et al. The adenosine A_{2A}receptor interacts with the actin-binding protein alpha-actinin. *J. Biol. Chem*. **2003**, 278, 37545–37552.

124. Morelli, M., et al. Adenosine A_{2A} receptors and Parkinson's disease. *Handb. Exp. Pharmacol*. **2009**, 193, 589–615.

125. Azdad, K., et al. Dopamine D_2 and adenosine A_{2A} receptors regulate NMDA-mediated excitation in accumbens neurons through A_{2A}-D_2 receptor heteromerization. *Neuropsychopharmacology*. **2009**, 34, 972–986.

126. Higley, M. J.,et al. Competitive regulation of synaptic Ca^{2+} influx by D_2 dopamine and A_{2A} adenosine receptors. *Nat. Neurosci*. **2010**, 13, 958–966.

127. Ferré, S., et al. An update on adenosine A_{2A}-dopamine D_2 receptor interactions. Implications for the function of G protein-coupled receptors. *Curr. Pharm. Des.* **2008**, 14, 1468–1474.

128. Tozzi, A., et al. The distinct role of medium spiny neurons and cholinergic interneurons in the D_2/A_{2A} receptor interaction in the striatum: Implications for Parkinson's disease. *J. Neurosci*. **2011**, 31, 1850–1862.

129. **Ungerstedt, U., et al.** 6-Hydroxydopamine-induced degeneration of central monoamine neurons. Eur. *J. Pharmacol*. **1968**, 5, 107–110.

130. Ungerstedt, U., et al. Quantitative recording of rotational behavior in rats after 6-hydroxy-dopamine lesions of the nigrostriatal dopamine system. *Brain. Res*. **1970**, 24, 485–493.

131. Bankiewicz, K. S., et al. MPTP-induced parkinsonism in nonhuman primates. *Methods Neurosci*. **1991**, 7, 168–182.

132. Jakowec, M.W., et al. 1-methyl-4-phenyl-1,2,3,6-tetrahydropyridine- induced lesion model of Parkinson's disease, with emphasis on mice and nonhuman primates. *Comp. Med.* **2004**, 54, 497–513.

133. Chen, J. F., et al. Neuroprotection by caffeine and A_{2A} adenosine receptor inactivation in a model of Parkinson's disease. *J. Neurosci*. **2001**, 21, RC143/ 1–RC143/6.

134. Grondin, R., et al. Antiparkinsonian effect of a new adenosine A_{2A} receptor antagonist in MPTP-treated monkeys. *Neurology*. **1999**, 52, 1673–1677.

135. Ongini, E., et al. Dual actions of A_{2A} adenosine receptor antagonists on motor dysfunction and neurodegenerative processes. *Drug Dev. Res*. **2001**, 52, 379–386.

136. El Yacoubi, M., et al. Adenosine A_{2A} receptors and depression. *Neurol*. **2003**, 61, S82–S87.

137. El Yacoubi, M., et al. Adenosine A_{2A} receptor antagonists are potential antidepressants: Evidence based on pharmacology and A_{2A} receptor knockout mice. *Br. J. of Pharm*. **2001**, 134, 68–77.

138. Palacios, N., et al. Caffeine and risk of Parkinson's disease in a large cohort of men and women. *Movement Disorders: Official Journal of the Movement Disorder Society*. **2012**, 27, 1276–1282.

139. Vickers, J.C., et al. The cause of neuronal degeneration in Alzheimer's disease. *Prog. Neurobiol.* **2000***,* 60, 139-165.

140. Dall'Igna, O. P., et al. Neuroprotection by caffeine and adenosine A_{2A} receptor blockade of beta-amyloid neurotoxicity. *Br. J. Pharmacol.* **2003***,* 138, 1207-1209.

141.Geiger, J.D., et al. Role of adenosine in the control of inflammatory events associated with acute and chronic neurodegenerative disorders. In: Cronstein, B., Szabo, C., Hasko, G. (Eds.) Adenosine receptors: Therapeutic aspects for inflammatory and immune diseases. *Taylor and Francis*. **2006.**

142. Cunha, R.A., et al. Potential therapeutic interest of adenosine A_{2A} receptors in psychiatric disorders. *Curr. Pharm. Des*. **2008**, 14, 1512-1524

143. Schiffmann, S.N., et al. Adenosine A_{2A} receptors and basal ganglia physiology. *Prog. Neurobiol*. **2007**, 83, 277- 292.

144. Dall'Igna, O.P., et al. Caffeine and adenosine $A(_{2a})$ receptor antagonists prevent beta-amyloid (25-35) induced cognitive deficits in mice. *Exp. Neurol.* **2007**, 203, 241-245.

145. Cunha, G.M.A., et al. Blocked of adenosine A_{2A} receptors prevents amyloid (Aβ1–42)-induced synaptotoxicity and memory impairment in rodents. *Purinergic. Signal.* **2006***,* 2, 135-136.

146. Wong, P.T., et al. Ornithine aminotransferase in Huntington's disease. *Brain Res*. **1982**, 231, 466–471.

147. Behrens, P.F., et al. Impaired glutamate transport and glutamate-glutamine cycling: downstream effects of the Huntington mutation. *Brain.* **2002**, 125, 1908–1922.

148. Shin, J.-Y., et al. Expression of mutant huntingtin in glial cells contributes to neuronal excitotoxicity. *J. Cell Biol*. **2005**, 171, 1001–1012.

149. Fan, M.M.Y., et al. N-methyl-D-aspartate (NMDA) receptor function and excitotoxicity in Huntington's disease. *Prog. Neurobiol*. **2007,** 81, 272–293.

150. Zeron, M.M., et al. Increased sensitivity to N-methyl-D-aspartate receptor mediated excitotoxicity in a mouse model of Huntington's disease. *Neuron.* **2002**, 33, 849–860.

151. **Li, L., et al.** Role of NR2B-type NMDA receptors in selective neurodegeneration in Huntington disease. *Neurobiol. Aging.* **2003**, 24, 1113–1121.

152. Li, L., et al. Enhanced striatal NR2Bcontaining N-methyl-D-aspartate receptor-mediated synaptic currents in a mouse model of Huntington disease. *J. Neurophysiol*. **2004,** 92, 2738–2746.

153. Rosin, D.L., et al. Immunohistochemical localization of adenosine A_{2A} receptors in the rat central nervous system. *J. Comp. Neurol*. **1998,** 401, 163–186.

154. Hettinger, B.D., et al. Ultrastructural localization of adenosine A_{2A} receptors suggests multiple cellular sites for modulation of GABAergic neurons in rat striatum. *J. Comp. Neurol*. **2001,** 431, 331–346.

155. Ciruela, F., et al. Presynaptic control of striatal glutamatergic neurotransmission by adenosine A_1-A_{2A} receptor heteromers. *J. Neurosci*. **2006,** 26, 2080–2087.

156. Rodrigues, R.J., et al. Co-localization and functional interaction between adenosine $A_{(2A)}$ and metabotropic group 5 receptors in glutamatergic nerve terminals of the rat striatum. *J. Neurochem*. **2005**, 92, 433–441.

157. Coney, A.M., et al. Role of adenosine and its receptors in the vasodilatation induced in the cerebral cortex of the rat by systemic hypoxia. *J. Physiol*. **1998,** 509, (Pt 2) 507–518.

158. Ngai, A.C., et al. Receptor subtypes mediating adenosine-induced dilation of cerebral arterioles. *Am. J. Physiol. Heart Circ*. *Physiol*. **2001**, 280, H2329–H2335.

159. Fields, R.D., et al. Purinergic signalling in neuron–glia interactions, *Nat. Rev. Neurosci*. **2006**, 7, 423–436.

160. Varani, K., et al. Aberrant amplification of $A_{(2A)}$ receptor signaling in striatal cells expressing mutant huntingtin. *FASEB J.* **2001,** 15, 1245–1247.

161. Blum, D., et al., et al. Striatal and cortical neurochemical changes induced by chronic metabolic compromise in the 3- nitropropionic model of Huntington's disease. *Neurobiol. Dis*. **2002,** 10, 410–426.

162. Chiang, M.-C., et al. YcAMP-response element-binding protein contributes to suppression of the A_{2A} adenosine receptor promoter by mutant Huntingtin with expanded polyglutamine residues. *J. Biol. Chem.* **2005**, 280, 14331–14340.

163. Tarditi, A., et al. Early and transient alteration of adenosine A_{2A} receptor signaling in a mouse model of Huntington disease. *Neurobiol. Dis*. **2006,** 23, 44–53.

164. Dhaenens, C.-M., et al. SA genetic variation in the ADORA2A gene modifies age at onset in Huntington's disease. *Neurobiol*. Dis. **2009**, 35, 474–476.

165. Lei, W., et al. Evidence for differential cortical input to direct pathway versus indirect pathway striatal projection neurons in rats. *J. Neurosci*. **2004,** 24, 8289–8299.

166. Corsi, A. C., et al. Striatal A_{2A} adenosine receptor antagonism differentially modifies striatal glutamate outflow in vivo in young and aged rats. *Neuro. Report.* **2000**, 11, 2591–2595.

167. Pintor, D. A., et al. SCH 58261 an adenosine A $_{(2A)}$ receptor antagonist reduces, only at low doses, K(+)-evoked glutamate release in the striatum. *Eur. J. Pharmacol*. **2001,** 421, 177–180.

168. Popoli, P., et al. Blockade of striatal adenosine A_{2A} receptor reduces, through a presynaptic mechanism, quinolinic acid-induced excitotoxicity: possible relevance to neuroprotective interventions in neurodegenerative diseases of the striatum. *J. Neurosci*. **2002,** 22, 1967–1975.

169. Tebano, M.T., et al. A. Adenosine A_{2A} receptor blockade differentially influences excitotoxic mechanisms at pre- and postsynaptic sites in the rat striatum. *J. Neurosci. Res*. **2004**, 77, 100–107.

170. Li, X.X., et al. Adenosine enhances glial glutamate efflux via A_{2A} adenosine receptors. *Life Sci*. **2001,** 68, 1343–1350.

171. Nishizaki, T., et al. A new neuromodulatory pathway with a glial contribution mediated via $A(_{2A})$ adenosine receptors. *Glia.* **2002,** 39, 133–147.

172. Nishizaki, T., et al. ATP- and adenosine-mediated signaling in the central nervous system: adenosine stimulates glutamate release from astrocytes via A_{2A} adenosine receptors. *J. Pharmacol*. Sci. **2004,** 94, 100–102.

173. Pintor, A., et al. Adenosine A_{2A} receptor antagonists prevent the increase in striatal glutamate levels induced by glutamate uptake inhibitors. *J. Neurochem*. **2004,** 89, 152–156.

174. **Wirkner, K., et al**. Inhibition by adenosine $A(_{2A})$ receptors of NMDA but not AMPA currents in rat neostriatal neurons. *Br. J. Pharmacol*. 130, **2000,** 259–269.

175. Ferrante, A., et al. Influence of CGS 21680, a selective adenosine $A(_{2A})$ receptor agonist, on NMDA receptor function and expression in the brain of Huntington's disease mice. *Brain. Res*. 1323, **2010,** 184–191.

176. Martire, A., et al. Remodeling of striatal NMDA receptors by chronic $A(_{2A})$ receptor blockade in Huntington's disease mice. *Neurobiol. Dis*. **2010**, 37, 99–105.

177. Nörenberg, W., et al. Effect of adenosine and some of its structura analogues on the conductance of NMDA receptor channels in a subset of rat neostriatal neurons. *Br. J. Pharmacol*. 122, **1997**, 71–80.

178. Popoli, P., et al. Functions, dysfunctions and possible therapeutic relevance of adenosine A_{2A} receptors in Huntington's disease. *Prog. Neurobiol*. 81, **2007**, 331–348.

179. Lubitz, D.K.V., et al. Cerebral ischemia in gerbils: effects of acute and chronic treatment with adenosine A_{2A} receptor agonist and antagonist. *Eur. J. Pharmacol*. **1995,** 287, 295–302.

180. Gao, Y., et al. JCGS 15943, an adenosine A_2 receptor antagonist, reduces cerebral ischemic injury in the Mongolian gerbil. *Life Sci*. **1994**, 55, PL61–PL65.

181. Phillis, J.W., et al. The effects of selective A_1 and A_{2a} adenosine receptor antagonists on cerebral ischemic injury in the gerbil. *Brain Res*. **1995**, 705, 79–84.

182. Monopoli, A., et al. Blockade of adenosine A_{2A} receptors by SCH 58261 results in neuroprotective effects in cerebral ischaemia in rats. *NeuroReport.* **1998**, 9, 3955–3959.

183. Chen, J.F., et al. $A(_{2A})$ adenosine receptor deficiency attenuates brain injury induced by transient focal ischemia in mice. J. *Neurosci*. **1999**, 19, 9192–9200.

184. Cunha, R.A., et al. Neuroprotection by adenosine in the brain: from $A(_1)$ receptor activation to A $(_{2A})$ receptor blockade. *Purinergic Signal.* **2005,** 1, 111–134.

185. Chen, J.F., et al. Adenosine A_{2A} receptors and brain injury: broad spectrum of neuroprotection, multifaceted actions and "fine tuning" modulation. *Prog. Neurobiol*. **2007**, 83, 310–331

186. Chen, J.F., et al. Modulation of ischemic brain injury and neuroinflammation by adenosine A_{2A} receptors. *Curr. Pharm. Des*. **2008**, 14, 1490–1499.

187. de Mendonça, A., et al. Therapeutic opportunities for caffeine in Alzheimer's disease and other neurodegenerative disorders. *J. Alzheimers Dis*. **2010**, 20, 1–2.

188. Carta, A.R., et al. Inactivation of neuronal forebrain A receptors protects dopaminergic neurons in a mouse model of Parkinson's disease. *J. Neurochem*. **2009**, 111, 1478–1489.

189. Dai, S.-S., et al. Local glutamate level dictates adenosine A_{2A} receptor regulation of neuroinflammation and traumatic brain injury. *J. Neurosci*. **2010**, 30, 5802–5810.

190. Yu, L., et al. Adenosine A_{2A} receptor antagonists exert motor and neuroprotective effects by distinct cellular mechanisms. *Ann. Neurol*. **2008**, 63, 338–346.

191. Gui, L., et al. Adenosine A_{2A} receptor deficiency reduces striatal glutamate outflow and attenuates brain injury induced by transient focal cerebral ischemia in mice. *Brain Res*. **2009**, 1297, 185–193.

192. Melani, A., et al. Selective adenosine A_{2A} receptor antagonism reduces JNK activation in oligodendrocytes after cerebral ischaemia. *Brain.* **2009**, 132, 1480–1495.

193. Chen, X., et al. Caffeine blocks disruption of blood brain barrier in a rabbit model of Alzheimer's disease. *J. Neuroinflammation*. **2008**, 5, 12.

194. Chen, X., et al. Caffeine protects against MPTP induced blood-brain barrier dysfunction in mouse striatum. *J. Neurochem*. **2008**, 107, 1147–1157.

195. Yu, L., et al. Selective inactivation or reconstitution of adenosine A_{2A} receptors in bone marrow cells reveals their significant contribution to the development of ischemic brain injury. *Nat. Med*. **2004**, 10, 1081–1087.

196. Zhao, X., et al. Caffeinol at the receptor level: anti-ischemic effect of N-methyl-D-aspartate receptor blockade is potentiated by caffeine. *Stroke*. 41, **2010**, 363–367.

197. Dash, P.K., et al. Post trauma administration of caffeine plus ethanol reduces contusion volume and improves working memory in rats. *J. Neurotrauma***. 2004**, 21, 1573–1583.
.
198. Pickel V.M., et al. Subcellular distributions of adenosine A_1 and A_{2A} receptors in the rat dorsomedial nucleus of the solitary tract at the level of the area postrema. *Synapse***. 2006**, 60, 496–509.

199. Svenningsson, P., et al. Distribution, biochemistry and function of striatal adenosine A_{2A} receptors. *Prog Neurobiol*. **1999**, 59, 355–396

200. Hasko, G., et al. Adenosine receptor signaling in the brain immune system. *Trends Pharmacol. Sci*. **2005**, 26, 511–516.

201. Hindley, S., et al. Stimulation of reactive astrogliosis in vivo by extracellular adenosine diphosphate or an adenosine A_2 receptor agonist. *J. Neurosc. Res*. **1994**, 38, 399–406.

202. Brambilla, R., et al. Blockade of A_{2A} adenosine receptors prevents basic fibroblast growth factor-induced reactive astrogliosis in rat striatal primary astrocytes. *Glia*. **2003**, 43, 190–194.

203. Brodie, C., et al. Activation of the A_{2A} adenosine receptor inhibits nitric oxide production in glial cells. *FEBS Lett.* **1998**, 429, 139–142.

204. **Fiebich B.L., et al**. Cyclooxygenase-2 expression in rat microglia is induced by adenosine A_{2A}-receptors. *Glia*. **1996**, 18, 152–160.

205. Saura, J., et al. Adenosine A_{2A} receptor stimulation potentiates nitric oxide release by activated microglia. *J. Neurochem*. **2005**, 95, 919–929.

206. Heese, K., et al. Nerve growth factor (NGF) expression in rat microglia is induced by adenosine A_{2A}-receptors. *Neurosci. Lett*. **1997**, 231, 83–86.

207. Abebe, W., et al. Effects of adenosine analogs on inositol 1,4,5-trisphosphate production in porcine coronary artery. *Vascul. Pharmacol.* **2002**, 39, 89–95.

208. Teng, B., et al. Involvement of p38-mitogen-activated protein kinase in adenosine receptor-mediated relaxation of coronary artery. *Am. J. Physiol. Heart. Circ. Physiol.* **2005**, 288, H2574–H2580.

209. Ray, C.J., et al. The cellular mechanisms by which adenosine evokes release of nitric oxide from rat aortic endothelium. *J. Physiol.* **2006**, 570, 85–96.

210. Jordan, J.E., et al. Adenosine A_2 receptor activation attenuates reperfusion injury by inhibiting neutrophil accumulation, superoxide generation and coronary endothelial adherence. *J. Pharmacol. Exp. Ther.* **1997**, 280, 301–309,

211. Llach, A., et al. Abnormal calcium handling in atrial fibrillation is linked to up-regulation of adenosine A_{2A} receptors. *Eur. Heart. J.* **2011**, 32, 721–729.

212. **Molina, C.E., et al**. Prevention of adenosine A_{2A} receptor activation diminishes beat-to-beat alternation in human atrial myocytes. *Basic. Res. Cardiol.* **2016,** 111, 5.

213. Fredholm, B.B., et al. Aspects of the general biology of adenosine A_{2A} signalling. *Prog. Neurobiol***. 2007**, 83, 263–276.

214. Mayr, B., et al. Transcriptional regulation by the phosphorylationdependent factor CREB. *Nat. Rev. Mol. Cell. Biol*. **2001**, 2, 599–609.

215. Lin, M.C., et al. Shear stress induction of the tissue factor gene. *J. Clin. Invest*. **1997**, 99, 737–744.

216. Kawasaki, H., et al. A family of cAMP-binding proteins that directly activate Rap1. *Science*. **1998**, 282, 2275–2279.

217. Sands, W.A., et al. Exchange protein activated by cyclic AMP (Epac)-mediated induction of suppressor of cytokine signalling 3 (SOCS-3) in vascular endothelial cells. *Mol. Cell. Biol*. **2006**, 26, 6333–6346.

218. Yoshimura, A., et al. SOCS proteins, cytokine signaling and immune regulation. *Nat. Rev. Immunol*. **2007**, 7, 454–465.

219. Khoa, N.D., et al. Inflammatory cytokines regulate function and expression of adensoine A_{2A} receptors in human monocytic THP-1 cells. *J. Immunol***. 2001**; 167:4026–4032.

220. Murphee, L.J., et al. Lipolpolysaccharide rapidly modify adenosine receptor transcripts in murine and human macrophages: role of NF-κB in A_{2A} adenosine receptor induction. *Biochem J*. **2005**, 391, 575–580.

221. Capecchi, P.L., et al. Up-regulation of A_{2A} adenosine receptor expression by TNF-alpha in PBMC of ptients with CHF: a regulatory mechanism of inflammation. *J Card Fail*. **2005**, 11(1), 67–73.

222. Morello, S., et al. IL-1beta and TNF-α regulation of the adenosine receptor (A_{2A}) expression: differential requirement for NF-kappa B binding to the proximal promoter. *J. Immunol*. **2006**, 177 (10), 7173–7183.

223. Sullivan, G.W., et al. The specific type IV phosphodiesterase inhibitor rolipram combined with adenosine reduces tumor necrosis factor-alpha-primed neutrophil oxidative activity. *Int. J. Immunopharmacol*. **1995**, 17(10), 793–803.

224. Haskó, G., et al. Shaping of monocyte and macrophage function by adenosine receptors. *Pharmacol Ther*. **2007**, 113, 264–275.

225. Cadieux, J.S., et al. Potentiation of neutrophil cyclooxygenase-2 by adenosine: an early anti-inflammatory signal. *J. Cell Sci*. **2005**, 118 (7), 1437–1447.

226. Flamand, N., et al. Cyclic AMP-mediated inhibition of 5-lypoxigenase translocation and leukotriene biosynthesis in human neutrophils. *Mol. Pharmacol*. **2002**, 62(2), 250–256.

227. Pouliot, M., et al. Adenosine up-regulatescyclooxigenase-2 in human granulocytes: impact of the balance of eicosanoid generation. *J. Immunol*. **2002**, 169 (9), 5279–5286.

228. McColl, S.R., et al. Immunomodulatory impact of the A_{2A} adenosine receptor on the profile of chemokine produced by neutrophils. *FASEB J*. **2006**, 20(1), 187–189.

229. St-Onge, M., et al. Impact of anti-inflammatory agents on the gene expression profile of stimulated human neutrophils: unravelling endogenous resoltution pathways. *Plos ONE*. **2009**, 3, e4902.

230. **Ferre, S., et al**. Stimulation of high-affinity adenosine A_2 receptors decreases the affinity of dopamine D_2 receptors in rat striatal membranes. *Proc. Natl. Acad. Sci. USA.* **1991,** 88, 7238–7241.

231. **Koupenova, M., et al**. A_{2B} adenosine receptor regulates hyperlipidemia and atherosclerosis. *Circulation.* **2012**, 125, 354–363.

232. Pedata, F., et al. Purinergic signalling in brain ischemia. *Neuropharmacology.* **2016,** 104, 105–130.

233. Sun, Y., et al. Adenosine A_{2B} Receptor: From Cell Biology to Human Diseases. **2016,** *Front Chem* 4, 37. **2016,**

234. Rosenberger, P., et al. Hypoxia-inducible factor-dependent induction of netrin-1 dampens inflammation caused by hypoxia. *Nat. Immunol.* **2009,** 10, 195–202.

235. **Sun, Y., et al**. A novel mechanism of control of NF_B activation and inflammation involving A_{2B} adenosine receptors. *J Cell Sci.* **2012,** 125, 4507–4517.

236. Moriyama, K., et al. Adenosine A_{2A} receptor is involved in cell surface expression of A_{2B} receptor. *J. Biol. Chem.* **2010,** 285, 39271–39288.

237. Gessi, S., et al. $A(_1)$ and $A(_3)$ adenosine receptors inhibit LPS-induced hypoxia-inducible factor-1 accumulation in murine astrocytes. *Pharmacol, Res.* **2013**, 76, 157–170.

238. Gu, L., et al. Early activation of nSMase2/ ceramide pathway in astrocytes is involved in ischemia-associated neuronal damage via inflammation in rat hippocampi. *J. Neuroinflammation.* **2013**, 10, 879.

239. Eltzschig, H.K., et al. Coordinated adenine nucleotide phosphohydrolysis and nucleoside signaling in posthypoxic endothelium: role of ectonucleotidases and adenosine A_{2B} receptors. *J. Exp. Med.* **2003**, 198. 783–796.

240. Hu, X., et al. Sustained Elevated Adenosine via ADORA2B Promotes Chronic Pain through Neuroimmune Interaction. *Cell. Reports.* **2016**, 16, 106–119.

241. Merighi, S., et al. A_{2B} adenosine receptors stimulate IL-6 production in primary murine microglia through p38 MAPK kinase pathway. *Pharmacol. Res.* **2017**, 117, 9–19.

242. Koscsó, B., et al. Adenosine augments IL-10 production by microglial cells through an A_{2B} adenosine receptor- mediated process. *J. Immunol.* **2012**, 188, 445– 453.

243. Merighi, S., et al. A_{2A} and A_{2B} adenosine receptors affect HIF-1α signaling in activated primary microglial cells. *Glia.* **2015**, 63, 1933–1952.

244. Janes, K., et al. A_3 adenosine receptor agonist prevents the development of paclitaxel-induced neuropat.hic pain by modulating spinal glial-restricted redox-dependent signaling pathways. *Pain.* **2014**, 155, 2560–2567.

245. Borea, P.A., et al. The A_3 adenosine receptor: history and perspectives. *Pharmacol Rev.* **2015**, 67, 74–102.

246. Fishman, P., et al. A_3 adenosine receptor as a target for cancer therapy. *Anticancer Drugs.* **2002**, 13, 437–443.

247. Melani, A., et al. Adenosine receptors in cerebral ischemia. *Int. Rev. Neurobiol.* **2014**, 119, 309–348.

248. Pugliese, A.M., et al. Role of adenosine A_3 receptors on CA1 hippocampal neurotransmission during oxygen-glucose deprivation episodes of different duration. *Biochem. Pharmacol.* **2007**, 74, 768–779.

249. Choi, I.Y., et al. A_3 adenosine receptor agonist reduces brain ischemic injury and inhibits inflammatory cell migration in rats. *Am. J. Pathol.* **2011**, 179, 2042–2052.

250. Lee, J.Y., at al. Activation of adenosine A_3 receptor suppresses lipopolysaccharide-induced TNF-α production through inhibition of PI 3-kinase/Akt and NF-kB activation in murine BV2 microglial cells. *Neurosci Lett.* **2006**, 396, 1–6.

251. Ohsawa, K., et al. Adenosine A_3 receptor is involved in ADP-induced microglial process extension and migration. *J. Neurochem.* **201**2, 121, 217–227.

252. Janes, K., et al. Identification of A_3 adenosine receptor agonists as novel non-narcotic analgesics. *Br. J. Pharmacol.* **2016**, 173, 1253–1267.

253. Sawynok, J., et al. Adenosine A_3 receptor activation produces nociceptive behaviour and edema by release of histamine and 5-hydroxytryptamine. *Eur J Pharmacol.* **1997**, 333, 1–7.

254. Wu, W-P., et al. Decreased inflammatory pain due to reduced carrageenan-induced inflammation in mice lacking adenosine A_3 receptors. *Neuroscience.* **2002**, 114, 523–527.

255. Chen, Z., et al. Controlling murine and rat chronic pain through A_3 adenosine receptor activation. *FASEB J.* **2012**, 26, 1855–1865.

256. Little, J.W., et al. Endogenous adenosine A_3 receptor activation selectively alleviates persistent pain states. *Brain.* **2012,** 138, 28–35.

257. **Janes, K., et al**. Spinal neuroimmune activation is independent of T-cell infiltration and attenuated by A_3 adenosine receptor agonists in a model of oxaliplatin-induced peripheral neuropathy. *Brain. Behav. Immun.* **2015,** 44, 91–99.

258. Varani, K., et al. The stimulation of $A(_3)$ adenosine receptors reduces bone-residing breast cancer in a rat preclinical model. *Eur. J. Cancer.* **2013,** 49, 482–491.

259. Chabre, M., et al. Monomeric G-protein-coupled receptor as a functional unit. *Biochemistry.* **2005,** 44, 9395–9403.

260. Whorton, M.R., et al. A monomeric G protein-coupled receptor isolated in a high density lipoprotein particle efficiently activates its G protein. *Proc. Natl. Acad. Sci. USA.* **2007,** 104, 7682–7687.

261. Whorton, M.R., et al. Efficient coupling of transducing to monomeric rhodopsin in a phospholipid bilayer. *J. Biol. Chem.* **2008,** 283, 4387–4394

262. White, J.F., et al. Dimerization of the class A G protein-coupled neurotensin receptor NTS1 alters G protein interaction. *Proc. Natl. Acad. Sci. USA.* **2007,** 104, 12199–12204.

263. Ciruela, F., et al. Immunological identification of A_1 adenosine receptors in brain cortex. *J. Neurosci. Res.* **1995,** 42, 818–828.

264. Yoshioka, K., et al. Hetero-oligomerization of adenosine A_1 receptors with P2Y1 receptors in rat brains. *FEBS. Lett.* **2002,** 531, 299–303.

265. Briddon, S.J., et al. Plasma membrane diffusion of G protein-coupled receptor oligomers. *Biochim Biophys Acta.* **2008,** 1783, 2262–2268.

266. Vidi, P.A., et al. Ligand-dependent oligomerization of dopamine D_2 and adenosine A_{2A} receptors in living neuronal cells. *Mol Pharmacol.* **2008 (a),** 74, 544–551.

267. Vidi, P.A., et al. Adenosine A_{2A} receptors assemble into higher-order oligomers at the plasma membrane. *FEBS Lett.* **2008 (b),** 582, 3985–3990.

268. Cristovao-Ferreira, S., et al. Modulation of GABA transport by adenosine A_1R-$A_{2A}R$ heteromers, which are coupled to both G_s- and $G(_i/_o)$-proteins. *J. Neurosci*. **2011**, 31, 15629–15639.

269. Cristovao-Ferreira, S., et al. A_1R-$A_{2A}R$ heteromers coupled to Gs and $G_i/_0$ proteins modulate GABA transport into astrocytes. *Purinergic Signal*. **2013**, 9, 433–449.

270. Hillion, J., et al. Coaggregation, cointernalization, and codesensitization of adenosine A_{2A} receptors and dopamine D2 receptors. *J. Biol. Chem.* **2002, 277,** 18091–18097.

271. **Kamiya, T., et al.** Oligomerization of adenosine A_{2A} and dopamine D_2 receptors in living cells. *Biochem Biophys. Res. Commun.* **2003, 306,** 544–549.

272. Canals, M., et al. Adenosine A_{2A}-dopamine $_{D2}$ receptorreceptor heteromerization: qualitative and quantitative assessment by fluorescence and bioluminescence energy transfer. *J. Biol. Chem.* **2003, 278,** 46741–46749.

273. Canals, M., et al. Homodimerization of adenosine A_{2A} receptors: qualitative and quantitative assessment by fluorescence and bioluminescence energy transfer. *J. Neurochem.* **2004, 88,** 726–734.

274. Orru, M., et al. Striatal pre- and postsynaptic profile of adenosine A_{2A} receptor antagonists. *PLoS One*. **2011**, 6, e16088.

275. Inventors; Bayer Aktiengesellschaft, Rosentreter, U., et al. Substituted 2-thio-3,5-dicyano-4-aryl-6-aminopyridines and the use thereof as adenosine receptor ligands. World patent WO01025210. **2001** Apr 12.

276. Beukers, M.W., et al. New, non-adenosine, high Potency agonists for the human adenosine A_{2B} receptor with an improved selectivity profile compared to the reference agonist N-ethylcarboxamidoadenosine. *J. Med. Chem*. **2004**, 47, 3707–3709.

277. Yan, L., et al. Adenosine receptor agonists: from basic medicinal chemistry to clinical development. *Exp. Opin. Emerg. Drugs*. **2003,** 8 537–576.

278. Gao, Z.G., et al. N^6-Substituted adenosine derivatives: selectivity, efficacy, and species differences at A_3 adenosine receptors. *Biochem. Pharmacol*. **2003,** 65, 1675–1684.

279. **Kiesman, W.F., et al**. A_1 adenosine receptor antagonists, agonists, and allosteric enhancers. *Handb. Exp. Pharmaco*l. **2009**, 193, 25–58 Review

280. Müller, C.E., et al. Recent developments in adenosine receptor ligands and their potential as novel drugs. *Bioch. Bioph. Act.* **2011**, 1808, 1290–1308

281. **Lauro, C., et al.** Adenosine A_1 receptors and microglial cells mediate CX3CL1-induced protection of hippocampal neurons against Glu-induced death. *Neuropsychopharmacology*. **2010**, 35, 1550–1559.

282. Knutsen, L.J., et al. N-Substituted adenosines as novel neuroprotective A_1 agonists with diminished hypotensive effects, *J. Med. Chem*. **1999,** 42, 3463–3477.

283. Zablocki, J.A., et al. Partial A_1 adenosine receptor agonists from a molecular perspective and their potential use as chronic ventricular rate control agents during atrial fibrillation (AF). *Curr. Top. Med. Chem*. **2004**, 4, 839–854.

284. Al Jaroudi, W., et al. Regadenoson: a new myocardial stress agent. *J. Am. Coll. Cardiol*. 54, **2009**, 1123–1130.

285. Mantell, S.J., et al. SAR of a series of inhaled A_{2A} agonists and comparison of inhaled pharmacokinetics in a preclinical model with clinical pharmacokinetic data. *Bioorg. Med. Chem. Lett*. **2009**, 19, 4471–4475.

286. El-Tayeb, A., et al. Nucleoside-5'-monophosphates as prodrugs of adenosine A_{2A} receptor agonists activated by ecto-5'-nucleotidase. *J. Med. Chem.* **2009,** 52, 7669–7677.

287. Awad, A.S., et al. Adenosine A_{2A} receptor activation attenuates inflammation and injury in diabetic nephropathy. *Am. J. Physiol. Renal. Physiol*. **2006**, 290, F828–F837.

288. Desai, A., et al. Adenosine A_{2A} receptor stimulation increases angiogenesis by down-regulating production of the antiangiogenic matrix protein thrombospondin 1. *Mol. Pharmacol*. **2005,** 67, 1406–1413.

289. Udelson, J.E., et al. Gibbons, Randomized, controlled dose-ranging study of the selective adenosine A_{2A} receptor agonist binodenoson for pharmacological stress as an adjunct to myocardial perfusion imaging. *Circulation.* **2004**, 109, 457–464.

290. Cerqueira, M.D., et al. Advances in pharmacologic agents in imaging: new A_{2A} receptor agonists. *Curr. Cardiol. Rep*. **2006,** 8, 119–122.

291. **Iskandrian, A.E., et al**. Adenosine versus regadenoson comparative evaluation in myocardial perfusion imaging: results of the ADVANCE phase 3 multicenter international trial. *J. Nucl. Cardiol*. **2007**, 14**,** 645–658.

292. Müller, C.E., et al. Xanthines as adenosine receptor antagonists. In Methylxanthines. In Handbook of Experimental Pharmacology, B.B. Fredholm, ed., Springer, **2011**, 200, 151–199.

293. Slawski, M.T., et al. Rolofylline: a selective adenosine 1 receptor antagonist for the treatment of heart failure. *Exp. Opin. Pharmacother*. **2009**, 10, 311–322.

294. Jacobson, K.A., et al. Adenosine receptors as therapeutic targets. *Nat. Rev. Drug Discov*. **2006**, 5, 247–264.

295. Arispe, N., et al. Direct activation of cystic fibrosis transmembrane conductance regulator channels by 8-cyclopentyl-1,3-dipropylxanthine (CPX) and 1,3-diallyl-8-cyclohexylxanthine (DAX). *J. Biol. Chem*. **1998,** 273, 5727–5734.

296. Wilson, C.N., et al. Adenosine receptors and asthma in humans. *Br. J. Pharmacol*. **2008**, 155, 475–486.

297. Müller, **C.E., et al.** A_1-adenosine receptor antagonists. *Exp. Opin. Ther*. Pat. **1997,** 7, 419–440.
298. Hess, S., et al. Recent advances in adenosine receptor antagonist research. *Exp. Opin. Ther*. **2001**, Pat. 11, 1533–1561.

299. Hocher, B., et al. Adenosine A_1 receptor antagonists in clinical research and development. *Kidney Int*. **2010**, 78, 438–445.

300. Müller, **C.E., et al.** Blocking striatal adenosine A_{2A} receptors: a new strategy for basal ganglia disorders. *Recent Pat. CNS Drug Discov*. **2007**, 2, 1–21.

301. Müller, **C.E., et al.** Blocking striatal adenosine A_{2A} receptors: a new strategy for basal ganglia disorders. *Frontiers in CNS Drug Discov.* **2010**, 1, 304–341.

302. Shah, U., et al. Recent progress in the discovery of adenosine A_{2A} receptor antagonists for the treatment of Parkinson's disease. *Curr. Opin. Drug Discov*. **2010**, 13, 466–480.

303. Sauer, R., et al. Water-soluble phosphate prodrugs of 1-propargyl-8-styrylxanthine derivatives. A_{2A}-selective adenosine receptor antagonists. J. *Med. Chem*. **2000**, 43, 440–448.

304. Vollmann, K., et al. Synthesis and properties of a new water-soluble prodrug of the adenosine A_{2A} receptor antagonist MSX-2, *Molecules.* **2008**, 13, 348–359.

305. Bilkei-Gorzo, A., et al. Adenosine receptor subtype-selective antagonists in inflammation and hyperalgesia. *Naunyn-Schmiedebergs Arch. Pharmacol*. **2008**, 377, 65–76.

306. Mott, A.M., et al. The adenosine A_{2A} antagonist MSX-3 reverses the effects of the dopamine antagonist haloperidol on effort-related decision making in a T-maze cost/benefit procedure. *Psychopharmacology*. **2009**, 204, 103–112.

307. Alexander, S.P., et al. [^{3}H]ZM241385 — an antagonist radioligand for adenosine A_{2A} receptors in brain. *Eur. J. Pharmacol*. **2001** 411, 205–210.

308. Hauser, R.A., et al. Tozadenant (SYN115) in patients with Parkinson's disease who have motor fluctuations on levodopa: a phase 2b, double-blind, randomised trial. *Lancet Neurol.* 13, **2014,** 767–776.

309. Kachroo, A., et al. Adenosine A_{2A} receptor gene disruption protects in an α-synuclein model of Parkinson's disease. *Ann. Neurol.* 71, **2012**, 278–282.

310. Ferreira, D.G., et al. Adenosine A_{2A} Receptors Modulate α-Synuclein Aggregation and Toxicity. *Cereb Cortex.* **2017**, 27, 718–730.

311. **Hu, Q., et al**. Aberrant adenosine A_{2A} receptor signaling contributes to neurodegeneration and cognitive impairments in a mouse model of synucleinopathy. *Exp. Neurol.* **2016**, 283, 213–223.

312. Li, J., et al. Oxidative stress and neurodegenerative disorders. *Int. J. Mol. Sci.* **2013**, *14*, 24438-24475.

313. Charoco, M., et al. A review on antioxidants, prooxidants and related controversy: Natural and synthetic compounds, screening and analysis methodologies and future perspectives. *Food and Chemical Toxicology.* **2013**, 51, 15–25

314. Turrens, J.F., et al. Mitochondrial formation of reactive oxygen species. *J. Physiol*. **2003**, *552*, 335–344.

315. Coon, M.J., et al. Ding, X.; Pernecky, S.J.; Vaz, A.D.N. Cytochrome P450: Progress and predictions. *FASEB J.* **1992***, 6*, 669–673.

316. Reed, J.R., et al. Backes, W.L. Formation of P450·P450 complexes and their effect on P450 function. *Pharmacol. Ther*. **2012**, *133*, 299–310. **317. DeLeo, F.R., et al**. Assembly of the phagocyte NADPH oxidase: Molecular interaction of oxidase proteins. *J. Leukoc. Biol*. **1996**, *60*, 677–691.

318. **Finkel, T. et al**. Redox-dependent signal transduction. *FEBS Lett*. **2000**, *476*, 52–54.

319. Gandhi, S., et al. Mechanism of oxidative stress in neurodegeneration. *Oxid. Med. Cell. Longev*. **2012**, *2012*, 428010.

320. Chance, B., et al. Hydroperoxide metabolism in mammalian organs. *Physiol. Rev.* **1979**, *59*, 527–605.

321. Packer, M.A., et al. Superoxide production by mitochondria in the presence of nitric oxide forms peroxynitrite. *Biochem. Mol. Biol. Int*. **1996**, *40*, 527–534.

322. Bringold, U., et al. Peroxynitrite formed by mitochondrial NO synthase promotes mitochondrial Ca^{2+} release. *Free Radic. Biol. Med.* **2000**, *29*, 343–348.

323. Stanley, B.A., et al. Thioredoxin reductase-2 is essential for keeping low levels of H_2O_2 emission from isolated heart mitochondria. *J. Biol. Chem*. **2011**, *286*, 33669–33677.

324. Lu, J., et al. The thioredoxin antioxidant system. *Free Radic. Biol. Med.* **2013**,

325. Massaad, C.A., et al. Reactive oxygen species in the regulation of synaptic plasticity and memory. *Antioxid. Redox Signal*. **2011**, *14*, 2013–2054.

326. Barros, A.I.R.N.A., et al. Effect of cooking on total vitamin C contents and antioxidant activity of sweet chestnuts (*Castanea sativa* Mill.). *Food Chem*. **2011**, 128, 165–172.

327. Burton, G.W., et al. Vitamin E: antioxidant activity, biokinetics, and bioavailability. *Annu. Rev. Nutr*. **1990**, 10, 357–382.

328. **Halpner, A.D., et al**. Protection by vitamin C of oxidant-induced loss of vitamin E in rat hepatocytes. *J. Nutr. Biochem*. **1998**, 9, 355–359.

329. Ross, D., et al. The generation and fate of glutathionyl radicals in biological systems, in Poli, G., et al., Free radicals in liver injury. *IRL Press. Oxford.* **1987**, 17-20.

330. Prutz, W.A. Chemical repair in DNA solutions containing thiols/or disulphides. Further evidence for disulphide radical anions acting as electron donors. *Int. J. Radiat. Biol.* **1989,** 56, 21-33.

331. Shindo, Y. Et al. Dose-response effects in acute ultraviolet irradiation on antioxidants and molecular markers of oxidation in murine epidermis. J. *Invest. Dermatol.* **1994,** 104, 470-475.

332. Valko, M., et al. Free radicals and antioxidants in normal physiological functions and human disease. *Int. J. Biochem. Cell Biol*. **2007**, 39, 44–84.

333. Rochette, L., et al. Direct and indirect antioxidant properties of α-lipoic acid and therapeutic potential. *Mol. Nutr. Food. Res.* **2013**, *57*, 114–125.

334. Raddatz, G., et al. Receptor site and stereospecifity of dihydrolipoamide dehydrogenase for R- and S-lipoamide: a molecular modeling study. *J. Biotechnol*. **1997**, 58, 89−100.

335. Fujiwara, K., et al. Lipoylation of Acyltransferase Components of α-Ketoacid Dehydrogenase Complexes. *J. Biol. Chem*. **1996**, 271, 12932−12936.

336. Akiba, S., et al. Assay of Protein- Bound Lipoic Acid in Tissues by a New Enzymatic Method. Anal. Biochem. 1998, 258, 299−304.

337. Wollin, S. D., et al. α-Lipoic Acid and Cardiovascular Disease. *J. Nutr*. **2003**, 133, 3327−3330.

338. Packer, L., et al. Vitamin E and alpha-lipoate: Role in antioxidant recycling and activation of the NF-κB transcription factor. *Mol. Aspects. Med*. **1993**, 14, 229−239.

339. Packer, L., et al. Alpha-lipoic acid as a biological antioxidant. *Free Radical Biol. Med*. **1995**, 19, 227−250.

340. Packer, L., et al. Alpha-lipoic acid: a metabolic antioxidant and potential redox modulator of transcription. *Adv. Pharmacol***. 1997**, 38, 79−101.

341. Packer, L., et al. α-Lipoic acid: A metabolic antioxidant which regulates NF-κB signal transduction and protects against oxidative injury. *Drug Metab. Rev*. **1998**, 30, 245−275.

342. Trujillo, M., et al. Peroxynitrite reaction with the reduced and the oxidized forms of lipoic acid: new insights into the reaction of peroxynitrite with thiols. *Arch. Biochem. Biophys***. 2002**, *397*, 91–98.

343. Ou, P., et al. Thioctic (lipoic) acid: a therapeutic metal-chelating antioxidant? *Biochem. Pharmacol.* **1995**, *50*, 123–126.

344. Suh, J. H., et al. Dietary supplementation with (R)-alpha-lipoic acid reverses the age-related accumulation of iron and depletion of antioxidants in the rat cerebral cortex. *Redox. Rep.* **2005**, 10, 52–60.

345. Bush, A. I., et al. Metal complexing agents as therapies for Alzheimer's disease. *Neurobiol. Aging.* **2002**, *23*, 1031– 1038.

346. Nagamatsu, M., et al. Lipoic acid improves nerve blood flow, reduces oxidative stress, and improves distal nerve conduction in experimental diabetic neuropathy. *Diabetes Care*. **1995**, 18(8), 1160–1167.

347. Ziegler, D., et al. Treatment of symptomatic diabetic polyneuropathy with the antioxidant alpha-lipoic acid: a meta-analysis. *Diabet Med*. **2004**, 21(2), 114–121.

348. Mijnhout, G.S., et al. Alpha lipoic Acid for symptomatic peripheral neuropathy in patients with diabetes: a meta-analysis of randomized controlled trials. *Int. J. Endocrinol*. **2012**, 2012, 1–8.

349. Li, Q.R., et al. Epalrestat protects against diabetic peripheral neuropathy by alleviating oxidative stress and inhibiting polyol pathway. *Neural. Regen. Res*. **2016**, 11(2), 345–351.

350. Li, P., et al. Clinical efficacy and safety of epalrestat in diabetic neuropathy-A multicenter randomized controlled clinical trial. *Chinese Journal of Endocrinology and Metabolism*. **2015**, 31(9), 743–747.

351. Hotta, N., et al. Long-term clinical effects of epalrestat, an aldose reductase inhibitor, on diabetic peripheral neuropathy: the 3-year, multicenter, comparative Aldose Reductase Inhibitor-Diabetes Complications Trial. *Diabetes Care*. **2006**, 29(7), 1538–1544.

352. Guo, Y., et al. Analysis the effect of lipoic acid combined with epalrestat in Chinese people with diabetes peripheral neuropathy. *Journal of Practical Diabetology*. **2017,**13(01), 15–18.

353. Wiernsperger, N.F., et al. Oxidative stress as a therapeutic target in diabetes: revisiting the controversy. *Diabetes Metab***. 2003**, 29, 579–585

354. Lü, J.M., et al. Chemical and molecular mechanisms of antioxidants: Experimental approaches and model systems. *J. Cell. Mol. Med*. **2010**, *14*, 840–860.

355. Cooke, M.S., et al. Does measurement of oxidative damage to DNA have clinical significance? *Clin. Chim. Acta.* **2006**, *365*, 30–49.

356. **Perez, M., et al**. Phosphorylated, but not native, tau protein assembles following reaction with the lipid peroxidation product, 4-hydroxy-2-nonenal. *FEBS Lett*. **2000**, *486*, 270–274.

357. Wataya, T., et al. High molecular weight neurofilament proteins are physiological substrates of adduction by the lipid peroxidation product hydroxynonenal. *J. Biol. Chem*. **2002**, *277*, 4644–4648.

358. Misonou, H., et al. Oxidative stress induces intracellular accumulation of amyloid beta-protein (Abeta) in human neuroblastoma cells. *Biochemistry.* **2000**, *39*, 6951–6959.

359. Gabuzda, D., et al. Inhibition of energy metabolism alters the processing of amyloid precursor protein and induces a potentially amyloidogenic derivative. *J. Biol. Chem.* **1994**, *269*, 13623–13628.

360. Apelt, J., et al. Aging related increase in oxidative stress correlates with developmental pattern of beta-secretase activity and beta-amyloid plaque formation in transgenic Tg2576 mice with Alzheimer like pathology. *Int. J. Dev. Neurosci.* **2004**, 22, 475–484.

361. Ghiso, J., et al. Cerebral amyloidosis, amyloid angiopathy, and their relationship to stroke and dementia. *J. Alzheimers Dis*. **2001**, *3*, 65–73.

362. Coma, M., et al. Oxidative stress triggers the amyloidogenic pathway in human vascular smooth muscle cells. *Neurobiol. Aging.* **2008**, *29*, 969–980.

363. Xiang, W., et al. Oxidative stress-induced posttranslational modifications of alpha-synuclein: Specific modification of alpha-synuclein by 4-hydroxy-2-nonenal increases dopaminergic toxicity. *Mol. Cell. Neurosci*. **2013**, *54*, 71–83.

364. Nekooki-Machida, Y., et al. Distinct conformations of *in vitro* and *in vivo* amyloids of huntingtin-exon1 show different cytotoxicity. *Proc. Natl. Acad. Sci. USA* **2009**, *106*, 9679–9684.

365. Mitomi, Y., et al. Post-aggregation oxidation of mutant huntingtin controls the interactions between aggregates. *J. Biol. Chem*. **2012**, *287*, 34764–34775.

366. Goswami, A., et al. Oxidative stress promotes mutant huntingtin aggregation and mutant huntingtin-dependent cell death by mimicking proteasomal malfunction. *Biochem. Biophys. Res. Commun*. **2006**, *342*, 184–190.

367. Zhuo, M., et al. Neuronal mechanism for neuropathic pain. *Mol. Pain*. **2007**, 3, 14.

368. Ma, W., et al. Does COX2-dependent PGE2 play a role in neuropathic pain? *Neurosci. Lett*. **2008**, 437, 165-169.

369. Tal, M., et al. A novel antioxidant alleviates heat hyperalgesia in rats with an experimental painful peripheral neuropathy. *Neur. Report*. **1996**, 7, 4-1382.

370. Khalil, Z., et al. Free radicals contribute to the reduction in peripheral vascular responses and the maintenance of therma hyperalgesia in rats with chronic constriction injury. *Pain*. **1999**, 79, 7-31.

371. Kim, H.K., et al. Reactive oxygen species (ROS) play an important role in rat model of neuropathic pain. *Pain*. **2004**, 111, 24-1116.

372. Naik, A.K., et al. Role of oxidative stress in pathophysiology of peripheral neuropathy and modulation by N-acetyl-L-cysteine in rats. *Eur. J. Pain*. **2006,** 10, 573–579.

373. Gamelin, E., et al. Clinical aspects and molecular basis of oxaliplatin neurotoxicity: Current management and development of preventive measures. *Semin. Oncol*. **2002**, 29, 21-33.

374. Di Cesare Mannelli, L., et al. Oxaliplatin-Induced Neuropathy: Oxidative Stress as Pathological Mechanism. Protective Effect of Silibinin. *The Journal of Pain*. **2012**, 13, 276-284.

375. Costenla, A.R., et al. Caffeine, adenosine receptors, and synaptic plasticity. *J. Alzheimer's Dis*. **2010**, 20, 25–34.

376. Costenla, A.R., et al. Adenosine modulates synaptic plasticity in hippocampal slices from aged rats. *Brain Res*. **1999**, 851, 228–234.

377. Costenla, A.R., et al. Enhanced role of adenosine $A_{(2A)}$ receptors in the modulation of LTP in the rat hippocampus upon ageing. *Eur. J. Neurosci*. **2011**, 34, 12–21.

378. Li, W., et al. Inactivation of adenosine A_{2A} receptors reverses working memory deficits at early stages of Huntington's disease models. *Neurobiol. Dis*. **2015**, 79, 70−80.

379. Armentero, M. T., et al. Past, present and future of A_{2A} adenosine receptor antagonists in the therapy of Parkinson's disease. *Pharmacol. Ther*. **2011**, 132, 280−299.

380. Preti, D., et al. History and perspective of A_{2A} adenosine receptor antagonists as potential therapeutic agents. *Med. Res. Rev*. **2015**, 35, 790−848.

381. Mohamed, R. A., et al. Role of adenosine A_{2A} receptor in cerebral ischemia reperfusion injury: signaling to phosphorylated extracellular signal-regulated protein kinase (pERK1/2). *Neuroscience*. **2016,** 314, 145−159.

382. Faivre, E., et al. Beneficial Effect of a Selective Adenosine A_{2A}Receptor Antagonist in the APPswe/PS1dE9 Mouse Model of Alzheimer's Disease. *Front. Mol. Neurosci*. **2018,** 11, 235

383. Silva, A.C., et al. Blockade of adenosine A_{2A} receptors recovers early deficits of memory and plasticity in the triple transgenic mouse model of Alzheimer's disease. *Neurob. of Dis*. **2018**, 117, 72–81.

384. Atack, J., et al. JNJ-40255293, a novel adenosine A_{2A}/A_1 antagonist with efficacy in preclinical models of Parkinson's disease. ACS *Chem. Neurosci*. **2014**, 5, 1005−1019.

385. Cechova, S, et al. A_1 receptors self regulate adenosine release in the striatum: evidence of autoreceptor characteristics. *Neuroscience.* **2010**, 171, 1006−1015.

386. Borycz, J., et al. Differential glutamate-dependent and glutamate independent adenosine A_1 receptor-mediated modulation of dopamine release in different striatal compartments. *J. Neurochem.* **2007**, 101, 355−363.

387. Colotta, V., et al. 1,2,4-Triazolo[4,3-a]quinoxalin-1-one moiety as an attractive scaffold to develop new potent and selective human A_3 adenosine receptor antagonists: synthesis, pharmacological and ligand-receptor modeling studies. *J. Med. Chem*. **2004**, 47, 3580−3590.

388. Colotta, V., et al. Synthesis of 4-Amino-6-(hetero)- arylalkylamino-1,2,4-triazolo[4,3-a]quinoxalin-1-one derivative as potent A_{2A} adenosine receptor antagonists. *Bioorg. Med. Chem*. **2003,** 11, 5509−5518.

389. **Lenzi, O., et al**. 4-Amido-2-aryl-1,2,4-triazolo[4,3-a]quinoxalin- 1-ones as new potent and selective human A_3 adenosine receptor antagonists. Synthesis, pharmacological evaluation and ligand-receptor modeling studies. J. *Med. Chem*. **2006**, 49, 3916−3925.

390. Morizzo, E., et al. Scouting human A_3 adenosine receptor antagonist binding mode using a molecular simplification approach: from triazoloquinoxaline to a pyrimidine skeleton as a key study. *J. Med. Chem*. **2007**, 50, 6596−6606.

391. Colotta, V., et al. Synthesis, ligand-receptor modeling studies and pharmacological evaluation of novel 4-modified-2-aryl- 1,2,4-triazolo[4,3-a]quinoxalin-1-one derivatives as potent and selective human A_3 Adenosine Receptor Antagonists. *Bioorg. Med. Chem*. **2008**, 16, 6086−6102.

392. Squarcialupi, L., et al. Exploring the 2- and 5-positions of the pyrazolo[4,3-*d*]pyrimidin-7-amino scaffold to target human A_1 and A_{2A} adenosine receptors. *Bioorg. Med. Chem*. **2016**, 24, 2794-2808.

393. Krimmel, B., et al. OH-radical induced degradation of hydroxybenzoic- and hydroxycinnamic acids and formation of aromatic products – a gamma radiolysis study. *Radiat. Phys. Chem*. **2010,** 79, 1247– 1254.

394. Terpinc, P., et al. Antioxidant properties of 4-vinyl derivatives of hydroxycinnamic acids. *Food Chem*. **2011,** 128, 62–68.

395. Hilton, J.W., et al. Antioxidants: function, types and necessity of inclusion in pet foods. *Can. Vet. J.* **1989,** 30, 682-684.

396. Amorati, R., et al. Antioxidant activity of obisphenols: the role of Intramolecular hydrogen bonding. *J. Org. Chem*. **2003,** 68, 5198-5204.

397. Lazer, E.S., et al. Antiinflammatory 2,6-di-tert-butyl-4-(2-arylethenyl)phenols. *J. Med. Chem*. **1989**, 32, 100-104.

398. Cummings, S.W., et al. Metabolism of 3-tert-butyl-4-hydroxyanisole by microsomal fractions and isolated rat hepatocytes. *Canc. Res*. **1985,** 45, 5617-5624.

399. Dacre, J.C., et al. The metabolism of 3,5-di-tert-butyl-4-hydroxytoluene and 3,5-ditert-butyl-4-hydroxybenzoic acid in the rabbit. *Biochem*. J. **1961,** 78, 758-766.

400. Suh, J.H., et al. Decline in transcriptional activity of Nrf2 causes age related loss of glutathione synthesis, which is reversible with lipoic acid. *Proc. Natl. Acad. Sci. U.S.A*. **2004**, 101(10), 3381–3386.

401. Kerksick, C., et al. The antioxidant role of glutathione and N-acety-L-cysteine supplements and exercise-induced oxidative stress. *J. Int. Soc. Sports.Nutr*. **2005**, 2, 38–44.

402. Jain, S.K., et al. L-cysteine supplementation lowers blood glucose, glycated hemoglobin, CRP, MCP-1, and oxidative stress and inhibits NF-κB activation in the livers of Zucker diabetic rats. *Free. Radic. Biol. Med*. **2009**, 46, 1633–1638.

403. Burton, G. W., et al. Autoxidation of biological molecules. 1. Antioxidant activity of vitamin E and related chainbreaking phenolic antioxidants in vitro. *J. Am. Chem. Soc*. **1981**, 103, 6472−6477.

404. Watanabe, T., et al. Protective effects of MCI-186 on cerebral ischemia: Possible involvement of free radical scavenging and antioxidant actions. *J. Pharmacol. Exp. Ther*. **1994**, 268, 1597–1604.

405. Wu, T., et al. Myocardial protection of MCI-186 in rabbit ischemia reperfusion. *Life. Sci.* **2002**, *71*, 2249–2255.

406. Banno, M., et al. The radical scavenger edaravone prevents oxidative neurotoxicity induced by peroxynitrite and activated microglia. *Neuropharm.* **2005**, *48*, 283–290.

407. Abe, S., et al. The reaction rate of edaravone(3-methyl-1-phenyl-2-pyrazolin-5-one (MCI-186)) with hydroxyl radical. *Chem. Pharm. Bull.* **2004**, *52*, 186–191,**408. Nakagawa, H., et al.** Radical scavenging by edaravone derivatives: efficient scavenging by 3-methyl-1-(pyridine-2-yl)-5-pyrazolone with an intramolecular base. *Bioorg. Med. Chem. Lett.* **2006**, *16*, 5939–5942.

409. Ono, S., et al. Density functional study of the radical reactions of 3-methyl-1-phenyl-2-pyrazolin-5-one (MCI-186): implication for the biological function of MCI-186 as a highly potent antioxidative radical scavenger. *J. Phys. Chem. A.* **1997**, *101*, 3769–3775.

410. Falsini, M., et al. The 1,2,4-triazolo[4,3-a]pyrazin-3-one as a versatile scaffold for the design of potent adenosine human receptor antagonists. Structural investigations to target the A_{2A} receptor. *J. Med. Chem*. **2017**, 60, 5772-5790.

411. Shawali, A. S., et al. Kinetics and mechanism of dehydrochlorination of N-aryl-C-ethoxycarbonylformohydrazidoyl chlorides. *Can. J. Chem*. **1986**, 64, 871−875.

412. Lozinskii, M. O., t al. Ethyl arylazochloroacetates and their reactions with morpholine and hydrazine hydrate. *Ukr. Khim. Zh*. **1967**, 33, 1295−1296.

413. Abbotto, A., et al. Diheteroarylmethanes. 8.1 Mapping charge and electron-withdrawing power of the 1,2,4-triazol-5-yl substituent. *J. Org. Chem*. **1999**, 64, 6756−6763.

414. Sharp, D. B., et al. Derivatives of 1,2,4-triazole and pyrazole. *J. Am. Chem. Soc*. **1946**, 68, 588−590.

415. Matiychuk, V. S.; et al. A New method for the synthesis of 1-aryl-1,2,4-triazole derivatives. *Synthesis*. **2011**, 2011, 1799−1813.

416. Inventors; Ironwood pharmaceuticals, Inc., Renhowe, P.A., et al. World patent WO2015/089182A1. **2015** Jun 18.

417. El Maatougui, A., et al. Discovery of potent and highly selective A_{2B} adenosine receptor antagonist chemotypes. *J. Med. Chem*. **2016**, 59, 1967−1983.

418. Alnouri, M. W., et al. Selectivity is species-dependent: Characterization of standard agonists and antagonists at human, rat, and mouse adenosine receptors. *Purinergic. Signalling*. **2015**, 11, 389−407.

419. Molecular Operating Environment; C.C.G., Inc.: 1255 University Street, Suite 1600, Montreal, Quebec, Canada, H3B 3X3, **2014**.

420. Jones, G. et al. Willett, P.; Glen, R. C.; Leach, A. R.; Taylor, R. Development and validation of a genetic algorithm for flexible docking. *J. Mol. Biol*. **1997**, 267, 727−748.

421. Huey, R., et al. Morris, G. M.; Olson, A. J.; Goodsell, D. S. A semiempirical free energy force field with charge-based desolvation. *J. Comput. Chem*. **2007**, 28, 1145−1152.

422. Morris, G. M., et al. AutoDock4 and AutoDockTools4: Automated docking with selective receptor flexibility. *J. Comput. Chem*. **2009**, 30, 2785−2791.

423. Jaakola, V. P., et al. The 2.6 angstrom crystal structure of a human A_{2A} adenosine receptor bound to an antagonist. *Science*. **2008**, 322, 1211−1217.

424. Dal Ben, D., et al. Adenosine receptor modeling: what does the A_{2A} crystal structure tell us? Curr. Top. *Med. Chem*. **2010**, 10, 993−1018.

425. Liu, W., et al. Structural basis for allosteric regulation of GPCRs by sodium ions. *Science*. **2012**, 337, 232−236.

426. **Squarcialupi, L., et al**. 7-Amino-2-phenylpyrazolo[4,3-d]pyrimidine derivatives: structural investigations at the 5-position to target A_1 and A_{2A} adenosine receptors. Molecular modeling and pharmacological studies. *Eur. J. Med. Chem*. **2014**, 84, 614−627.

427. Scatena, A., et al. 3-(Fur-2-yl)-10- (2-phenylethyl)-[1,2,4]triazino[4,3-a]benzimidazol-4(10H)-one, a novel adenosine receptor antagonist with A_{2A}-mediated neuroprotective effects. *ACS Chem. Neurosci*. **2011**, 2, 526−535.

428. **Zhao, Q., et al**. Protection against MPP^+-induced neurotoxicity in SH-SY5Y cells by tormentic acid via the activation of PI3-K/Akt/GSK3 pathway. *Neurochem. Int*. **2016**, 97, 117−123.

429. Giunta, S., et al. Dual blockade of the A_1 and A_{2A} adenosine receptor prevents amyloid beta toxicity in neuroblastoma cells exposed to aluminium chloride. *Int. J. Biochem. Cell Biol*. **2014**, 5, 122-136.

430. Yamada, K., et al. Antidepressant activity of the adenosine A_{2A} receptor antagonist, istradefylline (KW-6002) on learned helplessness in rats. *Psychopharmacology*. **2014**, 231, 2839−2849.

431. Kadowaki Horita, T., et al. Effects of the adenosine A_{2A} antagonist istradefylline on cognitive performance in rats with a 6-OHDA lesion in prefrontal cortex. *Psychopharmacology*. **2013**, 230, 345−352.

432. Ikeda, K., et al. Neuroprotection by adenosine A_{2A} receptor blockade in experimental models of Parkinson's disease. *J. Neurochem*. **2002**, 80, 262−270.

433. Gyoneva, S., et al. Adenosine A_{2A} receptor antagonism reverses inflammation-induced impairment of microglial process extension in a model of Parkinson's disease. *Neurobiol. Dis*. **2014**, 67, 191−202.

434. Blum, D., et al. Molecular pathways involved in the neurotoxicity of 6-OHDA, dopamine and MPTP: contribution to the apoptotic theory in Parkinson's disease. *Prog. Neurobiol*. **2001**, 65, 135−172.

435. Caulkett, P. W. R., et al. Preparation of (Amino)heteroaryl[1,2,4]triazolo[1,5-a]triazine and related compounds as adenosine A_2 receptor antagonists. EP 459702, May 23, **1991**.

436. Hutchison, A. J., et al. CGS21680, an A_2 selective adenosine receptor agonist with preferential hypotensive activity. *J. Pharmacol. Exp. Ther***. 1989**, 251, 47−55.

437. Rivera-Oliver, M., et al. Using caffeine and other adenosine receptor antagonists and agonists as therapeutic tools against neurodegenerative diseases. *a review, Life Sci*. **2014**, 101, 1-9.

438. Xu, K., et al. Neuroprotection by caffeine in the MPTP model of Parkinson's disease and its dependence on adenosine A_{2A} receptors. *Neuroscience*. **2016**, 322, 129–137.

439. Eskelinena, Marjo H., et al. Caffeine as a Protective Factor in Dementia and Alzheimer's Disease. *Journal of Alzheimer's Disease*. **2010**, 20, S167–S174.

440. **Kolahdouzan, M., et al**. The neuroprotective effects of caffeine in neurodegenerative diseases. *CNS Neurosci Ther*. **2017**, 23, 272–290.

441. Dall'Igna, O. P., et al. Caffeine and adenosine A_{2A} receptor antagonist prevent β-amyloid (25-35)-induced cognitive deficits in mice. *Experimental Neurology*. **2007**, 203, 241-245.

442. Di Cesare Mannelli, L., et al. Oxaliplatin-induced oxidative stress in nervous system-derived cellular models: could it correlate with in vivo neuropathy? *Free. Radic. Biol. Med*. **2013**, 61, 143-50.

443. Faria, J. Et al. Comparative study of the neurotoxicological effects of tramadol and tapentadol in SH-SY5Y. *cells. Toxicology*. **2016**, 359, 1-10.

444. Branca, J.J.V., et al. Selenium and zinc: Two key players against cadmium-induced neuronal toxicity. *Toxicol In Vitro*. **2018**, 48, 159-169.

445. Zanardelli, M., et al. Oxaliplatin Neurotoxicity Involves Peroxisome Alterations. PPARγ Agonism as Preventive Pharmacological Approach. *Plos ONE*. **2014,** 9(7), e102758.

446. de Lera Ruiz, M., et al. Adenosine A_{2A} receptor as a drug discovery target. *J. Med. Chem*. **2013**, 57, 3623−3650.

447. Headrick, J. P., et al. Cardiovascular adenosine receptors: expression, actions and interactions. *Pharmacol. Ther*. **2013**, 140, 92−111.

448. Gao, Z. G., et al. Emerging adenosine receptor agonists. *Expert Opin. Emerging Drugs*. **2007**, 12, 479−492.

449. Lappas, C. M., et al. Adenosine A_{2A} agonists in development for the treatment of inflammation. *Expert Opin. Invest. Drugs*. **2005**, 14, 797−806.

450. Varani, K., et al. Oxidative/nitrosative stress selectively altered A_{2B} adenosine receptors in chronic obstructive pulmonary disease. *FASEB J*. **2010**, 24, 1192−1204.

451. Soudijn, W., et al. Medicinal chemistry of adenosine A_1 receptor ligands. *Curr Top Med Chem*. **2003**, 3, 355–367.

452. Gao, Z.G., et al. Site-directed mutagenesis studies of human A($_{2A}$) adenosine receptors: involvement of glu(13) and his(278) in ligand binding and sodium modulation. *Biochem Pharmacol*. **2000**, 60, 661–668.

453. Kim, S.K., et al. Modeling the adenosine receptors: comparison of the binding domains of A_{2A} agonists and antagonists. *J. Med. Chem*. **2003**, 46, 4847–4859.

454. Jacobson, K.A., et al. A neoceptor approach to unraveling microscopic interactions between the human A_{2A} adenosine receptor and its agonists. *Chem. Biol*. **2005**, 12, 237–247.

455. Inventors; Bayer Aktiengesellschaft, Rosentreter, U., et al. Preparation of 2-heteroarylmethyltio-3,5-dicyano-4-phenyl-6-aminopyridines as adenosine receptor selective ligands. World patent WO03008384. **200.3** Jan 30.

4**56. Chang, L.C., et al.** A series of ligands displaying a remarkable agonistic-antagonistic profile at the adenosine A_1 receptor. *J. Med. Chem*. **2005**, 48, 2045–2053.

457. Galli, U., et al. The Guareschi Pyridine Scaffold as a Valuable Platform for the Identification of Selective PI3K Inhibitors. *Molec*. **2015**, 20, 17275-17287.

458. Smith, P.K. et al. Measurement of Protein Using Bicinchoninic Acid. *Anal. Biochem*. **1985**, 150, 76-85.

459. Cheng, Y., et al. Relationship between the inhibition constant (K1) and the concentration of inhibitor which causes 50 per cent inhibition (I50) of an enzymatic reaction. Biochem Pharmacol. **1973**, 22, 3099-3108.